MSc Thesis Report

Learning from Orderbook Features in Intraday Electricity Market

ME-MME

Ruochen Wu

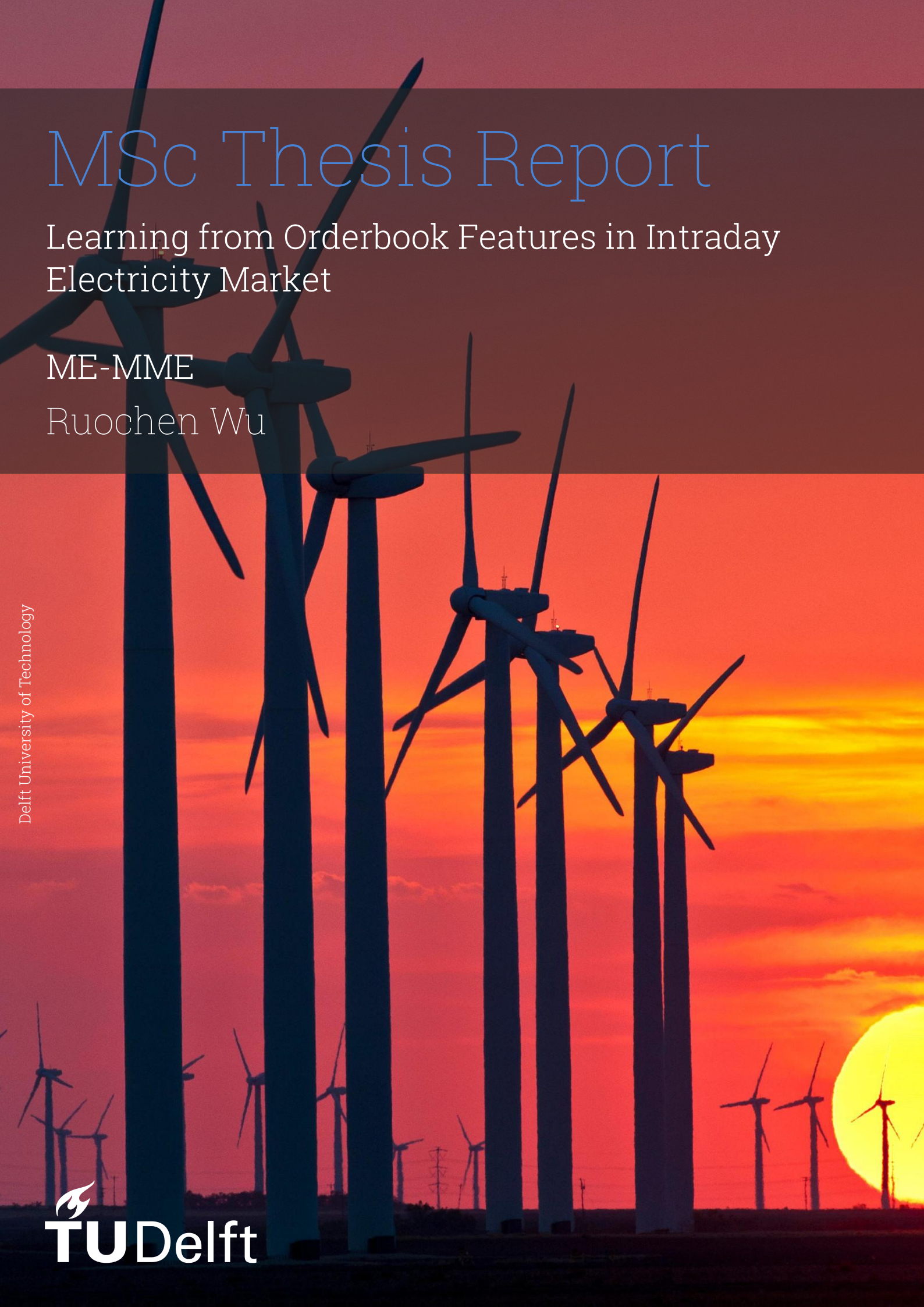

Delft University of Technology

TU Delft

MSc Thesis Report

Learning from Orderbook Features in Intraday Electricity Market

ME54035

Ruochen

Wu

Supervisor:	Dr. J. Cremer, R. Yu
Chair:	Dr. J. Jovanova
Project Duration:	January 13th, 2025 - June 23rd, 2025
Faculty:	Faculty of Mechanical Engineering, Delft
Report NO.:	2025.MME.9088

TU Delft

Preface

This report represents the final product of my MSc thesis and constitutes part of the ME54035 MSc Graduation Project. It also incorporates elements from my earlier literature research. This work marks my first academic exploration in the field of data mining applied to the energy market, as well as my first systematic and focused research in machine learning and artificial intelligence applications.

As someone who has been passionate about mathematical statistics since childhood, and a former Olympiad mathematics competitor, I feel deeply fortunate to have had the opportunity to center my graduation project on data mining in the European energy markets. This project represents a significant personal milestone and has provided me with valuable experience and motivation to pursue further research in AI applications.

My graduation project officially began in January 2025, and by June 2025, the main experimental pipelines were completed. In the first phase of exploration, I dedicated several months to investigating the frontier of interpretable price prediction in intraday electricity markets using the KolmogorovArnold Network (KAN). Although KAN appeared theoretically promising as a white-box deep learning model, the symbolification process led to unacceptable loss, and its performance, after conversion, fell below that of statistical machine learning methodsdespite the black-box KAN showing strong results. Moreover, it required significantly more computation time. Although this phase of research was ultimately disappointing in terms of results, it was intellectually stimulating and led me to develop several novel ideas.

In the second phase, building upon the findings from the first, I shifted toward developing a classifier for price anomaly detection and designed corresponding gating networks. However, the lack of an authoritative definition of abnormal prices made this direction difficult to validate. Moreover, the improvement to pointwise prediction brought by gating networks proved to be marginal. These two exploratory directions were disheartening, especially for a newcomer to the field. However, they deepened my understanding of the inherent uncertainty in scientific research and ultimately fueled my enthusiasm to return to foundational ideas and pursue more robust solutions.

The third phase of explorationserving as the baseline for this reportwas inspired by a Q&A during a literature research group meeting in November 2024. I clearly recall my ambition to build unified models for predicting across different countries and regions, but I struggled to answer the challenge: "Why not train a separate model for each market?" This moment led me to explore generalization across markets and to design and conduct what became the most intellectually rewarding part of this project: the generalization assessment.

This project also had a profound impact on my personal philosophy. It made me fall in love with examining and refining machine learning models from a philosophical perspective, appreciating not only their function but also their conceptual underpinnings.

I would like to express my heartfelt gratitude to those who supported me throughout this journey. I am

especially grateful to my project chair, Jovana, an outstanding and empathetic mentor who supported me throughout my second year at TU Delft, both during my Research Assignment and during this Graduation Project. I am also deeply thankful to my supervisor, Jochen, a knowledgeable and creative researcher whose challenges and encouragement often left a lasting impression. Furthermore, I would like to thank my daily supervisor, Runyao, a patient and talented data scientist. We connected several months before the project officially started, and he guided me from the theoretical foundations of domain knowledge, algorithms, and AI models. He has always been open to discussing ideas and generous in his tolerance of my beginners mistakes.

I would also like to thank the Faculty of Mechanical Engineering at TU Delft and the MME program for providing a rich and forward-looking academic environment. Finally, I must express my deepest appreciation to my parents, Mr. and Mrs. Wu, who have supported every step of my development. Their consistent psychological and material support has allowed me to freely pursue my interests and carve out a unique professional path.

Ruochen Wu
Delft, July 2025

Abstract

Intraday electricity markets (IDM), which is designed to correct forecast error of renewable energy generations and enable energy trading, are characterized by high volatility and rapid price fluctuations, which not only provide market participants with strong motivation to make accurate price predictions, but also present significant challenges. The use of machine learning methods for price prediction has become a major trend in recent research. However, in previous studies, only a few specific features, such as Volume-Weighted Average Price (VWAP) and last transaction price [1, 2, 3], have been applied, while the rich features embedded in orderbooks have not received sufficient attention. Furthermore, while quantile regression tasks, which provide richer information for trading strategies, have been employed in IDM price prediction, they have generally been confined to statistical models [4, 5]. Deep learning-based quantile regression, capable of capturing nonlinear relationships and incorporating uncertainty, has yet to be applied. Additionally, in current research, IDM price prediction is often based on a specific orderbook, and thus, the generalization of prediction methods across different orderbooks, as well as their structural similarities across different markets and product types, has not been convincingly addressed.

To address the challenges mentioned above, this report focuses on the German and Austrian markets over continuous trading periods from January 2022 to January 2025, considering both hourly and quarter-hourly products. A total of 384 feature candidates were extracted, including percentiles, momentum, and volatility of prices and trading volumes on both buy and sell sides across multiple time windows. For the extracted feature candidates, we propose an innovative feature selection approach based on their correlation with normal and extreme price labels. Comparative experiments demonstrate that this algorithm outperforms L1-based selection and Principal Component Analysis (PCA) compression in quantile forecast evaluations. Based on the selected features, Quantile LightGBM (QLGBM), Quantile Extreme Gradient Boosting (QXGB), Quantile Multilayer Perceptron (QMLP), and Quantile KolmogorovArnold Network (QKAN) were used to predict the labels, providing a comprehensive set of benchmarks. Additionally, generalization studies across markets and products were conducted using transfer learning, with multiple strategies such as zero-shot, fine-tuning, and joint learning applied. The results reveal valuable insights into the relationships between different markets and product types.

Contents

1

Introduction

1.1. Background

1.1.1. Renewable Energy Integration

The rapid rise in global energy demand [6, 7] has made balancing energy production with environmental protection an increasingly urgent challenge [8], influencing global economic stability [9]. In response, European Union (EU) countries are accelerating their efforts to reduce reliance on fossil fuels, which have long dominated their energy systems [10, 11, 12]. This transition is not only reshaping the EUs electricity market but also triggering far-reaching changes in its economic and environmental policies.

Driven by sustainability goals, renewable energy sources (RES) are steadily increasing and are expected to continue rising in their share of the EUs overall energy consumption [13]. As shown in Figures 1.1 [14] and 1.2 [15], Figure 1.1 presents the energy consumption structure of the EU in 2022 and outlines the projected energy consumption structure for the 2030 targets. Meanwhile, Figure 1.2 illustrates the increase in RES consumption share across EU countries from 2011 to 2020.

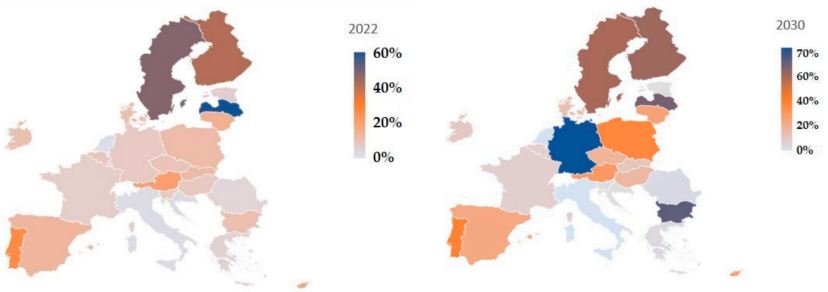

Figure 1.1: The share of RES in final energy consumption in industry in the EU. [14]

There exist several key challenges in the widespread adoption of RES, and one of them is the varying predictability levels among different RES. The primary components of RES include hydropower, wind power, solar power, and solid biofuels. Among these, hydropower is generally regarded as highly predictable due to its temporal and spatial consistency [16]. This consistency allows for better planning

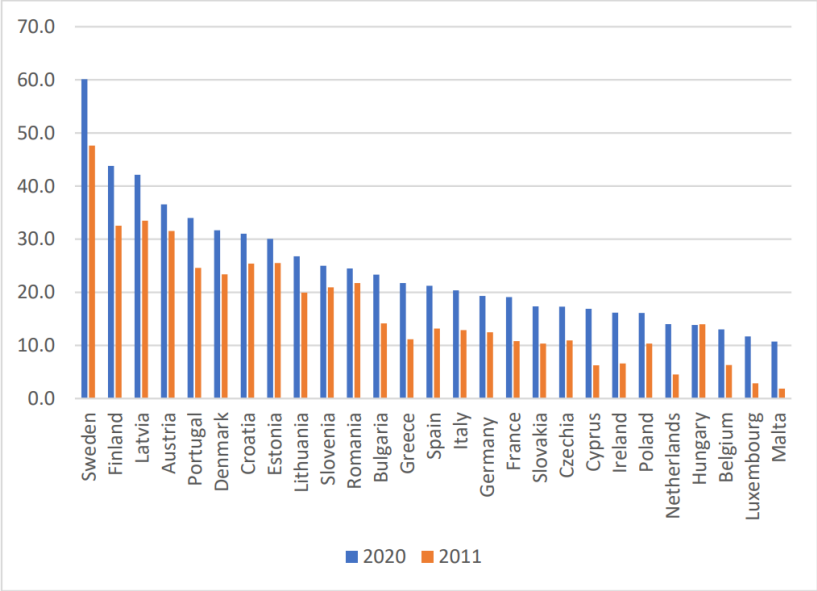

Figure 1.2: Share of energy from renewable sources [15]

and integration into the energy grid, as the flow of water can be forecast with a high degree of accuracy, based on historical data and seasonal patterns. In contrast, wind and solar power are often considered less predictable, as their generation is strongly influenced by variable weather conditions [17]. For example, wind power generation can fluctuate due to shifts in wind speed, which are difficult to forecast accurately over long periods. Similarly, solar power generation is dependent on sunlight, which can be affected by cloud cover, time of day, and seasonal variation.

The unpredictability of wind and solar energy is shown to impact the predictability of the EU's electricity market [18]. As illustrated in Figure 1.3 [19], wind and solar together accounted for over 50% of the EUs renewable energy share in 2022. This increasing proportion of variable renewable energy (VRE) sources has significant implications for the stability and operation of the EU electricity grid. As reliance on wind and solar power grows, there is an increasing need for more sophisticated grid management techniques to ensure that supply consistently aligns with demand, even when these variable sources are unavailable.

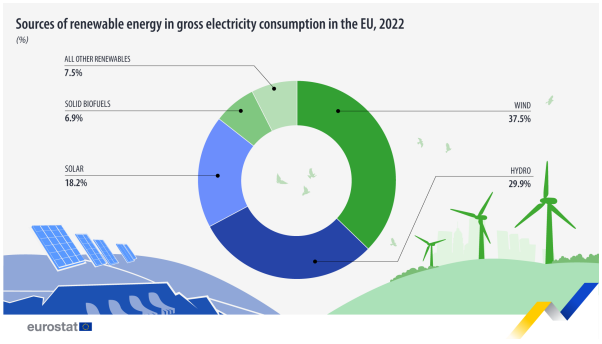

Figure 1.3: Composition of renewable energy in the EU in 2022. [19]

To support the balance between supply and demand proposed above, energy markets have emerged as critical structures within the energy sector. These markets serve multiple purposes: they ensure a stable

and reliable energy supply, reduce waste on the production side, prevent shortages on the consumer side, and offer mechanisms to manage the inherent risks associated with fluctuating supply and demand [20, 21, 22].

Additionally, energy markets play an important role in optimizing the structure of energy generation [23, 24], particularly by promoting the use of renewable sources that typically have lower marginal costs [25]. While long-term markets contribute to stability across the entire energy supply chain, short-term markets are designed to address volatility and manage uncertainties in real time.

1.1.2. Energy Trading in Intraday Market

Among energy markets, intraday power markets play an essential role as part of short-term power management systems, enabling rapid adjustments to meet demand shifts. By allowing transactions throughout the day, IDM provides flexibility and efficiency [26, 27], helping to mitigate short-term risks in energy supply and demand.

Market participants, including electricity producers, consumers, market operators, and system operators, interact within these markets to balance supply and demand. In addition to players such as utilities, traders, aggregators, and demand response providers are becoming increasingly important in managing grid stability [28], especially with the integration of renewable energy.

Currently, Power Exchanges (PXs) [29, 30] such as EPEX actively participate in IDM, which operates based on Continuous Trading (CT) rules [31, 32]. In Germany and Austria, for example, market participants can engage in buying and selling electricity within 15-minute CT auction intervals [33]. Evidence suggests that market dynamics have improved with the adoption of these quarter-hour trading intervals, resulting in a notable increase in transaction volume (TV), enhanced market flexibility, and greater price stability in the electricity market [33, 31, 32].

The integration of European electricity markets has become increasingly important as countries work together to balance supply and demand across borders [34]. Cross-border trading enables electricity to flow more efficiently between countries, enhancing market liquidity and reducing price volatility. As part of the European Union's broader energy strategy, efforts to integrate national markets into a unified European electricity market are helping to create a more resilient and efficient energy system that can better accommodate the growing share of renewable energy, illustrated as Figure 1.4 [35].

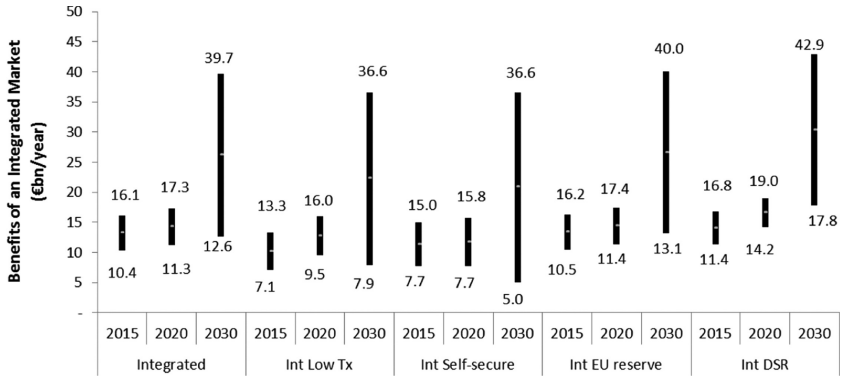

Figure 1.4: Range of annual cost savings in integration scenarios relative to Baseline, 20152030. [35]

1.1.3. Importance of Price Forecast

As the proportion of VRE increases mentioned in Section 1.1.1, forecasting plays a crucial role in addressing the challenges of supply-demand balancing within the electricity market [36]. Accurate predictions of renewable generation and demand patterns allow operators to allocate resources more effectively, mitigate risks of over- or under-generation, and optimize system operations. Price forecasting, relies on variables such as historical orderbook data and weather forecasts to improve accuracy. These predictions help market participants make informed decisions, manage financial risks, and adjust strategies to market fluctuations [29].

In energy transactions, both electricity sellers and buyers aim to minimize risk and maximize revenue. For sellers, primarily power generators, the main risk lies in overcapacity during certain periods, which can drive prices down. RES, with their low marginal costs [37], are prioritized for generation whenever feasible. As a result, when RES output is high and supply exceeds demand, prices tend to drop. Fossil fuel plants operating during these low-price periods risk unnecessary fuel consumption and financial losses [38]. On the other hand, when RES generation is low, electricity prices rise, and fossil fuel plants can capitalize on these high-price periods for greater profits. Therefore, accurate price forecasting is essential for maximizing seller profits by enabling informed trading strategies.

For buyers, the primary risk stems from insufficient supply, potentially leading to power outages. Blackouts can disrupt industrial operations, businesses, and daily life. If bids are set too low, theres a risk of not securing enough power, while setting them too high may reduce profit margins. Thus, precise price forecasting and balanced bidding strategies are crucial to ensuring a stable supply while optimizing financial outcomes for buyers [39].

Price forecasting can also benefit large consumers, such as industrial facilities, by helping them optimize production schedules. When low electricity prices are anticipated, these consumers can increase production during these periods, maximizing their profit margins while reducing operational costs. This strategy not only increases profitability but also alleviates grid stress during peak price periods, when electricity demandand pricesare typically higher. By aligning production with expected price fluctuations, large-scale consumers can contribute to grid stability while optimizing their own financial outcomes.

1.2. Intraday Market

1.2.1. Mechanism and Types of Orders

Generally, CID allows market participants to react swiftly to fluctuations in demand, supply, and electricity prices. Each trading interval presents an opportunity to buy or sell electricity for specific time slots, typically within hours. Market participantsincluding power producers, retailers, and consumerscan place orders throughout the day, adjusting their strategies based on real-time market conditions. For example, if a wind farm generates more electricity than expected, traders can sell the excess on the CID market, while consumers or retailers can take advantage of lower prices when surplus generation is available.

The flexibility of CID provides a strong hedge against the uncertainty introduced by renewable energy sources (RES) and fluctuating load, which are often intermittent and unpredictable [40]. The continuous nature of the market allows for ongoing adjustments to orders, helping balance supply and demand more effectively than markets with fixed trading times. As a result, IDM, particularly CID, has become an

essential tool for dynamic grid balancing, especially in regions with high RES penetration.

The CID market offers various types of orders, such as market order and limit order, to meet the specific needs of market participants, each designed to serve distinct purposes and enable different strategies for managing electricity trading based on price expectations, volume constraints, and risk tolerance [41].

Market Orders are orders which are executed at the best available price in the market at the time of placement. These orders are typically used when immediate execution is prioritized over price control. For example, a power producer seeking to sell excess electricity may place a market order to ensure the trade is executed quickly, regardless of the price.

Limit Orders, by contrast, specify a price limit at which the participant is willing to buy or sell electricity. These orders are only executed if the market price meets or exceeds the specified price. If the price is not favorable, the order remains open until it can be matched. Limit orders are commonly used to ensure price control and minimize the risk of trading at undesirable prices. Moreover, limit orders can be partially executed if there is insufficient volume to fulfill the entire order at the specified price.

In summary, the CID market provides significant flexibility through a variety of order types, enabling participants to optimize their trading strategies. Power producers may use limit orders to sell electricity when prices are high, while retailers or consumers can place market orders to secure electricity at lower prices during surplus periods. This flexibility helps market participants plan ahead and mitigate exposure to price volatility.

1.2.2. Clearing Models and Processes

Order clearing in the CID market is facilitated by two primary models: the Immediate Order Clearing (IOC) model and the Partial Order Clearing (POC) model [42]. These models determine how orders are executed and handled when they are submitted to the market, particularly in relation to how they match with available orders and the conditions under which unfulfilled parts of the order are managed.

The IOC model is designed to ensure that an order is executed immediately for the available quantity. If there is insufficient liquidity in the market to fulfill the entire order at the time of placement, the unfilled portion of the order is canceled. This model is typically used by market participants who prioritize speed and certainty in execution, as they are willing to accept immediate execution at the available price without waiting for the full order to be matched. For example, a power producer might use an IOC order to sell excess electricity when market conditions are favorable and there is a need for quick execution.

In contrast, the POC model allows for partial execution of an order. If the full quantity cannot be fulfilled immediately, a portion of the order is matched with available counterpart orders, and the remaining volume stays active in the market, pending future matching. This flexibility is particularly useful for market participants who are willing to accept partial fulfillment of their order but still want the remaining volume to be executed at a later time. The POC model is often employed in situations where there is a degree of flexibility in execution, and market participants are not seeking immediate fulfillment of the entire order. For instance, a retailer might place a POC order to buy electricity at a specific price, knowing that some portion of the order can be filled immediately, with the remaining part being executed as more favorable offers become available.

Both IOC and POC models enhance the efficiency of order clearing in the CID market by offering market

participants flexibility in how their orders are executed and by ensuring that orders are processed in line with their immediate needs and trading strategies. These models contribute to a more dynamic market by allowing orders to be processed under different conditions, ensuring that liquidity is maintained and that supply and demand can be matched effectively within the real-time trading environment.

In the CID market, submitted limit orders are processed differently depending on whether they are bid or ask orders. For an ask order, its price is compared to the best bid price available in the shared order book. If the price of the ask order is less than or equal to the best bid price, the ask order is cleared with the best bid order. The cleared volume is determined by the smaller of the two volumes (order volume and best bid volume). Any remaining volume from the ask order is added to the shared order book.

As shown in Figure 1.5a [42], the transaction mechanism operates such that a transaction occurs when a bid (buy) order matches an ask (sell) order. This happens when the price of the bid order is greater than or equal to the best available ask price. Conversely, as illustrated in Figure 1.5b [42], if the best bid price is lower than the best ask price, the CID transaction cannot occur.

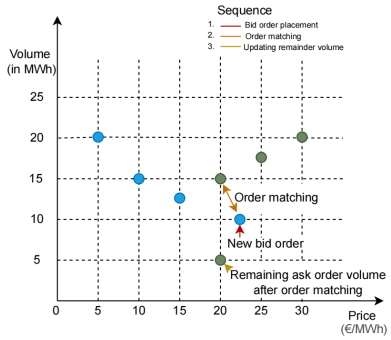

(a) Illustration of price-volume curves in continuous intraday market with the best bid and ask prices matching. [42]

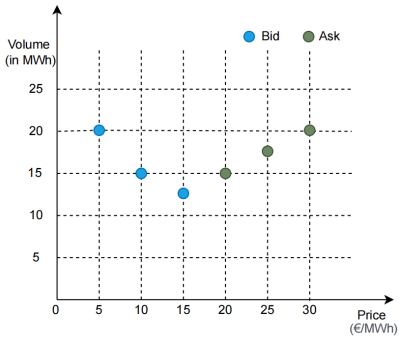

(b) Illustration of price-volume curves in continuous intraday market when orders do not match. [42]

Figure 1.5: Illustration of price-volume curves with prices matching (Figure 2.1-A) and with prices not matching (Figure 2.1-B).

Figure 1.6 [42] illustrates an example of CID market clearing with a dynamic timeline. Initially, a bid of 4 MWh is posted at 20/MWh. It remains in the market as no ask (offer) order is available to match with this bid. Subsequently, an offer of 14 MWh is posted at 30/MWh. Since this offer is at a higher price than the bid at 20/MWh, no match occurs. Later, a bid of 14 MWh is posted at 35/MWh and is fully matched with the offer at 30/MWh. Then, an offer of 6 MWh is posted at 18/MWh, which is partially matched with the bid at 20/MWh. The remaining 2 MWh of the offer stays in the market until a bid of 2 MWh is posted at 22/MWh, which is fully matched.

Similarly, a bid order is cleared with the best ask order if its price exceeds the best ask price. The remaining volume, if any, is also added to the shared order book following this process.

It is worth mentioning that in the European Power Exchange Spot (EPEX SPOT) transactions, once a transaction is completed, it is generally settled at the seller's price, even if the buyer's bid may be higher than this price. When the top bid and ask in the order book are tradable in terms of price, the bid with the highest price and the ask with the lowest price are matched first.

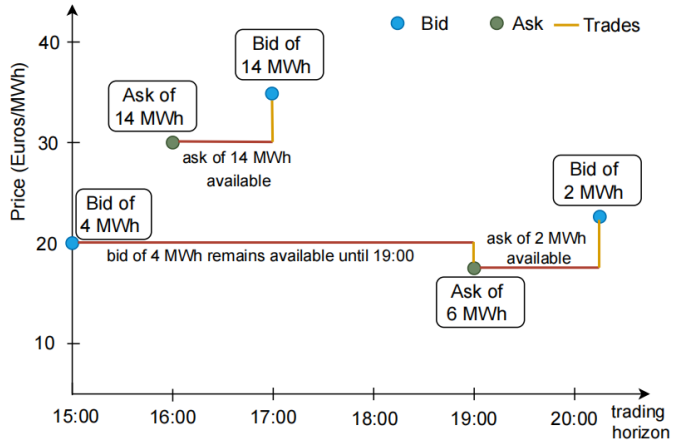

Figure 1.6: Example of CID market clearing. [42]

1.3. Orderbook

1.3.1. Orderbook Data

In the intraday electricity market, orderbook data refers to the collection of all orders placed by market participants, including details such as price, volume, side, transaction time, delivery time, order type, etc. This data reflects participants' willingness to buy or sell at specific prices and plays a crucial role in matching transactions [43]. Orderbook data provides valuable insights into market liquidity and demand, enabling traders to make informed decisions regarding the optimal timing and pricing for their trades.

1.3.2. Delivery Time and Transaction Time

The delivery start time refers to the moment when electricity begins to be delivered, while the delivery end time refers to the moment when electricity delivery is finished.

For simplicity, we refer delivery start time as delivery time in this report. It represents the actual time at which the electricity is delivered, typically occurring within hours or minutes after the transaction takes place in intraday trading.

Transaction time, on the other hand, is when a buy or sell order is placed and accepted in the market, marking the agreement between buyer and seller on the price and quantity of electricity. Unlike delivery time, transaction time indicates when the market participants agree on the terms of the trade, rather than when the electricity is actually consumed.

Together, delivery time and transaction time create a time-series structure [44] in the CID orderbook, reflecting the temporal relationship between when the trade occurs and when the electricity is delivered.

EPEX SPOT offers 24 hourly (60-minute) and 96 quarter-hourly (15-minute) products in the Austrian CID market. Each product corresponds to electricity delivery during specific time intervals throughout the day, with the delivery time referring to the start of the electricity delivery for simplicity.

1.4. Objective

This report aims to develop a comprehensive data-driven framework for probabilistic intraday electricity price prediction using features derived from orderbook data. Additionally, it seeks to gain insights into the relationships between features and labels within the orderbook, as well as across different orderbooks.

Intraday electricity markets are known for their high volatility and rapid price fluctuations, posing significant challenges for accurate forecasting and decision-making. Existing studies typically rely on a limited set of handcrafted features, such as volume-weighted average price (VWAP) or the last transaction price. However, the rich microstructural data from the orderbook remains largely underutilized. While traditional statistical learning models like linear quantile regression (LQR) and Least Absolute Shrinkage and Selection Operator (LASSO) have been widely applied, advanced machine learning techniques that can capture nonlinear relationships and complex uncertainties are still underexplored in this field. Furthermore, most current methods are developed and validated within a single market or product type, with limited research on their generalization across different markets and product types.

Based on this, the report is structured around the following three central research questions:

- ***What are the predictive features derived from the orderbook that can improve price prediction?***
- ***How can deep learning architectures improve performance in quantile forecasting of price labels compared to traditional statistical learning models***
- ***Through the generalization studies across different markets and products, what structural similarities on price prediction can be learned?***

1.5. Report Structure

As shown in Figure 1.7, this report is divided into Five chapters. Chapter 1 provides background knowledge, including an overview of renewable energy and the energy market. It discusses the impact of the energy market on electricity generation and highlights the importance of forecasting. In addition, it introduces the fundamental characteristics of the intraday electricity market (IDM) and defines key terminologies relevant to the energy market.

Chapter 2 presents a literature review focusing on relevant previous studies. Dozens of works on electricity price prediction are examined, covering both statistical machine learning models and deep learning approaches. Various quantile regression frameworks adopted in prior research are also discussed. Additionally, emerging trends in generalization and transfer learning within the field are briefly outlined.

Chapter 3 introduces all methodologies utilized in this report. It describes the extraction of datasets from raw orderbooks and provides definitions for all labels, cases, and feature candidates. The quantile regression framework is also presented, including the loss function, evaluation metrics, and significance testing for performance differences. In addition, the preparatory components for all experiments are outlined, such as feature selection approaches, model benchmarks, and transfer learning settings.

Chapter 4 presents the main experimental results, including feature selection, model comparison, and generalization studies across different countries and product types. Several insights are proposed based on the analysis of these results.

Finally, Chapter 5 provides a concise conclusion on the research question and each subquestion, drawing on the experimental results and analysis. It summarizes the key findings, discusses their implications,

and reflects on how the outcomes contribute to the understanding of the problem. Additionally, potential directions for future research are suggested based on the insights gained from this study.

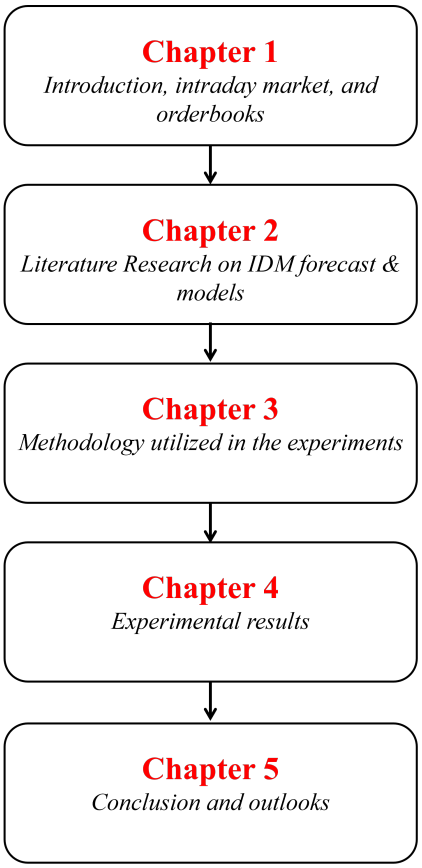

Figure 1.7: Report structure

2

Literature Research

2.1. Machine Learning for Intraday Price Prediction

In the context of IDM, statistical models have proven to be effective tools for predicting short-term electricity price fluctuations [2]. Unlike neural network-based approaches, which rely on complex and deep learning architectures, statistical models typically include traditional machine learning algorithms such as regression analysis, decision trees, support vector machines (SVM), and ensemble methods like random forests (RF) and gradient boosting. These models focus on capturing linear and non-linear relationships in historical data, leveraging statistical patterns and market behaviors. By incorporating factors like demand, supply, weather conditions, and historical price trends, statistical models can provide valuable insights for market participants seeking to anticipate IDM price movements with a balance of interpretability and accuracy.

Pape, Christian, and Hagemann et al. [27] developed a regression model for predicting German intraday market (IDM) electricity prices, incorporating the supply stack model of electricity supply and demand. In addition to fundamental supply stack effects, their model was enriched with factors such as start-up costs, market state variables, and trading behavior, capturing price impacts beyond pure supply and demand dynamics. Their findings indicate that including these additional factors significantly enhances the accuracy of IDM price predictions. Furthermore, their study highlights the value of incorporating day-ahead prices as a feature for intraday price forecasting, demonstrating that this approach tends to improve predictive performance. Additionally, their results support the rationale for using past prices as predictors for IDM prices, reinforcing the notion that historical price patterns contain valuable information for short-term electricity market forecasting.

Lasso regression has opened new avenues for the application of statistical machine learning models in IDM price prediction. Research conducted by Ziel [45] indicates that lasso-based methods consistently outperform traditional autoregressive (AR) models in forecasting intraday electricity prices. These lasso-implied structures have demonstrated strong predictive accuracy in short-term electricity price forecasting across multiple studies [5], further reinforcing their reliability in energy market modeling.

Building on this foundation, Narajewski and Ziel [2] found that both lasso and elastic net techniques offer

substantial improvements in forecast accuracy compared to conventional electricity price forecasting (EPF) models. Their findings highlight the potential of these advanced regularization methods to enhance precision in electricity market predictions, supporting their growing importance in energy economics and strategic market planning. Moreover, these studies suggest the possibility of inherent correlations between different time periods within the intraday market. Understanding these temporal relationships could provide deeper insights into market dynamics and contribute to the development of more effective predictive models.

Christoph Scholz et al. [46] conducted a comprehensive study to predict future IDM prices across different time intervals using EPEX SPOT data, employing both tree-based ensemble methods (eXtreme Gradient Boosting, XGBoost, and Random Forest, RF) and deep learning techniques, specifically Long Short-Term Memory (LSTM) networks. Their findings demonstrated that XGBoost and RF significantly outperformed baseline models based on VWAP and Last Price, highlighting the effectiveness of these machine learning approaches in IDM price forecasting. Notably, the study revealed the exceptional accuracy of XGBoost, with its predictive performance in certain time intervals even surpassing that of deep learning models. This unexpected result underscored the potential of tree-based ensemble methods in financial time series forecasting, especially in scenarios where deep learning models may not always yield superior results. However, the study also showed that the LSTM model, developed as part of their analysis, slightly outperformed XGBoost in terms of predictive accuracy, particularly for longer prediction intervals. This suggests that LSTM networks are particularly adept at capturing complex temporal dependencies and long-term trends in electricity price data, offering an advantage in forecasting scenarios where such patterns are critical.

Englund and Axel [47] utilized AR models, XGBoost, and Deep Neural Networks (DNN) to forecast IDM prices in Sweden's SE3 region, leveraging data from Nord Pool. Their findings highlighted the superior performance of the Elastic Net regularized ARX model in predicting sell-side prices, demonstrating its robustness in capturing market dynamics. Additionally, they explored the challenges associated with forecasting both buyer and seller prices, concluding that predicting buyer prices is inherently more difficult due to greater market uncertainty. Furthermore, their study revealed the limitations of the employed statistical models in detecting anomalies.

Kath and Christopher [48] built up regression models as prediction models to insight the influence from Cross-Border Intraday Project (XBID) to German IDM electricity prices. The results illustrate the low correlation between them, which means the XBID is not suggested to set as a feature of forecasting.

Deep learning (DL) refers to neural networks with multiple hidden layers [49], and has gained prominence as a powerful tool for forecasting in various domains [50]. In the context of intraday electricity price forecasting, deep learning modelsparticularly architectures such as Multilayer Perceptron (MLP), Convolutional Neural Networks (CNN), and Recurrent Neural Networks (RNNs) with Long Short-Term Memory (LSTM) unitshave proven to be highly effective in capturing complex, nonlinear relationships within the data [51]. These models are particularly adept at learning intricate, hierarchical patterns from historical price data, as well as from external variables like weather conditions, demand fluctuations, and market sentiment. This ability to capture dynamic and time-dependent patterns distinguishes deep learning models from statistical machine learning models, which often struggle with such complexities.

Monteiro et al. [52] developed a new set of intraday session models for price forecasting, referred to as the Intraday Session Model for Price Forecasting (ISMPF), based on MLP architectures. These models

are specifically designed to predict the hourly prices across the six intraday periods of the IDM in the Iberian electricity market (MIBEL). The inputs to the model aggregate a variety of relevant time-series data, including the hourly prices from the past few days, as well as key variables such as hourly electricity demand, power generation from various types of electricity production in the region, and day-ahead demand forecasts. Additionally, the model incorporates wind power generation forecasts and weather dataspecifically, hourly wind speed, temperature, and solar radiationas well as the hourly prices from both the MIBEL daily period and the previous intraday period. By utilizing such a comprehensive set of features, the ISMPF models aim to capture the complex relationships and dependencies that influence intraday electricity prices, making them highly suited for accurate forecasting in the dynamic MIBEL market.

Oksuz, Ilkay and Ugurlu et al. [53] employed a range of forecasting models, including linear regression, lasso-based ARX, ANN, and RNN, with specific attention to LSTM and GRU, to predict IDM electricity prices in Türkiye. Through a comparative analysis of these different models, the results revealed that neural network-based methods outperformed both linear regression and lasso ARX models in terms of forecast accuracy. Notably, the Diebold-Mariano test indicated that the RNN architecture was statistically significantly superior to the ANN model. This is particularly important, as time-dependent tasks are best handled by models capable of remembering previous time points, a strength inherent in RNNs due to their memory component. Additionally, the study found that GRU models demonstrated superior performance compared to LSTM, highlighting the advantages of GRU in capturing complex temporal dependencies more efficiently. Another key finding was that the forecasting performance for the day-ahead price and intraday price spread was more accurate than the forecast for the actual IDM prices. This suggests that models can more reliably predict price trends or spreads over short-term horizons compared to specific price points, further enhancing the understanding of price behavior in the electricity market.

Vijn [54] employed MLP models for both point and interval forecasts of IDM electricity prices in the Netherlands and Germany. The results demonstrate that the MLP model is highly effective at capturing nonlinear relationships in the data, yielding improved point forecasts in out-of-sample testing. However, when similar architectures were trained on multiple quantiles, they did not outperform the quantile regression mean of the considered point forecasts, suggesting that MLP may not fully leverage the benefits of quantile-specific information for interval predictions. Additionally, the study highlights that the relative and absolute accuracy of all forecasts is highly sensitive to factors such as the delivery time and the prevailing price regime.

Kolberg and Waage [55] developed a deep learning model based on LSTM networks for forecasting prices in the IDM Elbas market of the Nordic electricity trading platform, Nord Pool. The results indicate that this newly developed LSTM model significantly outperforms simple domain-based heuristics and most of the models in two established benchmarks: econometric models and other machine learning-based forecasting methods. Notably, despite the increased complexity of the LSTM model, the study shows that incorporating additional relevant datasuch as weather forecasts from SMHI via Montel, alongside Nord Pool market datasubstantially enhances the models predictive performance. This suggests that the inclusion of weather-related factors, which play a crucial role in influencing electricity prices, further refines the models ability to anticipate market movements with greater accuracy, highlighting the importance of integrating external data sources into deep learning-based forecasting models.

Eide and Viken [56] focused on price prediction using intraday data from the NO2 region in southern

Norway, which is characterized by strong intraday liquidity. They evaluated several deep learning architectures, including LSTM, GRU, Deep Autoregressive Model (DeepAR), and Time Fusion Transformer (TFT), through a comprehensive comparative analysis. The results demonstrated that LSTM and GRU models outperformed the other methods in terms of prediction accuracy for IDM prices. Furthermore, the study highlighted that incorporating a probabilistic classifier significantly enhanced the classification performance compared to directly using predicted symbol differences. This approach suggests that probabilistic models can better capture uncertainty in predictions, providing more reliable forecasts for market participants.

Klç et al. [57] examined the IDM spot market in the DK1 grid area of Denmark, utilizing a variety of forecasting models, including XGBoost, RF, LightGBM, Support Vector Regression with Radial Basis Function (SVR-RBF), K-Nearest Neighbors (KNN), Seasonal Autoregressive Integrated Moving Average (SARIMA), CNN, and LSTM networks for IDM price prediction. The researchers first established that accurate electricity price forecasting (EPF) could significantly increase profits, even with relatively simple trading strategies. The comparative experimental results revealed that both LSTM and CNN models exhibited strong performance in predicting IDM prices. Building on these findings, the study proposed and successfully deployed a multi-step prediction framework, combining LSTM and CNN models, to enhance forecasting accuracy over multiple time steps. This approach emphasizes the power of combining deep learning techniques to improve predictive performance in the highly volatile intraday electricity market.

Collectively, these studies underscore the growing role of statistical and machine learning models in IDM price forecasting, offering both methodological advancements and practical insights. While no single approach consistently outperforms others across all market conditions, the integration of regularization techniques, ensemble methods, and external market factors has proven beneficial in enhancing predictive accuracy. Furthermore, the trade-off between model complexity and interpretability remains a key consideration, as simpler models like AR with exogenous variables can, in certain contexts, rival more sophisticated machine learning techniques. These findings emphasize the need for continuous exploration of feature selection, market-specific dynamics, and hybrid modeling approaches to further refine IDM forecasting methodologies.

Given the high volatility and uncertainty in intraday electricity markets, these factors are critical concerns for both electricity sellers and buyers. One of the main motivations for using forecasts based on quantile regressors is their ability to quantify uncertainty [58]. This approach helps market participants estimate the likelihood of extreme price events and develop more robust strategies for trading, bidding, and hedging, thereby improving their risk management capabilities [59]. Moreover, the availability of multiple quantile forecasts provides richer information in designing trading strategies [60].

The reliability of quantile forecast models is commonly evaluated using metrics such as the quantile cross rate (QCR) [61], which focuses on identifying anomalies in the predicted quantiles and evaluating the consistency of the model's outputs.

K. Maciejowska et al. [60] employed a quantile regression-based method proposed Factor Quantile Regression Averaging (FQRA) to generate interval forecasts of electricity spot prices in the British power market. Their results showed that FQRA produced more accurate prediction intervals compared to both the benchmark ARX model and the original QRA method.

Bartosz Uniejewski and R. Weron [62] proposed LASSO QRA (LQRA), which incorporates regular-

ization into the Quantile Regression Averaging (QRA) framework. The method was validated using datasets from the Polish and Nordic power markets. Results showed that LQRA outperformed several benchmark models in terms of the Kupiec test, pinball score, conditional predictive accuracy, and financial gains from trading strategies.

Yuki Osone and Daisuke Kodaira [63] applied a QR approach with general predictors to forecast short-term electricity spot prices in the UK market. It also demonstrated strong predictive accuracy and robustness, with limited degradation in performance when previous-day prices were excluded due to bidding constraints.

2.2. Cross-Domain Generalization

In this report, cross-domain generalization refers to the generalizability across countries and forecasting targets. The motivation for this line of research is largely driven by the perspective of policy-makers, as improved generalization can support more informed regulation and policy design [64], while enhancing situational awareness of electricity markets [65].

Currently, generalization studies based on transfer learning have not yet been explored.

2.3. Chapter Conclusion

While substantial progress has been made in the prediction of short-term energy prices, there remains considerable potential in exploring feature candidates derived directly from raw orderbook data. The microstructural information embedded in orderbooks remains largely untapped, and further extraction and utilization of these features could offer valuable insights into price forecasting.

Research on quantile forecasting, which incorporates uncertainty into predictions, has been proposed in various applications. However, the integration of quantile forecasting with different deep learning architectures for intraday electricity price prediction has not been widely explored. While some efforts have been made, there is still a significant gap in fully leveraging these approaches to address nonlinear dependencies and capture complex uncertainty structures, which traditional statistical models often fail to handle.

Moreover, while some studies have explored the generalization of models across different datasets, there has yet to be a systematic investigation of the generalization capabilities of models trained on different orderbooks.

3

Methodology

3.1. Data Sources and Preprocessing

3.1.1. Datasets Acquisition and Extraction

We follow the methodology from [66] and use orderbook data purchased from the European Power Exchange Spot (EPEX Spot). This data provides detailed insights into market dynamics, including key attributes such as delivery start time, product type, price, volume, side, OrderID, transaction time, and action code. Orders can be placed up to five minutes before each delivery start time, with transaction details recorded upon matching. Different types of products, such as hourly (60-min) and quarter-hourly (15-min), are provided. We filter out unmatched orders, as they do not contribute to market-clearing outcomes. The pseudocode of the filtering algorithm is described in Table 3.1.

3.1.2. Labels Description

In this report, we focus on three prediction targets: ID_1, ID_2, and ID_3. We follow the definition of ID_x from [66], which can be expressed as follows:

$$\mathrm{ID}_x \;=\; \frac{\sum\limits_{s\in\{+,-\}}\;\sum\limits_{t\in[t_d-\Delta,\,t_d-\delta_c]} P_t^{(s)}\,V_t^{(s)}}{\sum\limits_{s\in\{+,-\}}\;\sum\limits_{t\in[t_d-\Delta,\,t_d-\delta_c]} V_t^{(s)}}, \tag{3.1}$$

where t_d denotes the delivery time, and t is the transaction time. The market side $s \in \{+,-\}$ corresponds to buy $(+)$ and sell $(-)$ orders. Here, $P_t^{(s)} = \{p_1, p_2, ..., p_{n_t^{(s)}}\}$ and $V_t^{(s)} = \{v_1, v_2, ..., v_{n_t^{(s)}}\}$ denote the price and volume of a trade on side s at time t. The trading window is defined by $\Delta = 60 \times x\,\mathrm{min}$, where $x = 1, 2, 3$ for $\mathrm{ID}_1, \mathrm{ID}_2, \mathrm{ID}_3$, respectively. The parameter δ_c specifies the limited trading period before delivery (30 minutes for Germany, 5 minutes for Austria) for control zones.

In addition to the three indices mentioned above, this report considers two countries, Germany (DE) and Austria (AT), as well as two types of products with different resolutions: hourly (h) and quarter-hourly (qh).

Table 3.1: Algorith of Filtering the Raw Orderbooks [66]

Algorithm 1: Orderbook Filtering

Input: Raw orderbook files
Initialize data structures for storing processed orders
for all orderbook files **do**
  Load orderbook
  Classify orders by product type (hourly/quarter-hourly)
  if hourly products exist **then**
    Group records by OrderID and transaction time
    Filter entries with action codes "P" or "M"
    Compute traded volume between consecutive updates
    Aggregate processed hourly trades
  end if
  if quarter-hourly products exist **then**
    Apply the same processing steps as hourly products
    Aggregate processed quarter-hourly trades
  end if
end for
Return Aggregated and filtered orderbook

3.1.3. Features Description

We evaluate five encoding benchmarks. Let $\mathcal{T}_W = [t_d - \Delta - W,\ t_d - \Delta]$ denote a historical look-back window of size W, and $\mathcal{T}_\infty = (-\infty,\ t_d - \Delta]$ the full transaction history available prior to prediction. All trades are indexed by transaction time t and market side $s \in \{+, -\}$. The time windows considered in this report are shown as Formula 3.2.

$$W \in \{1, 5, 15, 60, 180, \infty\} \tag{3.2}$$

From the raw datasets, we extracted 32 features separately from the buying and selling sides, each potentially relevant to the prediction of the target labels. Many of these features are based on percentile statistics, with the specific quantiles considered in this report defined in Formula 3.3.

$$T = \{10\%, 25\%, 45\%, 50\%, 55\%, 75\%, 90\%\} \tag{3.3}$$

As a result, each target label is associated with a total of **384** potential features. A detailed description of the features is provided in Table 3.2.

3.2. Features Selection and Models Comparison

3.2.1. Principal Component Analysis (PCA) Compression

PCA compression is a non-parametric method that achieves dimensionality reduction and data compression through linear transformation [67]. It effectively reduces data redundancy and storage requirements

Table 3.2: Extracted Features and Equations

Feature	Equation
First Price	$P_{first} = p_1$
Last Price	$P_{last} = p_{n^{(s)}_{t\in\mathcal{T}_W}}$
Mean Price	$P_{mean} = \frac{\sum_{t\in\mathcal{T}_W} P_t^{(s)}}{n^{(s)}_{t\in\mathcal{T}_W}}$
Minimum Price	$P_{min} = \min(P^{(s)}_{t\in\mathcal{T}_W})$
Maximum Price	$P_{max} = \max(P^{(s)}_{t\in\mathcal{T}_W})$
Price Volatility	$P_{vol} = \sqrt{\frac{1}{n^{(s)}_{t\in\mathcal{T}_W}} \sum_{i=1}^{n^{(s)}_{t\in\mathcal{T}_W}} (p_i - P_{mean})^2}$
Delta Price	$\delta P = P_{last} - P_{first}$
First Volume	$V_{first} = v_1$
Last Volume	$V_{last} = v_{n^{(s)}_{t\in\mathcal{T}_W}}$
Mean Volume	$V_{mean} = \frac{\sum_{t\in\mathcal{T}_W} V_t^{(s)}}{n^{(s)}_{t\in\mathcal{T}_W}}$
Minimum Volume	$V_{min} = \min(V^{(s)}_{t\in\mathcal{T}_W})$
Maximum Volume	$V_{max} = \max(V^{(s)}_{t\in\mathcal{T}_W})$
Volume Volatility	$V_{vol} = \sqrt{\frac{1}{n^{(s)}_{t\in\mathcal{T}_W}} \sum_{i=1}^{n^{(s)}_{t\in\mathcal{T}_W}} (v_i - V_{mean})^2}$
Delta Volume	$\delta V = V_{last} - V_{first}$
VWAP	$VWAP = \frac{\sum_{t\in\mathcal{T}_W} P_t^{(s)} V_t^{(s)}}{\sum_{t\in\mathcal{T}_W} V_t^{(s)}}$
Momentum	$M = \frac{P_{last} - VWAP_W}{VWAP_W}$
Sum Volume	$sum\_V = \sum_{t\in\mathcal{T}_W} V_t^{(s)}$
Trade Count	$N_{trade} = n^{(s)}_{t\in\mathcal{T}_W}$
Price Percentile	$Percentile(P^{(s)}_{t\in\mathcal{T}_W}, \tau) \vert \tau \in T$
Volume Percentile	$Percentile(V^{(s)}_{t\in\mathcal{T}_W}, \tau) \vert \tau \in T$

while preserving the essential information.

Given a data matrix $\mathbf{X} \in \mathbb{R}^{n\times d}$, where n is the number of samples and d is the original dimensionality, the first step is to center the data by subtracting the mean:

$$\bar{\mathbf{x}} = \frac{1}{n}\sum_{i=1}^{n} \mathbf{x}_i, \tag{3.4}$$

$$\mathbf{X}_{centered} = \mathbf{X} - \mathbf{1}_n \bar{\mathbf{x}}^\top, \tag{3.5}$$

where $\mathbf{1}_n$ is an n-dimensional vector of ones. The covariance matrix $\mathbf{\Sigma}$ is then computed as

$$\mathbf{\Sigma} = \frac{1}{n-1}\mathbf{X}^\top_{centered}\mathbf{X}_{centered}. \tag{3.6}$$

Performing eigen-decomposition on $\mathbf{\Sigma}$ yields eigenvalues and eigenvectors:

$$\mathbf{\Sigma} = \mathbf{U}\mathbf{\Lambda}\mathbf{U}^\top, \tag{3.7}$$

where $\mathbf{\Lambda} = \text{diag}(\lambda_1, \lambda_2, \ldots, \lambda_d)$ with $\lambda_1 \geq \lambda_2 \geq \cdots \geq \lambda_d \geq 0$ representing the variances explained by each principal component. The proportion of variance explained by the i-th component is

$$r_i = \frac{\lambda_i}{\sum_{j=1}^{d} \lambda_j}. \tag{3.8}$$

To retain a specified amount of variance η, the smallest number of principal components k is selected such that the cumulative variance satisfies

$$\sum_{i=1}^{k} r_i \geq \eta, \eta \in (0, 1]. \tag{3.9}$$

The data is then projected onto the subspace spanned by the selected eigenvectors $\mathbf{W} = [\mathbf{u}_1, \mathbf{u}_2, \ldots, \mathbf{u}_k]$:

$$\mathbf{Z} = \mathbf{X}_{centered}\mathbf{W}, \tag{3.10}$$

where $\mathbf{Z} \in \mathbb{R}^{n \times k}$ is a compressed representation. Using the PCA method, the original feature matrix $\mathbf{X} \in \mathbb{R}^{n \times d}$ is transformed into the reduced matrix $\mathbf{Z} \in \mathbb{R}^{n \times k}$.

3.2.2. L1-Penalty Selection

To perform feature selection via linear quantile regressor, we incorporate an L_1-norm regularization term into the original loss function to encourage sparsity [68]. Specifically, for quantile regression with quantile loss L_τ, the overall objective function combines the quantile loss and the L_1 penalty weighted by a regularization parameter $\alpha \geq 0$.

Formally, the optimization problem can be written as minimizing the following loss function:

$$\min_{\boldsymbol{\beta}} \sum_{i=1}^{n} L_\tau(y_i, \mathbf{x}_i^\top \boldsymbol{\beta}) + \alpha \|\boldsymbol{\beta}\|_1, \tag{3.11}$$

where $\mathbf{x}_i \in \mathbb{R}^d$ is the feature vector for the i-th observation, $\boldsymbol{\beta} \in \mathbb{R}^d$ is the coefficient vector, and $\|\boldsymbol{\beta}\|_1 = \sum_{j=1}^{d} |\beta_j|$ is the L_1-norm of $\boldsymbol{\beta}$.

The tuning parameter α controls the strength of regularization: larger values of α result in more coefficients being shrunk toward zero, thus selecting fewer features. The selection results for each case were tested using an QMLP model with Optuna.

$$q \in \{0.800, 0.900, 0.950, 0.980, 0.990, 0.995\},$$
$$n \in \{2, 4, 8, 16, 32, 64\} \tag{3.12}$$

3.2.3. Intersectional Percentile- and Correlation-based Feature Selection Algorithm (IPC)

Intersectional Percentile- and Correlation-based Feature Selection Algorithm (IPC) is a method for selecting features with the highest relevance, emphasizing extreme values by increasing their weights. As illustrated in Figure 3.1, the full dataset is divided into the IN-section and OUT-section based on the percentages of the prediction label. Using the time index, all feature candidates are assigned to one of the two sections (the blue and red sections correspond to the OUT-section and IN-section, respectively). The correlation coefficients for the IN-section, where $y \in [Q_l, Q_h]$, and for the OUT-section, where $y \in (-\infty, Q_l) \cup (Q_h, +\infty)$, are computed independently. These coefficients are then averaged to yield the correlation score between the current feature and the target. The values Q_l and Q_h represent the lower and upper limits of the IN-section, respectively, and can be computed using Formula 3.13.

$$Q_h = 0.5 + 0.5q, Q_l = 0.5 - 0.5q \tag{3.13}$$

where $q \in (0, 1)$ means the quantile constraint, which is a hyperparameter of IPC.

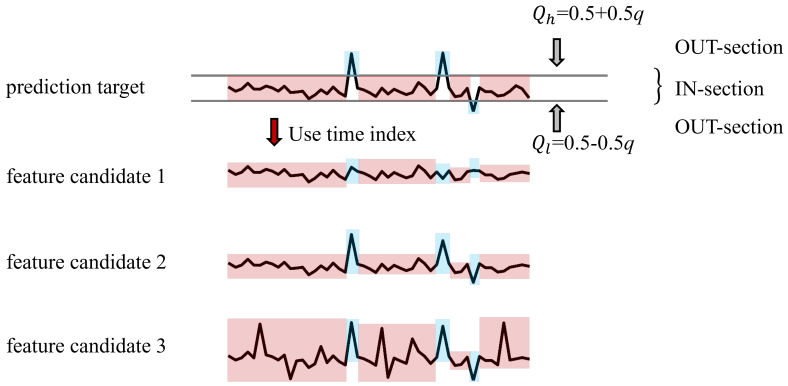

Figure 3.1: The features selection using Focal Correlation Filter (IPC). [35]

Specifically, Pearson and Spearman's Correlation Coefficients are used to calculate the correlation for each section. Formulas 3.14 and 3.15 represent the calculations for Pearson and Spearman's Correlation Coefficients, respectively.

$$r_p = \frac{\sum(X_i - \bar{X})(Y_i - \bar{Y})}{\sqrt{\sum(X_i - \bar{X})^2 \sum(Y_i - \bar{Y})^2}} \tag{3.14}$$

$$r_s = \frac{\text{cov}\,[R[X], R[Y]]}{\sigma_{R[X]}\sigma_{R[Y]}} \tag{3.15}$$

Where X_i and Y_i refer to data points in the dataset, $\bar{X}$ and $\bar{Y}$ represent the mean values of X and Y, respectively, and r is the Pearson correlation coefficient. $\text{cov}\,[R[X], R[Y]]$ is the covariance of the rank variables, and $\sigma_{R[X]}$ and $\sigma_{R[Y]}$ are the standard deviations of the rank variables.

More details of the algorithm of IPC are illustrated in 3.3.

Table 3.3: Algorithm for IPC

Algorithm 2: Feature Filtering and Selection

Input:
N: a set of number of top features e.g. [100, 500, 1000, ...]
Q: a set of quantile constraints e.g. [0.5, 0.8, ...]
$X_h, Y_c \leftarrow$ Load feature and label data
$L^*_{val} \leftarrow$ Initialize validation loss as infinite value ∞
for q in Q **do**
  $Q_l, Q_h \leftarrow$ Calculate quantile bounds using formula $0.5 \pm q/2$
  $P_l, P_h \leftarrow$ Calculate price bounds of Y_c using Q_l and Q_h
  $X_{in} \leftarrow$ Filter X_h where Y_c is inside (P_l, P_h)
  $X_{out} \leftarrow$ Filter X_h where Y_c is outside (P_l, P_h)
  $C_{in} \leftarrow$ Calculate correlation of X_{in} with label Y_c
  $C_{out} \leftarrow$ Calculate correlation of X_{out} with label Y_c
  for n in N **do**
    $F_{in} \leftarrow$ Extract n top features from C_{in}
    $F_{out} \leftarrow$ Extract n top features from C_{out}
    $F_{int} \leftarrow$ Take intersection of top features $F_{in} \cap F_{out}$
    for α in A **do**
      $L_{val} \leftarrow$ Calculate validation loss with feature set F_{int}
      $F \leftarrow$ Get filtered feature set where coefficients are not zero
      if $L_{val} < L^*_{val}$ **then**
        $L^*_{val} \leftarrow$ Update validation loss with L_{val}
        $F^* \leftarrow$ Update optimal feature set with F
      end if
    end for
  end for
end for
Return F^*

3.3. Machine Learning Models

3.3.1. Liniear Quantile Regression (LQR)

Quantile regression estimates the conditional quantiles of the response variable, rather than focusing solely on the conditional mean [69]. This approach allows for modeling the entire distribution of possible outcomes, rather than a single expected value. Forecasts derived from quantile regression are referred to as quantile forecasts. Compared to pointwise forecasts, quantile forecasts not only capture uncertainty [70, 71], which is essential for risk assessment [72], but also offer greater flexibility by not requiring assumptions about specific error distributions [73]. Furthermore, in situations where the data

distribution is skewed or exhibits heavy tails [74, 72], quantile forecasts tend to provide higher accuracy.

LQR models the relationship between the input features and the target variable, focusing on linear relationships and using linear programming (LP) for optimization.

LR is widely regarded as a fundamental statistical learning method for analyzing the linear relationship between labels and features [75, 76, 77]. The LR model can be expressed as:

$$\begin{aligned} y_i = \hat{y} + \epsilon &= \beta_0 + \beta_1 x_1 + \beta_2 x_2 + \cdots + \beta_p x_p + \epsilon \\ &= \mathbf{X_i}\beta + \epsilon \end{aligned} \tag{3.16}$$

Here, y represents the true labels to be predicted, while $\hat{y}$ denotes the model's predicted values. Each feature is represented by x_i, with $\mathbf{X}_i$ defined as the vector containing all features and constants. The regression coefficients, β_j, describe the contribution of individual features, collectively expressed as the vector $\boldsymbol{\beta}$. The residual term ϵ accounts for prediction errors. The coefficients β_j are determined by minimizing the error between observed (y) and predicted ($\hat{y}$) values, ensuring the model effectively captures the linear relationship in an interpretable framework.

The purpose of regularization is to prevent overfitting and enhance the generalization capability of the model. This subsection primarily focuses on L_1 (Lasso) and L_2 (Ridge) regularization. In this report, we simply focus on L1-penalty. Building on the example above, the processes of LR combined with lasso net can be expressed as Formula .

$$\arg\min_{\beta} J = \arg\min_{\beta} L_{func} + \lambda_1 \sum_{j=1}^{p} |\beta_j| \tag{3.17}$$

From the form of the additional regularization term in the objective function, we can observe that lasso tends to induce sparsity, meaning that the β_j values of less important features are directly reduced to 0. Lasso performs feature selection based on the Sparsity Assumption. In contrast, by penalizing both $|\beta_j|$ and β_j^2, elastic net is capable of selecting important features while assigning appropriate weights to weakly related features.

3.3.2. Quantile Multilayer Perceptron (QMLP)

Quantile Multilayer Perceptron (QMLP) is a neural network model that extends the Multilayer Perceptron (MLP) to predict conditional quantiles by incorporating quantile loss into the training process.

In an MLP, the input to a neuron in the l-th layer is derived from the output of the previous layer and is computed as:

$$z_j^{(l)} = \sum_i w_{ij}^{(l)} h_i^{(l-1)} + b_j^{(l)},$$

where $w_{ij}^{(l)}$ is the weight, $h_i^{(l-1)}$ is the output of the i-th neuron in the previous layer, and $b_j^{(l)}$ is the bias term. The output of the neuron is:

$$h_j^{(l)} = \sigma(z_j^{(l)}),$$

with σ being the activation function. For an MLP with L layers, the input is $\mathbf{x}$, and the output of the final layer is $\hat{y}$. For regression tasks, the output layer typically uses a linear activation function:

$$\hat{y} = \mathbf{w}^{(L)} \cdot \mathbf{h}^{(L-1)} + b^{(L)}.$$

The goal is to minimize the loss function, such as the MSE:

$$\mathcal{L}(\mathbf{y}, \hat{y}) = \frac{1}{n} \sum_{i=1}^{n} (y_i - \hat{y}_i)^2 .$$

The weights and biases are updated via gradient descent:

$$w_{ij}^{(l)} \leftarrow w_{ij}^{(l)} - \eta \frac{\partial \mathcal{L}}{\partial w_{ij}^{(l)}}, \quad b_j^{(l)} \leftarrow b_j^{(l)} - \eta \frac{\partial \mathcal{L}}{\partial b_j^{(l)}}.$$

where η is the learning rate. The model gradually converges to minimize the loss function through iterative updates.

3.3.3. Quantile Kolmogorov-Arnold Networks (QKAN)

KAN is an innovative deep learning architecture with the relocation of learnable activation functions. More theory and information of KAN will be mentioned in Chapter D. Quantile KAN extends the KAN to make quantile forecast by utilizing quantile loss.

3.3.4. Quantile LightGBM (QLGBM)

LightGBM is a gradient boosting framework that uses decision trees, optimized for efficiency and speed, and is particularly effective with large datasets due to its histogram-based approach.

The model prediction is initialized with a simple baseline, typically the mean of the target values:

$$\hat{y}_i^{(0)} = \bar{y} = \frac{1}{n} \sum_{i=1}^{n} y_i. \tag{3.18}$$

The goal is to iteratively minimize the total loss function J, such as MSE:

$$J = \sum_{i=1}^{n} \mathcal{L}(y_i, \hat{y}_i), \quad \text{where} \quad \mathcal{L}(y_i, \hat{y}_i) = \frac{1}{2}(y_i - \hat{y}_i)^2. \tag{3.19}$$

At each iteration t, the updates follow the same principles as XGBoost. The model computes the residual $r_i^{(t)}$ as:

$$r_i^{(t)} = y_i - \hat{y}_i^{(t-1)}, \tag{3.20}$$

and fits a new decision tree $f_t(x)$ to these residuals. The prediction is then updated:

$$\hat{y}_i^{(t)} = \hat{y}_i^{(t-1)} + f_t(x_i). \tag{3.21}$$

LightGBM constructs trees using a *leaf-wise growth strategy*, where the leaf node with the highest potential gain is split first. This approach creates deeper, asymmetrical trees and reduces training error more efficiently, albeit with a higher risk of overfitting. To optimize the split points, LightGBM uses a *histogram-based algorithm*. Continuous feature values are binned into discrete buckets, significantly speeding up split point computation. For a given feature x_j and split value s, the gain is computed as:

$$\text{Gain}(x_j, s) = \frac{1}{2}\left(\frac{\left(\sum_{i\in I_L} g_i\right)^2}{\sum_{i\in I_L} h_i} + \frac{\left(\sum_{i\in I_R} g_i\right)^2}{\sum_{i\in I_R} h_i} - \frac{\left(\sum_{i\in I} g_i\right)^2}{\sum_{i\in I} h_i}\right), \tag{3.22}$$

where I_L and I_R represent the left and right child nodes after the split, and g_i and h_i are the gradient and Hessian values for sample i.

After T iterations, the final prediction is given by:

$$\hat{y}_i = \sum_{t=1}^{T} f_t(x_i). \tag{3.23}$$

LightGBM follows the same gradient boosting principles, with each tree learning the residuals of the previous iteration. However, its *leaf-wise growth strategy* and *histogram-based split point optimization* distinguish it, enabling faster training and more efficient handling of large-scale data, albeit with a greater risk of overfitting.

3.3.5. Quantile XGBoost (QXGB)

XGBoost is a highly efficient gradient boosting algorithm based on decision trees, known for its regularization capabilities and excellent performance in classification and regression tasks.

XGBoost can be considered as a gradient boosting method that iteratively builds an ensemble model by adding decision trees to minimize the loss function. Let the dataset consist of n samples, where y_i represents the true value of the i-th sample, and $\hat{y}_i^{(t)}$ represents the model's prediction after the t-th iteration. Initially, the model prediction is set to a baseline value, typically the mean of all target values:

$$\hat{y}_i^{(0)} = \bar{y} = \frac{1}{n}\sum_{i=1}^{n} y_i. \tag{3.24}$$

The objective of XGBoost is to iteratively minimize the total loss function, J, which for regression tasks is often MSE:

$$J = \sum_{i=1}^{n} \mathcal{L}(y_i, \hat{y}_i), \quad \text{where} \quad \mathcal{L}(y_i, \hat{y}_i) = \frac{1}{2}(y_i - \hat{y}_i)^2. \tag{3.25}$$

At each iteration t, the model computes the residual $r_i^{(t)}$, representing the difference between the true value y_i and the current prediction $\hat{y}_i^{(t-1)}$:

$$r_i^{(t)} = y_i - \hat{y}_i^{(t-1)}. \tag{3.26}$$

The goal of the new decision tree $f_t(x)$ is to predict these residuals as accurately as possible. By fitting $f_t(x)$ to the residuals, the model effectively minimizes the discrepancy between the predictions and the true values. The prediction is updated at the end of each iteration:

$$\hat{y}_i^{(t)} = \hat{y}_i^{(t-1)} + f_t(x_i), \tag{3.27}$$

where $f_t(x_i)$ is the output of the new tree for sample i.

To efficiently optimize the loss function, XGBoost approximates it using a second-order Taylor expansion around the previous predictions $\hat{y}_i^{(t-1)}$:

$$\mathcal{L}(y_i, \hat{y}_i^{(t-1)} + f_t(x_i)) \approx \mathcal{L}(y_i, \hat{y}_i^{(t-1)}) + g_i f_t(x_i) + \frac{1}{2} h_i f_t(x_i)^2, \tag{3.28}$$

where $g_i = \frac{\partial \mathcal{L}(y_i, \hat{y}_i)}{\partial \hat{y}_i}$ is the first derivative (gradient) and $h_i = \frac{\partial^2 \mathcal{L}(y_i, \hat{y}_i)}{\partial \hat{y}_i^2}$ is the second derivative (Hessian). Substituting this expansion into the total loss function gives:

$$J(f_t) = \sum_{i=1}^{n} \left[g_i f_t(x_i) + \frac{1}{2} h_i f_t(x_i)^2 \right]. \tag{3.29}$$

The tree $f_t(x)$ is constructed to minimize $J(f_t)$, ensuring that it effectively reduces the gradient and improves the model.

After T iterations, the final prediction for each sample is the sum of the outputs of all decision trees:

$$\hat{y}_i = \sum_{t=1}^{T} f_t(x_i). \tag{3.30}$$

This process incrementally refines the model by fitting each new tree to the residuals of the previous predictions. Unlike random forest, which uses bagging and builds trees independently, XGBoost leverages all samples at each iteration and sequentially builds trees that focus on reducing the residuals, ensuring an efficient optimization of the loss function.

3.4. Transfer Learning and Model Generalization

Generalization refers to a machine learning model's ability to maintain good performance on new data or tasks, i.e., its ability to adapt to new datasets or tasks [78]. Transfer learning is a machine learning approach aimed at transferring knowledge gained from the source case (A) to the target case (B) which is related but different [79]. The generalization of models is typically demonstrated through testing after transfer learning.

The transfer learning strategies considered in this report include separate training, zero-shot learning, fine-tuning, and joint learning, as shown in Table 3.4. Separate training refers to the scenario where cases A and B are trained, validated, and tested independently. Zero-shot learning involves using a model trained and validated on case A and directly testing it on case B. Fine-tuning refers to using a model pre-trained on case A and then fine-tuning it for several epochs using a small subset of the dataset from case B. Joint learning involves merging the datasets of case A and case B, training and validating the model on the combined data, and then testing it on case B.

Table 3.4: Transfer learning strategies mentioned in the report

Strategy Name	Description
Separate Training	$A/A, B/B$
Zero-shot	$B/A, A/B$
Fine-tuning	$B \rightarrow A/A, A \rightarrow B/B$
Joint Learning	$A + B/A, A + B/B$

3.5. Evaluation

3.5.1. Loss Function

The experiments of this report are based on the quantile regression framework mentioned as Section 3.5.1. For a given $\alpha \in (0, 1)$, the loss function for a quantile regressor is shown in Formula 3.31.

$$L_{func} = L_{\alpha}(y_i, \hat{y}_{\alpha,i}) = \begin{cases} \alpha \cdot (y_i - \hat{y}_i), & \text{if } y_i \geq \hat{y}_i, \\ (1 - \alpha) \cdot (\hat{y}_i - y_i), & \text{if } y_i < \hat{y}_i, \end{cases} \tag{3.31}$$

where y_i is the true value and $\hat{y}_i$ is the predicted quantile for the $i - th$ sample. This loss penalizes over-predictions and under-predictions differently depending on the quantile level α . When predicting upper quantiles ($\alpha > 0.5$), higher penalties are applied to under-predictions, whereas for lower quantiles ($\alpha < 0.5$), over-predictions incur higher penalties.

All quantiles considered in this report are shown in Formula 3.32.

$$A = \{10\%, 25\%, 45\%, 50\%, 55\%, 75\%, 90\%\} \tag{3.32}$$

3.5.2. Metrics

Average quantile loss (AQL) is employed to estimate conditional quantiles of the target distribution. Since our model employs a multi-task learning framework, the AQL is computed as the mean quantile

loss across all samples and quantiles:

$$\text{AQL} = \frac{1}{|A|N} \sum_{\alpha \in A} \sum_{i=1}^{N} L_\alpha(y_i, \hat{y}_{\alpha,i}), \tag{3.33}$$

where Q represents the set of quantiles being predicted, and N is the total number of samples. Lower AQL values indicate better overall performance in quantile prediction.

The Root Mean Squared Error (RMSE) evaluates the accuracy of pointwise predictions by penalizing larger errors more heavily than smaller ones. It is particularly sensitive to outliers and provides an overall measure of prediction quality. RMSE is calculated as Formula 3.34.

$$\text{RMSE} = \sqrt{\frac{1}{N} \sum_{i=1}^{N} (y_i - \hat{y}_i)^2}, \tag{3.34}$$

where y_i represents the true value, $\hat{y}_i$ is the predicted value, and N is the total number of samples.

The Mean Absolute Error (MAE) measures the average magnitude of prediction errors, treating all deviations equally regardless of their direction. Unlike RMSE, MAE is more robust to outliers, making it a reliable metric for assessing average prediction accuracy. It is computed as:

$$\text{MAE} = \frac{1}{N} \sum_{i=1}^{N} |y_i - \hat{y}_i|, \tag{3.35}$$

where y_i and $\hat{y}_i$ are the true and predicted values, respectively.

The Coefficient of Determination (R^2) quantifies the proportion of variance in the target variable that is explained by the predictions. A value of $R^2 = 1$ indicates perfect predictions, whereas $R^2 = 0$ suggests that the model performs no better than predicting the mean of the true values. It is defined as:

$$R^2 = 1 - \frac{\sum_{i=1}^{N} (y_i - \hat{y}_i)^2}{\sum_{i=1}^{N} (y_i - \bar{y})^2}, \tag{3.36}$$

where $\bar{y}$ is the mean of the true values y_i, and the numerator and denominator represent the residual sum of squares and the total sum of squares, respectively.

The Average Quantile Crossing Rate (AQCR) is utilized to quantify the frequency of quantile crossing violations. The quantile crossing indicator for a quantile pair (α_l, α_u) with $\alpha_l < \alpha_u$ is:

$$C_{\alpha_l, \alpha_u}(\hat{y}_{l,i}, \hat{y}_{u,i}) = \mathbb{I}(\hat{y}_{l,i} > \hat{y}_{u,i}), \tag{3.37}$$

where $\mathbb{I}(\cdot)$ is an indicator function that returns 1 if the condition inside is true and 0 otherwise. We aggregate the crossing indicators to compute the AQCR across N samples as:

$$\text{AQCR} = \frac{1}{N} \sum_{i=1}^{N} C_{\alpha_l, \alpha_u}(\hat{y}_{l,i}, \hat{y}_{u,i}) \tag{3.38}$$

Smaller AQCR values indicate fewer quantile crossing violations, reflecting more reliable predictions.

3.5.3. Diebold-Mariano Test

The Diebold-Mariano (DM) test is a statistical test used to compare the predictive accuracy of two competing forecast models. It tests the null hypothesis that the two models have the same forecast accuracy against the alternative that one model outperforms the other [80].

Let the forecast errors for models 1 and 2 at time t. The forecast error for each model can be calculated as:

$$L_{t,j} = \frac{1}{|A|} \sum_{\alpha \in A} L_\alpha(y_{\text{true},i}, \hat{y}^{(j)}_{\alpha,i}) \tag{3.39}$$

Where $L_{t,1}$ and $L_{t,2}$ represent the forecast errors for model 1 and model 2, respectively, and L_α refers to the quantile loss shown in Formula 3.31 in this report. The difference between model 1 and model 2 at time t can be expressed as:

$$d_t = L_{t,1} - L_{t,2} \tag{3.40}$$

The sample mean and variance of the difference sequence d_t are:

$$\bar{d} = \frac{1}{T} \sum_{t=1}^{T} d_t, \tag{3.41}$$

$$\sigma_d = \sqrt{\frac{1}{T-1} \sum_{t=1}^{T} (d_t - \bar{d})^2} \tag{3.42}$$

where T is the sample size.

Next, the DM statistic is calculated as:

$$DM = \frac{\bar{d}}{\sigma_d / \sqrt{T}} \tag{3.43}$$

where $\bar{d}$ is the sample mean of the differences, σ_d is the sample standard deviation, and T is the sample size. The sign of the DM statistic provides insight into which model performs better: a **positive DM statistic** indicates that model 2 (the later model) outperforms model 1 (the earlier model), while a **negative DM statistic** indicates the opposite.

To test the significance of the DM statistic, we compute the p-value assuming the DM statistic follows a standard normal distribution (Z-distribution). The p-value is calculated as:

$$p\text{-value} = 2(1 - \Phi(|DM|)) \tag{3.44}$$

where $\Phi(\cdot)$ is the cumulative distribution function (CDF) of the standard normal distribution, and $|DM|$ is the absolute value of the DM statistic.

A p-value less than 0.05 suggests rejecting the null hypothesis, indicating the result is statistically significant and unlikely due to chance. If the p-value is greater than 0.05, we fail to reject the null hypothesis, meaning there's insufficient evidence for a significant difference.

4

Experiments and Results

4.1. Features Selection

4.1.1. Experimental Setup

The objective of feature selection is to identify, from the 384 feature candidates in each case, a subset of selected features, providing insights into the relationships among feature candidates & labels. The evaluation of performance primarily focuses on AQL and the number of selected features (N_{input}), along with assessments of AQCR and pointwise forecast performance. Three approaches are discussed in this section: Principal Component Analysis (PCA) Compression, L1-based Selection, and Intersectional Percentile- and Correlation-based Feature Selection Algorithm (IPC).

The order book data are split into training (Jan 2022–Dec 2023), validation (Jan–Jun 2024), and testing (Jul–Dec 2024) datasets. All predictions are based on the quantile regression framework proposed in Section 3.5, with a set of quantiles specified in Formula 3.32. For ID1, ID2, and ID3, predictions are made 60, 120, and 180 minutes prior to each delivery time, respectively. The performance of pointwise predictions for the median quantile is evaluated using MAE, RMSE, and R^2, while the probabilistic predictions are assessed using AQL and AQCR, as discussed in more detail in Section 3.5.2. All potential features under consideration are listed in Table 3.2. All experiments were conducted using the NVIDIA GeForce RTX 4060 GPU.

4.1.2. PCA Compression Results

PCA compressors with an explained variance ratio (EVR) shown as Formula 4.1 are considered and experimented with. The compressor for each case, which yields the optimal validation loss, was tested using an QMLP model with Optuna to find the optimal set of hyperparameters. The Optuna configuration in all experiments was set to $n_{trial} = 100$.

$$e_v \in \{0.800, 0.900, 0.950, 0.990\} \tag{4.1}$$

To illustrate the relationship between the explained variance ratio (EVR) and the number of compo-

nents N_p for each case, a cumulative explained variance plot is presented in Figure 4.1, with the 95% threshold highlighted. Several key EVR thresholds and their corresponding numbers of components after compression are summarized in Table 4.1.

Table 4.1: Number of components (N_p) versus key EVR thresholds in PCA compressors

Case Desc.	$N_p \vert e_v = 0.80$	$N_p \vert e_v = 0.90$	$N_p \vert e_v = 0.95$	$N_p \vert e_v = 0.99$
ID1 DE h	31	60	84	142
ID1 AT h	20	43	66	122
ID2 DE h	28	58	86	151
ID2 AT h	15	33	53	102
ID3 DE h	32	62	88	149
ID3 AT h	12	26	44	87
ID1 DE qh	26	55	81	142
ID1 AT qh	19	43	65	127
ID2 DE qh	27	56	82	142
ID2 AT qh	15	34	54	103
ID3 DE qh	26	53	79	142
ID3 AT qh	12	27	44	86

Table 4.3 presents the testing performance of PCA compressors using QMLP models. Only the compressor with the optimal validation loss for each case is shown.

4.1.3. L1-Penalty Selection Results

In this section, LQR models with L1 regularization are employed, with the regularization strength specified in Formula 4.2. The feature selection results for each case are the union sets of the selections across all quantiles.

$$\alpha_{L_1} \in \{0, 1e^{-5}, 1e^{-3}, 5e^{-3}, 1e^{-2}, 5e^{-2}, 1e^{-1}\} \tag{4.2}$$

To illustrate the relationship between the L1 regularization strength α and the number of selected features N_f, Table 4.2 presents several key values of α and their corresponding N_f. After validation, the optimal L1-based selector for each case is tested and shown in Table 4.3. All details of selected features are shown in Table A.1.

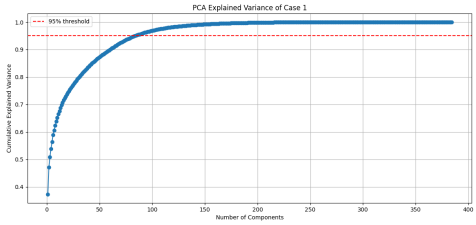

(A) Case ID1 DE h

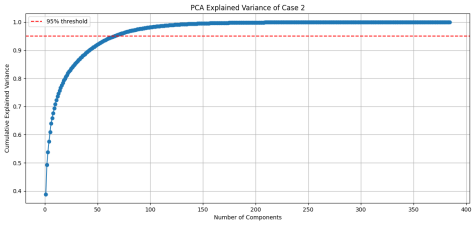

(B) Case ID1 AT h

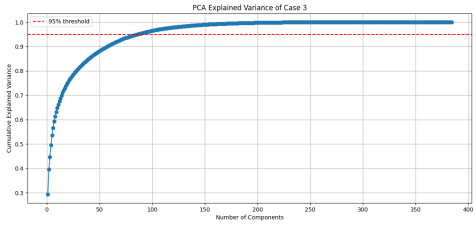

(C) Case ID2 DE h

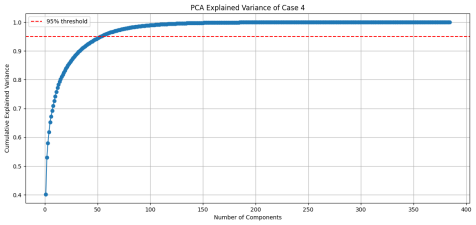

(D) Case ID2 AT h

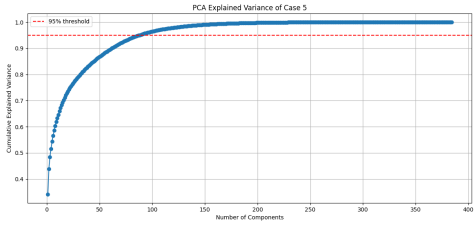

(E) Case ID3 DE h

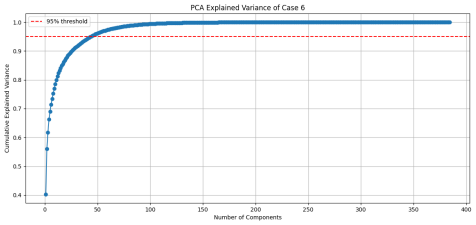

(F) Case ID3 AT h

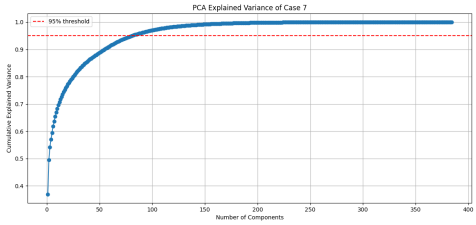

(G) Case ID1 DE qh

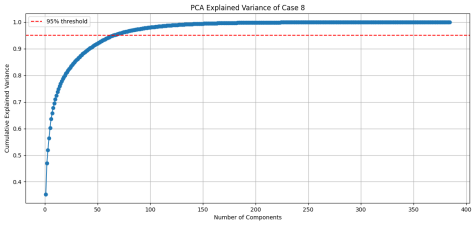

(H) Case ID1 AT qh

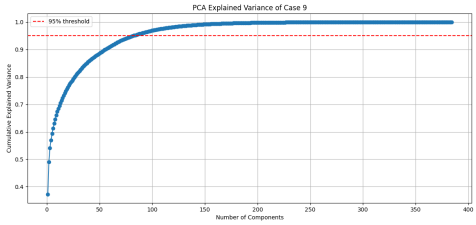

(I) Case ID2 DE qh

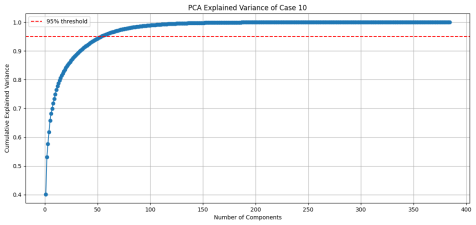

(J) Case ID2 AT qh

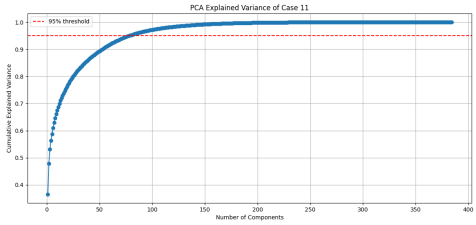

(K) Case ID3 DE qh

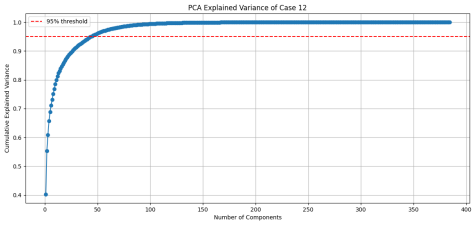

(L) Case ID3 AT qh

Figure 4.1: Cumulative explained variance plot of all cases

Table 4.2: Number of selected features (N_f) vs L1 regularization strength α

Case Desc.	$N_f \vert \alpha = 1e^{-5}$	$N_f \vert \alpha = 1e^{-3}$	$N_f \vert \alpha = 1e^{-2}$	$N_f \vert \alpha = 1e^{-1}$
ID1 DE h	368	245	53	14
ID1 AT h	373	249	87	50
ID2 DE h	364	240	40	18
ID2 AT h	366	241	75	33
ID3 DE h	371	243	46	16
ID3 AT h	355	208	66	38
ID1 DE qh	365	216	54	18
ID1 AT qh	372	212	70	39
ID2 DE qh	371	218	51	23
ID2 AT qh	363	193	86	55
ID3 DE qh	369	215	59	24
ID3 AT qh	351	176	85	54

Afterwards, the filtered features are input to QMLP models with Optuna for testing. The testing performance results are shown as Table 4.3.

4.1.4. IPC Selection Results

In this section, the quantile constraint q and the number of top features n are specified in Formula 3.12.

During the training and validation process, all details of selected features are shown in Table A.2. The testing performance results are shown as Table 4.3.

4.1.5. Experiment Conslusion

The testing performance of all three feature selection approaches is presented in Table 4.3. Detailed information on the selected features is provided in Appendix A. The testing performance of multi-head models, where different quantiles share a uniform set of selected features, is shown in Appendix B.

In all twelve cases, IPC outperforms the other two approaches in quantile forecast performance. Therefore, the comparison of approaches indicates that IPC selectors have distinct advantages. Additionally, IPC selectors achieve the lowest AQCR in 9 out of the 12 cases. In terms of pointwise forecast performance, IPC achieves optimal results in 11, 10, and 10 cases for MAE, RMSE, and Rš, respectively. Consequently, IPC selectors and the selected features are used in the experiments in Sections 4.2 and 4.3.

Preliminary analysis of the IPC-selected features, presented in Table A.2, highlights the importance of percentile prices as input features. Among the 84 selected feature sets and 1276 feature occurrences, percentile prices appeared in 82 of the selected feature sets, accounting for 628 occurrences, or 49.2%. Table A.3 shows the top 5 most important features selected based on the coefficients of each feature in the LQR model (if a feature set contains fewer than 5 elements, it is not expanded). Among these top 5 features, percentile prices appeared in 77 of the selected feature sets and accounted for 192 occurrences, or 46.4%, across the 84 feature sets and 414 feature occurrences.

For further insight into the selected features from IPC selectors, we calculated the intersection of

selected feature sets across different quantiles, indices, markets, and contracts. Table A.4 shows the shared selected features among quantiles within the same case, indicating that only two cases have a shared feature. The rarity of shared features among quantiles supports the rationale that different features are selected for prediction in different quantiles, to some extent.

Tables A.5, A.6, and A.7 illustrate the shared selected features across indices, markets, and contracts. Less than half of the cases (35.7%) share features across indices at the same quantile, with only the $q10$ quantile having shared features in all cases. The shared features across contracts generally exceed those across markets, indicating that IPC selectors show a higher degree of similarity in feature selection across contracts than across markets.

Table 4.3: Testing performance of comparison among three selection modes in all cases. The best results are shown in **bold**. The units of AQL, RMSE, and MAE are expressed in /MWh, while AQCR is reported in %. All metrics are denormalized.

Case Desc.	Selection Method	AQL	AQCR	MAE	RMSE	R2
ID1 DE h	PCA	5.48	86.27	13.13	35.76	0.84
	L1	5.57	68.40	12.05	33.48	0.86
	IPC	**4.82**	**10.35**	**11.82**	**30.92**	**0.88**
ID1 AT h	PCA	8.20	59.25	20.26	40.80	0.75
	L1	8.02	46.46	19.56	43.90	0.72
	IPC	**7.87**	**2.76**	**19.43**	**40.06**	**0.76**
ID2 DE h	PCA	4.39	63.44	10.69	29.03	0.87
	L1	4.17	86.68	9.49	26.68	0.89
	IPC	**3.82**	**2.06**	**9.41**	**25.98**	**0.90**
ID2 AT h	PCA	5.11	76.35	12.06	**30.27**	**0.79**
	L1	6.68	52.32	**11.70**	30.81	0.79
	IPC	**4.83**	**9.31**	11.77	31.11	0.78
ID3 DE h	PCA	4.65	74.25	11.04	29.15	0.86
	L1	5.92	89.56	10.19	27.89	0.87
	IPC	**4.03**	**8.27**	**10.01**	**27.29**	**0.88**
ID3 AT h	PCA	5.07	42.65	12.54	29.41	0.79
	L1	5.02	34.95	12.14	29.66	0.78
	IPC	**4.91**	**5.03**	**11.97**	**29.05**	**0.79**
ID1 DE qh	PCA	23.72	97.92	53.46	98.56	0.31
	L1	9.54	**31.38**	20.09	66.96	0.68
	IPC	**8.26**	37.00	**18.62**	**55.70**	**0.78**
ID1 AT qh	PCA	12.63	47.76	32.05	107.60	0.35
	L1	12.36	**5.47**	30.76	105.75	0.37
	IPC	**12.33**	10.16	**30.69**	**105.06**	**0.38**
ID2 DE qh	PCA	12.80	95.74	25.66	55.62	0.70
	L1	9.41	68.57	18.99	53.07	0.72

Case Desc.	Selection Method	AQL	AQCR	MAE	RMSE	R2
	IPC	**7.57**	**20.97**	**17.57**	**51.06**	**0.75**
ID2 AT qh	PCA	7.52	82.29	18.31	66.87	0.50
	L1	7.51	74.27	18.58	**66.63**	**0.51**
	IPC	**7.40**	**15.11**	**18.10**	66.80	0.51
ID3 DE qh	PCA	15.56	92.11	31.22	61.57	0.58
	L1	9.29	**72.07**	21.01	52.06	0.70
	IPC	**7.41**	77.01	**17.43**	**49.70**	**0.73**
ID3 AT qh	PCA	7.34	88.45	17.82	52.26	0.57
	L1	7.31	32.10	17.65	52.20	0.57
	IPC	**7.25**	**2.17**	**17.59**	**52.10**	**0.58**

4.2. Probabilistic Price Prediction

4.2.1. Experimental Setup

The objective of the models' comparison is to train and validate a quantile regressor using multiple models with different architectures, while maintaining the same input features, and ultimately compare the testing performance to gain insights into model selection. The training, validation, and testing sets are split as described in Section 4.1.1, and the quantile framework, along with the hardware used, remain consistent. The Optuna configuration in all experiments was set to $n_{\text{trial}} = 100$. The evaluation focuses primarily on AQL, while also considering AQCR and several pointwise performance metrics.

Quantile Multilayer Perceptron (QMLP), Quantile Kolmogorov-Arnold Networks (QKAN), Quantile LightGBM (QLGBM), and Quantile XGBoost (QXGB) models were considered and experimented.

4.2.2. Experiments Results & Conclusion

After training and validation using the same selected features, the testing performance is presented in Table 4.4.

The results show that the deep learning models, QMLP and QKAN, outperform the tree-based models, LightGBM and XGBoost, in all cases, as demonstrated in terms of quantile forecast performance, model AQCR, and pointwise forecast performance. Specifically, in terms of quantile forecast performance, the traditional neural network-based QMLP achieves the lowest AQL in 10 out of 12 cases, while QKAN shares the remaining 2 cases. In terms of model AQCR, QMLP achieves the lowest crossing rate in 9 cases. From the perspective of pointwise forecast performance, QMLP outperforms in MAE, RMSE, and R^2 in 12, 10, and 10 cases, respectively, while QKAN excels in RMSE and R2 in 2 cases. This suggests QMLPs advantage in handling extreme values.

In conclusion, the above experiments confirm the superiority of deep learning methods in terms of quantile forecast performance, model AQCR and pointwise forecast performance. Additionally, as an innovative deep learning architecture, QKAN can be considered as an alternative, demonstrating better performance than QMLP in some cases.

Table 4.4: Testing performance of models comparison. The best results are shown in **bold**. The units of AQL, RMSE,and MAE are expressed in /MWh, while AQCR is reported in %. All metrics are denormalized.

Case Desc.	Model	AQL	AQCR	MAE	RMSE	R2
ID1 DE h	QKAN	4.87	49.51	12.06	34.67	0.85
	QLGBM	5.23	26.52	12.60	42.87	0.77
	QMLP	**4.82**	**10.35**	**11.82**	**30.92**	**0.88**
	QXGB	5.23	26.52	12.60	42.87	0.77
ID1 AT h	QKAN	8.04	72.53	19.87	50.69	0.62
	QLGBM	8.13	22.08	19.87	53.52	0.58
	QMLP	**7.87**	**2.76**	**19.43**	**40.06**	**0.76**
	QXGB	8.13	22.08	19.87	53.52	0.58
ID2 DE h	QKAN	3.85	6.98	9.47	26.95	0.89
	QLGBM	4.15	56.13	10.01	33.46	0.83
	QMLP	**3.82**	**2.06**	**9.41**	**25.98**	**0.90**
	QXGB	4.15	56.13	10.01	33.46	0.83
ID2 AT h	QKAN	4.91	36.74	11.90	32.34	0.76
	QLGBM	4.90	37.33	11.90	32.09	0.77
	QMLP	**4.83**	**9.31**	**11.77**	**31.11**	**0.78**
	QXGB	4.90	37.33	11.90	32.09	0.77
ID3 DE h	QKAN	4.04	33.23	10.09	27.54	0.88
	QLGBM	4.24	36.40	10.32	30.36	0.85
	QMLP	**4.03**	**8.27**	**10.01**	**27.29**	**0.88**
	QXGB	4.24	36.40	10.32	30.36	0.85
ID3 AT h	QKAN	4.99	20.07	12.02	29.22	0.79
	QLGBM	4.98	23.76	12.05	29.31	0.79
	QMLP	**4.91**	**5.03**	**11.97**	**29.05**	**0.79**
	QXGB	4.98	23.76	12.05	29.31	0.79
ID1 DE qh	QKAN	8.73	54.69	19.02	55.99	0.78
	QLGBM	9.16	**34.63**	20.00	74.68	0.60
	QMLP	**8.26**	37.00	**18.62**	**55.70**	**0.78**
	QXGB	9.16	**34.63**	20.00	74.68	0.60
ID1 AT qh	QKAN	12.48	21.41	30.83	**100.17**	**0.44**
	QLGBM	12.54	**8.97**	30.97	113.60	0.28
	QMLP	**12.33**	10.16	**30.69**	105.06	0.38
	QXGB	12.54	**8.97**	30.97	113.60	0.28
ID2 DE qh	QKAN	**7.55**	25.92	17.73	51.51	0.74
	QLGBM	7.88	21.47	18.28	58.40	0.67
	QMLP	7.57	**20.97**	**17.57**	**51.06**	**0.75**
	QXGB	7.88	21.47	18.28	58.40	0.67

Case Desc.	Model	AQL	AQCR	MAE	RMSE	R2
ID2 AT qh	QKAN	7.51	59.50	18.21	71.29	0.44
	QLGBM	7.49	24.91	18.21	69.97	0.46
	QMLP	**7.40**	**15.11**	**18.10**	**66.80**	**0.51**
	QXGB	7.49	24.91	18.21	69.97	0.46
ID3 DE qh	QKAN	**7.32**	59.46	17.56	**49.52**	**0.73**
	QLGBM	7.56	**40.93**	17.76	52.59	0.69
	QMLP	7.41	77.01	**17.43**	49.70	0.73
	QXGB	7.56	**40.93**	17.76	52.59	0.69
ID3 AT qh	QKAN	7.27	35.05	17.65	**51.97**	**0.58**
	QLGBM	7.30	10.94	17.82	52.06	0.58
	QMLP	**7.25**	**2.17**	**17.59**	52.10	0.58
	QXGB	7.30	10.94	17.82	52.06	0.58

4.3. Generalization Assessment

4.3.1. Experimental Setup

The objective of the generalization research across countries is to explore the transferability of models between Germany and Austria, aiming to uncover cross-country structural similarities. The training, validation, and testing sets are split as described in Section 4.1.1, and the quantile framework, along with the hardware used, remain consistent. The Optuna configuration in all experiments was set to $n_{\text{trial}} = 100$. The evaluation focuses primarily on AQL, while also considering AQCR and several pointwise performance metrics.

It is generally accepted that fine-tuning requires significantly fewer training epochs than pretraining [81]. In separate training, joint training, zero-shot learning, and pretraining, the number of training epochs is set to 50. However, in fine-tuning, the number of training epochs is limited to 10 [82]. Additionally, fine-tuning is required to use only a small subset [83] of the training data from the target case (case B). Therefore, the number of samples extracted from the training set of case B is defined by Formula 4.3, and the strategy of extracting x data points is referred to as "*x shots.*" Although X_G includes elements that are significantly larger than those typically used in fine-tuning with x, for the sake of gaining insights, we will use X_G in the generalization results, while X_F will be used in the other experiments.

$$\begin{aligned} x \in X_G &= \{1, 5, 10, 50, 100, 500, 1000\} \\ x \in X_F &= \{1, 5, 10, 50\} \end{aligned} \tag{4.3}$$

Additionally, the fine-tuning datasets use the same scalers as the corresponding pretraining datasets, as the weights of the pretrained model were adapted to the scaled dataset during pretraining. In the generalization research, layer freezing is applied, where all hidden layers except for the final layer are frozen, leaving only the last hidden layer and the output layer available for fine-tuning. This approach is designed to preserve the knowledge acquired during pretraining on case A. In joint learning, the dataset is constructed by evenly interleaving data from both case A and case B. The results of the comparison studies on scalers and freezing techniques are presented in Tables B.5, B.6, B.8, and B.9.

4.3.2. Cross-Market Generalization

Based on the conclusions from Section 4.1 and Section 4.2, generalization across markets (between Germany and Austria) experiments were conducted using four transfer learning strategies. To assess the statistical significance of the differences between the results of separate training and other strategies, the DM test on AQL, as proposed in Section 3.5.3, was employed. The results include the DM_stat and p_value. These results are presented in Table 4.5. The Case Desc. in the table refers to the target case (case B).

Table 4.5: Generation results with different transfer learning strategies across countries. All results are based on testing datasets of hourly products. The best results are highlighted in **bold**. The units of AQL, RMSE, and MAE are expressed in /MWh, while AQCR is reported in %. All metrics are denormalized. The **Case Desc.** refers to case B. In the **DM test results**, model 1 corresponds to the separate training approach for the current case, while model 2 represents the strategy applied in this row.

Case Desc.	Trans. Strategy	AQL	AQCR	MAE	RMSE	R2	DM_stat	p_value
ID1 DE h	sepa	**4.82**	10.35	**11.82**	30.92	0.88	0.00	nan
	joint	5.02	10.15	12.06	31.76	0.88	-5.41	0.00
	zero	5.26	9.17	12.68	30.28	0.89	-7.21	0.00
	1 shot	5.01	25.25	12.06	29.44	0.89	-3.03	0.00
	5 shots	5.65	39.86	12.51	29.48	0.89	-12.45	0.00
	10 shots	5.33	34.41	12.68	30.96	0.88	-11.29	0.00
	50 shots	5.20	**9.08**	12.68	30.89	0.88	-7.97	0.00
	100 shots	5.40	30.62	12.80	30.96	0.88	-11.43	0.00
	500 shots	5.17	17.53	12.32	30.79	0.88	-7.60	0.00
	1000 shots	5.08	30.22	12.02	**29.94**	**0.89**	-5.67	0.00
ID1 AT h	sepa	7.87	**2.76**	19.43	40.06	0.76	0.00	nan
	joint	**7.84**	9.22	19.27	41.02	0.75	1.23	0.22
	zero	8.03	17.10	19.19	**33.65**	**0.83**	-2.83	0.00
	1 shot	8.13	30.62	19.17	33.71	0.83	-5.38	0.00
	5 shots	8.02	10.65	19.37	35.56	0.81	-2.36	0.02
	10 shots	8.03	30.78	19.20	34.80	0.82	-3.42	0.00
	50 shots	7.95	13.48	19.25	35.11	0.82	-1.88	0.06
	100 shots	7.92	9.01	19.16	34.33	0.83	-0.96	0.34
	500 shots	7.87	19.89	**19.14**	33.71	0.83	0.03	0.97
	1000 shots	7.85	27.25	19.38	36.63	0.80	0.76	0.45
ID2 DE h	sepa	**3.82**	**2.06**	**9.41**	25.98	0.90	0.00	nan
	joint	3.90	9.90	9.89	26.92	0.89	-3.87	0.00
	zero	4.08	10.44	9.93	25.41	0.90	-7.22	0.00
	1 shot	4.07	75.74	9.62	25.12	0.91	-4.93	0.00
	5 shots	4.01	40.82	9.80	25.18	0.91	-4.06	0.00
	10 shots	4.00	63.33	9.75	**25.16**	**0.91**	-4.12	0.00
	50 shots	4.13	29.63	9.67	25.50	0.90	-10.87	0.00
	100 shots	4.02	22.65	9.57	25.56	0.90	-6.93	0.00
	500 shots	4.05	18.69	9.55	25.50	0.90	-8.00	0.00

Case Desc.	Trans. Strategy	AQL	AQCR	MAE	RMSE	R2	DM_stat	p_value
	1000 shots	4.00	14.27	9.54	25.48	0.90	-6.26	0.00
ID2 AT h	sepa	4.83	9.31	11.77	31.11	0.78	0.00	nan
	joint	4.78	**7.43**	11.61	28.90	0.81	0.99	0.32
	zero	4.81	35.79	11.58	**28.58**	**0.82**	0.34	0.73
	1 shot	4.83	22.72	**11.48**	28.63	0.81	0.00	1.00
	5 shots	4.80	43.49	11.75	28.98	0.81	0.59	0.55
	10 shots	4.90	44.17	11.98	29.59	0.80	-1.35	0.18
	50 shots	4.84	23.17	12.44	29.74	0.80	-0.15	0.88
	100 shots	4.79	21.77	11.97	29.31	0.81	0.69	0.49
	500 shots	4.76	17.10	11.67	29.09	0.81	1.39	0.16
	1000 shots	**4.75**	19.71	11.73	29.66	0.80	1.60	0.11
ID3 DE h	sepa	**4.03**	**8.27**	**10.01**	**27.29**	**0.88**	0.00	nan
	joint	4.10	23.90	10.31	29.35	0.86	-3.86	0.00
	zero	4.26	10.33	10.55	27.80	0.87	-10.48	0.00
	1 shot	4.27	27.84	10.38	27.83	0.87	-8.69	0.00
	5 shots	5.60	88.34	16.58	32.55	0.83	-30.67	0.00
	10 shots	4.92	67.66	13.47	29.15	0.86	-25.42	0.00
	50 shots	4.33	81.63	10.60	27.87	0.87	-12.04	0.00
	100 shots	4.24	29.94	10.41	27.78	0.87	-9.25	0.00
	500 shots	4.19	62.22	10.17	27.73	0.87	-8.09	0.00
	1000 shots	4.19	19.12	10.32	27.81	0.87	-8.31	0.00
ID3 AT h	sepa	4.91	**5.03**	11.97	29.05	0.79	0.00	nan
	joint	**4.89**	6.66	**11.85**	28.81	0.80	1.70	0.09
	zero	4.95	24.64	11.95	**28.79**	**0.80**	-3.13	0.00
	1 shot	5.01	62.38	12.07	28.85	0.80	-6.58	0.00
	5 shots	5.55	48.81	13.89	30.59	0.77	-13.45	0.00
	10 shots	5.14	56.76	12.17	28.84	0.80	-10.87	0.00
	50 shots	4.97	28.63	12.05	29.07	0.79	-4.80	0.00
	100 shots	5.27	47.29	12.86	29.58	0.79	-12.73	0.00
	500 shots	4.94	7.43	12.22	29.04	0.79	-2.36	0.02
	1000 shots	4.92	7.34	12.00	28.93	0.79	-1.38	0.17
ID1 DE qh	sepa	**8.26**	**37.00**	**18.62**	**55.70**	**0.78**	0.00	nan
	joint	9.03	71.02	19.04	60.93	0.73	-19.87	0.00
	zero	10.25	80.95	21.80	64.44	0.70	-27.58	0.00
	1 shot	9.94	82.15	21.09	64.06	0.71	-23.12	0.00
	5 shots	10.56	90.11	21.48	64.66	0.70	-28.61	0.00
	10 shots	10.41	84.52	21.20	64.40	0.70	-26.23	0.00
	50 shots	10.40	80.88	21.41	64.65	0.70	-22.98	0.00
	100 shots	10.52	81.68	21.25	64.55	0.70	-26.19	0.00
	500 shots	10.41	77.02	21.23	64.54	0.70	-25.85	0.00
	1000 shots	10.59	76.95	20.78	64.53	0.70	-27.09	0.00

Case Desc.	Trans. Strategy	AQL	AQCR	MAE	RMSE	R2	DM_stat	p_value
ID1 AT qh	sepa	**12.33**	10.16	30.69	105.06	0.38	0.00	nan
	joint	12.38	**7.10**	**30.10**	100.68	0.43	-1.88	0.06
	zero	13.14	40.31	31.17	94.77	0.50	-19.31	0.00
	1 shot	14.69	90.06	39.19	95.34	0.49	-35.58	0.00
	5 shots	13.09	55.99	31.47	**94.09**	**0.50**	-17.56	0.00
	10 shots	12.83	69.20	30.78	96.76	0.47	-15.59	0.00
	50 shots	12.91	62.85	30.83	97.84	0.46	-18.26	0.00
	100 shots	12.75	75.68	30.69	97.08	0.47	-13.94	0.00
	500 shots	12.69	45.27	30.75	98.43	0.46	-12.79	0.00
	1000 shots	12.57	20.04	30.69	98.44	0.46	-8.89	0.00
ID2 DE qh	sepa	**7.57**	20.97	**17.57**	**51.06**	**0.75**	0.00	nan
	joint	7.84	32.51	18.23	52.01	0.74	-13.79	0.00
	zero	8.11	71.14	18.88	52.85	0.73	-15.95	0.00
	1 shot	8.21	83.30	18.86	52.90	0.73	-18.69	0.00
	5 shots	9.34	91.63	19.02	53.19	0.72	-41.43	0.00
	10 shots	8.24	46.84	18.84	53.11	0.72	-18.62	0.00
	50 shots	8.24	53.91	18.95	53.19	0.72	-19.59	0.00
	100 shots	8.60	34.61	19.04	53.19	0.72	-30.95	0.00
	500 shots	8.57	50.49	18.93	53.15	0.72	-29.51	0.00
	1000 shots	8.93	**18.00**	19.28	53.52	0.72	-37.70	0.00
ID2 AT qh	sepa	**7.40**	15.11	18.10	66.80	0.51	0.00	nan
	joint	7.40	**4.07**	17.95	67.61	0.49	-0.30	0.76
	zero	7.76	32.20	18.16	**64.61**	**0.54**	-17.48	0.00
	1 shot	8.47	72.66	19.15	64.68	0.54	-34.83	0.00
	5 shots	7.56	51.84	17.91	64.53	0.54	-9.17	0.00
	10 shots	7.57	41.48	17.88	64.80	0.53	-10.50	0.00
	50 shots	7.56	15.65	**17.86**	64.99	0.53	-10.45	0.00
	100 shots	7.51	35.81	17.87	64.98	0.53	-8.69	0.00
	500 shots	7.45	19.41	17.86	64.99	0.53	-3.79	0.00
	1000 shots	7.40	26.38	17.95	65.47	0.53	-0.49	0.62
ID3 DE qh	sepa	**7.41**	77.01	**17.43**	**49.70**	**0.73**	0.00	nan
	joint	8.52	**60.11**	19.19	50.53	0.72	-39.67	0.00
	zero	9.29	81.61	18.60	50.56	0.72	-26.26	0.00
	1 shot	9.24	87.55	18.41	50.47	0.72	-25.86	0.00
	5 shots	9.66	89.98	18.05	50.21	0.72	-30.43	0.00
	10 shots	9.07	80.52	19.08	50.55	0.72	-23.44	0.00
	50 shots	9.18	81.98	17.89	50.15	0.72	-24.74	0.00
	100 shots	9.47	76.08	18.09	50.54	0.72	-28.30	0.00
	500 shots	9.20	82.76	17.88	50.47	0.72	-25.51	0.00
	1000 shots	9.30	84.08	17.71	50.33	0.72	-26.77	0.00
ID3 AT qh	sepa	7.25	**2.17**	**17.59**	52.10	0.58	0.00	nan

Case Desc.	Trans. Strategy	AQL	AQCR	MAE	RMSE	R2	DM_stat	p_value
	joint	**7.22**	11.71	17.67	51.96	0.58	2.08	0.04
	zero	7.58	33.23	17.90	51.83	0.58	-18.64	0.00
	1 shot	7.88	67.98	18.08	51.89	0.58	-27.91	0.00
	5 shots	7.82	85.11	17.82	51.81	0.58	-33.76	0.00
	10 shots	7.45	59.31	17.81	51.81	0.58	-13.90	0.00
	50 shots	7.46	43.67	17.79	51.80	0.58	-14.74	0.00
	100 shots	7.42	47.30	17.74	51.78	0.58	-11.27	0.00
	500 shots	7.41	54.08	17.75	51.78	0.58	-12.00	0.00
	1000 shots	7.34	71.69	17.64	**51.76**	**0.58**	-7.24	0.00

4.3.3. Cross-Product Generalization

Based on the conclusions from Section 4.1 and Section 4.2, generalization across different types of products experiments were conducted using four transfer learning strategies. To assess the statistical significance of the differences between the results of separate training and other strategies, the DM test based on quantile loss, as proposed in Section 3.5.3, was employed. The results include the DM_stat and p_value. These results are presented in Table 4.6. The Case Desc. in the table refers to the target case (case B).

Table 4.6: Generation results with different transfer learning strategies across products in German market. All results are based on testing datasets. The best results are highlighted in **bold**. The units of AQL, RMSE, and MAE are expressed in /MWh, while AQCR is reported in %. All metrics are denormalized. The **Case Desc.** refers to case B. In the **DM test results**, model 1 corresponds to the separate training approach for the current case, while model 2 represents the strategy applied in this row.

Case Desc.	Trans. Strategy	AQL	AQCR	MAE	RMSE	R2	DM_stat	p_value
ID1 DE h	sepa	4.82	10.35	11.82	30.92	0.88	0.00	nan
	joint	5.01	60.11	**11.58**	**26.43**	**0.91**	-2.69	0.01
	zero	5.31	14.00	12.12	28.40	0.90	-7.49	0.00
	1 shot	4.94	70.78	11.78	27.51	0.91	-2.09	0.04
	5 shots	5.31	23.60	12.01	27.02	0.91	-5.72	0.00
	10 shots	5.18	82.24	12.98	30.39	0.89	-6.42	0.00
	50 shots	5.00	35.65	12.28	30.15	0.89	-3.13	0.00
	100 shots	5.06	68.79	12.58	30.04	0.89	-4.17	0.00
	500 shots	4.95	7.66	12.44	30.07	0.89	-2.33	0.02
	1000 shots	**4.81**	**3.10**	12.12	30.58	0.89	0.18	0.86
ID1 AT h	sepa	**7.87**	2.76	**19.43**	**40.06**	**0.76**	0.00	nan
	joint	8.03	5.37	20.12	45.70	0.69	-2.26	0.02
	zero	8.24	7.20	19.88	44.15	0.71	-5.93	0.00
	1 shot	8.17	9.54	19.70	43.91	0.72	-4.61	0.00
	5 shots	8.24	4.98	19.77	44.03	0.71	-6.06	0.00
	10 shots	8.23	**1.56**	20.06	44.37	0.71	-4.79	0.00
	50 shots	8.18	1.79	19.85	44.04	0.71	-4.39	0.00
	100 shots	8.38	2.56	19.72	43.93	0.72	-9.79	0.00

Case Desc.	Trans. Strategy	AQL	AQCR	MAE	RMSE	R2	DM_stat	p_value
	500 shots	8.14	10.83	19.80	44.03	0.71	-4.78	0.00
	1000 shots	8.12	2.22	19.67	43.92	0.72	-3.49	0.00
ID2 DE h	sepa	**3.82**	**2.06**	9.41	**25.98**	**0.90**	0.00	nan
	joint	4.06	43.28	9.46	26.12	0.90	-11.03	0.00
	zero	4.32	33.91	9.44	27.01	0.89	-24.41	0.00
	1 shot	4.07	57.19	9.68	26.79	0.89	-13.20	0.00
	5 shots	4.33	37.92	9.70	26.37	0.90	-21.44	0.00
	10 shots	4.26	48.27	9.72	26.41	0.90	-20.87	0.00
	50 shots	4.09	24.62	**9.41**	26.74	0.89	-11.36	0.00
	100 shots	4.03	12.77	9.50	26.73	0.89	-11.15	0.00
	500 shots	4.17	4.89	9.44	26.61	0.89	-15.61	0.00
	1000 shots	3.93	13.98	9.47	27.02	0.89	-5.86	0.00
ID2 AT h	sepa	**4.83**	9.31	**11.77**	**31.11**	**0.78**	0.00	nan
	joint	4.90	42.99	12.05	32.36	0.76	-2.35	0.02
	zero	4.91	**3.19**	12.17	31.39	0.78	-3.33	0.00
	1 shot	4.96	11.94	11.98	31.17	0.78	-5.44	0.00
	5 shots	5.00	46.48	12.38	31.41	0.78	-5.38	0.00
	10 shots	5.15	4.98	12.03	31.40	0.78	-12.19	0.00
	50 shots	5.02	5.78	12.58	31.77	0.77	-7.12	0.00
	100 shots	4.94	24.42	12.02	31.29	0.78	-4.27	0.00
	500 shots	4.91	6.14	12.12	31.40	0.78	-2.88	0.00
	1000 shots	4.89	14.50	12.04	31.46	0.78	-2.17	0.03
ID3 DE h	sepa	**4.03**	**8.27**	**10.01**	27.29	0.88	0.00	nan
	joint	4.12	21.00	10.09	**27.45**	**0.88**	-2.84	0.00
	zero	4.32	29.42	10.03	27.90	0.87	-13.14	0.00
	1 shot	4.24	65.05	10.27	27.97	0.87	-9.41	0.00
	5 shots	4.30	63.87	10.04	28.01	0.87	-10.46	0.00
	10 shots	4.27	17.24	10.15	28.00	0.87	-14.80	0.00
	50 shots	4.22	37.49	10.05	27.87	0.87	-11.36	0.00
	100 shots	4.23	28.92	10.08	27.86	0.87	-13.61	0.00
	500 shots	4.21	34.56	10.09	27.96	0.87	-10.86	0.00
	1000 shots	4.18	9.38	10.24	28.07	0.87	-6.67	0.00
ID3 AT h	sepa	**4.91**	5.03	**11.97**	**29.05**	**0.79**	0.00	nan
	joint	5.02	3.94	12.20	29.61	0.78	-7.79	0.00
	zero	5.04	12.59	12.33	29.73	0.78	-9.54	0.00
	1 shot	5.07	63.99	12.20	29.70	0.78	-11.26	0.00
	5 shots	5.17	31.60	13.04	30.06	0.78	-11.37	0.00
	10 shots	5.14	2.81	12.32	29.66	0.78	-13.91	0.00
	50 shots	5.10	**2.74**	12.48	29.95	0.78	-13.16	0.00
	100 shots	5.14	18.80	12.75	29.96	0.78	-11.91	0.00
	500 shots	5.08	4.42	12.43	29.74	0.78	-11.01	0.00

Case Desc.	Trans. Strategy	AQL	AQCR	MAE	RMSE	R2	DM_stat	p_value
	1000 shots	5.02	15.92	12.26	29.70	0.78	-8.84	0.00
ID1 DE qh	sepa	8.26	37.00	18.62	**55.70**	**0.78**	0.00	nan
	joint	8.19	35.38	**18.49**	58.71	0.75	2.57	0.01
	zero	**8.17**	53.30	18.60	64.45	0.70	1.38	0.17
	1 shot	8.90	86.69	19.42	66.32	0.69	-8.53	0.00
	5 shots	8.15	76.37	18.50	64.12	0.71	1.80	0.07
	10 shots	8.30	35.48	18.76	65.82	0.69	-0.46	0.65
	50 shots	8.46	78.36	18.79	66.43	0.68	-2.35	0.02
	100 shots	8.43	14.84	18.74	66.56	0.68	-2.03	0.04
	500 shots	8.38	15.61	18.63	64.68	0.70	-1.80	0.07
	1000 shots	8.43	**10.87**	18.59	64.90	0.70	-2.70	0.01
ID1 AT qh	sepa	12.33	10.16	30.69	105.06	0.38	0.00	nan
	joint	**12.33**	10.26	30.72	103.26	0.40	0.38	0.70
	zero	12.59	7.58	30.60	101.04	0.43	-8.08	0.00
	1 shot	13.65	62.37	31.48	**99.72**	**0.44**	-23.56	0.00
	5 shots	12.64	55.42	30.57	100.36	0.43	-9.88	0.00
	10 shots	12.56	38.24	30.64	102.17	0.41	-8.16	0.00
	50 shots	12.50	41.68	30.60	101.76	0.42	-6.24	0.00
	100 shots	12.47	48.35	**30.53**	101.33	0.42	-5.16	0.00
	500 shots	12.44	21.69	30.68	102.12	0.41	-4.31	0.00
	1000 shots	12.40	**4.57**	30.71	101.42	0.42	-2.38	0.02
ID2 DE qh	sepa	7.57	20.97	17.57	51.06	0.75	0.00	nan
	joint	7.59	44.34	**17.53**	**50.27**	**0.75**	-0.81	0.42
	zero	**7.44**	19.06	17.58	50.59	0.75	7.35	0.00
	1 shot	7.67	41.08	18.13	51.43	0.74	-4.58	0.00
	5 shots	8.53	81.66	22.11	56.20	0.69	-29.23	0.00
	10 shots	7.57	19.14	17.85	54.23	0.71	0.01	0.99
	50 shots	7.55	**11.44**	17.94	53.42	0.72	1.08	0.28
	100 shots	7.72	49.62	18.08	50.89	0.75	-9.94	0.00
	500 shots	7.57	22.47	17.74	51.13	0.74	0.54	0.59
	1000 shots	7.81	45.47	18.82	51.61	0.74	-17.41	0.00
ID2 AT qh	sepa	**7.40**	15.11	18.10	66.80	0.51	0.00	nan
	joint	7.40	43.34	18.00	65.93	0.52	-0.07	0.94
	zero	7.44	21.00	**17.92**	65.11	0.53	-3.64	0.00
	1 shot	8.87	82.04	19.65	**64.84**	**0.53**	-45.93	0.00
	5 shots	7.53	7.84	19.12	66.06	0.52	-8.14	0.00
	10 shots	7.40	29.78	17.94	65.14	0.53	-0.20	0.84
	50 shots	7.57	31.57	19.14	66.42	0.51	-11.70	0.00
	100 shots	7.62	51.17	19.11	66.50	0.51	-14.26	0.00
	500 shots	7.42	**7.64**	18.30	65.94	0.52	-2.22	0.03
	1000 shots	7.43	10.14	18.40	66.18	0.51	-3.09	0.00

Case Desc.	Trans. Strategy	AQL	AQCR	MAE	RMSE	R2	DM_stat	p_value
ID3 DE qh	sepa	7.41	77.01	**17.43**	49.70	0.73	0.00	nan
	joint	**7.38**	38.30	17.45	**49.08**	**0.73**	2.36	0.02
	zero	7.84	**17.07**	18.24	57.11	0.64	-4.57	0.00
	1 shot	8.44	44.99	19.71	57.19	0.64	-11.22	0.00
	5 shots	8.12	67.83	18.64	58.32	0.62	-7.15	0.00
	10 shots	8.33	65.41	18.90	57.48	0.63	-9.91	0.00
	50 shots	7.88	23.69	18.31	57.36	0.64	-4.87	0.00
	100 shots	7.96	52.95	18.31	58.67	0.62	-5.60	0.00
	500 shots	7.87	62.26	18.16	56.80	0.64	-4.90	0.00
	1000 shots	7.96	51.25	18.24	57.67	0.63	-5.82	0.00
ID3 AT qh	sepa	7.25	**2.17**	17.59	52.10	0.58	0.00	nan
	joint	**7.23**	5.18	17.52	52.12	0.58	1.51	0.13
	zero	7.26	10.64	**17.51**	**51.67**	**0.58**	-1.98	0.05
	1 shot	7.82	82.70	19.90	52.68	0.57	-31.26	0.00
	5 shots	7.39	43.46	18.37	52.29	0.57	-9.48	0.00
	10 shots	7.35	28.88	18.29	52.24	0.57	-7.48	0.00
	50 shots	7.31	33.93	17.54	51.88	0.58	-6.62	0.00
	100 shots	7.31	32.75	18.05	51.99	0.58	-5.25	0.00
	500 shots	7.32	4.28	18.21	52.05	0.58	-6.08	0.00
	1000 shots	7.32	12.07	18.19	52.04	0.58	-5.92	0.00

4.3.4. Experiments Conclusion

Experimental Findings

The results in 4.5 highlight the similarities in the underlying structure between the German and Austrian markets, as reflected in both hourly and quarter-hourly product prices. However, there are notable differences in generalization between the two countries. In the six cases for the German market, various transfer learning strategies involving Austrian datasets were found to perform significantly worse than the separate training approach in terms of quantile forecast performance. In contrast, for the Austrian market, joint learning in all six cases was found to perform at least not significantly worse than the separate training approach. Additionally, transfer learning strategies showed potential for improving pointwise price forecast performance for the Austrian market.

The results in 4.6 demonstrate the similarities in structure between the hourly and quarter-hourly products in both the German and Austrian markets, while also highlighting significant differences in generalization across the two product types. In predicting the six cases for hourly product prices, all transfer learning strategiesincluding zero-shot, fine-tuning, and joint learningthat involved quarter-hourly product prices were found to perform significantly worse than separate training in terms of quantile forecast performance. However, for quarter-hourly products, joint learning was found to perform at least not significantly worse than separate training in terms of quantile forecast performance.

Analysis and Insights

The asymmetric transfer effect observed in the experimental results may stem from differences in the number of trades between different cases, which means the variation in the number of trades per

data point used to extract features and labels from raw order books. Table 4.7 shows the average number of trades across different cases. When studying generalization across markets, for $\delta = 60\text{min}, 120\text{min}, 180\text{min}$, the average number of trades for German hourly contracts is approximately 12.00, 13.79, and 13.66 times that of Austria, while for German qh contracts, the average number of trades is about 8.25, 8.66, and 8.80 times that in Austria. When studying generalization across products, for $\delta = 60\text{min}, 120\text{min}, 180\text{min}$, the average number of trades for hourly contracts in the German market is approximately 2.11, 2.43, and 2.65 times that for qh contracts, while in the Austrian market, the average number of trades for hourly contracts is about 1.45, 1.53, and 1.71 times that for qh contracts.

The ratio of average trades between these different cases not only affects whether the asymmetric transfer effect occurs, but also influences the degree of this effect. In the generalization across markets study, joint learning outperforms separate learning in all three cases for hourly contracts, whereas for qh contracts, this occurs in only one case. This can be explained by the greater difference in average trading numbers for hourly contracts compared to qh contracts between countries. Similarly, in the generalization across products study, joint learning outperforms separate learning in predicting ID1 and ID3 in both the German and Austrian markets. However, in the German market, this performance improvement is considered significant by the DM test, whereas in the Austrian market, the performance improvements in both cases are not considered significant.

In conclusion, the experimental results from the generalization research support the hypothesis that the asymmetric transfer effect arises from differences in trading number in raw orderbooks. Generally, higher trading numbers tend to lead to more stable price distributions, meaning they are less influenced by extreme prices. Thus, when there is a similarity between features and labels of case A and case B, joint learning involving cases with higher trading numbers may improve predictive performance.

Table 4.7: Average number of trades of cases

Case Desc.	Avg. Num. Trades
ID1 DE h	2528.20
ID1 AT h	210.68
ID1 DE qh	1200.19
ID1 AT qh	145.39
ID2 DE h	1579.21
ID2 AT h	114.53
ID2 DE qh	648.92
ID2 AT qh	74.93
ID3 DE h	1043.28
ID3 AT h	76.37
ID3 DE qh	393.79
ID3 AT qh	44.76

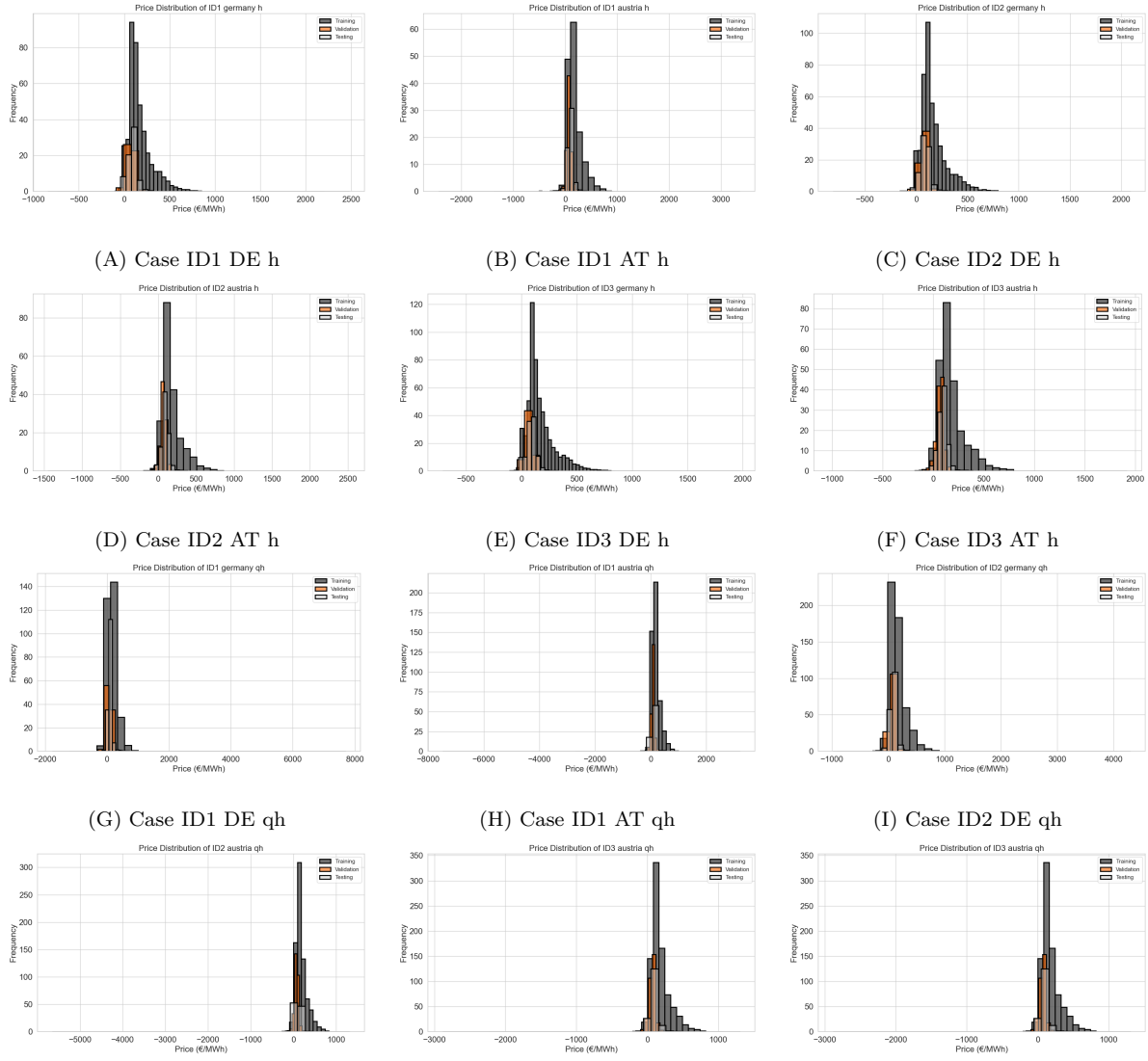

(A) Case ID1 DE h (B) Case ID1 AT h (C) Case ID2 DE h

(D) Case ID2 AT h (E) Case ID3 DE h (F) Case ID3 AT h

(G) Case ID1 DE qh (H) Case ID1 AT qh (I) Case ID2 DE qh

(J) Case ID2 AT qh (K) Case ID3 DE qh (L) Case ID3 AT qh

Figure 4.2: Cumulative explained variance plot of all cases

5

Conclusion

5.1. Report Conclusion

This report focuses on extracting additional internal microstructure from IDM orderbooks, exploring the application of deep learning for quantile forecasting, and examining generalization across different orderbooks. We conducted a series of experiments to predict the prices of hourly and quarter-hourly products in the intraday markets of Germany and Austria, specifically for ID1, ID2, and ID3 prices, covering a total of 12 cases. These experiments provided valuable insights through comparative studies between different markets and product types.

Now, let us address the research questions posed in Section 1.4.

- ***What are the predictive features derived from the orderbook that can improve price prediction?***

During feature selection, alongside commonly used features such as VWAP and last prices, the importance of percentile prices was emphasized and validated. Furthermore, we introduced the Intersectional Percentile- and Correlation-based Feature Selection Algorithm (IPC) and demonstrated its advantages over PCA compression and L1-based selection in terms of quantile forecast performance across all 12 cases. Additionally, we analyzed the shared features and top 5 features selected by IPC and provided insights based on these findings.

- ***How can deep learning architectures improve performance in quantile forecasting of price labels compared to traditional statistical learning models?***

Building on the conclusions from feature selection, probabilistic price prediction was implemented. We applied prediction models based on Quantile LightGBM (QLGBM), Quantile Extreme Gradient Boosting (QXGB), Quantile Multilayer Perceptron (QMLP), and Quantile KolmogorovArnold Network (QKAN). Extensive benchmarking indicated the advantages of deep learning models for quantile forecasting of IDM prices.

- ***Through the generalization research across different markets and products, what structural similarities on price prediction can be learned?***

Subsequent research focused on assessing generalization across markets (Germany and Austria) and products (hourly and quarter-hourly). We observed differences in transfer learning strategies across countries and product types. The results showed that all mentioned transfer learning strategies significantly worsened the quantile forecast in Germany, while joint learning did not significantly deteriorate and possibly even improved forecast performance in Austria. Similarly, transfer learning strategies significantly worsened the quantile forecast for hourly contracts, but joint learning did not significantly worsen and might even improve the quantile forecast for qh contracts. Additionally, we proposed and analyzed the relationship between this asymmetric transfer effect and the number of trades. These insights provide references for model developers and market regulators.

5.2. Outlooks and Future Work

Firstly, the cross-country and cross-product generalization should be further validated using data from other countries, such as Norway and Germany. Additional generalization assessments could provide further insights, such as whether the structural similarities between different markets are strongly correlated with geographical location.

Moreover, temporal generalization assessment presents another potential area of exploration, offering valuable insights into market structure changes for policymakers and market regulators. This could also help quantify the actual effects of policy changes following their implementation.

Additionally, methods to effectively reduce AQCR should be explored and studied. In this research, the crossing rate between different quantiles was only monitored through AQCR, but no effective solution was proposed to reduce it. A high crossing rate may adversely affect the reliability of quantile forecast models.

Finally, based on the quantile forecasting approach proposed in this report, a new trading strategy should be developed. Compared to pointwise forecast models, quantile forecast models provide richer information, and whether this can be translated into gains in profitability is a topic worthy of future research.

References

[1] Grzegorz Marcjasz, Bartosz Uniejewski, and Rafa Weron. "Beating the naveCombining LASSO with nave intraday electricity price forecasts". In: *Energies* 13.7 (2020), p. 1667.

[2] Micha Narajewski and Florian Ziel. "Econometric modelling and forecasting of intraday electricity prices". In: *Journal of Commodity Markets* 19 (2020), p. 100107.

[3] Tomasz Serafin, Grzegorz Marcjasz, and Rafa Weron. "Trading on short-term path forecasts of intraday electricity prices". In: *Energy Economics* 112 (2022), p. 106125.

[4] José R Andrade et al. "Probabilistic price forecasting for day-ahead and intraday markets: Beyond the statistical model". In: *Sustainability* 9.11 (2017), p. 1990.

[5] Bartosz Uniejewski, Grzegorz Marcjasz, and Rafa Weron. "Understanding intraday electricity markets: Variable selection and very short-term price forecasting using LASSO". In: *International Journal of Forecasting* 35.4 (2019), pp. 1533–1547.

[6] Stephen Karekezi and John Kimani. "Have power sector reforms increased access to electricity among the poor in East Africa?" In: *Energy for Sustainable Development* 8.4 (2004), pp. 10–25.

[7] MR Nouni, SC Mullick, and TC Kandpal. "Providing electricity access to remote areas in India: Niche areas for decentralized electricity supply". In: *Renewable energy* 34.2 (2009), pp. 430–434.

[8] Xiangwen Wu et al. "Emissions of CO2, CH4, and N2O fluxes from forest soil in permafrost region of Daxingan Mountains, northeast China". In: *International Journal of Environmental Research and Public Health* 16.16 (2019), p. 2999.

[9] Siti Zawiyah Azmi et al. "Trend and status of air quality at three different monitoring stations in the Klang Valley, Malaysia". In: *Air Quality, Atmosphere & Health* 3 (2010), pp. 53–64.

[10] Roberto Álvarez et al. "Analysis of low carbon super credit policy efficiency in European Union greenhouse gas emissions". In: *Energy* 82 (2015), pp. 996–1010.

[11] Jarosaw Brodny and Magdalena Tutak. "Analyzing similarities between the European Union countries in terms of the structure and volume of energy production from renewable energy sources". In: *Energies* 13.4 (2020), p. 913.

[12] Roberto Álvarez et al. "Analysis of low carbon super credit policy efficiency in European Union greenhouse gas emissions". In: *Energy* 82 (2015), pp. 996–1010.

[13] Eurostat. *Energy from renewable sources*. 2024. URL: `http://www.europarl.europa.eu/factsheets/en/sheet/70/energia-ze-zrodel` (visited on 11/01/2024).

[14] Boena Gajdzik et al. "Renewable Energy Share in European Industry: Analysis and Extrapolation of Trends in EU Countries". In: *Energies* (2024). DOI: `10.3390/en17112476`.

[15] M. Ste and Mariola Grzebyk. "Statistical Analysis of the Level of Development of Renewable Energy Sources in the Countries of the European Union". In: *Energies* (2022). DOI: `10.3390/en15218278`.

[16] José D Morcillo, Fabiola Angulo, and Carlos J Franco. “Analyzing the hydroelectricity variability on power markets from a system dynamics and dynamic systems perspective: Seasonality and ENSO phenomenon”. In: *Energies* 13.9 (2020), p. 2381.

[17] Mehrnaz Anvari et al. “Short term fluctuations of wind and solar power systems”. In: *New Journal of Physics* 18.6 (2016), p. 063027.

[18] I González-Aparicio and Andreas Zucker. “Impact of wind power uncertainty forecasting on the market integration of wind energy in Spain”. In: *Applied energy* 159 (2015), pp. 334–349.

[19] Eurostat. *Electricity from renewable sources up to 41% in 2022*. 2024. URL: %5Curl%7Bhttps://ec.europa.eu/eurostat/web/products-eurostat-news/w/ddn-20240221-1%7D (visited on 11/01/2024).

[20] Aitor Ciarreta, Peru Muniain, and Ainhoa Zarraga. “Modeling and forecasting realized volatility in German–Austrian continuous intraday electricity prices”. In: *Journal of Forecasting* 36.6 (2017), pp. 680–690.

[21] Ulfar Linnet. “Tools supporting wind energy trade in deregulated markets”. In: *Master’s Thesis, Technical University of Denmark* (2005).

[22] Richard Green. “Electricity liberalisation in Europehow competitive will it be?” In: *Energy Policy* 34.16 (2006), pp. 2532–2541.

[23] Lingchunzi Li et al. “Forward contracting and spot trading in electricity markets”. In: *Annals of Operations Research* (2023), pp. 1–45.

[24] Peter Cramton. “Electricity market design”. In: *Oxford Review of Economic Policy* 33.4 (2017), pp. 589–612.

[25] P. Zweifel, Aaron Praktiknjo, and G. Erdmann. “Markets for Electricity”. In: (2017), pp. 269–296. DOI: 10.1007/978-3-662-53022-1_12.

[26] Orhan Altu Karabiber and George Xydis. “Electricity price forecasting in the Danish day-ahead market using the TBATS, ANN and ARIMA methods”. In: *Energies* 12.5 (2019), p. 928.

[27] Christian Pape, Simon Hagemann, and Christoph Weber. “Are fundamentals enough? Explaining price variations in the German day-ahead and intraday power market”. In: *Energy Economics* 54 (2016), pp. 376–387.

[28] Selina Kerscher and Pablo Arboleya. “The key role of aggregators in the energy transition under the latest European regulatory framework”. In: *International Journal of Electrical Power & Energy Systems* 134 (2022), p. 107361.

[29] Hong Lam Le, Valentin Ilea, and Cristian Bovo. “Integrated European intra-day electricity market: Rules, modeling and analysis”. In: *Applied energy* 238 (2019), pp. 258–273.

[30] Valentin Ilea, Cristian Bovo, et al. “Impact of the price coupling of regions project on the day-ahead electricity market in Italy”. In: *2017 IEEE Manchester PowerTech*. IEEE. 2017, pp. 1–6.

[31] Rüdiger Kiesel and Florentina Paraschiv. “Econometric analysis of 15-minute intraday electricity prices”. In: *Energy Economics* 64 (2017), pp. 77–90.

[32] Christian Pape. “The impact of intraday markets on the market value of flexibilityDecomposing effects on profile and the imbalance costs”. In: *Energy Economics* 76 (2018), pp. 186–201.

[33] Karsten Neuhoff et al. “Intraday markets for power: Discretizing the continuous trading?” In: (2016).

[34] David Newbery, Goran Strbac, and Ivan Viehoff. “The benefits of integrating European electricity markets”. In: *Energy Policy* 94 (2016), pp. 253–263.

[35] Venizelos Venizelou and Andreas Poullikkas. “Trend Analysis of Cross-Border Electricity Trading in Pan-European Network”. In: *Energies* 17.21 (2024), p. 5318.

[36] Angelica Gianfreda, Francesco Ravazzolo, and Luca Rossini. “Comparing the forecasting performances of linear models for electricity prices with high RES penetration”. In: *International Journal of Forecasting* 36.3 (2020), pp. 974–986.

[37] Christoph Kost et al. “Levelized cost of electricity-renewable energy technologies”. In: (2013).

[38] Jan Dobschinski et al. “The potential of advanced shortest-term forecasts and dynamic prediction intervals for reducing the wind power induced reserve requirements”. In: (2010).

[39] Hannele Holttinen. “Handling of wind power forecast errors in the Nordic power market”. In: *2006 International Conference on Probabilistic Methods Applied to Power Systems*. IEEE. 2006, pp. 1–6.

[40] Oluwadare Badejo and Marianthi Ierapetritou. “Mathematical programming approach to optimize tactical and operational supply chain decisions under disruptions”. In: *Industrial & Engineering Chemistry Research* 61.45 (2022), pp. 16747–16763.

[41] Priyanka Shinde, I. Kouveliotis-Lysikatos, and M. Amelin. “Multistage Stochastic Programming for VPP Trading in Continuous Intraday Electricity Markets”. In: *IEEE Transactions on Sustainable Energy* 13 (2021), pp. 1037–1048. DOI: 10.36227/TECHRXIV.14999496.V1.

[42] Priyanka Shinde. “Efficient Trading in the Short-term Electricity Markets for Integration of Renewable Energy Sources: Multistage Stochastic and Agent-based Modeling Approaches for Continuous Intraday Electricity Market”. PhD thesis. KTH Royal Institute of Technology, 2023.

[43] Henry Martin and Scott Otterson. “German intraday electricity market analysis and modeling based on the limit order book”. In: *2018 15th international conference on the European energy market (EEM)*. IEEE. 2018, pp. 1–6.

[44] Gustavo EAPA Batista et al. “CID: an efficient complexity-invariant distance for time series”. In: *Data Mining and Knowledge Discovery* 28 (2014), pp. 634–669.

[45] Florian Ziel. “Forecasting electricity spot prices using lasso: On capturing the autoregressive intraday structure”. In: *IEEE Transactions on Power Systems* 31.6 (2016), pp. 4977–4987.

[46] Christoph Scholz et al. “Towards the prediction of electricity prices at the intraday market using shallow and deep-learning methods”. In: *Mining Data for Financial Applications: 5th ECML PKDD Workshop, MIDAS 2020, Ghent, Belgium, September 18, 2020, Revised Selected Papers 5*. Springer. 2021, pp. 101–118.

[47] Axel Englund. *Evaluation of Machine Learning Models for Intraday Price Forecasting in the Renewable Energy Sector*. 2024.

[48] Christopher Kath. “Modeling intraday markets under the new advances of the cross-border intraday project (XBID): Evidence from the German intraday market”. In: *Energies* 12.22 (2019), p. 4339.

[49] Christian O'Leary et al. "A comparison of deep learning vs traditional machine learning for electricity price forecasting". In: *2021 4th International Conference on Information and Computer Technologies (ICICT)*. IEEE. 2021, pp. 6–12.

[50] Abdulaziz Almalaq and George Edwards. "A review of deep learning methods applied on load forecasting". In: *2017 16th IEEE international conference on machine learning and applications (ICMLA)*. IEEE. 2017, pp. 511–516.

[51] Mauro Castelli, Ale Groznik, and Ale Popovi. "Forecasting electricity prices: A machine learning approach". In: *algorithms* 13.5 (2020), p. 119.

[52] Claudio Monteiro et al. "Short-term price forecasting models based on artificial neural networks for intraday sessions in the Iberian electricity market". In: *Energies* 9.9 (2016), p. 721.

[53] Ilkay Oksuz and Umut Ugurlu. "Neural network based model comparison for intraday electricity price forecasting". In: *Energies* 12.23 (2019), p. 4557.

[54] TP Timo Vijn. "Point and interval forecasting of short-term electricity price with machine learning: A theoretical and practical evaluation of benchmark accuracies for the Dutch intraday market". PhD thesis. Delft University of Technology, 2021.

[55] Johannes Krokeide Kolberg and Kristin Waage. "Artificial Intelligence and Nord Pools intraday electricity market Elbas: a demonstration and pragmatic evaluation of employing deep learning for price prediction: using extensive market data and spatio-temporal weather forecasts". MA thesis. 2018.

[56] Sondre Eide and Olai Viken. "Bu y on Intraday Market or not: A Deep Learning Approach: A decision tool for buyers in the Norwegian electricity markets to decide optimal market to purchase electricity". MA thesis. 2022.

[57] Deniz Kenan Klç, Peter Nielsen, and Amila Thibbotuwawa. "Intraday Electricity Price Forecasting via LSTM and Trading Strategy for the Power Market: A Case Study of the West Denmark DK1 Grid Region". In: *Energies* 17.12 (2024), p. 2909.

[58] J. Nowotarski and R. Weron. "Computing electricity spot price prediction intervals using quantile regression and forecast averaging". In: *Computational Statistics* 30 (2014), pp. 791–803. DOI: 10.1007/s00180-014-0523-0.

[59] Bartosz Uniejewski. "Enhancing Accuracy of Probabilistic Electricity Price Forecasting: A Comparative Study of Novel Quantile Regression Averaging Generalization". In: *2023 19th International Conference on the European Energy Market (EEM)* (2023), pp. 1–5. DOI: 10.1109/EEM58374.2023.10161748.

[60] K. Maciejowska, J. Nowotarski, and R. Weron. "Probabilistic forecasting of electricity spot prices using Factor Quantile Regression Averaging". In: *International Journal of Forecasting* 32 (2016), pp. 957–965. DOI: 10.1016/J.IJFORECAST.2014.12.004.

[61] H. Bondell, B. Reich, and H. Wang. "Noncrossing quantile regression curve estimation." In: *Biometrika* 97 4 (2010), pp. 825–838. DOI: 10.1093/BIOMET/ASQ048.

[62] Bartosz Uniejewski and R. Weron. "Regularized quantile regression averaging for probabilistic electricity price forecasting". In: *Energy Economics* (2021). DOI: 10.1016/J.ENECO.2021.105121.

[63] Yuki Osone and Daisuke Kodaira. "Quantile Regression for Probabilistic Electricity Price Forecasting in the U.K. Electricity Market". In: *IEEE Access* 13 (2025), pp. 10083–10093. DOI: 10.1109/ACCESS.2025.3528450.

[64] Haolin Yang and K. Schell. “Real-time electricity price forecasting of wind farms with deep neural network transfer learning and hybrid datasets”. In: *Applied Energy* 299 (2021), p. 117242. DOI: 10.1016/J.APENERGY.2021.117242.

[65] Ali Hooshmand and Ratnesh K. Sharma. “Energy Predictive Models with Limited Data using Transfer Learning”. In: *Proceedings of the Tenth ACM International Conference on Future Energy Systems* (2019). DOI: 10.1145/3307772.3328284.

[66] Runyao Yu et al. “OrderFusion: Encoding Orderbook for Probabilistic Intraday Price Prediction”. In: *arXiv preprint arXiv:2502.06830* (2025).

[67] Hervé Abdi and Lynne J Williams. “Principal component analysis”. In: *Wiley interdisciplinary reviews: computational statistics* 2.4 (2010), pp. 433–459.

[68] Elham Abdul-Razik Ismail. “Behavior of lasso quantile regression with small sample sizes”. In: *J. Multidiscip. Eng. Sci. Technol* 2 (2015), pp. 388–394.

[69] Elisabeth Waldmann. “Quantile regression: A short story on how and why”. In: *Statistical Modelling* 18 (2018), pp. 203–218. DOI: 10.1177/1471082X18759142.

[70] Sanlei Dang et al. “A Quantile Regression Random Forest-Based Short-Term Load Probabilistic Forecasting Method”. In: *Energies* (2022). DOI: 10.3390/en15020663.

[71] Vilde Jensen, F. Bianchi, and S. N. Anfinsen. “Ensemble Conformalized Quantile Regression for Probabilistic Time Series Forecasting”. In: *IEEE Transactions on Neural Networks and Learning Systems* 35 (2022), pp. 9014–9025. DOI: 10.1109/TNNLS.2022.3217694.

[72] Chengliang Xu et al. “Quantile regression based probabilistic forecasting of renewable energy generation and building electrical load: A state of the art review”. In: *Journal of Building Engineering* (2023). DOI: 10.1016/j.jobe.2023.107772.

[73] C. Wan et al. “Direct Quantile Regression for Nonparametric Probabilistic Forecasting of Wind Power Generation”. In: *IEEE Transactions on Power Systems* 32 (2017), pp. 2767–2778. DOI: 10.1109/TPWRS.2016.2625101.

[74] Huiting Tian, Andrew Yim, and D. Newton. “Tail-Heaviness, Asymmetry, and Profitability Forecasting by Quantile Regression”. In: *Forecasting Models eJournal* (2020). DOI: 10.2139/ssrn.3008666.

[75] Douglas C Montgomery, Elizabeth A Peck, and G Geoffrey Vining. *Introduction to linear regression analysis*. John Wiley & Sons, 2021.

[76] S Weisberg. *Applied linear regression*. 2005.

[77] Xiaogang Su, Xin Yan, and Chih-Ling Tsai. “Linear regression”. In: *Wiley Interdisciplinary Reviews: Computational Statistics* 4.3 (2012), pp. 275–294.

[78] F. Knoll et al. “Assessment of the generalization of learned image reconstruction and the potential for transfer learning”. In: *Magnetic Resonance in Medicine* 81 (2019), pp. 116–128. DOI: 10.1002/mrm.27355.

[79] Jianjun Su et al. “Enhanced transfer learning with data augmentation”. In: *Eng. Appl. Artif. Intell.* 129 (2024), p. 107602. DOI: 10.1016/j.engappai.2023.107602.

[80] Firas Ahmmed Mohammed and Moamen Abbas Mousa. “Applying Diebold–Mariano Test”. In: *Theory and Applications of Time Series Analysis: Selected Contributions from ITISE 2019* (2020), p. 443.

[81] Nagwa Elaraby, S. Barakat, and A. Rezk. “A conditional GAN-based approach for enhancing transfer learning performance in few-shot HCR tasks”. In: *Scientific Reports* 12 (2022). DOI: 10.1038/s41598-022-20654-1.

[82] Yung-Kyun Noh et al. “Transfer learning for automated optical inspection”. In: *2017 International Joint Conference on Neural Networks (IJCNN)* (2017), pp. 2517–2524. DOI: 10.1109/IJCNN.2017.7966162.

[83] Lei Zhao et al. “Hybrid Fine-Tuning Strategy for Few-Shot Classification”. In: *Computational Intelligence and Neuroscience* 2022 (2022). DOI: 10.1155/2022/9620755.

[84] Anastasia-M Leventi-Peetz and Kai Weber. “Rashomon effect and consistency in explainable artificial intelligence (XAI)”. In: *Proceedings of the Future Technologies Conference*. Springer. 2022, pp. 796–808.

[85] Joanna Janczura and Edyta Wójcik. “Dynamic short-term risk management strategies for the choice of electricity market based on probabilistic forecasts of profit and risk measures. The German and the Polish market case study”. In: *Energy Economics* 110 (2022), p. 106015.

[86] Ziming Liu et al. “Kan: Kolmogorov-arnold networks”. In: *arXiv preprint arXiv:2404.19756* (2024).

[87] Ziming Liu et al. “Kan 2.0: Kolmogorov-arnold networks meet science”. In: *arXiv preprint arXiv:2408.10205* (2024).

[88] Johannes Schmidt-Hieber. “The Kolmogorov–Arnold representation theorem revisited”. In: *Neural networks* 137 (2021), pp. 119–126.

[89] William J Gordon and Richard F Riesenfeld. “B-spline curves and surfaces”. In: *Computer aided geometric design*. Elsevier, 1974, pp. 95–126.

[90] Jinfeng Xu et al. “FourierKAN-GCF: Fourier Kolmogorov-Arnold Network–An Effective and Efficient Feature Transformation for Graph Collaborative Filtering”. In: *arXiv preprint arXiv:2406.01034* (2024).

[91] Lianqiang Li, Jie Zhu, and Ming-Ting Sun. “Deep learning based method for pruning deep neural networks”. In: *2019 IEEE International Conference on Multimedia & Expo Workshops (ICMEW)*. IEEE. 2019, pp. 312–317.

[92] Cristian J Vaca-Rubio et al. “Kolmogorov-arnold networks (kans) for time series analysis”. In: *arXiv preprint arXiv:2405.08790* (2024).

[93] Roman Bresson et al. “Kagnns: Kolmogorov-arnold networks meet graph learning”. In: *arXiv preprint arXiv:2406.18380* (2024).

[94] Timothy O Hodson. “Root mean square error (RMSE) or mean absolute error (MAE): When to use them or not”. In: *Geoscientific Model Development Discussions* 2022 (2022), pp. 1–10.

[95] Tsung-Yi Lin et al. “Focal loss for dense object detection”. In: *Proceedings of the IEEE international conference on computer vision*. 2017, pp. 2980–2988.

A

Supplementary Results

A.1. Feature Selection Results

A.1.1. L1-Penalty Selectors Results

Table A.1: Selected features of L1-penalty selectors

Case Desc.	Quantile	Num Features	Features
ID1 DE h	10	73	['MaxP_full_sell', 'DeltaP_full_sell', 'FirstV_full_sell', 'SumV_full_sell', 'TradeCount_full_sell', 'PctlP_10_full_sell', 'PctlV_90_full_sell', 'FirstP_180_sell', 'MinP_180_sell', 'VolumeVolatility_180_sell', 'PctlP_10_180_sell', 'PctlV_25_180_sell', 'PctlV_75_180_sell', 'PriceVolatility_60_sell', 'FirstV_60_sell', 'Momentum_60_sell', 'PctlV_25_60_sell', 'PriceVolatility_15_sell', 'DeltaP_15_sell', 'FirstV_15_sell', 'MaxV_15_sell', 'MedianV_5_sell', 'PctlV_10_5_sell', 'PctlV_90_5_sell', 'FirstV_1_sell', 'SumV_1_sell', 'PctlP_10_1_sell', 'PctlP_55_1_sell', 'PctlV_55_1_sell', 'PctlV_75_1_sell', 'PctlV_90_1_sell', 'FirstP_full_buy', 'MinP_full_buy', 'MaxP_full_buy', 'PriceVolatility_full_buy', 'FirstV_full_buy', 'MedianV_full_buy', 'VolumeVolatility_full_buy', 'DeltaV_full_buy', 'PctlV_45_full_buy', 'PctlV_55_full_buy', 'FirstP_180_buy', 'MinP_180_buy', 'TradeCount_180_buy', 'PctlV_55_180_buy', 'PctlV_75_180_buy', 'MinP_60_buy', 'PriceVolatility_60_buy', 'MeanV_60_buy', 'TradeCount_60_buy', 'PctlV_10_60_buy', 'PctlV_90_60_buy', 'PriceVolatility_15_buy', 'DeltaP_15_buy', 'MaxV_15_buy', 'TradeCount_15_buy', 'PctlV_10_15_buy', 'PctlV_55_15_buy', 'MinP_5_buy', 'DeltaP_5_buy', 'TradeCount_5_buy', 'PctlV_55_5_buy', 'PctlV_90_5_buy', 'MinP_1_buy', 'MaxP_1_buy', 'PriceVolatility_1_buy', 'DeltaP_1_buy', 'MaxV_1_buy', 'SumV_1_buy', 'PctlP_10_1_buy', 'PctlV_10_1_buy', 'PctlV_45_1_buy', 'PctlV_90_1_buy']

Case Desc.	Quantile	Num Features	Features
	25	93	['MaxP_full_sell', 'PriceVolatility_full_sell', 'DeltaP_full_sell', 'FirstV_full_sell', 'Momentum_full_sell', 'SumV_full_sell', 'TradeCount_full_sell', 'PctlV_25_full_sell', 'PctlV_45_full_sell', 'PctlV_55_full_sell', 'PctlV_90_full_sell', 'LastP_180_sell', 'MinP_180_sell', 'FirstV_180_sell', 'VolumeVolatility_180_sell', 'Momentum_180_sell', 'PctlP_10_180_sell', 'PctlV_10_180_sell', 'PriceVolatility_60_sell', 'FirstV_60_sell', 'MedianV_60_sell', 'PctlV_10_60_sell', 'PctlV_90_60_sell', 'PriceVolatility_15_sell', 'DeltaP_15_sell', 'SumV_15_sell', 'TradeCount_15_sell', 'PctlV_25_15_sell', 'PctlV_75_15_sell', 'FirstP_5_sell', 'MinV_5_sell', 'Momentum_5_sell', 'PctlV_10_5_sell', 'PriceVolatility_1_sell', 'FirstV_1_sell', 'MedianV_1_sell', 'MinV_1_sell', 'MaxV_1_sell', 'Momentum_1_sell', 'SumV_1_sell', 'PctlP_25_1_sell', 'PctlP_55_1_sell', 'PctlV_55_1_sell', 'PctlV_90_1_sell', 'FirstP_full_buy', 'MinP_full_buy', 'PriceVolatility_full_buy', 'FirstV_full_buy', 'MedianV_full_buy', 'VolumeVolatility_full_buy', 'DeltaV_full_buy', 'Momentum_full_buy', 'PctlV_10_full_buy', 'PctlV_55_full_buy', 'FirstP_180_buy', 'FirstV_180_buy', 'MeanV_180_buy', 'TradeCount_180_buy', 'MinP_60_buy', 'PriceVolatility_60_buy', 'FirstV_60_buy', 'MaxV_60_buy', 'Momentum_60_buy', 'PctlV_10_60_buy', 'MaxP_15_buy', 'DeltaP_15_buy', 'FirstV_15_buy', 'MaxV_15_buy', 'Momentum_15_buy', 'TradeCount_15_buy', 'PctlV_25_15_buy', 'PctlV_75_15_buy', 'MinP_5_buy', 'MinV_5_buy', 'VolumeVolatility_5_buy', 'Momentum_5_buy', 'SumV_5_buy', 'TradeCount_5_buy', 'PctlP_90_5_buy', 'PctlV_90_5_buy', 'FirstP_1_buy', 'MinP_1_buy', 'MaxP_1_buy', 'PriceVolatility_1_buy', 'FirstV_1_buy', 'MaxV_1_buy', 'VWAP_1_buy', 'SumV_1_buy', 'PctlP_10_1_buy', 'PctlP_75_1_buy', 'PctlP_90_1_buy', 'PctlV_10_1_buy', 'PctlV_90_1_buy']
	45	52	['DeltaP_full_sell', 'DeltaV_full_sell', 'Momentum_full_sell', 'TradeCount_full_sell', 'PctlV_25_full_sell', 'PctlV_90_full_sell', 'PriceVolatility_180_sell', 'MaxV_180_sell', 'VolumeVolatility_180_sell', 'Momentum_180_sell', 'PriceVolatility_60_sell', 'TradeCount_60_sell', 'LastP_15_sell', 'MinP_15_sell', 'SumV_15_sell', 'TradeCount_15_sell', 'FirstP_5_sell', 'PctlP_45_5_sell', 'PctlV_10_5_sell', 'PctlV_90_5_sell', 'MinV_1_sell', 'VolumeVolatility_1_sell', 'TradeCount_1_sell', 'PctlP_75_1_sell', 'FirstP_full_buy', 'PriceVolatility_full_buy', 'VolumeVolatility_full_buy', 'PctlV_10_full_buy', 'FirstP_180_buy', 'SumV_180_buy', 'TradeCount_180_buy', 'LastP_60_buy', 'MeanV_60_buy', 'MaxV_60_buy', 'DeltaP_15_buy', 'FirstV_15_buy', 'TradeCount_15_buy', 'PctlP_90_15_buy', 'PctlV_25_15_buy', 'PctlV_90_15_buy', 'MinP_5_buy', 'DeltaV_5_buy', 'TradeCount_5_buy', 'PctlP_10_5_buy', 'PctlV_75_5_buy', 'PctlV_90_5_buy', 'MinP_1_buy', 'PriceVolatility_1_buy', 'SumV_1_buy', 'PctlP_10_1_buy', 'PctlP_75_1_buy', 'PctlV_75_1_buy']
	50	20	['LastP_full_sell', 'DeltaP_full_sell', 'TradeCount_full_sell', 'TradeCount_60_sell', 'SumV_15_sell', 'TradeCount_15_sell', 'MedianP_5_sell', 'PctlP_75_1_sell', 'SumV_180_buy', 'LastP_60_buy', 'MeanV_60_buy', 'SumV_15_buy', 'TradeCount_15_buy', 'PctlP_90_15_buy', 'TradeCount_5_buy', 'PctlP_10_5_buy', 'MinP_1_buy', 'SumV_1_buy', 'PctlP_10_1_buy', 'PctlP_75_1_buy']
	55	24	['TradeCount_full_sell', 'TradeCount_60_sell', 'LastP_15_sell', 'SumV_15_sell', 'TradeCount_15_sell', 'FirstP_5_sell', 'MedianP_5_sell', 'PctlP_75_1_sell', 'PctlP_90_1_sell', 'FirstP_full_buy', 'MeanV_180_buy', 'LastP_60_buy', 'MeanV_60_buy', 'SumV_15_buy', 'TradeCount_15_buy', 'PctlP_90_15_buy', 'SumV_5_buy', 'TradeCount_5_buy', 'PctlP_10_5_buy', 'PctlP_25_5_buy', 'MinP_1_buy', 'SumV_1_buy', 'PctlP_10_1_buy', 'PctlP_75_1_buy']
	75	23	['DeltaP_full_sell', 'TradeCount_60_sell', 'SumV_15_sell', 'TradeCount_15_sell', 'FirstP_5_sell', 'MedianP_5_sell', 'MaxP_5_sell', 'PctlP_25_5_sell', 'VWAP_1_sell', 'PctlP_90_1_sell', 'FirstP_full_buy', 'MeanV_180_buy', 'LastP_60_buy', 'MedianV_60_buy', 'MeanV_60_buy', 'SumV_15_buy', 'TradeCount_15_buy', 'PctlP_90_15_buy', 'PctlP_90_5_buy', 'MinP_1_buy', 'SumV_1_buy', 'TradeCount_1_buy', 'PctlP_10_1_buy']

Case Desc.	Quantile	Num Features	Features
	90	120	['LastP_full_sell', 'MinP_full_sell', 'PriceVolatility_full_sell', 'DeltaP_full_sell', 'FirstV_full_sell', 'MeanV_full_sell', 'Momentum_full_sell', 'PctlP_10_full_sell', 'PctlV_10_full_sell', 'PctlV_45_full_sell', 'MinP_180_sell', 'MaxP_180_sell', 'PriceVolatility_180_sell', 'DeltaP_180_sell', 'FirstV_180_sell', 'MedianV_180_sell', 'MaxV_180_sell', 'Momentum_180_sell', 'SumV_180_sell', 'PctlV_10_180_sell', 'PctlV_90_180_sell', 'MaxP_60_sell', 'PriceVolatility_60_sell', 'MedianV_60_sell', 'MaxV_60_sell', 'Momentum_60_sell', 'TradeCount_60_sell', 'PctlV_10_60_sell', 'PctlV_25_60_sell', 'PctlV_55_60_sell', 'PctlV_90_60_sell', 'MinP_15_sell', 'DeltaP_15_sell', 'FirstV_15_sell', 'MedianV_15_sell', 'VolumeVolatility_15_sell', 'Momentum_15_sell', 'SumV_15_sell', 'TradeCount_15_sell', 'PctlV_10_15_sell', 'PctlV_25_15_sell', 'PctlV_75_15_sell', 'PctlV_90_15_sell', 'MaxP_5_sell', 'PriceVolatility_5_sell', 'DeltaP_5_sell', 'FirstV_5_sell', 'MedianV_5_sell', 'MinV_5_sell', 'VolumeVolatility_5_sell', 'Momentum_5_sell', 'TradeCount_5_sell', 'PctlP_25_5_sell', 'PctlV_10_5_sell', 'PctlV_25_5_sell', 'PctlV_75_5_sell', 'PctlV_90_5_sell', 'FirstP_1_sell', 'MinP_1_sell', 'FirstV_1_sell', 'MinV_1_sell', 'MaxV_1_sell', 'VWAP_1_sell', 'Momentum_1_sell', 'SumV_1_sell', 'TradeCount_1_sell', 'PctlP_10_1_sell', 'PctlV_45_1_sell', 'PctlV_55_1_sell', 'PctlV_90_1_sell', 'FirstP_full_buy', 'MinP_full_buy', 'PriceVolatility_full_buy', 'MaxV_full_buy', 'TradeCount_full_buy', 'PctlV_25_full_buy', 'PctlV_55_full_buy', 'MinP_180_buy', 'MaxP_180_buy', 'FirstV_180_buy', 'MaxV_180_buy', 'DeltaV_180_buy', 'PctlV_10_180_buy', 'PctlV_45_180_buy', 'PctlV_75_180_buy', 'PctlV_90_180_buy', 'FirstP_60_buy', 'PriceVolatility_60_buy', 'FirstV_60_buy', 'MeanV_60_buy', 'Momentum_60_buy', 'PctlV_45_60_buy', 'PctlV_55_60_buy', 'MaxP_15_buy', 'PriceVolatility_15_buy', 'DeltaP_15_buy', 'Momentum_15_buy', 'SumV_15_buy', 'TradeCount_15_buy', 'PctlP_90_15_buy', 'PctlV_25_15_buy', 'PctlV_45_15_buy', 'PctlV_90_15_buy', 'MaxP_5_buy', 'DeltaP_5_buy', 'FirstV_5_buy', 'MaxV_5_buy', 'SumV_5_buy', 'PctlV_45_5_buy', 'PctlV_55_5_buy', 'PctlV_75_5_buy', 'MinP_1_buy', 'PriceVolatility_1_buy', 'DeltaP_1_buy', 'FirstV_1_buy', 'MinV_1_buy', 'MaxV_1_buy', 'Momentum_1_buy', 'SumV_1_buy', 'TradeCount_1_buy']
ID1 AT h	10	40	['MinP_full_sell', 'PriceVolatility_full_sell', 'DeltaP_full_sell', 'MaxV_full_sell', 'VolumeVolatility_full_sell', 'PctlP_10_full_sell', 'PctlV_25_full_sell', 'DeltaP_180_sell', 'MaxV_180_sell', 'TradeCount_180_sell', 'PctlP_10_180_sell', 'PctlV_10_180_sell', 'PctlV_75_180_sell', 'DeltaP_60_sell', 'TradeCount_60_sell', 'TradeCount_15_sell', 'PctlP_25_15_sell', 'PctlV_75_15_sell', 'VWAP_5_sell', 'VWAP_1_sell', 'MinP_full_buy', 'DeltaV_full_buy', 'SumV_full_buy', 'PctlV_25_full_buy', 'MinP_180_buy', 'PctlV_90_180_buy', 'MinP_60_buy', 'TradeCount_60_buy', 'PctlV_90_60_buy', 'FirstP_15_buy', 'MaxP_15_buy', 'MinV_15_buy', 'MaxV_15_buy', 'TradeCount_15_buy', 'PctlP_10_15_buy', 'MaxV_5_buy', 'PctlV_75_5_buy', 'FirstP_1_buy', 'MinP_1_buy', 'MedianV_1_buy']
	25	24	['PctlP_10_full_sell', 'PctlP_45_full_sell', 'TradeCount_180_sell', 'PctlP_25_180_sell', 'TradeCount_60_sell', 'PctlP_25_60_sell', 'PctlP_25_15_sell', 'VWAP_5_sell', 'FirstP_1_sell', 'LastP_1_sell', 'PctlP_75_1_sell', 'PctlP_90_1_sell', 'MinP_full_buy', 'PctlP_10_full_buy', 'MinP_180_buy', 'VWAP_60_buy', 'SumV_60_buy', 'FirstP_15_buy', 'MedianP_15_buy', 'TradeCount_15_buy', 'PctlP_10_15_buy', 'FirstP_1_buy', 'MeanP_1_buy', 'PctlP_10_1_buy']
	45	27	['VWAP_full_sell', 'PctlP_45_full_sell', 'PctlP_75_full_sell', 'VWAP_180_sell', 'TradeCount_180_sell', 'VWAP_60_sell', 'TradeCount_60_sell', 'PctlP_45_15_sell', 'VWAP_5_sell', 'PctlP_55_5_sell', 'LastP_1_sell', 'PctlP_90_1_sell', 'VWAP_full_buy', 'PctlP_55_180_buy', 'SumV_60_buy', 'TradeCount_60_buy', 'FirstP_15_buy', 'MedianP_15_buy', 'TradeCount_15_buy', 'PctlP_10_15_buy', 'PctlP_45_15_buy', 'MedianP_5_buy', 'PctlP_25_5_buy', 'FirstP_1_buy', 'MeanP_1_buy', 'VWAP_1_buy', 'PctlP_25_1_buy']

Case Desc.	Quantile	Num Features	Features
	50	25	['PctlP_75_full_sell', 'VWAP_180_sell', 'TradeCount_180_sell', 'VWAP_60_sell', 'TradeCount_60_sell', 'PctlP_75_60_sell', 'VWAP_15_sell', 'PctlP_45_15_sell', 'PctlP_75_15_sell', 'VWAP_5_sell', 'LastP_1_sell', 'MaxP_1_sell', 'PctlP_90_1_sell', 'VWAP_full_buy', 'PctlP_75_full_buy', 'PctlP_55_180_buy', 'TradeCount_60_buy', 'FirstP_15_buy', 'TradeCount_15_buy', 'PctlP_45_15_buy', 'MedianP_5_buy', 'FirstP_1_buy', 'MeanP_1_buy', 'VWAP_1_buy', 'PctlP_25_1_buy']
	55	22	['FirstP_full_sell', 'PctlP_90_full_sell', 'TradeCount_60_sell', 'PctlP_75_60_sell', 'VWAP_15_sell', 'PctlP_75_15_sell', 'VWAP_5_sell', 'PctlP_75_5_sell', 'LastP_1_sell', 'MaxP_1_sell', 'PctlP_90_1_sell', 'VWAP_full_buy', 'PctlP_75_full_buy', 'PctlP_55_180_buy', 'TradeCount_60_buy', 'MedianP_15_buy', 'TradeCount_15_buy', 'PctlP_45_15_buy', 'PctlP_45_5_buy', 'FirstP_1_buy', 'VWAP_1_buy', 'PctlP_25_1_buy']
	75	45	['MaxP_full_sell', 'PriceVolatility_full_sell', 'VolumeVolatility_full_sell', 'PctlV_90_full_sell', 'MaxP_180_sell', 'FirstV_180_sell', 'MinV_180_sell', 'TradeCount_180_sell', 'MaxP_60_sell', 'DeltaP_60_sell', 'Momentum_60_sell', 'TradeCount_60_sell', 'PctlV_75_60_sell', 'MaxP_15_sell', 'DeltaP_15_sell', 'LastV_15_sell', 'MinV_15_sell', 'TradeCount_15_sell', 'PctlV_90_15_sell', 'LastP_5_sell', 'MaxP_5_sell', 'MinV_5_sell', 'VWAP_5_sell', 'TradeCount_5_sell', 'PctlP_25_5_sell', 'PctlP_55_5_sell', 'PctlV_90_5_sell', 'MaxP_1_sell', 'PctlP_90_1_sell', 'FirstP_full_buy', 'MinV_full_buy', 'Momentum_full_buy', 'PctlP_75_full_buy', 'PctlP_90_full_buy', 'FirstV_180_buy', 'DeltaV_180_buy', 'TradeCount_180_buy', 'TradeCount_60_buy', 'PctlV_25_60_buy', 'MedianP_15_buy', 'TradeCount_15_buy', 'Momentum_5_buy', 'VolumeVolatility_1_buy', 'PctlP_10_1_buy', 'PctlP_45_1_buy']
	90	67	['FirstP_full_sell', 'MinP_full_sell', 'MaxP_full_sell', 'PriceVolatility_full_sell', 'FirstV_full_sell', 'MedianV_full_sell', 'MinV_full_sell', 'VolumeVolatility_full_sell', 'TradeCount_full_sell', 'PctlV_25_full_sell', 'PctlV_90_full_sell', 'MaxP_180_sell', 'PriceVolatility_180_sell', 'FirstV_180_sell', 'MinV_180_sell', 'MaxP_60_sell', 'Momentum_60_sell', 'TradeCount_60_sell', 'PctlV_10_60_sell', 'PctlV_75_60_sell', 'PctlV_90_60_sell', 'MaxP_15_sell', 'DeltaP_15_sell', 'FirstV_15_sell', 'MinV_15_sell', 'TradeCount_15_sell', 'PctlV_90_15_sell', 'FirstP_5_sell', 'MaxP_5_sell', 'PriceVolatility_5_sell', 'MinV_5_sell', 'TradeCount_5_sell', 'PctlP_10_5_sell', 'PctlP_90_5_sell', 'PctlV_55_5_sell', 'FirstV_1_sell', 'DeltaV_1_sell', 'TradeCount_1_sell', 'MaxP_full_buy', 'MaxV_full_buy', 'PctlP_75_full_buy', 'PctlP_90_full_buy', 'PctlV_75_full_buy', 'FirstV_180_buy', 'MinV_180_buy', 'DeltaV_180_buy', 'TradeCount_180_buy', 'PctlV_90_180_buy', 'MinP_60_buy', 'VolumeVolatility_60_buy', 'DeltaV_60_buy', 'SumV_60_buy', 'TradeCount_60_buy', 'PctlV_25_60_buy', 'MedianP_15_buy', 'MaxP_15_buy', 'TradeCount_15_buy', 'PctlV_10_15_buy', 'MaxV_5_buy', 'PctlP_25_5_buy', 'PctlV_55_5_buy', 'VolumeVolatility_1_buy', 'TradeCount_1_buy', 'PctlP_10_1_buy', 'PctlP_25_1_buy', 'PctlP_45_1_buy', 'PctlV_55_1_buy']

Case Desc.	Quantile	Num Features	Features
ID2 DE h	10	119	['FirstP_full_sell', 'MaxP_full_sell', 'PriceVolatility_full_sell', 'VolumeVolatility_full_sell', 'SumV_full_sell', 'TradeCount_full_sell', 'PctlP_90_full_sell', 'PctlV_45_full_sell', 'PctlV_90_full_sell', 'FirstP_180_sell', 'MinP_180_sell', 'MaxP_180_sell', 'FirstV_180_sell', 'VolumeVolatility_180_sell', 'Momentum_180_sell', 'PctlV_10_180_sell', 'PctlV_25_180_sell', 'PctlV_55_180_sell', 'FirstP_60_sell', 'MinP_60_sell', 'MedianV_60_sell', 'MaxV_60_sell', 'VolumeVolatility_60_sell', 'Momentum_60_sell', 'PctlV_10_60_sell', 'PctlV_75_60_sell', 'PctlV_90_60_sell', 'MinP_15_sell', 'VolumeVolatility_15_sell', 'TradeCount_15_sell', 'PctlP_25_15_sell', 'PctlV_25_15_sell', 'PctlV_45_15_sell', 'PctlV_90_15_sell', 'FirstP_5_sell', 'MinP_5_sell', 'DeltaP_5_sell', 'MedianV_5_sell', 'MaxV_5_sell', 'VolumeVolatility_5_sell', 'TradeCount_5_sell', 'PctlP_10_5_sell', 'PctlP_75_5_sell', 'PctlV_10_5_sell', 'PctlV_45_5_sell', 'FirstP_1_sell', 'MinP_1_sell', 'PriceVolatility_1_sell', 'LastV_1_sell', 'MedianV_1_sell', 'MaxV_1_sell', 'SumV_1_sell', 'PctlV_75_1_sell', 'FirstP_full_buy', 'MinP_full_buy', 'MaxP_full_buy', 'PriceVolatility_full_buy', 'FirstV_full_buy', 'MedianV_full_buy', 'MaxV_full_buy', 'VolumeVolatility_full_buy', 'Momentum_full_buy', 'TradeCount_full_buy', 'PctlV_25_full_buy', 'FirstP_180_buy', 'MinP_180_buy', 'MaxP_180_buy', 'PriceVolatility_180_buy', 'MaxV_180_buy', 'Momentum_180_buy', 'PctlV_90_180_buy', 'PctlV_25_180_buy', 'PctlV_45_180_buy', 'PctlV_90_180_buy', 'FirstP_60_buy', 'MinP_60_buy', 'PriceVolatility_60_buy', 'FirstV_60_buy', 'MaxV_60_buy', 'TradeCount_60_buy', 'PctlP_90_60_buy', 'PctlV_10_60_buy', 'PctlV_25_60_buy', 'PctlV_55_60_buy', 'FirstP_15_buy', 'MinP_15_buy', 'MaxP_15_buy', 'PriceVolatility_15_buy', 'DeltaP_15_buy', 'MedianV_15_buy', 'MinV_15_buy', 'MaxV_15_buy', 'DeltaV_15_buy', 'Momentum_15_buy', 'TradeCount_15_buy', 'PctlP_90_15_buy', 'PctlV_25_15_buy', 'PctlV_45_15_buy', 'PctlV_75_15_buy', 'MinP_5_buy', 'DeltaP_5_buy', 'FirstV_5_buy', 'MinV_5_buy', 'TradeCount_5_buy', 'PctlP_55_5_buy', 'PctlV_90_5_buy', 'PctlV_10_5_buy', 'PctlV_25_5_buy', 'PctlV_45_5_buy', 'PctlV_75_5_buy', 'MinP_1_buy', 'MaxP_1_buy', 'FirstV_1_buy', 'MinV_1_buy', 'VolumeVolatility_1_buy', 'VWAP_1_buy', 'Momentum_1_buy', 'PctlP_75_1_buy', 'PctlV_55_1_buy']
	25	74	['FirstP_full_sell', 'MinP_full_sell', 'MaxP_full_sell', 'PriceVolatility_full_sell', 'FirstV_full_sell', 'Momentum_full_sell', 'SumV_full_sell', 'PctlV_90_full_sell', 'MinP_180_sell', 'FirstV_180_sell', 'PctlV_10_180_sell', 'PctlV_75_180_sell', 'PctlV_90_180_sell', 'MaxV_60_sell', 'PctlV_10_60_sell', 'PctlV_75_60_sell', 'MeanV_15_sell', 'MinV_15_sell', 'VolumeVolatility_15_sell', 'TradeCount_15_sell', 'PctlP_25_15_sell', 'FirstP_5_sell', 'MinP_5_sell', 'PriceVolatility_5_sell', 'MinV_5_sell', 'VolumeVolatility_5_sell', 'TradeCount_5_sell', 'PctlP_75_5_sell', 'PctlV_45_5_sell', 'PctlV_75_5_sell', 'PctlV_90_5_sell', 'MinP_1_sell', 'PriceVolatility_1_sell', 'MaxV_1_sell', 'Momentum_1_sell', 'SumV_1_sell', 'PctlV_10_1_sell', 'FirstP_full_buy', 'MinP_full_buy', 'PriceVolatility_full_buy', 'FirstV_full_buy', 'MedianV_full_buy', 'PctlV_10_full_buy', 'MinP_180_buy', 'PriceVolatility_180_buy', 'MaxV_180_buy', 'PctlV_25_180_buy', 'MinP_60_buy', 'FirstV_60_buy', 'TradeCount_60_buy', 'PctlV_10_60_buy', 'PctlV_25_60_buy', 'MinP_15_buy', 'MinV_15_buy', 'VolumeVolatility_15_buy', 'TradeCount_15_buy', 'PctlV_10_15_buy', 'PctlV_25_15_buy', 'PctlV_55_15_buy', 'FirstP_5_buy', 'MeanP_5_buy', 'MinP_5_buy', 'MaxP_5_buy', 'DeltaP_5_buy', 'FirstV_5_buy', 'Momentum_5_buy', 'TradeCount_5_buy', 'PctlV_10_5_buy', 'PctlV_75_5_buy', 'PctlV_90_5_buy', 'MaxV_1_buy', 'Momentum_1_buy', 'PctlP_75_1_buy', 'PctlV_75_1_buy']
	45	11	['TradeCount_full_sell', 'PctlP_25_15_sell', 'PctlP_75_5_sell', 'PctlP_90_5_sell', 'MinP_full_buy', 'MeanP_60_buy', 'MeanP_15_buy', 'MinP_15_buy', 'PctlP_10_15_buy', 'FirstP_5_buy', 'MinP_5_buy']

Case Desc.	Quantile	Num Features	Features
	50	37	['FirstP_full_sell', 'TradeCount_full_sell', 'PctlV_10_full_sell', 'Momentum_180_sell', 'PctlV_75_180_sell', 'FirstV_60_sell', 'Momentum_15_sell', 'PctlP_25_15_sell', 'MaxP_5_sell', 'MeanV_5_sell', 'Momentum_5_sell', 'PctlP_75_5_sell', 'PctlP_90_5_sell', 'PctlV_10_5_sell', 'PctlV_55_5_sell', 'MeanV_1_sell', 'MaxV_1_sell', 'TradeCount_1_sell', 'PctlV_75_1_sell', 'MinP_full_buy', 'PriceVolatility_full_buy', 'FirstP_180_buy', 'SumV_180_buy', 'PctlV_55_180_buy', 'PctlV_75_180_buy', 'MeanP_15_buy', 'MinP_15_buy', 'SumV_15_buy', 'TradeCount_15_buy', 'PctlP_10_15_buy', 'FirstP_5_buy', 'MeanP_5_buy', 'MinP_5_buy', 'MaxP_5_buy', 'PctlV_10_5_buy', 'DeltaP_1_buy', 'TradeCount_1_buy']
	55	10	['PctlP_25_15_sell', 'MaxP_5_sell', 'PctlP_75_5_sell', 'PctlP_90_5_sell', 'PctlV_75_180_buy', 'MeanP_60_buy', 'MeanP_15_buy', 'PctlP_10_15_buy', 'PctlP_55_15_buy', 'MinP_5_buy']
	75	11	['MaxP_full_sell', 'DeltaP_full_sell', 'MaxP_180_sell', 'MaxP_15_sell', 'MaxP_5_sell', 'PctlP_55_5_sell', 'TradeCount_1_sell', 'PctlV_75_180_buy', 'MeanP_15_buy', 'PctlP_10_5_buy', 'TradeCount_1_buy']
	90	114	['FirstP_full_sell', 'MinP_full_sell', 'MaxP_full_sell', 'PriceVolatility_full_sell', 'FirstV_full_sell', 'MeanV_full_sell', 'MaxV_full_sell', 'VolumeVolatility_full_sell', 'Momentum_full_sell', 'PctlP_10_full_sell', 'PctlV_10_full_sell', 'PctlV_90_full_sell', 'MinP_180_sell', 'MaxP_180_sell', 'FirstV_180_sell', 'MaxV_180_sell', 'PctlP_10_180_sell', 'PctlV_10_180_sell', 'PctlV_55_180_sell', 'MinP_60_sell', 'MaxP_60_sell', 'FirstV_60_sell', 'MedianV_60_sell', 'SumV_60_sell', 'PctlV_10_60_sell', 'PctlV_45_60_sell', 'MinP_15_sell', 'MaxP_15_sell', 'FirstV_15_sell', 'MinV_15_sell', 'VolumeVolatility_15_sell', 'DeltaV_15_sell', 'Momentum_15_sell', 'SumV_15_sell', 'TradeCount_15_sell', 'PctlP_25_15_sell', 'PctlV_25_15_sell', 'PctlV_45_15_sell', 'PctlV_55_15_sell', 'PctlV_90_15_sell', 'FirstP_5_sell', 'PriceVolatility_5_sell', 'MedianV_5_sell', 'MinV_5_sell', 'MaxV_5_sell', 'Momentum_5_sell', 'PctlP_10_5_sell', 'PctlP_25_5_sell', 'PctlV_10_5_sell', 'PctlV_25_5_sell', 'PctlV_75_5_sell', 'PctlV_90_5_sell', 'MinP_1_sell', 'DeltaP_1_sell', 'FirstV_1_sell', 'MaxV_1_sell', 'Momentum_1_sell', 'SumV_1_sell', 'PctlP_45_1_sell', 'PctlV_25_1_sell', 'PctlV_45_1_sell', 'PctlV_75_1_sell', 'PctlV_90_1_sell', 'FirstP_full_buy', 'MinP_full_buy', 'MeanV_full_buy', 'Momentum_full_buy', 'TradeCount_full_buy', 'PctlP_10_full_buy', 'PctlV_10_full_buy', 'PctlV_45_full_buy', 'PctlV_55_full_buy', 'PctlV_90_full_buy', 'FirstP_180_buy', 'FirstV_180_buy', 'PctlV_10_180_buy', 'PctlV_25_180_buy', 'PctlV_55_180_buy', 'PctlV_75_180_buy', 'FirstP_60_buy', 'MaxP_60_buy', 'PriceVolatility_60_buy', 'FirstV_60_buy', 'MaxV_60_buy', 'DeltaV_60_buy', 'Momentum_60_buy', 'MinV_15_buy', 'DeltaV_15_buy', 'Momentum_15_buy', 'TradeCount_15_buy', 'PctlP_75_15_buy', 'PctlP_90_15_buy', 'PctlV_10_15_buy', 'PctlV_45_15_buy', 'FirstP_5_buy', 'MaxP_5_buy', 'DeltaP_5_buy', 'FirstV_5_buy', 'MinV_5_buy', 'MaxV_5_buy', 'PctlP_10_5_buy', 'PctlV_10_5_buy', 'PctlV_25_5_buy', 'PctlV_45_5_buy', 'PctlV_55_5_buy', 'PctlV_75_5_buy', 'MinP_1_buy', 'PriceVolatility_1_buy', 'FirstV_1_buy', 'VolumeVolatility_1_buy', 'SumV_1_buy', 'PctlP_55_1_buy', 'PctlP_90_1_buy', 'PctlV_75_1_buy']
ID2 AT h	10	36	['MinP_full_sell', 'PriceVolatility_full_sell', 'DeltaP_full_sell', 'MeanV_full_sell', 'MinV_full_sell', 'DeltaP_180_sell', 'FirstV_180_sell', 'VolumeVolatility_180_sell', 'MinP_60_sell', 'PriceVolatility_60_sell', 'DeltaP_60_sell', 'FirstV_60_sell', 'MeanV_60_sell', 'MinV_60_sell', 'PctlP_25_60_sell', 'PctlV_75_60_sell', 'MinP_15_sell', 'PctlP_10_15_sell', 'LastP_5_sell', 'MaxP_5_sell', 'MaxP_1_sell', 'VWAP_1_sell', 'MinP_full_buy', 'PriceVolatility_full_buy', 'MinV_full_buy', 'MaxV_full_buy', 'Momentum_full_buy', 'SumV_full_buy', 'MinP_180_buy', 'MinP_60_buy', 'PriceVolatility_60_buy', 'MinV_60_buy', 'TradeCount_60_buy', 'DeltaP_15_buy', 'TradeCount_15_buy', 'MinP_5_buy']
	25	16	['MinP_full_sell', 'PctlP_10_full_sell', 'MinP_180_sell', 'PctlP_25_60_sell', 'MinP_15_sell', 'LastP_5_sell', 'MinP_5_sell', 'MaxP_5_sell', 'VWAP_5_sell', 'PctlP_75_5_sell', 'MinP_1_sell', 'VWAP_1_sell', 'MinP_full_buy', 'MinP_180_buy', 'MinP_60_buy', 'MinP_1_buy']

Case Desc.	Quantile	Num Features	Features
	45	46	['PctlP_55_full_sell', 'PctlV_10_full_sell', 'PctlV_25_full_sell', 'VolumeVolatility_180_sell', 'VWAP_180_sell', 'SumV_180_sell', 'TradeCount_180_sell', 'FirstV_60_sell', 'DeltaV_60_sell', 'VWAP_60_sell', 'SumV_60_sell', 'TradeCount_60_sell', 'MedianP_15_sell', 'DeltaP_15_sell', 'MinV_15_sell', 'VolumeVolatility_15_sell', 'VWAP_15_sell', 'PctlP_75_15_sell', 'LastP_5_sell', 'MaxP_5_sell', 'VWAP_5_sell', 'MaxP_1_sell', 'FirstV_1_sell', 'VWAP_1_sell', 'PctlP_75_1_sell', 'FirstP_full_buy', 'LastP_full_buy', 'MinP_full_buy', 'VolumeVolatility_full_buy', 'Momentum_full_buy', 'TradeCount_full_buy', 'FirstP_180_buy', 'MinP_180_buy', 'PctlP_45_180_buy', 'PctlV_90_180_buy', 'MinP_60_buy', 'MinV_60_buy', 'TradeCount_60_buy', 'PctlP_25_60_buy', 'PctlP_45_60_buy', 'PctlV_90_60_buy', 'FirstV_15_buy', 'TradeCount_15_buy', 'PctlV_90_15_buy', 'MinP_1_buy', 'PctlP_45_1_buy']
	50	41	['PriceVolatility_full_sell', 'PctlP_75_full_sell', 'PctlV_10_full_sell', 'PctlV_75_full_sell', 'VolumeVolatility_180_sell', 'SumV_180_sell', 'TradeCount_180_sell', 'PctlP_75_180_sell', 'PctlP_90_180_sell', 'MaxP_60_sell', 'DeltaV_60_sell', 'VWAP_60_sell', 'TradeCount_60_sell', 'DeltaP_15_sell', 'MinV_15_sell', 'MaxV_15_sell', 'VWAP_15_sell', 'LastP_5_sell', 'MaxP_5_sell', 'PctlP_90_5_sell', 'MaxP_1_sell', 'FirstV_1_sell', 'VWAP_1_sell', 'PctlP_75_1_sell', 'FirstP_full_buy', 'LastP_full_buy', 'VolumeVolatility_full_buy', 'FirstP_180_buy', 'PctlP_45_180_buy', 'PctlV_90_180_buy', 'MinP_60_buy', 'MinV_60_buy', 'TradeCount_60_buy', 'PctlP_25_60_buy', 'PctlP_45_60_buy', 'MinP_15_buy', 'TradeCount_15_buy', 'PctlV_90_15_buy', 'MinP_1_buy', 'TradeCount_1_buy', 'PctlP_45_1_buy']
	55	20	['PctlP_75_full_sell', 'TradeCount_180_sell', 'PctlP_90_180_sell', 'MaxP_60_sell', 'VWAP_60_sell', 'LastP_5_sell', 'MaxP_5_sell', 'VWAP_5_sell', 'PctlP_90_5_sell', 'VWAP_1_sell', 'PctlP_75_1_sell', 'PctlP_90_1_sell', 'FirstP_full_buy', 'LastP_full_buy', 'FirstP_180_buy', 'PctlP_45_180_buy', 'PctlP_45_60_buy', 'TradeCount_15_buy', 'MinP_1_buy', 'PctlP_45_1_buy']
	75	39	['MaxP_full_sell', 'PriceVolatility_full_sell', 'SumV_full_sell', 'PctlV_10_full_sell', 'PctlV_90_full_sell', 'MaxP_180_sell', 'VolumeVolatility_180_sell', 'SumV_180_sell', 'TradeCount_180_sell', 'PctlV_90_180_sell', 'PctlV_25_180_sell', 'MaxP_60_sell', 'MinV_60_sell', 'SumV_60_sell', 'TradeCount_60_sell', 'DeltaP_15_sell', 'MinV_15_sell', 'VWAP_15_sell', 'PctlP_90_15_sell', 'PctlV_75_15_sell', 'LastP_5_sell', 'MaxP_5_sell', 'Momentum_5_sell', 'PctlP_90_5_sell', 'MinV_1_sell', 'Momentum_1_sell', 'FirstP_full_buy', 'LastP_full_buy', 'PriceVolatility_full_buy', 'MaxV_full_buy', 'VolumeVolatility_full_buy', 'PctlP_75_full_buy', 'PctlP_90_full_buy', 'PctlP_75_180_buy', 'VWAP_15_buy', 'MaxP_5_buy', 'VWAP_5_buy', 'MaxP_1_buy', 'PctlP_45_1_buy']
	90	32	['MaxP_full_sell', 'PriceVolatility_full_sell', 'SumV_full_sell', 'TradeCount_full_sell', 'PctlV_10_full_sell', 'PctlV_25_full_sell', 'MaxP_180_sell', 'PriceVolatility_180_sell', 'DeltaP_180_sell', 'PctlV_10_180_sell', 'PctlV_25_180_sell', 'MaxP_60_sell', 'DeltaP_60_sell', 'MinV_60_sell', 'SumV_60_sell', 'TradeCount_60_sell', 'MaxP_15_sell', 'DeltaP_15_sell', 'PriceVolatility_5_sell', 'MaxP_1_sell', 'PriceVolatility_1_sell', 'Momentum_1_sell', 'PctlP_90_1_sell', 'PriceVolatility_full_buy', 'PctlP_90_180_buy', 'LastP_60_buy', 'MaxP_60_buy', 'DeltaP_60_buy', 'MaxP_15_buy', 'VWAP_15_buy', 'VWAP_5_buy', 'MaxP_1_buy']

Case Desc.	Quantile	Num Features	Features
ID3 DE h	10	61	['MinP_full_sell', 'MaxP_full_sell', 'PriceVolatility_full_sell', 'DeltaP_full_sell', 'LastV_full_sell', 'MaxV_full_sell', 'SumV_full_sell', 'TradeCount_full_sell', 'PctlP_10_full_sell', 'PctlV_75_full_sell', 'PctlV_90_full_sell', 'MinP_180_sell', 'PriceVolatility_180_sell', 'DeltaP_180_sell', 'Momentum_180_sell', 'SumV_180_sell', 'PctlV_10_180_sell', 'FirstP_60_sell', 'MinP_60_sell', 'FirstV_60_sell', 'TradeCount_60_sell', 'PctlP_10_60_sell', 'PctlV_10_60_sell', 'PctlV_45_60_sell', 'DeltaP_15_sell', 'TradeCount_15_sell', 'LastP_5_sell', 'MedianP_5_sell', 'MinP_5_sell', 'MinV_5_sell', 'VolumeVolatility_5_sell', 'DeltaV_5_sell', 'Momentum_5_sell', 'PctlP_90_5_sell', 'FirstP_1_sell', 'FirstV_1_sell', 'MaxV_1_sell', 'Momentum_1_sell', 'TradeCount_1_sell', 'MinP_full_buy', 'FirstV_full_buy', 'DeltaP_180_buy', 'MaxV_180_buy', 'PctlV_75_180_buy', 'MinP_60_buy', 'PriceVolatility_60_buy', 'PctlV_75_60_buy', 'MinP_15_buy', 'SumV_15_buy', 'PctlP_10_15_buy', 'PctlV_10_15_buy', 'FirstV_5_buy', 'Momentum_5_buy', 'PctlP_25_5_buy', 'PctlV_10_5_buy', 'PriceVolatility_1_buy', 'DeltaP_1_buy', 'FirstV_1_buy', 'Momentum_1_buy', 'TradeCount_1_buy', 'PctlV_25_1_buy']
	25	41	['PriceVolatility_full_sell', 'Momentum_full_sell', 'SumV_full_sell', 'PctlV_75_full_sell', 'PctlV_90_full_sell', 'MinP_180_sell', 'FirstP_60_sell', 'MinP_60_sell', 'FirstV_60_sell', 'PctlP_10_60_sell', 'PctlV_10_60_sell', 'Momentum_15_sell', 'PctlP_25_15_sell', 'LastP_5_sell', 'MeanP_5_sell', 'MinV_5_sell', 'Momentum_5_sell', 'PctlP_90_5_sell', 'MaxV_1_sell', 'TradeCount_1_sell', 'MinP_full_buy', 'DeltaP_full_buy', 'MeanP_60_buy', 'MinP_60_buy', 'MaxP_60_buy', 'MinP_15_buy', 'PriceVolatility_15_buy', 'MaxV_15_buy', 'SumV_15_buy', 'PctlP_10_15_buy', 'PctlP_55_15_buy', 'PctlV_10_15_buy', 'PriceVolatility_5_buy', 'FirstV_5_buy', 'DeltaV_5_buy', 'Momentum_5_buy', 'TradeCount_5_buy', 'PctlP_25_5_buy', 'DeltaP_1_buy', 'Momentum_1_buy', 'TradeCount_1_buy']
	45	51	['DeltaP_full_sell', 'Momentum_full_sell', 'SumV_full_sell', 'PctlV_90_full_sell', 'MaxV_180_sell', 'PctlV_25_180_sell', 'FirstV_60_sell', 'Momentum_60_sell', 'PctlV_10_60_sell', 'MedianV_15_sell', 'Momentum_15_sell', 'PctlP_10_15_sell', 'PctlP_25_15_sell', 'PctlP_75_15_sell', 'LastP_5_sell', 'MaxP_5_sell', 'Momentum_5_sell', 'PctlP_90_5_sell', 'PctlV_55_5_sell', 'PctlV_55_1_sell', 'FirstV_full_buy', 'PctlV_10_full_buy', 'Momentum_180_buy', 'PctlP_75_180_buy', 'PctlV_25_180_buy', 'MedianV_60_buy', 'MinP_60_buy', 'MedianV_60_buy', 'MaxV_60_buy', 'PctlP_10_60_buy', 'PctlP_55_60_buy', 'FirstP_15_buy', 'MinP_15_buy', 'MaxV_15_buy', 'SumV_15_buy', 'PctlP_10_15_buy', 'PctlP_25_15_buy', 'PctlP_55_15_buy', 'PctlV_10_15_buy', 'PriceVolatility_5_buy', 'FirstV_5_buy', 'MaxV_5_buy', 'TradeCount_5_buy', 'PctlP_25_5_buy', 'PctlP_75_5_buy', 'PriceVolatility_1_buy', 'DeltaP_1_buy', 'FirstV_1_buy', 'DeltaV_1_buy', 'Momentum_1_buy', 'TradeCount_1_buy']
	50	50	['DeltaP_full_sell', 'SumV_full_sell', 'PctlV_90_full_sell', 'PctlV_25_180_sell', 'FirstV_60_sell', 'Momentum_60_sell', 'PctlV_10_60_sell', 'MedianV_15_sell', 'Momentum_15_sell', 'PctlP_10_15_sell', 'PctlP_25_15_sell', 'PctlP_75_15_sell', 'LastP_5_sell', 'MaxP_5_sell', 'MedianV_5_sell', 'Momentum_5_sell', 'PctlP_90_5_sell', 'PctlV_90_5_sell', 'PctlP_90_1_sell', 'PctlV_45_1_sell', 'MinP_full_buy', 'FirstV_full_buy', 'MaxV_full_buy', 'PctlV_10_full_buy', 'Momentum_180_buy', 'PctlP_75_180_buy', 'PctlV_25_180_buy', 'PctlV_55_180_buy', 'MedianV_60_buy', 'MinP_60_buy', 'MedianV_60_buy', 'PctlP_25_60_buy', 'PctlP_55_60_buy', 'MinP_15_buy', 'PriceVolatility_15_buy', 'MaxV_15_buy', 'PctlP_10_15_buy', 'PctlP_75_15_buy', 'PctlV_10_15_buy', 'PctlV_25_15_buy', 'PriceVolatility_5_buy', 'TradeCount_5_buy', 'PctlP_10_5_buy', 'PctlP_25_5_buy', 'PctlP_75_5_buy', 'PriceVolatility_1_buy', 'DeltaP_1_buy', 'MinV_1_buy', 'DeltaV_1_buy', 'TradeCount_1_buy']
	55	17	['VWAP_15_sell', 'PctlP_75_15_sell', 'PctlP_90_15_sell', 'LastP_5_sell', 'MaxP_5_sell', 'PctlP_90_5_sell', 'MaxP_1_sell', 'PctlV_25_180_buy', 'PctlV_55_180_buy', 'MedianV_60_buy', 'PctlV_55_60_buy', 'MedianP_15_buy', 'MinP_15_buy', 'PctlP_10_15_buy', 'PctlP_10_5_buy', 'PctlP_25_5_buy', 'PctlP_75_5_buy']

Case Desc.	Quantile	Num Features	Features
	75	208	['FirstP_full_sell', 'MeanP_full_sell', 'MinP_full_sell', 'MaxP_full_sell', 'PriceVolatility_full_sell', 'DeltaP_full_sell', 'LastV_full_sell', 'MedianV_full_sell', 'VolumeVolatility_full_sell', 'DeltaV_full_sell', 'Momentum_full_sell', 'SumV_full_sell', 'PctlP_10_full_sell', 'PctlV_10_full_sell', 'PctlV_25_full_sell', 'PctlV_55_full_sell', 'PctlV_75_full_sell', 'PctlV_90_full_sell', 'MeanP_180_sell', 'MinP_180_sell', 'MaxP_180_sell', 'PriceVolatility_180_sell', 'DeltaP_180_sell', 'MedianV_180_sell', 'MeanV_180_sell', 'MinV_180_sell', 'MaxV_180_sell', 'VolumeVolatility_180_sell', 'DeltaV_180_sell', 'Momentum_180_sell', 'TradeCount_180_sell', 'PctlP_10_180_sell', 'PctlP_90_180_sell', 'PctlV_10_180_sell', 'PctlV_45_180_sell', 'PctlV_55_180_sell', 'PctlV_75_180_sell', 'PctlV_90_180_sell', 'MinP_60_sell', 'PriceVolatility_60_sell', 'DeltaP_60_sell', 'MedianV_60_sell', 'MaxV_60_sell', 'DeltaV_60_sell', 'VWAP_60_sell', 'Momentum_60_sell', 'SumV_60_sell', 'PctlP_10_60_sell', 'PctlP_25_60_sell', 'PctlV_10_60_sell', 'PctlV_25_60_sell', 'PctlV_45_60_sell', 'PctlV_55_60_sell', 'PctlV_90_60_sell', 'MaxP_15_sell', 'PriceVolatility_15_sell', 'DeltaP_15_sell', 'FirstV_15_sell', 'MedianV_15_sell', 'MeanV_15_sell', 'MinV_15_sell', 'MaxV_15_sell', 'VolumeVolatility_15_sell', 'Momentum_15_sell', 'SumV_15_sell', 'TradeCount_15_sell', 'PctlP_10_15_sell', 'PctlP_25_15_sell', 'PctlP_45_15_sell', 'PctlP_90_15_sell', 'PctlV_10_15_sell', 'PctlV_55_15_sell', 'PctlV_75_15_sell', 'PctlV_90_15_sell', 'MinP_5_sell', 'MaxP_5_sell', 'PriceVolatility_5_sell', 'DeltaP_5_sell', 'FirstV_5_sell', 'MedianV_5_sell', 'MinV_5_sell', 'MaxV_5_sell', 'Momentum_5_sell', 'SumV_5_sell', 'TradeCount_5_sell', 'PctlP_10_5_sell', 'PctlP_25_5_sell', 'PctlP_45_5_sell', 'PctlV_10_5_sell', 'PctlV_25_5_sell', 'PctlV_45_5_sell', 'PctlV_75_5_sell', 'PctlV_90_5_sell', 'MinP_1_sell', 'DeltaP_1_sell', 'FirstV_1_sell', 'MinV_1_sell', 'MaxV_1_sell', 'VolumeVolatility_1_sell', 'Momentum_1_sell', 'SumV_1_sell', 'TradeCount_1_sell', 'PctlV_10_1_sell', 'PctlV_25_1_sell', 'PctlV_45_1_sell', 'PctlV_55_1_sell', 'PctlV_75_1_sell', 'PctlV_90_1_sell', 'MinP_full_buy', 'MaxP_full_buy', 'PriceVolatility_full_buy', 'DeltaP_full_buy', 'MeanV_full_buy', 'MaxV_full_buy', 'VolumeVolatility_full_buy', 'DeltaV_full_buy', 'Momentum_full_buy', 'PctlP_10_full_buy', 'PctlP_90_full_buy', 'PctlV_10_full_buy', 'PctlV_25_full_buy', 'PctlV_55_full_buy', 'PctlV_75_full_buy', 'PctlV_90_full_buy', 'MaxP_180_buy', 'DeltaP_180_buy', 'FirstV_180_buy', 'MinP_180_buy', 'MaxP_180_buy', 'Momentum_180_buy', 'SumV_180_buy', 'PctlP_55_180_buy', 'PctlP_75_180_buy', 'PctlP_90_180_buy', 'PctlV_10_180_buy', 'PctlV_25_180_buy', 'PctlV_45_180_buy', 'PctlV_55_180_buy', 'PctlV_75_180_buy', 'PctlV_90_180_buy', 'FirstP_60_buy', 'MeanP_60_buy', 'MaxP_60_buy', 'FirstV_60_buy', 'MinV_60_buy', 'MaxV_60_buy', 'VolumeVolatility_60_buy', 'Momentum_60_buy', 'TradeCount_60_buy', 'PctlP_55_60_buy', 'PctlP_75_60_buy', 'PctlP_90_60_buy', 'PctlV_10_60_buy', 'PctlV_55_60_buy', 'PctlV_75_60_buy', 'PctlV_90_60_buy', 'MinP_15_buy', 'MaxP_15_buy', 'PriceVolatility_15_buy', 'FirstV_15_buy', 'MinV_15_buy', 'MaxV_15_buy', 'VolumeVolatility_15_buy', 'Momentum_15_buy', 'SumV_15_buy', 'TradeCount_15_buy', 'PctlP_10_15_buy', 'PctlP_75_15_buy', 'PctlP_90_15_buy', 'PctlV_10_15_buy', 'PctlV_25_15_buy', 'PctlV_45_15_buy', 'PctlV_55_15_buy', 'PctlV_75_15_buy', 'PctlV_90_15_buy', 'MinP_5_buy', 'PriceVolatility_5_buy', 'DeltaP_5_buy', 'FirstV_5_buy', 'LastV_5_buy', 'MedianV_5_buy', 'MeanV_5_buy', 'MinV_5_buy', 'MaxV_5_buy', 'Momentum_5_buy', 'PctlP_10_5_buy', 'PctlP_25_5_buy', 'PctlP_45_5_buy', 'PctlV_10_5_buy', 'PctlV_25_5_buy', 'PctlV_45_5_buy', 'PctlV_75_5_buy', 'PctlV_90_5_buy', 'MaxP_1_buy', 'PriceVolatility_1_buy', 'DeltaP_1_buy', 'LastV_1_buy', 'MedianV_1_buy', 'MinV_1_buy', 'MaxV_1_buy', 'VolumeVolatility_1_buy', 'DeltaV_1_buy', 'Momentum_1_buy', 'TradeCount_1_buy', 'PctlP_90_1_buy', 'PctlV_10_1_buy', 'PctlV_25_1_buy', 'PctlV_75_1_buy', 'PctlV_90_1_buy']

Case Desc.	Quantile	Num Features	Features
	90	164	['FirstP_full_sell', 'MinP_full_sell', 'MaxP_full_sell', 'FirstV_full_sell', 'MedianV_full_sell', 'MeanV_full_sell', 'Momentum_full_sell', 'TradeCount_full_sell', 'PctlP_10_full_sell', 'PctlP_25_full_sell', 'PctlP_90_full_sell', 'PctlV_10_full_sell', 'PctlV_25_full_sell', 'PctlV_45_full_sell', 'PctlV_55_full_sell', 'PctlV_75_full_sell', 'MinP_180_sell', 'MaxP_180_sell', 'PriceVolatility_180_sell', 'DeltaP_180_sell', 'FirstV_180_sell', 'MeanV_180_sell', 'MinV_180_sell', 'VolumeVolatility_180_sell', 'PctlP_90_180_sell', 'PctlV_10_180_sell', 'PctlV_45_180_sell', 'PctlV_90_180_sell', 'FirstP_60_sell', 'MeanP_60_sell', 'MaxP_60_sell', 'FirstV_60_sell', 'MedianV_60_sell', 'MinV_60_sell', 'MaxV_60_sell', 'VolumeVolatility_60_sell', 'PctlP_10_60_sell', 'PctlP_25_60_sell', 'PctlV_10_60_sell', 'PctlV_25_60_sell', 'PctlV_45_60_sell', 'PctlV_55_60_sell', 'MinP_15_sell', 'MaxP_15_sell', 'PriceVolatility_15_sell', 'DeltaP_15_sell', 'FirstV_15_sell', 'MedianV_15_sell', 'MeanV_15_sell', 'MaxV_15_sell', 'Momentum_15_sell', 'SumV_15_sell', 'TradeCount_15_sell', 'PctlP_10_15_sell', 'PctlP_25_15_sell', 'PctlP_90_15_sell', 'PctlV_10_15_sell', 'PctlV_90_15_sell', 'MaxP_5_sell', 'DeltaP_5_sell', 'FirstV_5_sell', 'MedianV_5_sell', 'MinV_5_sell', 'VolumeVolatility_5_sell', 'Momentum_5_sell', 'SumV_5_sell', 'PctlP_10_5_sell', 'PctlP_25_5_sell', 'PctlP_45_5_sell', 'PctlP_90_5_sell', 'PctlV_10_5_sell', 'PctlV_55_5_sell', 'PctlV_75_5_sell', 'PctlV_90_5_sell', 'PriceVolatility_1_sell', 'DeltaP_1_sell', 'FirstV_1_sell', 'MinV_1_sell', 'VolumeVolatility_1_sell', 'Momentum_1_sell', 'PctlP_25_1_sell', 'PctlV_55_1_sell', 'PctlV_75_1_sell', 'PctlV_90_1_sell', 'FirstP_full_buy', 'PriceVolatility_full_buy', 'MeanV_full_buy', 'MaxV_full_buy', 'DeltaV_full_buy', 'Momentum_full_buy', 'PctlP_10_full_buy', 'PctlP_25_full_buy', 'PctlP_90_full_buy', 'PctlV_10_full_buy', 'PctlV_25_full_buy', 'PctlV_45_full_buy', 'PctlV_55_full_buy', 'PctlV_90_full_buy', 'MinP_180_buy', 'MaxP_180_buy', 'PriceVolatility_180_buy', 'DeltaP_180_buy', 'FirstV_180_buy', 'MinV_180_buy', 'MaxV_180_buy', 'Momentum_180_buy', 'SumV_180_buy', 'PctlP_75_180_buy', 'PctlP_90_180_buy', 'PctlV_10_180_buy', 'PctlV_25_180_buy', 'PctlV_45_180_buy', 'PctlV_55_180_buy', 'PctlV_75_180_buy', 'PctlV_90_180_buy', 'FirstP_60_buy', 'MaxP_60_buy', 'MaxV_60_buy', 'TradeCount_60_buy', 'PctlP_55_60_buy', 'PctlP_75_60_buy', 'PctlP_90_60_buy', 'PctlV_10_60_buy', 'PctlV_75_60_buy', 'PctlV_90_60_buy', 'FirstP_15_buy', 'MaxP_15_buy', 'PriceVolatility_15_buy', 'FirstV_15_buy', 'MedianV_15_buy', 'MeanV_15_buy', 'MinV_15_buy', 'MaxV_15_buy', 'Momentum_15_buy', 'PctlP_90_15_buy', 'PctlV_25_15_buy', 'PctlV_75_15_buy', 'PctlV_90_15_buy', 'FirstP_5_buy', 'MinP_5_buy', 'PriceVolatility_5_buy', 'DeltaP_5_buy', 'FirstV_5_buy', 'MeanV_5_buy', 'MinV_5_buy', 'VolumeVolatility_5_buy', 'TradeCount_5_buy', 'PctlP_10_5_buy', 'PctlP_25_5_buy', 'PctlP_90_5_buy', 'PctlV_25_5_buy', 'PctlV_75_5_buy', 'PctlV_90_5_buy', 'PriceVolatility_1_buy', 'DeltaP_1_buy', 'FirstV_1_buy', 'LastV_1_buy', 'MinV_1_buy', 'VolumeVolatility_1_buy', 'Momentum_1_buy', 'TradeCount_1_buy', 'PctlV_55_1_buy', 'PctlV_75_1_buy', 'PctlV_90_1_buy']
ID3 AT h	10	50	['PriceVolatility_full_sell', 'DeltaP_full_sell', 'LastV_full_sell', 'MeanV_full_sell', 'MinV_full_sell', 'MaxV_full_sell', 'TradeCount_full_sell', 'PctlP_10_full_sell', 'PctlV_10_full_sell', 'PctlV_25_full_sell', 'PriceVolatility_180_sell', 'DeltaP_180_sell', 'PctlV_75_180_sell', 'PriceVolatility_60_sell', 'MaxV_60_sell', 'Momentum_60_sell', 'PctlP_10_60_sell', 'FirstP_15_sell', 'MinP_15_sell', 'FirstV_15_sell', 'VolumeVolatility_15_sell', 'PctlV_45_15_sell', 'FirstP_5_sell', 'MinP_5_sell', 'PctlP_45_5_sell', 'FirstP_1_sell', 'MaxP_1_sell', 'SumV_1_sell', 'PctlV_90_1_sell', 'MinP_full_buy', 'FirstV_full_buy', 'MinV_full_buy', 'SumV_full_buy', 'TradeCount_full_buy', 'PctlV_45_full_buy', 'MinP_180_buy', 'DeltaP_180_buy', 'MinV_180_buy', 'PriceVolatility_60_buy', 'MaxV_60_buy', 'Momentum_60_buy', 'SumV_60_buy', 'TradeCount_60_buy', 'PctlV_90_60_buy', 'MinP_15_buy', 'FirstV_15_buy', 'DeltaP_5_buy', 'MinV_5_buy', 'VolumeVolatility_5_buy', 'TradeCount_1_buy']
	25	16	['LastP_180_sell', 'MinP_180_sell', 'MinP_60_sell', 'FirstP_15_sell', 'PctlP_25_15_sell', 'FirstP_5_sell', 'MinP_5_sell', 'VWAP_5_sell', 'PctlP_10_5_sell', 'PctlP_25_5_sell', 'PctlP_25_1_sell', 'MinP_full_buy', 'MinP_180_buy', 'MinP_60_buy', 'MinP_15_buy', 'MinP_1_buy']

Case Desc.	Quantile	Num Features	Features
	45	20	['LastP_full_sell', 'PctlP_55_full_sell', 'FirstP_60_sell', 'MinP_60_sell', 'FirstP_5_sell', 'MedianP_5_sell', 'VWAP_5_sell', 'PctlP_45_5_sell', 'FirstP_1_sell', 'MaxP_1_sell', 'FirstP_full_buy', 'MinP_full_buy', 'PctlP_45_full_buy', 'FirstP_180_buy', 'LastP_180_buy', 'PctlP_45_180_buy', 'MinP_60_buy', 'MinP_15_buy', 'MinP_5_buy', 'MinP_1_buy']
	50	19	['LastP_full_sell', 'PctlP_75_full_sell', 'FirstP_60_sell', 'FirstP_5_sell', 'PctlP_45_5_sell', 'FirstP_1_sell', 'MaxP_1_sell', 'FirstP_full_buy', 'PctlP_45_full_buy', 'PctlP_90_full_buy', 'FirstP_180_buy', 'LastP_180_buy', 'PctlP_45_180_buy', 'PctlP_90_180_buy', 'FirstP_60_buy', 'MinP_60_buy', 'MaxP_60_buy', 'MinP_15_buy', 'MinP_5_buy']
	55	19	['LastP_full_sell', 'PctlP_75_full_sell', 'PctlP_90_full_sell', 'MaxP_180_sell', 'FirstP_60_sell', 'PctlP_45_5_sell', 'FirstP_1_sell', 'MaxP_1_sell', 'FirstP_full_buy', 'LastP_full_buy', 'PctlP_45_full_buy', 'PctlP_75_full_buy', 'PctlP_90_full_buy', 'LastP_180_buy', 'PctlP_45_180_buy', 'MaxP_60_buy', 'MinP_15_buy', 'MinP_5_buy', 'MinP_1_buy']
	75	39	['PriceVolatility_full_sell', 'MaxV_full_sell', 'Momentum_full_sell', 'SumV_full_sell', 'TradeCount_full_sell', 'PctlV_10_full_sell', 'PctlV_25_full_sell', 'PctlV_90_full_sell', 'LastP_180_sell', 'MaxP_180_sell', 'PriceVolatility_180_sell', 'VolumeVolatility_180_sell', 'SumV_180_sell', 'PctlP_90_180_sell', 'VolumeVolatility_60_sell', 'Momentum_15_sell', 'LastV_5_sell', 'Momentum_5_sell', 'PctlP_45_5_sell', 'PctlP_90_5_sell', 'MaxP_1_sell', 'DeltaV_1_sell', 'SumV_1_sell', 'PctlP_90_1_sell', 'FirstP_full_buy', 'LastP_full_buy', 'MedianV_full_buy', 'MaxV_full_buy', 'SumV_full_buy', 'TradeCount_full_buy', 'PctlP_90_full_buy', 'PctlP_45_180_buy', 'MaxP_60_buy', 'PctlP_45_60_buy', 'PctlP_55_60_buy', 'PctlP_75_60_buy', 'PctlP_90_60_buy', 'PctlP_90_15_buy', 'PctlP_90_1_buy']

Case Desc.	Quantile	Num Features	Features
	90	138	['MinP_full_sell', 'MaxP_full_sell', 'PriceVolatility_full_sell', 'DeltaP_full_sell', 'FirstV_full_sell', 'MedianV_full_sell', 'MinV_full_sell', 'MaxV_full_sell', 'Momentum_full_sell', 'SumV_full_sell', 'TradeCount_full_sell', 'PctlP_25_full_sell', 'PctlP_55_full_sell', 'PctlV_10_full_sell', 'PctlV_25_full_sell', 'PctlV_45_full_sell', 'PctlV_75_full_sell', 'PctlV_90_full_sell', 'MinP_180_sell', 'MaxP_180_sell', 'PriceVolatility_180_sell', 'DeltaP_180_sell', 'LastV_180_sell', 'MeanV_180_sell', 'MinV_180_sell', 'MaxV_180_sell', 'DeltaV_180_sell', 'Momentum_180_sell', 'SumV_180_sell', 'PctlV_10_180_sell', 'PctlV_25_180_sell', 'PctlV_45_180_sell', 'PctlV_55_180_sell', 'PctlV_75_180_sell', 'PctlV_90_180_sell', 'FirstP_60_sell', 'PriceVolatility_60_sell', 'FirstV_60_sell', 'MinV_60_sell', 'MaxV_60_sell', 'VolumeVolatility_60_sell', 'SumV_60_sell', 'TradeCount_60_sell', 'PctlV_10_60_sell', 'PctlV_25_60_sell', 'PctlV_55_60_sell', 'PctlV_90_60_sell', 'PriceVolatility_15_sell', 'DeltaP_15_sell', 'FirstV_15_sell', 'LastV_15_sell', 'MinV_15_sell', 'SumV_15_sell', 'TradeCount_15_sell', 'PctlV_45_15_sell', 'PctlV_75_15_sell', 'PctlV_90_15_sell', 'PriceVolatility_5_sell', 'MinV_5_sell', 'VolumeVolatility_5_sell', 'Momentum_5_sell', 'TradeCount_5_sell', 'PctlV_45_5_sell', 'PctlV_75_5_sell', 'FirstP_1_sell', 'MinP_1_sell', 'MaxP_1_sell', 'PriceVolatility_1_sell', 'DeltaP_1_sell', 'MedianV_1_sell', 'MinV_1_sell', 'VolumeVolatility_1_sell', 'DeltaV_1_sell', 'SumV_1_sell', 'PctlP_10_1_sell', 'PctlV_10_1_sell', 'PctlV_55_1_sell', 'PctlV_90_1_sell', 'FirstP_full_buy', 'MinP_full_buy', 'MaxP_full_buy', 'PriceVolatility_full_buy', 'FirstV_full_buy', 'MinV_full_buy', 'MaxV_full_buy', 'Momentum_full_buy', 'TradeCount_full_buy', 'PctlP_45_full_buy', 'PctlP_75_full_buy', 'PctlP_90_full_buy', 'PctlV_10_full_buy', 'PctlV_25_full_buy', 'PctlV_55_full_buy', 'PctlV_90_full_buy', 'LastP_180_buy', 'PriceVolatility_180_buy', 'MinV_180_buy', 'MaxV_180_buy', 'Momentum_180_buy', 'SumV_180_buy', 'TradeCount_180_buy', 'PctlP_45_180_buy', 'PctlV_25_180_buy', 'PctlV_55_180_buy', 'PctlV_90_180_buy', 'PriceVolatility_60_buy', 'DeltaP_60_buy', 'FirstV_60_buy', 'LastV_60_buy', 'MeanV_60_buy', 'MinV_60_buy', 'MaxV_60_buy', 'Momentum_60_buy', 'SumV_60_buy', 'PctlP_55_60_buy', 'PctlP_75_60_buy', 'PctlP_90_60_buy', 'PctlV_10_60_buy', 'PctlV_75_60_buy', 'PctlV_90_60_buy', 'MinP_15_buy', 'MaxP_15_buy', 'PriceVolatility_15_buy', 'FirstV_15_buy', 'MinV_15_buy', 'MaxV_15_buy', 'VolumeVolatility_15_buy', 'Momentum_15_buy', 'SumV_15_buy', 'TradeCount_15_buy', 'PctlP_10_15_buy', 'PctlP_75_15_buy', 'PctlP_90_15_buy', 'PctlV_10_15_buy', 'PctlV_25_15_buy', 'PctlV_45_15_buy', 'PctlV_55_15_buy', 'PctlV_75_15_buy', 'PctlV_90_15_buy', 'MinP_5_buy', 'PriceVolatility_5_buy', 'DeltaP_5_buy', 'FirstV_5_buy', 'LastV_5_buy', 'MedianV_5_buy', 'MeanV_5_buy', 'MinV_5_buy', 'MaxV_5_buy', 'Momentum_5_buy', 'PctlP_10_5_buy', 'PctlP_25_5_buy', 'PctlP_45_5_buy', 'PctlV_10_5_buy', 'PctlV_25_5_buy', 'PctlV_45_5_buy', 'PctlV_75_5_buy', 'PctlV_90_5_buy', 'MinP_1_buy', 'DeltaP_1_buy', 'FirstV_1_buy', 'MinV_1_buy', 'MaxV_1_buy', 'VolumeVolatility_1_buy', 'Momentum_1_buy', 'SumV_1_buy', 'TradeCount_1_buy', 'PctlP_90_1_buy', 'PctlV_10_1_buy', 'PctlV_25_1_buy', 'PctlV_75_1_buy', 'PctlV_90_1_buy']
ID1 DE qh	10	4	['TradeCount_180_sell', 'MinP_180_buy', 'MinP_60_buy', 'MinP_15_buy']
	25	10	['TradeCount_180_sell', 'PctlP_10_180_sell', 'PctlP_10_15_sell', 'MinP_180_buy', 'LastP_60_buy', 'MinP_60_buy', 'MinP_15_buy', 'MinP_5_buy', 'PctlP_10_5_buy', 'MinP_1_buy']
	45	14	['MinP_180_sell', 'TradeCount_180_sell', 'LastP_1_sell', 'PctlP_45_1_sell', 'PctlP_10_180_buy', 'LastP_60_buy', 'VWAP_60_buy', 'PctlP_10_60_buy', 'PctlP_25_60_buy', 'MinP_5_buy', 'PctlP_10_5_buy', 'PctlP_25_5_buy', 'MinP_1_buy', 'PctlP_10_1_buy']
	50	17	['MinP_180_sell', 'TradeCount_180_sell', 'PctlP_25_180_sell', 'LastP_1_sell', 'PctlP_45_1_sell', 'PctlP_75_1_sell', 'VWAP_180_buy', 'PctlP_10_180_buy', 'LastP_60_buy', 'VWAP_60_buy', 'PctlP_10_60_buy', 'PctlP_25_60_buy', 'PctlP_45_60_buy', 'PctlP_10_5_buy', 'PctlP_25_5_buy', 'MinP_1_buy', 'PctlP_10_1_buy']

Case Desc.	Quantile	Num Features	Features
	55	13	['MinP_180_sell', 'TradeCount_180_sell', 'LastP_1_sell', 'PctlP_45_1_sell', 'PctlP_75_1_sell', 'LastP_180_buy', 'LastP_60_buy', 'VWAP_60_buy', 'PctlP_45_60_buy', 'PctlP_10_5_buy', 'PctlP_25_5_buy', 'MinP_1_buy', 'PctlP_10_1_buy']
	75	13	['LastP_5_sell', 'PctlP_90_5_sell', 'MaxP_1_sell', 'PctlP_45_1_sell', 'PctlP_75_1_sell', 'LastP_full_buy', 'PctlP_90_180_buy', 'VWAP_60_buy', 'PctlP_90_60_buy', 'PctlP_25_5_buy', 'MinP_1_buy', 'MaxP_1_buy', 'PctlP_10_1_buy']
	90	10	['LastP_180_sell', 'PctlP_90_5_sell', 'MaxP_1_sell', 'PctlP_45_1_sell', 'PctlP_75_1_sell', 'PctlP_90_180_buy', 'PctlP_90_60_buy', 'LastP_15_buy', 'PctlP_25_5_buy', 'MaxP_1_buy']
ID1 AT qh	10	18	['MeanV_full_sell', 'PctlP_10_full_sell', 'PctlV_45_full_sell', 'PctlP_25_60_sell', 'VWAP_15_sell', 'PctlP_45_15_sell', 'VWAP_5_sell', 'MeanV_full_buy', 'SumV_full_buy', 'MinP_180_buy', 'MinP_60_buy', 'TradeCount_60_buy', 'MeanP_15_buy', 'MinP_15_buy', 'VolumeVolatility_15_buy', 'TradeCount_15_buy', 'PctlV_90_15_buy', 'PctlV_90_5_buy']
	25	22	['PctlP_10_full_sell', 'PctlP_25_full_sell', 'TradeCount_180_sell', 'TradeCount_60_sell', 'PctlP_25_60_sell', 'VWAP_15_sell', 'PctlP_55_15_sell', 'PctlP_75_15_sell', 'VWAP_5_sell', 'PctlP_90_5_sell', 'SumV_full_buy', 'TradeCount_full_buy', 'MinP_180_buy', 'MinP_60_buy', 'TradeCount_60_buy', 'MeanP_15_buy', 'MinP_15_buy', 'MaxP_15_buy', 'TradeCount_15_buy', 'PctlP_10_15_buy', 'MaxP_5_buy', 'PctlV_90_5_buy']
	45	20	['MedianP_full_sell', 'VWAP_full_sell', 'PctlP_25_full_sell', 'PctlP_55_full_sell', 'PctlP_75_full_sell', 'VWAP_60_sell', 'PctlP_45_60_sell', 'PctlP_55_60_sell', 'PctlP_55_15_sell', 'PctlP_75_15_sell', 'PctlP_90_15_sell', 'MaxP_5_sell', 'VWAP_5_sell', 'MaxP_1_sell', 'FirstP_full_buy', 'VWAP_full_buy', 'PctlP_25_full_buy', 'MeanP_15_buy', 'PctlP_10_15_buy', 'PctlP_25_15_buy']
	50	24	['MedianP_full_sell', 'VWAP_full_sell', 'PctlP_25_full_sell', 'PctlP_55_full_sell', 'PctlP_75_full_sell', 'FirstP_180_sell', 'VWAP_180_sell', 'VWAP_60_sell', 'PctlP_45_60_sell', 'PctlP_55_60_sell', 'VWAP_15_sell', 'PctlP_55_15_sell', 'PctlP_75_15_sell', 'PctlP_90_15_sell', 'MaxP_5_sell', 'VWAP_5_sell', 'MaxP_1_sell', 'FirstP_full_buy', 'VWAP_full_buy', 'PctlP_25_full_buy', 'PctlP_55_60_buy', 'MeanP_15_buy', 'PctlP_10_15_buy', 'PctlP_25_15_buy']
	55	22	['PctlP_55_full_sell', 'PctlP_75_full_sell', 'FirstP_180_sell', 'VWAP_180_sell', 'VWAP_60_sell', 'PctlP_55_60_sell', 'PctlP_75_60_sell', 'MaxP_15_sell', 'VWAP_15_sell', 'PctlP_55_15_sell', 'PctlP_75_15_sell', 'PctlP_90_15_sell', 'MaxP_5_sell', 'VWAP_5_sell', 'MaxP_1_sell', 'FirstP_full_buy', 'VWAP_full_buy', 'PctlP_25_full_buy', 'PctlP_55_60_buy', 'MeanP_15_buy', 'PctlP_10_15_buy', 'PctlP_25_15_buy']
	75	33	['LastP_full_sell', 'MedianV_full_sell', 'MeanV_full_sell', 'SumV_full_sell', 'PctlP_90_full_sell', 'MaxP_180_sell', 'MaxP_60_sell', 'SumV_60_sell', 'TradeCount_60_sell', 'PctlP_90_60_sell', 'MeanP_15_sell', 'MaxP_15_sell', 'SumV_15_sell', 'PctlP_25_15_sell', 'PctlP_55_15_sell', 'PctlP_90_15_sell', 'MaxP_5_sell', 'MaxP_1_sell', 'FirstP_full_buy', 'PctlP_75_full_buy', 'PctlP_90_full_buy', 'FirstP_180_buy', 'VWAP_180_buy', 'PctlP_75_180_buy', 'TradeCount_60_buy', 'PctlP_55_60_buy', 'MeanP_15_buy', 'PctlP_10_15_buy', 'PctlP_25_15_buy', 'FirstP_5_buy', 'MeanP_5_buy', 'MaxP_5_buy', 'MaxP_1_buy']
	90	33	['LastP_full_sell', 'MaxP_full_sell', 'FirstV_full_sell', 'MedianV_full_sell', 'MeanV_full_sell', 'MinV_full_sell', 'MaxV_full_sell', 'SumV_full_sell', 'PctlP_90_full_sell', 'PctlV_25_full_sell', 'PctlV_45_full_sell', 'MaxP_180_sell', 'MaxP_60_sell', 'FirstP_15_sell', 'MeanP_15_sell', 'MaxP_15_sell', 'SumV_15_sell', 'PctlP_55_15_sell', 'PctlP_90_15_sell', 'MaxP_1_sell', 'FirstP_full_buy', 'MinV_full_buy', 'PctlP_90_full_buy', 'PctlV_25_full_buy', 'PctlV_45_full_buy', 'FirstP_180_buy', 'TradeCount_60_buy', 'TradeCount_15_buy', 'FirstP_5_buy', 'MeanP_5_buy', 'VWAP_5_buy', 'MaxP_1_buy', 'TradeCount_1_buy']

Case Desc.	Quantile	Num Features	Features
ID2 DE qh	10	11	['PctlV_90_full_sell', 'TradeCount_180_sell', 'PriceVolatility_15_sell', 'PctlP_75_1_sell', 'MaxP_full_buy', 'DeltaP_full_buy', 'MinP_180_buy', 'TradeCount_180_buy', 'MinP_60_buy', 'MeanP_15_buy', 'MinP_15_buy']
	25	17	['MinP_full_sell', 'PctlP_10_full_sell', 'PctlV_90_full_sell', 'TradeCount_180_sell', 'LastP_15_sell', 'MaxP_1_sell', 'PctlP_75_1_sell', 'PctlP_90_1_sell', 'MaxP_full_buy', 'DeltaP_full_buy', 'PctlV_90_full_buy', 'MinP_180_buy', 'MaxP_180_buy', 'TradeCount_180_buy', 'MinP_60_buy', 'MinP_15_buy', 'MinP_5_buy']
	45	18	['MinP_full_sell', 'PctlV_90_full_sell', 'TradeCount_180_sell', 'PctlP_10_180_sell', 'MinP_5_sell', 'MaxP_5_sell', 'PctlP_90_5_sell', 'MaxP_1_sell', 'PctlP_90_1_sell', 'DeltaP_full_buy', 'PctlP_10_180_buy', 'PctlP_10_60_buy', 'FirstP_15_buy', 'LastP_15_buy', 'MeanP_15_buy', 'MinP_15_buy', 'PctlP_10_15_buy', 'MinP_5_buy']
	50	22	['MinP_full_sell', 'TradeCount_full_sell', 'PctlV_90_full_sell', 'MinP_180_sell', 'TradeCount_180_sell', 'PctlP_10_180_sell', 'LastP_15_sell', 'MaxP_5_sell', 'PctlP_90_5_sell', 'MaxP_1_sell', 'PctlP_90_1_sell', 'DeltaP_full_buy', 'PctlP_10_180_buy', 'PctlP_10_60_buy', 'FirstP_15_buy', 'MeanP_15_buy', 'MinP_15_buy', 'PctlP_10_15_buy', 'LastP_5_buy', 'MinP_5_buy', 'MinP_1_buy', 'PctlP_10_1_buy']
	55	17	['MinP_full_sell', 'MeanP_180_sell', 'TradeCount_180_sell', 'PctlP_55_60_sell', 'MaxP_15_sell', 'MaxP_5_sell', 'PctlP_90_5_sell', 'MaxP_1_sell', 'LastP_full_buy', 'DeltaP_full_buy', 'PctlP_10_60_buy', 'FirstP_15_buy', 'MeanP_15_buy', 'MinP_15_buy', 'PctlP_10_15_buy', 'MinP_5_buy', 'MinP_1_buy']
	75	19	['MinP_full_sell', 'MaxP_full_sell', 'MinP_180_sell', 'PctlP_90_180_sell', 'TradeCount_60_sell', 'PctlP_90_60_sell', 'MaxP_15_sell', 'MaxP_5_sell', 'PctlP_90_5_sell', 'MaxP_1_sell', 'PctlP_75_1_sell', 'LastP_full_buy', 'DeltaP_full_buy', 'PctlP_75_60_buy', 'FirstP_15_buy', 'PctlP_45_15_buy', 'MinP_5_buy', 'VWAP_1_buy', 'PctlP_10_1_buy']
	90	21	['MinP_full_sell', 'MaxP_full_sell', 'DeltaP_full_sell', 'MaxV_full_sell', 'PctlV_45_full_sell', 'MaxP_180_sell', 'MaxP_60_sell', 'MinV_60_sell', 'MaxP_15_sell', 'MaxP_5_sell', 'PctlP_75_1_sell', 'LastP_full_buy', 'DeltaP_full_buy', 'MeanV_full_buy', 'PctlV_45_full_buy', 'TradeCount_180_buy', 'PctlP_75_15_buy', 'MaxP_1_buy', 'VWAP_1_buy', 'PctlP_10_1_buy', 'PctlP_25_1_buy']
ID2 AT qh	10	33	['MinP_full_sell', 'PriceVolatility_full_sell', 'MedianV_full_sell', 'MeanV_full_sell', 'MinV_full_sell', 'MaxV_full_sell', 'SumV_full_sell', 'PctlP_10_full_sell', 'PctlV_45_full_sell', 'LastP_180_sell', 'MinP_180_sell', 'PriceVolatility_180_sell', 'DeltaP_180_sell', 'PctlP_10_180_sell', 'MinP_60_sell', 'MinP_15_sell', 'MinP_1_sell', 'MinP_full_buy', 'MeanV_full_buy', 'MinV_full_buy', 'TradeCount_full_buy', 'PctlP_10_full_buy', 'PctlV_90_full_buy', 'MinP_180_buy', 'PriceVolatility_180_buy', 'MaxV_180_buy', 'TradeCount_180_buy', 'PctlP_10_180_buy', 'PctlV_90_180_buy', 'MinP_60_buy', 'LastP_15_buy', 'MinP_15_buy', 'MinP_1_buy']
	25	23	['PctlP_10_full_sell', 'PctlP_25_full_sell', 'PctlP_45_full_sell', 'LastP_180_sell', 'MinP_180_sell', 'VWAP_180_sell', 'PctlP_10_180_sell', 'PctlP_25_180_sell', 'MinP_60_sell', 'PctlP_10_15_sell', 'PctlP_10_5_sell', 'MinP_1_sell', 'PctlP_10_1_sell', 'FirstP_full_buy', 'PctlP_10_full_buy', 'PctlP_10_180_buy', 'MinP_60_buy', 'LastP_15_buy', 'MinP_15_buy', 'MinP_5_buy', 'PctlP_10_5_buy', 'MinP_1_buy', 'PctlP_10_1_buy']

Case Desc.	Quantile	Num Features	Features
	45	189	['FirstP_full_sell', 'MinP_full_sell', 'MaxP_full_sell', 'PriceVolatility_full_sell', 'FirstV_full_sell', 'LastV_full_sell', 'MedianV_full_sell', 'MinV_full_sell', 'VolumeVolatility_full_sell', 'VWAP_full_sell', 'Momentum_full_sell', 'SumV_full_sell', 'TradeCount_full_sell', 'PctlP_10_full_sell', 'PctlP_55_full_sell', 'PctlP_75_full_sell', 'PctlP_90_full_sell', 'PctlV_25_full_sell', 'PctlV_45_full_sell', 'PctlV_55_full_sell', 'PctlV_75_full_sell', 'PctlV_90_full_sell', 'LastP_180_sell', 'PriceVolatility_180_sell', 'DeltaP_180_sell', 'MedianV_180_sell', 'MeanV_180_sell', 'MinV_180_sell', 'MaxV_180_sell', 'DeltaV_180_sell', 'VWAP_180_sell', 'Momentum_180_sell', 'TradeCount_180_sell', 'PctlV_10_180_sell', 'PctlV_25_180_sell', 'PctlV_45_180_sell', 'PctlV_55_180_sell', 'PctlV_90_180_sell', 'MaxP_60_sell', 'PriceVolatility_60_sell', 'DeltaP_60_sell', 'LastV_60_sell', 'MedianV_60_sell', 'MeanV_60_sell', 'MinV_60_sell', 'MaxV_60_sell', 'VWAP_60_sell', 'Momentum_60_sell', 'SumV_60_sell', 'TradeCount_60_sell', 'PctlP_25_60_sell', 'PctlP_90_60_sell', 'PctlV_25_60_sell', 'PctlV_45_60_sell', 'PctlV_55_60_sell', 'PctlV_75_60_sell', 'PctlV_90_60_sell', 'MaxP_15_sell', 'PriceVolatility_15_sell', 'DeltaP_15_sell', 'FirstV_15_sell', 'MinV_15_sell', 'MaxV_15_sell', 'VolumeVolatility_15_sell', 'VWAP_15_sell', 'Momentum_15_sell', 'TradeCount_15_sell', 'PctlP_10_15_sell', 'PctlP_55_15_sell', 'PctlV_25_15_sell', 'PctlV_45_15_sell', 'PctlV_55_15_sell', 'PctlV_75_15_sell', 'MaxP_5_sell', 'PriceVolatility_5_sell', 'DeltaP_5_sell', 'LastV_5_sell', 'MaxV_5_sell', 'VolumeVolatility_5_sell', 'DeltaV_5_sell', 'VWAP_5_sell', 'Momentum_5_sell', 'SumV_5_sell', 'PctlP_75_5_sell', 'PctlV_10_5_sell', 'PctlV_25_5_sell', 'PctlV_90_5_sell', 'FirstP_1_sell', 'PriceVolatility_1_sell', 'FirstV_1_sell', 'MedianV_1_sell', 'MinV_1_sell', 'MaxV_1_sell', 'SumV_1_sell', 'TradeCount_1_sell', 'PctlV_75_1_sell', 'PctlV_90_1_sell', 'FirstP_full_buy', 'MeanP_full_buy', 'MinP_full_buy', 'PriceVolatility_full_buy', 'LastV_full_buy', 'MedianV_full_buy', 'MeanV_full_buy', 'MinV_full_buy', 'MaxV_full_buy', 'VolumeVolatility_full_buy', 'DeltaV_full_buy', 'VWAP_full_buy', 'Momentum_full_buy', 'SumV_full_buy', 'TradeCount_full_buy', 'PctlP_45_full_buy', 'PctlP_90_full_buy', 'PctlV_10_full_buy', 'PctlV_25_full_buy', 'PctlV_45_full_buy', 'PctlV_75_full_buy', 'PctlV_90_full_buy', 'FirstP_180_buy', 'MinP_180_buy', 'PriceVolatility_180_buy', 'LastV_180_buy', 'MedianV_180_buy', 'MinV_180_buy', 'MaxV_180_buy', 'DeltaV_180_buy', 'VWAP_180_buy', 'Momentum_180_buy', 'SumV_180_buy', 'TradeCount_180_buy', 'PctlV_10_180_buy', 'PctlV_25_180_buy', 'PctlV_45_180_buy', 'PctlV_55_180_buy', 'PctlV_75_180_buy', 'PctlV_90_180_buy', 'MinP_60_buy', 'PriceVolatility_60_buy', 'DeltaP_60_buy', 'MeanV_60_buy', 'MinV_60_buy', 'MaxV_60_buy', 'SumV_60_buy', 'TradeCount_60_buy', 'PctlP_25_60_buy', 'PctlP_55_60_buy', 'PctlV_25_60_buy', 'PctlV_45_60_buy', 'PctlV_55_60_buy', 'PctlV_75_60_buy', 'MinP_15_buy', 'DeltaP_15_buy', 'FirstV_15_buy', 'MeanV_15_buy', 'MinV_15_buy', 'MaxV_15_buy', 'Momentum_15_buy', 'SumV_15_buy', 'TradeCount_15_buy', 'PctlV_25_15_buy', 'PctlV_45_15_buy', 'PctlV_55_15_buy', 'PctlV_75_15_buy', 'PctlV_90_15_buy', 'DeltaP_5_buy', 'FirstV_5_buy', 'LastV_5_buy', 'MinV_5_buy', 'MaxV_5_buy', 'VWAP_5_buy', 'Momentum_5_buy', 'TradeCount_5_buy', 'PctlP_10_5_buy', 'PctlP_55_5_buy', 'PctlV_55_5_buy', 'PctlV_75_5_buy', 'PctlV_90_5_buy', 'FirstP_1_buy', 'DeltaP_1_buy', 'MaxV_1_buy', 'VolumeVolatility_1_buy', 'DeltaV_1_buy', 'Momentum_1_buy', 'TradeCount_1_buy', 'PctlV_25_1_buy', 'PctlV_55_1_buy', 'PctlV_75_1_buy', 'PctlV_90_1_buy']

Case Desc.	Quantile	Num Features	Features
	50	200	['FirstP_full_sell', 'MinP_full_sell', 'MaxP_full_sell', 'PriceVolatility_full_sell', 'FirstV_full_sell', 'LastV_full_sell', 'MedianV_full_sell', 'MeanV_full_sell', 'MinV_full_sell', 'MaxV_full_sell', 'VolumeVolatility_full_sell', 'Momentum_full_sell', 'SumV_full_sell', 'TradeCount_full_sell', 'PctlP_10_full_sell', 'PctlP_55_full_sell', 'PctlP_75_full_sell', 'PctlP_90_full_sell', 'PctlV_10_full_sell', 'PctlV_25_full_sell', 'PctlV_45_full_sell', 'PctlV_55_full_sell', 'PctlV_90_full_sell', 'FirstP_180_sell', 'LastP_180_sell', 'MedianP_180_sell', 'LastV_180_sell', 'MedianV_180_sell', 'MeanV_180_sell', 'MinV_180_sell', 'VolumeVolatility_180_sell', 'DeltaV_180_sell', 'VWAP_180_sell', 'Momentum_180_sell', 'SumV_180_sell', 'TradeCount_180_sell', 'PctlV_10_180_sell', 'PctlV_45_180_sell', 'PctlV_55_180_sell', 'PctlV_75_180_sell', 'PctlV_90_180_sell', 'MinP_60_sell', 'MaxP_60_sell', 'PriceVolatility_60_sell', 'DeltaP_60_sell', 'LastV_60_sell', 'MedianV_60_sell', 'MeanV_60_sell', 'MinV_60_sell', 'MaxV_60_sell', 'VolumeVolatility_60_sell', 'DeltaV_60_sell', 'VWAP_60_sell', 'Momentum_60_sell', 'SumV_60_sell', 'TradeCount_60_sell', 'PctlP_25_60_sell', 'PctlP_90_60_sell', 'PctlV_10_60_sell', 'PctlV_25_60_sell', 'PctlV_55_60_sell', 'PctlV_75_60_sell', 'PctlV_90_60_sell', 'MaxP_15_sell', 'DeltaP_15_sell', 'FirstV_15_sell', 'MinV_15_sell', 'MaxV_15_sell', 'VolumeVolatility_15_sell', 'VWAP_15_sell', 'Momentum_15_sell', 'SumV_15_sell', 'TradeCount_15_sell', 'PctlP_10_15_sell', 'PctlV_25_15_sell', 'PctlV_45_15_sell', 'PctlV_55_15_sell', 'PctlV_75_15_sell', 'MaxP_5_sell', 'PriceVolatility_5_sell', 'DeltaP_5_sell', 'LastV_5_sell', 'MaxV_5_sell', 'DeltaV_5_sell', 'SumV_5_sell', 'TradeCount_5_sell', 'PctlP_55_5_sell', 'PctlV_10_5_sell', 'PctlV_25_5_sell', 'PctlV_75_5_sell', 'PctlV_90_5_sell', 'FirstP_1_sell', 'PriceVolatility_1_sell', 'FirstV_1_sell', 'MinV_1_sell', 'MaxV_1_sell', 'SumV_1_sell', 'TradeCount_1_sell', 'PctlV_45_1_sell', 'PctlV_55_1_sell', 'PctlV_75_1_sell', 'PctlV_90_1_sell', 'FirstP_full_buy', 'MedianP_full_buy', 'MeanP_full_buy', 'MinP_full_buy', 'PriceVolatility_full_buy', 'LastV_full_buy', 'MeanV_full_buy', 'MinV_full_buy', 'MaxV_full_buy', 'VolumeVolatility_full_buy', 'DeltaV_full_buy', 'VWAP_full_buy', 'Momentum_full_buy', 'SumV_full_buy', 'TradeCount_full_buy', 'PctlP_45_full_buy', 'PctlP_90_full_buy', 'PctlV_10_full_buy', 'PctlV_25_full_buy', 'PctlV_45_full_buy', 'PctlV_75_full_buy', 'PctlV_90_full_buy', 'FirstP_180_buy', 'MinP_180_buy', 'PriceVolatility_180_buy', 'LastV_180_buy', 'MedianV_180_buy', 'MinV_180_buy', 'DeltaV_180_buy', 'VWAP_180_buy', 'Momentum_180_buy', 'SumV_180_buy', 'TradeCount_180_buy', 'PctlV_10_180_buy', 'PctlV_25_180_buy', 'PctlV_45_180_buy', 'PctlV_55_180_buy', 'PctlV_75_180_buy', 'PctlV_90_180_buy', 'MinP_60_buy', 'PriceVolatility_60_buy', 'DeltaP_60_buy', 'LastV_60_buy', 'MeanV_60_buy', 'MinV_60_buy', 'MaxV_60_buy', 'SumV_60_buy', 'TradeCount_60_buy', 'PctlP_25_60_buy', 'PctlP_55_60_buy', 'PctlV_25_60_buy', 'PctlV_45_60_buy', 'PctlV_55_60_buy', 'PctlV_75_60_buy', 'MinP_15_buy', 'DeltaP_15_buy', 'FirstV_15_buy', 'MeanV_15_buy', 'MinV_15_buy', 'MaxV_15_buy', 'Momentum_15_buy', 'SumV_15_buy', 'TradeCount_15_buy', 'PctlV_25_15_buy', 'PctlV_45_15_buy', 'PctlV_55_15_buy', 'PctlV_75_15_buy', 'PctlV_90_15_buy', 'DeltaP_5_buy', 'FirstV_5_buy', 'LastV_5_buy', 'MinV_5_buy', 'MaxV_5_buy', 'VWAP_5_buy', 'Momentum_5_buy', 'TradeCount_5_buy', 'PctlP_10_5_buy', 'PctlP_55_5_buy', 'PctlV_55_5_buy', 'PctlV_75_5_buy', 'PctlV_90_5_buy', 'FirstP_1_buy', 'DeltaP_1_buy', 'MaxV_1_buy', 'VolumeVolatility_1_buy', 'DeltaV_1_buy', 'Momentum_1_buy', 'TradeCount_1_buy', 'PctlV_25_1_buy', 'PctlV_55_1_buy', 'PctlV_75_1_buy', 'PctlV_90_1_buy']

Case Desc.	Quantile	Num Features	Features
	55	198	['FirstP_full_sell', 'MinP_full_sell', 'MaxP_full_sell', 'PriceVolatility_full_sell', 'FirstV_full_sell', 'LastV_full_sell', 'MedianV_full_sell', 'MeanV_full_sell', 'MinV_full_sell', 'MaxV_full_sell', 'VolumeVolatility_full_sell', 'Momentum_full_sell', 'SumV_full_sell', 'TradeCount_full_sell', 'PctlP_75_full_sell', 'PctlP_90_full_sell', 'PctlV_10_full_sell', 'PctlV_25_full_sell', 'PctlV_55_full_sell', 'PctlV_75_full_sell', 'PctlV_90_full_sell', 'FirstP_180_sell', 'LastP_180_sell', 'MedianP_180_sell', 'PriceVolatility_180_sell', 'LastV_180_sell', 'MedianV_180_sell', 'MeanV_180_sell', 'MinV_180_sell', 'MaxV_180_sell', 'VolumeVolatility_180_sell', 'DeltaV_180_sell', 'VWAP_180_sell', 'Momentum_180_sell', 'SumV_180_sell', 'TradeCount_180_sell', 'PctlV_25_180_sell', 'PctlV_45_180_sell', 'PctlV_55_180_sell', 'PctlV_75_180_sell', 'PctlV_90_180_sell', 'MaxP_60_sell', 'PriceVolatility_60_sell', 'DeltaP_60_sell', 'FirstV_60_sell', 'LastV_60_sell', 'MedianV_60_sell', 'MeanV_60_sell', 'MinV_60_sell', 'MaxV_60_sell', 'VWAP_60_sell', 'Momentum_60_sell', 'SumV_60_sell', 'TradeCount_60_sell', 'PctlP_25_60_sell', 'PctlP_90_60_sell', 'PctlV_10_60_sell', 'PctlV_25_60_sell', 'PctlV_45_60_sell', 'PctlV_55_60_sell', 'PctlV_75_60_sell', 'PctlV_90_60_sell', 'MaxP_15_sell', 'PriceVolatility_15_sell', 'DeltaP_15_sell', 'FirstV_15_sell', 'MinV_15_sell', 'MaxV_15_sell', 'VolumeVolatility_15_sell', 'VWAP_15_sell', 'Momentum_15_sell', 'SumV_15_sell', 'TradeCount_15_sell', 'PctlP_10_15_sell', 'PctlV_25_15_sell', 'PctlV_45_15_sell', 'PctlV_55_15_sell', 'PctlV_75_15_sell', 'MaxP_5_sell', 'PriceVolatility_5_sell', 'DeltaP_5_sell', 'LastV_5_sell', 'MaxV_5_sell', 'DeltaV_5_sell', 'Momentum_5_sell', 'SumV_5_sell', 'TradeCount_5_sell', 'PctlP_55_5_sell', 'PctlV_10_5_sell', 'PctlV_25_5_sell', 'PctlV_55_5_sell', 'PctlV_75_5_sell', 'PctlV_90_5_sell', 'FirstP_1_sell', 'PriceVolatility_1_sell', 'FirstV_1_sell', 'MinV_1_sell', 'MaxV_1_sell', 'SumV_1_sell', 'TradeCount_1_sell', 'PctlV_45_1_sell', 'PctlV_55_1_sell', 'PctlV_75_1_sell', 'PctlV_90_1_sell', 'FirstP_full_buy', 'MedianP_full_buy', 'MinP_full_buy', 'PriceVolatility_full_buy', 'LastV_full_buy', 'MedianV_full_buy', 'MeanV_full_buy', 'MinV_full_buy', 'MaxV_full_buy', 'VolumeVolatility_full_buy', 'DeltaV_full_buy', 'Momentum_full_buy', 'SumV_full_buy', 'TradeCount_full_buy', 'PctlP_45_full_buy', 'PctlP_75_full_buy', 'PctlP_90_full_buy', 'PctlV_10_full_buy', 'PctlV_45_full_buy', 'PctlV_55_full_buy', 'PctlV_75_full_buy', 'PctlV_90_full_buy', 'FirstP_180_buy', 'LastP_180_buy', 'MaxP_180_buy', 'PriceVolatility_180_buy', 'MedianV_180_buy', 'MeanV_180_buy', 'MinV_180_buy', 'DeltaV_180_buy', 'VWAP_180_buy', 'Momentum_180_buy', 'SumV_180_buy', 'TradeCount_180_buy', 'PctlV_10_180_buy', 'PctlV_25_180_buy', 'PctlV_45_180_buy', 'PctlV_55_180_buy', 'PctlV_75_180_buy', 'PctlV_90_180_buy', 'MinP_60_buy', 'PriceVolatility_60_buy', 'DeltaP_60_buy', 'LastV_60_buy', 'MeanV_60_buy', 'MinV_60_buy', 'MaxV_60_buy', 'DeltaV_60_buy', 'Momentum_60_buy', 'SumV_60_buy', 'TradeCount_60_buy', 'PctlP_25_60_buy', 'PctlP_55_60_buy', 'PctlV_25_60_buy', 'PctlV_45_60_buy', 'PctlV_55_60_buy', 'PctlV_75_60_buy', 'MinP_15_buy', 'PriceVolatility_15_buy', 'DeltaP_15_buy', 'MaxV_15_buy', 'DeltaV_15_buy', 'Momentum_15_buy', 'TradeCount_15_buy', 'PctlV_10_15_buy', 'PctlV_25_15_buy', 'PctlV_45_15_buy', 'PctlV_55_15_buy', 'PctlV_90_15_buy', 'PriceVolatility_5_buy', 'DeltaP_5_buy', 'FirstV_5_buy', 'LastV_5_buy', 'MinV_5_buy', 'VolumeVolatility_5_buy', 'Momentum_5_buy', 'SumV_5_buy', 'TradeCount_5_buy', 'PctlP_10_5_buy', 'PctlV_45_5_buy', 'PctlV_75_5_buy', 'FirstP_1_buy', 'PriceVolatility_1_buy', 'MinV_1_buy', 'MaxV_1_buy', 'VolumeVolatility_1_buy', 'DeltaV_1_buy', 'SumV_1_buy', 'TradeCount_1_buy', 'PctlV_55_1_buy', 'PctlV_25_1_buy', 'PctlV_45_1_buy', 'PctlV_55_1_buy', 'PctlV_90_1_buy']
	75	24	['SumV_full_sell', 'PctlP_75_full_sell', 'PctlP_90_full_sell', 'PctlV_90_full_sell', 'LastP_180_sell', 'MaxP_180_sell', 'TradeCount_180_sell', 'PctlP_90_180_sell', 'MaxP_60_sell', 'PctlP_90_60_sell', 'MaxP_15_sell', 'VWAP_15_sell', 'MedianP_5_sell', 'MaxP_1_sell', 'FirstP_full_buy', 'PctlP_75_full_buy', 'PctlP_90_full_buy', 'MaxP_180_buy', 'MaxP_60_buy', 'LastP_15_buy', 'MaxP_15_buy', 'MeanP_1_buy', 'MaxP_1_buy', 'PctlP_55_1_buy']

Case Desc.	Quantile	Num Features	Features
	90	18	['SumV_full_sell', 'TradeCount_full_sell', 'PctlP_90_full_sell', 'PctlV_90_full_sell', 'MaxP_180_sell', 'PriceVolatility_180_sell', 'MaxP_60_sell', 'MaxP_15_sell', 'LastP_5_sell', 'MaxP_1_sell', 'FirstP_full_buy', 'MaxP_full_buy', 'PctlP_90_full_buy', 'MaxP_180_buy', 'LastP_60_buy', 'MaxP_60_buy', 'MaxP_15_buy', 'MaxP_1_buy']
ID3 DE qh	10	14	['MinP_full_sell', 'TradeCount_180_sell', 'TradeCount_60_sell', 'FirstP_5_sell', 'MeanP_5_sell', 'MaxP_1_sell', 'MaxP_full_buy', 'MinP_180_buy', 'MaxP_180_buy', 'TradeCount_180_buy', 'MinP_60_buy', 'MinP_15_buy', 'MinP_1_buy', 'PctlP_10_1_buy']
	25	19	['MinP_full_sell', 'PctlV_90_full_sell', 'TradeCount_180_sell', 'TradeCount_60_sell', 'PctlP_55_15_sell', 'PctlP_75_15_sell', 'FirstP_5_sell', 'MeanP_5_sell', 'PctlP_55_5_sell', 'PctlP_75_5_sell', 'PctlP_90_5_sell', 'MaxP_1_sell', 'MaxP_full_buy', 'MinP_180_buy', 'TradeCount_180_buy', 'MinP_60_buy', 'PctlP_10_60_buy', 'MinP_15_buy', 'PctlP_10_1_buy']
	45	17	['MinP_full_sell', 'TradeCount_180_sell', 'PctlP_45_60_sell', 'PctlP_75_15_sell', 'PctlP_90_15_sell', 'MeanP_5_sell', 'MaxP_5_sell', 'PctlP_90_5_sell', 'MaxP_1_sell', 'MinP_180_buy', 'VWAP_180_buy', 'MinP_60_buy', 'PctlP_10_60_buy', 'PctlP_25_60_buy', 'MinP_15_buy', 'MinP_1_buy', 'PctlP_10_1_buy']
	50	15	['MinP_full_sell', 'TradeCount_180_sell', 'PctlP_45_60_sell', 'PctlP_75_15_sell', 'PctlP_90_15_sell', 'MaxP_5_sell', 'MaxP_1_sell', 'PctlP_90_1_sell', 'VWAP_180_buy', 'MinP_60_buy', 'PctlP_10_60_buy', 'PctlP_25_60_buy', 'MinP_15_buy', 'PctlP_10_15_buy', 'MinP_1_buy']
	55	17	['MinP_full_sell', 'TradeCount_180_sell', 'PctlP_45_60_sell', 'PctlP_75_60_sell', 'PctlP_90_15_sell', 'MaxP_5_sell', 'PctlP_90_5_sell', 'MaxP_1_sell', 'PctlP_90_1_sell', 'VWAP_180_buy', 'PctlP_10_60_buy', 'PctlP_25_60_buy', 'PctlP_45_60_buy', 'MinP_15_buy', 'PctlP_10_15_buy', 'MinP_5_buy', 'MinP_1_buy']
	75	16	['MinP_full_sell', 'MeanP_180_sell', 'PctlP_90_180_sell', 'MeanP_60_sell', 'PctlP_75_60_sell', 'PctlP_90_60_sell', 'MaxP_15_sell', 'PctlP_90_15_sell', 'MaxP_5_sell', 'PctlP_90_1_sell', 'PctlP_75_180_buy', 'MedianP_60_buy', 'PctlP_25_60_buy', 'PctlP_45_60_buy', 'PctlP_10_15_buy', 'MinP_1_buy']
	90	21	['MinP_full_sell', 'MaxP_full_sell', 'DeltaP_full_sell', 'MedianV_full_sell', 'PctlV_25_full_sell', 'MaxP_180_sell', 'MaxP_60_sell', 'PctlP_90_60_sell', 'MaxP_15_sell', 'PctlP_90_15_sell', 'MaxP_1_sell', 'PctlP_90_1_sell', 'DeltaP_full_buy', 'FirstV_full_buy', 'MeanV_full_buy', 'PctlV_25_full_buy', 'PctlV_75_full_buy', 'TradeCount_180_buy', 'PctlP_25_15_buy', 'FirstP_5_buy', 'MinP_1_buy']
ID3 AT qh	10	12	['PctlP_10_full_sell', 'MinP_180_sell', 'PctlP_10_180_sell', 'MinP_5_sell', 'MinP_1_sell', 'TradeCount_full_buy', 'MinP_180_buy', 'MinP_15_buy', 'MinP_5_buy', 'PctlP_10_full_buy', 'PctlP_10_180_buy', 'PctlP_10_60_buy']
	25	21	['LastP_full_sell', 'MedianP_full_sell', 'VWAP_full_sell', 'PctlP_10_full_sell', 'PctlP_25_full_sell', 'VWAP_180_sell', 'PctlP_25_180_sell', 'MinP_1_sell', 'FirstP_full_buy', 'TradeCount_full_buy', 'MinP_180_buy', 'VWAP_60_buy', 'MinP_15_buy', 'LastP_5_buy', 'MinP_1_buy', 'VWAP_1_buy', 'PctlP_10_full_buy', 'PctlP_25_full_buy', 'PctlP_10_180_buy', 'PctlP_10_60_buy', 'PctlP_10_5_buy']
	45	17	['LastP_full_sell', 'MedianP_full_sell', 'MeanP_full_sell', 'VWAP_180_sell', 'MeanP_60_sell', 'MeanP_1_sell', 'MinP_1_sell', 'VWAP_1_sell', 'FirstP_full_buy', 'MeanP_full_buy', 'MeanP_60_buy', 'LastP_15_buy', 'MinP_15_buy', 'VWAP_1_buy', 'PctlP_25_full_buy', 'PctlP_10_15_buy', 'PctlP_10_5_buy']
	50	17	['LastP_full_sell', 'MeanP_full_sell', 'PctlP_55_full_sell', 'VWAP_180_sell', 'PctlP_75_60_sell', 'MaxP_15_sell', 'FirstP_1_sell', 'MeanP_1_sell', 'VWAP_1_sell', 'FirstP_full_buy', 'MeanP_full_buy', 'MeanP_60_buy', 'LastP_15_buy', 'MeanP_15_buy', 'MinP_15_buy', 'VWAP_1_buy', 'PctlP_10_5_buy']

Case Desc.	Quantile	Num Features	Features
	55	23	['LastP_full_sell', 'MeanP_full_sell', 'PctlP_55_full_sell', 'PctlP_75_full_sell', 'VWAP_180_sell', 'PctlP_75_180_sell', 'VWAP_60_sell', 'PctlP_75_60_sell', 'PctlP_90_60_sell', 'MaxP_15_sell', 'MaxP_5_sell', 'FirstP_1_sell', 'MeanP_1_sell', 'FirstP_full_buy', 'MeanP_full_buy', 'MaxP_180_buy', 'MeanP_60_buy', 'LastP_15_buy', 'MeanP_15_buy', 'MinP_15_buy', 'VWAP_1_buy', 'PctlP_55_full_buy', 'PctlP_75_full_buy']
	75	171	['FirstP_full_sell', 'MinP_full_sell', 'MaxP_full_sell', 'PriceVolatility_full_sell', 'FirstV_full_sell', 'LastV_full_sell', 'MedianV_full_sell', 'MeanV_full_sell', 'MinV_full_sell', 'MaxV_full_sell', 'VolumeVolatility_full_sell', 'Momentum_full_sell', 'SumV_full_sell', 'TradeCount_full_sell', 'PctlP_10_full_sell', 'PctlP_25_full_sell', 'PctlP_90_full_sell', 'PctlV_10_full_sell', 'PctlV_25_full_sell', 'PctlV_45_full_sell', 'PctlV_55_full_sell', 'PctlV_75_full_sell', 'PctlV_90_full_sell', 'MaxP_180_sell', 'PriceVolatility_180_sell', 'DeltaP_180_sell', 'FirstV_180_sell', 'LastV_180_sell', 'MedianV_180_sell', 'MeanV_180_sell', 'MinV_180_sell', 'MaxV_180_sell', 'VolumeVolatility_180_sell', 'Momentum_180_sell', 'SumV_180_sell', 'TradeCount_180_sell', 'PctlP_10_180_sell', 'PctlP_55_180_sell', 'PctlP_90_180_sell', 'PctlV_10_180_sell', 'PctlV_45_180_sell', 'PctlV_55_180_sell', 'PctlV_75_180_sell', 'FirstP_60_sell', 'LastP_60_sell', 'PriceVolatility_60_sell', 'FirstV_60_sell', 'MedianV_60_sell', 'MeanV_60_sell', 'MinV_60_sell', 'MaxV_60_sell', 'VolumeVolatility_60_sell', 'Momentum_60_sell', 'TradeCount_60_sell', 'PctlV_25_60_sell', 'PctlV_45_60_sell', 'PctlV_75_60_sell', 'PctlV_90_60_sell', 'FirstP_15_sell', 'PriceVolatility_15_sell', 'FirstV_15_sell', 'MedianV_15_sell', 'MinV_15_sell', 'MaxV_15_sell', 'VolumeVolatility_15_sell', 'Momentum_15_sell', 'SumV_15_sell', 'TradeCount_15_sell', 'PriceVolatility_5_sell', 'DeltaP_5_sell', 'FirstV_5_sell', 'MedianV_5_sell', 'MeanV_5_sell', 'VolumeVolatility_5_sell', 'Momentum_5_sell', 'SumV_5_sell', 'PctlV_90_5_sell', 'FirstP_1_sell', 'MinP_1_sell', 'PriceVolatility_1_sell', 'FirstV_1_sell', 'MinV_1_sell', 'Momentum_1_sell', 'SumV_1_sell', 'TradeCount_1_sell', 'PctlV_55_1_sell', 'FirstP_full_buy', 'MinP_full_buy', 'MaxP_full_buy', 'PriceVolatility_full_buy', 'FirstV_full_buy', 'LastV_full_buy', 'MinV_full_buy', 'MaxV_full_buy', 'VolumeVolatility_full_buy', 'VWAP_full_buy', 'Momentum_full_buy', 'SumV_full_buy', 'TradeCount_full_buy', 'FirstP_180_buy', 'MinP_180_buy', 'MaxP_180_buy', 'PriceVolatility_180_buy', 'MeanV_180_buy', 'MinV_180_buy', 'MaxV_180_buy', 'VolumeVolatility_180_buy', 'VWAP_180_buy', 'Momentum_180_buy', 'FirstP_60_buy', 'PriceVolatility_60_buy', 'LastV_60_buy', 'MeanV_60_buy', 'MinV_60_buy', 'MaxV_60_buy', 'VolumeVolatility_60_buy', 'DeltaV_60_buy', 'Momentum_60_buy', 'SumV_60_buy', 'TradeCount_60_buy', 'MinP_15_buy', 'MaxP_15_buy', 'PriceVolatility_15_buy', 'DeltaP_15_buy', 'FirstV_15_buy', 'MaxV_15_buy', 'SumV_15_buy', 'TradeCount_15_buy', 'DeltaP_5_buy', 'MedianV_5_buy', 'MinV_5_buy', 'VolumeVolatility_5_buy', 'DeltaV_5_buy', 'Momentum_5_buy', 'SumV_5_buy', 'TradeCount_5_buy', 'FirstP_1_buy', 'PriceVolatility_1_buy', 'FirstV_1_buy', 'MeanV_1_buy', 'MaxV_1_buy', 'DeltaV_1_buy', 'VWAP_1_buy', 'SumV_1_buy', 'TradeCount_1_buy', 'PctlP_10_full_buy', 'PctlP_25_full_buy', 'PctlP_55_full_buy', 'PctlP_90_full_buy', 'PctlV_25_full_buy', 'PctlV_45_full_buy', 'PctlV_55_full_buy', 'PctlV_75_full_buy', 'PctlP_75_180_buy', 'PctlP_90_180_buy', 'PctlV_45_180_buy', 'PctlV_55_180_buy', 'PctlV_75_180_buy', 'PctlV_90_180_buy', 'PctlV_10_60_buy', 'PctlV_25_60_buy', 'PctlV_45_60_buy', 'PctlV_55_60_buy', 'PctlV_25_15_buy', 'PctlV_45_15_buy', 'PctlV_75_15_buy', 'PctlV_90_15_buy', 'PctlV_25_5_buy', 'PctlV_45_5_buy', 'PctlV_75_5_buy', 'PctlV_10_1_buy']
	90	19	['MaxV_full_sell', 'SumV_full_sell', 'TradeCount_full_sell', 'PctlP_90_full_sell', 'PctlV_90_full_sell', 'MaxP_180_sell', 'TradeCount_180_sell', 'LastP_60_sell', 'MaxP_60_sell', 'MaxP_1_sell', 'FirstP_full_buy', 'LastP_full_buy', 'MaxP_full_buy', 'TradeCount_full_buy', 'MaxP_180_buy', 'TradeCount_180_buy', 'MaxP_1_buy', 'PctlP_90_full_buy', 'PctlP_90_15_buy']

A.1.2. IPC Selectors Results

Table A.2: Selected features of IPC selectors

Case Desc.	Quantile	Num Features	Features
ID1 DE h	10	33	['MinP_15_buy', 'MinP_5_buy', 'MeanP_60_sell', 'MedianP_5_sell', 'VWAP_60_buy', 'MinP_1_buy', 'PctlP_45_5_buy', 'PctlP_10_1_buy', 'PctlP_55_1_sell', 'PctlP_25_1_buy', 'MaxP_1_sell', 'PctlP_75_180_buy', 'PctlP_45_1_buy', 'PctlP_75_180_sell', 'LastP_full_buy', 'PctlP_10_60_sell', 'PctlP_75_1_buy', 'VWAP_180_sell', 'PctlP_10_5_sell', 'PctlP_90_full_sell', 'FirstP_5_sell', 'MinP_60_buy', 'PctlP_90_15_sell', 'PctlP_10_1_sell', 'FirstP_15_buy', 'PctlP_90_15_buy', 'MaxP_15_sell', 'PctlP_90_5_buy', 'PctlP_25_180_sell', 'MeanP_full_buy', 'MaxP_60_sell', 'PctlP_25_full_sell', 'MaxP_180_sell']
	25	10	['MinP_5_buy', 'VWAP_60_sell', 'MeanP_60_sell', 'PctlP_10_5_buy', 'PctlP_75_60_buy', 'PctlP_45_15_buy', 'PctlP_55_15_sell', 'PctlP_25_60_buy', 'PctlP_45_5_sell', 'MedianP_5_sell']
	45	4	['PctlP_75_60_sell', 'MinP_5_buy', 'MeanP_60_sell', 'PctlP_10_5_buy']
	50	3	['MinP_5_buy', 'MeanP_60_sell', 'PctlP_10_5_buy']
	55	3	['MinP_5_buy', 'MeanP_60_sell', 'PctlP_10_5_buy']
	75	10	['PctlP_10_1_buy', 'PctlP_25_5_buy', 'PctlP_25_1_buy', 'MedianP_5_sell', 'LastP_full_buy', 'PctlP_90_1_sell', 'VWAP_5_sell', 'PctlP_75_60_buy', 'MinP_60_buy', 'VWAP_15_buy']
	90	22	['MinP_15_buy', 'PctlP_55_60_buy', 'MedianP_60_buy', 'MeanP_60_sell', 'MedianP_5_sell', 'VWAP_60_buy', 'PctlP_55_15_buy', 'PctlP_75_60_buy', 'VWAP_15_buy', 'PctlP_25_5_sell', 'PctlP_75_15_sell', 'PctlP_45_5_buy', 'PctlP_10_1_buy', 'VWAP_5_sell', 'PctlP_25_1_buy', 'MaxP_1_sell', 'PctlP_45_1_sell', 'PctlP_10_60_buy', 'FirstP_5_buy', 'LastP_full_buy', 'VWAP_1_buy', 'PctlP_90_60_sell']
ID1 AT h	10	15	['VWAP_5_sell', 'PctlP_90_1_sell', 'VWAP_180_sell', 'VWAP_15_buy', 'PctlP_10_5_buy', 'LastP_full_sell', 'PctlP_90_full_sell', 'VWAP_full_buy', 'PctlP_55_1_buy', 'FirstP_15_buy', 'MaxP_180_sell', 'MinP_15_buy', 'PctlP_10_full_sell', 'PctlP_10_180_sell', 'FirstP_180_buy']
	25	10	['VWAP_5_sell', 'PctlP_90_1_sell', 'PctlP_55_5_sell', 'PctlP_25_15_sell', 'PctlP_10_1_buy', 'LastP_full_sell', 'VWAP_180_sell', 'PctlP_45_60_sell', 'PctlP_10_15_buy', 'VWAP_180_buy']
	45	8	['PctlP_75_60_sell', 'VWAP_15_sell', 'VWAP_1_sell', 'VWAP_5_sell', 'PctlP_45_15_buy', 'MeanP_5_sell', 'PctlP_25_15_sell', 'PctlP_90_1_sell']
	50	7	['PctlP_75_60_sell', 'VWAP_15_sell', 'VWAP_1_sell', 'VWAP_5_sell', 'PctlP_45_15_buy', 'PctlP_75_5_sell', 'MeanP_1_sell']
	55	7	['PctlP_75_60_sell', 'VWAP_15_sell', 'PctlP_90_60_sell', 'VWAP_5_sell', 'PctlP_45_15_buy', 'PctlP_75_5_sell', 'MeanP_1_sell']
	75	25	['MedianP_15_buy', 'FirstP_5_sell', 'PctlP_90_5_sell', 'PctlP_90_15_sell', 'MedianP_5_sell', 'MaxP_15_sell', 'MaxP_1_sell', 'PctlP_55_60_sell', 'PctlP_10_1_buy', 'PctlP_10_5_buy', 'PctlP_45_1_buy', 'LastP_full_sell', 'PctlP_10_5_sell', 'MinP_1_sell', 'FirstP_15_sell', 'VWAP_180_buy', 'MaxP_60_sell', 'VWAP_full_buy', 'PctlP_75_full_buy', 'MinP_5_sell', 'PctlP_10_180_buy', 'MinP_15_sell', 'MaxP_full_sell', 'MinP_60_buy', 'PctlP_55_15_buy']
	90	21	['MaxP_1_sell', 'PctlP_45_15_buy', 'MaxP_15_sell', 'PctlP_25_5_buy', 'PctlP_25_5_sell', 'PctlP_45_1_buy', 'PctlP_10_1_buy', 'LastP_full_sell', 'PctlP_10_5_buy', 'PctlP_10_5_sell', 'PctlP_55_180_buy', 'FirstP_15_sell', 'MaxP_60_sell', 'VWAP_full_buy', 'PctlP_75_full_buy', 'PctlP_45_full_sell', 'PctlP_25_full_sell', 'MinP_60_buy', 'FirstP_180_sell', 'MinP_180_buy', 'MaxP_full_sell']
ID2 DE h	10	20	['MaxP_15_sell', 'PctlP_10_15_buy', 'MinP_15_buy', 'PctlP_90_5_sell', 'PctlP_75_5_sell', 'PctlP_75_60_sell', 'MeanP_5_sell', 'MaxP_180_sell', 'VWAP_60_sell', 'PctlP_25_60_sell', 'PctlP_10_60_buy', 'MinP_60_buy', 'VWAP_60_buy', 'PctlP_90_full_sell', 'MeanP_180_buy', 'MinP_180_buy', 'VWAP_full_sell', 'PctlP_25_full_sell', 'PctlP_10_full_buy', 'MaxP_full_sell']

Case Desc.	Quantile	Num Features	Features
	25	24	['MaxP_15_sell', 'PctlP_10_15_buy', 'MinP_15_buy', 'PctlP_90_5_sell', 'PctlP_75_5_sell', 'MaxP_60_sell', 'PctlP_25_15_sell', 'PctlP_75_1_sell', 'VWAP_15_buy', 'PctlP_25_5_sell', 'PctlP_25_60_sell', 'PctlP_10_60_buy', 'MeanP_5_sell', 'MaxP_180_sell', 'MeanP_15_buy', 'PctlP_90_full_sell', 'PctlP_10_180_buy', 'MeanP_180_sell', 'PctlP_75_full_buy', 'MinP_180_buy', 'PctlP_25_full_sell', 'VWAP_full_sell', 'VWAP_180_buy', 'MaxP_full_sell']
	45	23	['MedianP_15_buy', 'PctlP_10_15_buy', 'MinP_15_buy', 'PctlP_90_5_sell', 'MaxP_5_sell', 'MaxP_60_sell', 'PctlP_75_5_sell', 'MinP_5_buy', 'PctlP_25_15_sell', 'VWAP_15_buy', 'PctlP_25_5_sell', 'MeanP_5_sell', 'MaxP_180_sell', 'PctlP_10_60_buy', 'VWAP_60_buy', 'PctlP_75_180_sell', 'PctlP_75_180_buy', 'MeanP_15_buy', 'PctlP_90_full_sell', 'VWAP_5_buy', 'PctlP_25_full_sell', 'PctlP_10_full_buy', 'PctlP_10_full_sell']
	50	9	['PctlP_10_15_buy', 'MinP_15_buy', 'PctlP_90_5_sell', 'MaxP_5_sell', 'PctlP_75_5_sell', 'MinP_5_buy', 'MaxP_180_sell', 'MeanP_1_sell', 'VWAP_15_sell']
	55	7	['MaxP_15_sell', 'PctlP_10_15_buy', 'PctlP_90_5_sell', 'MaxP_5_sell', 'MaxP_60_sell', 'PctlP_75_5_sell', 'MinP_5_buy']
	75	10	['MaxP_15_sell', 'PctlP_10_5_buy', 'MaxP_5_sell', 'PctlP_45_5_sell', 'MinP_60_buy', 'VWAP_15_buy', 'PctlP_90_180_sell', 'PctlP_10_180_buy', 'PctlP_10_180_sell', 'PctlP_45_full_sell']
	90	16	['MaxP_15_sell', 'PctlP_45_5_buy', 'MaxP_60_sell', 'PctlP_10_5_buy', 'PctlP_90_15_buy', 'PctlP_25_15_sell', 'MaxP_180_sell', 'MinP_60_buy', 'PctlP_10_60_sell', 'VWAP_5_buy', 'PctlP_10_180_sell', 'MinP_180_buy', 'PctlP_10_full_buy', 'PctlP_10_full_sell', 'MaxP_full_sell', 'FirstP_60_buy']
ID2 AT h	10	30	['MaxP_5_sell', 'VWAP_60_sell', 'PctlP_45_15_sell', 'PctlP_45_60_buy', 'LastP_full_sell', 'PctlP_90_60_sell', 'PctlP_25_60_buy', 'MaxP_60_sell', 'VWAP_60_buy', 'PctlP_25_60_sell', 'MinP_1_sell', 'MinP_15_sell', 'PctlP_45_180_sell', 'MinP_60_buy', 'PctlP_25_180_sell', 'MedianP_180_buy', 'PctlP_10_60_sell', 'FirstP_60_buy', 'MaxP_180_sell', 'VWAP_full_sell', 'MinP_1_buy', 'PctlP_55_full_sell', 'FirstP_15_buy', 'PctlP_25_full_sell', 'VWAP_full_buy', 'MinP_180_buy', 'PctlP_90_full_sell', 'MinP_60_sell', 'PctlP_90_5_buy', 'LastP_full_buy']
	25	15	['VWAP_60_sell', 'MaxP_5_sell', 'PctlP_45_60_buy', 'PctlP_90_60_sell', 'VWAP_1_sell', 'VWAP_5_sell', 'PctlP_75_60_sell', 'PctlP_90_15_sell', 'FirstP_5_sell', 'MeanP_15_sell', 'PctlP_25_60_buy', 'VWAP_60_buy', 'MeanP_1_sell', 'MaxP_60_sell', 'MedianP_60_buy']
	45	9	['VWAP_60_sell', 'PctlP_45_60_buy', 'VWAP_60_buy', 'PctlP_25_60_buy', 'MaxP_1_sell', 'MaxP_5_sell', 'VWAP_1_sell', 'MeanP_5_sell', 'PctlP_55_15_sell']
	50	9	['VWAP_60_sell', 'PctlP_45_60_buy', 'VWAP_60_buy', 'PctlP_25_60_buy', 'MaxP_1_sell', 'MaxP_5_sell', 'PctlP_90_5_sell', 'VWAP_1_sell', 'PctlP_55_15_sell']
	55	35	['VWAP_60_sell', 'MaxP_5_sell', 'PctlP_90_5_sell', 'PctlP_45_60_buy', 'PctlP_75_1_sell', 'VWAP_15_sell', 'FirstP_1_sell', 'VWAP_5_sell', 'VWAP_60_buy', 'MaxP_60_sell', 'LastP_full_sell', 'FirstP_15_sell', 'PctlP_55_60_buy', 'PctlP_45_1_buy', 'PctlP_75_60_buy', 'VWAP_180_sell', 'FirstP_1_buy', 'MinP_1_sell', 'PctlP_45_180_buy', 'PctlP_75_15_buy', 'PctlP_55_1_buy', 'PctlP_55_5_buy', 'MaxP_1_buy', 'FirstP_60_buy', 'PctlP_45_180_sell', 'FirstP_15_buy', 'MinP_15_buy', 'MinP_1_buy', 'PctlP_10_60_sell', 'PctlP_90_60_buy', 'LastP_full_buy', 'PctlP_90_180_buy', 'PctlP_75_full_sell', 'PctlP_55_full_sell', 'PctlP_25_full_sell']
	75	32	['PctlP_90_1_sell', 'PctlP_90_5_sell', 'MaxP_5_sell', 'VWAP_15_sell', 'PctlP_45_60_buy', 'LastP_full_sell', 'PctlP_25_60_buy', 'PctlP_25_5_sell', 'MaxP_60_sell', 'PctlP_25_60_sell', 'FirstP_15_sell', 'VWAP_180_sell', 'PctlP_45_180_buy', 'PctlP_25_180_buy', 'PctlP_90_180_sell', 'PctlP_45_180_sell', 'PctlP_10_180_buy', 'FirstP_60_buy', 'MaxP_180_sell', 'FirstP_1_buy', 'VWAP_full_sell', 'MeanP_full_buy', 'VWAP_5_buy', 'VWAP_15_buy', 'MinP_15_buy', 'FirstP_15_buy', 'PctlP_25_full_sell', 'PctlP_10_full_buy', 'MinP_180_buy', 'PctlP_90_full_sell', 'MaxP_1_buy', 'LastP_full_buy']

Case Desc.	Quantile	Num Features	Features
	90	33	['PctlP_90_1_sell', 'MaxP_1_sell', 'PctlP_90_15_sell', 'VWAP_60_sell', 'MaxP_15_sell', 'LastP_full_sell', 'PctlP_25_60_buy', 'MaxP_60_sell', 'PctlP_10_5_sell', 'MedianP_60_buy', 'FirstP_15_sell', 'MinP_1_sell', 'PctlP_90_180_sell', 'PctlP_45_180_sell', 'MinP_60_buy', 'VWAP_180_buy', 'FirstP_60_buy', 'FirstP_60_sell', 'PctlP_25_15_buy', 'MaxP_180_sell', 'FirstP_5_buy', 'MeanP_full_buy', 'MinP_15_buy', 'PctlP_55_180_buy', 'PctlP_25_full_sell', 'VWAP_full_buy', 'PctlP_10_full_buy', 'MinP_180_buy', 'PctlP_90_full_sell', 'PctlP_90_180_buy', 'MaxP_1_buy', 'MaxP_5_buy', 'LastP_full_buy']
ID3 DE h	10	15	['PctlP_10_15_buy', 'MinP_15_buy', 'MaxP_5_sell', 'PctlP_10_60_buy', 'MedianP_5_sell', 'MinP_60_buy', 'PctlP_55_60_buy', 'PctlP_10_180_buy', 'MaxP_180_sell', 'MinP_180_buy', 'PctlP_90_full_sell', 'MeanP_full_sell', 'MaxP_full_sell', 'MinP_full_buy', 'MeanP_60_buy']
	25	16	['PctlP_10_15_buy', 'PctlP_90_5_sell', 'MaxP_5_sell', 'MinP_15_buy', 'PctlP_25_5_buy', 'PctlP_10_60_buy', 'MaxP_60_sell', 'MedianP_180_buy', 'MaxP_180_sell', 'PctlP_10_180_buy', 'PctlP_90_full_sell', 'MinP_180_buy', 'PctlP_10_full_buy', 'MeanP_180_sell', 'MeanP_full_sell', 'MaxP_full_sell']
	45	18	['PctlP_10_15_buy', 'PctlP_75_15_sell', 'PctlP_90_15_sell', 'MinP_15_buy', 'PctlP_90_5_sell', 'MaxP_5_sell', 'PctlP_45_15_buy', 'PctlP_25_60_buy', 'PctlP_55_15_buy', 'PctlP_10_60_buy', 'PctlP_10_5_buy', 'PctlP_25_5_buy', 'MinP_5_buy', 'MedianP_5_buy', 'PctlP_75_15_buy', 'MaxP_60_sell', 'PctlP_90_180_sell', 'MeanP_5_buy']
	50	15	['PctlP_10_15_buy', 'PctlP_75_15_sell', 'PctlP_90_15_sell', 'MinP_15_buy', 'PctlP_90_5_sell', 'MaxP_5_sell', 'PctlP_45_15_buy', 'PctlP_25_60_buy', 'PctlP_10_5_buy', 'PctlP_25_5_buy', 'PctlP_90_60_sell', 'MedianP_5_buy', 'PctlP_75_15_buy', 'PctlP_45_60_buy', 'MaxP_60_sell']
	55	14	['PctlP_10_15_buy', 'PctlP_90_5_sell', 'PctlP_75_15_sell', 'MaxP_5_sell', 'PctlP_90_15_sell', 'MinP_15_buy', 'PctlP_10_5_buy', 'PctlP_25_5_buy', 'PctlP_10_1_buy', 'MinP_60_buy', 'PctlP_45_180_sell', 'PctlP_55_180_buy', 'PctlP_90_full_sell', 'PctlP_10_full_buy']
	75	22	['PctlP_90_15_sell', 'MaxP_15_sell', 'PctlP_10_15_buy', 'MaxP_5_sell', 'PctlP_10_5_buy', 'MinP_5_buy', 'MinP_1_buy', 'PctlP_45_5_sell', 'VWAP_1_buy', 'MedianP_1_buy', 'PctlP_90_180_sell', 'MaxP_180_sell', 'PctlP_55_180_buy', 'PctlP_25_5_sell', 'VWAP_5_sell', 'PctlP_25_180_sell', 'PctlP_90_full_sell', 'PctlP_45_1_sell', 'PctlP_25_full_sell', 'PctlP_10_full_buy', 'PctlP_25_1_sell', 'VWAP_60_sell']
	90	24	['PctlP_90_15_sell', 'MaxP_15_sell', 'MaxP_5_sell', 'PctlP_10_5_buy', 'MaxP_60_sell', 'PctlP_90_180_sell', 'PctlP_45_full_sell', 'VWAP_5_sell', 'MaxP_180_sell', 'PctlP_25_full_buy', 'MeanP_5_sell', 'PctlP_25_full_sell', 'PctlP_90_full_sell', 'PctlP_10_full_buy', 'VWAP_180_sell', 'VWAP_1_sell', 'MaxP_full_sell', 'MeanP_60_sell', 'PctlP_45_1_sell', 'PctlP_25_1_sell', 'PctlP_10_full_sell', 'FirstP_1_sell', 'PctlP_25_15_sell', 'MeanP_60_buy']
ID3 AT h	10	19	['PctlP_45_5_sell', 'LastP_full_sell', 'FirstP_1_sell', 'MinP_15_buy', 'MinP_5_buy', 'FirstP_15_sell', 'MinP_5_sell', 'MaxP_60_sell', 'PctlP_10_60_sell', 'FirstP_5_buy', 'PctlP_90_180_sell', 'MinP_180_buy', 'MaxP_180_sell', 'LastP_full_buy', 'PctlP_10_15_buy', 'MaxP_5_buy', 'PctlP_75_full_sell', 'PctlP_10_full_buy', 'VWAP_full_buy']
	25	11	['LastP_full_sell', 'PctlP_25_5_sell', 'PctlP_25_15_sell', 'FirstP_5_sell', 'MinP_5_buy', 'MinP_1_buy', 'PctlP_10_5_sell', 'MinP_60_buy', 'MinP_5_sell', 'PctlP_10_60_sell', 'PctlP_10_180_buy']
	45	13	['LastP_full_sell', 'MedianP_5_sell', 'PctlP_25_5_sell', 'FirstP_1_sell', 'FirstP_5_sell', 'MinP_1_buy', 'MinP_5_buy', 'LastP_full_buy', 'MinP_60_buy', 'FirstP_60_sell', 'MinP_60_sell', 'MinP_180_buy', 'PctlP_45_full_buy']
	50	10	['LastP_full_sell', 'PctlP_45_5_sell', 'LastP_full_buy', 'FirstP_1_sell', 'FirstP_5_sell', 'MinP_1_buy', 'MinP_5_buy', 'FirstP_60_sell', 'PctlP_75_full_sell', 'PctlP_45_full_buy']
	55	13	['PctlP_45_5_sell', 'LastP_full_sell', 'MaxP_1_sell', 'FirstP_1_sell', 'MinP_15_buy', 'FirstP_5_sell', 'MinP_5_buy', 'MinP_1_buy', 'FirstP_60_sell', 'MaxP_180_sell', 'LastP_full_buy', 'PctlP_45_full_buy', 'PctlP_75_full_sell']

Case Desc.	Quantile	Num Features	Features
	75	23	['LastP_full_sell', 'MaxP_1_sell', 'PctlP_90_1_sell', 'LastP_full_buy', 'PctlP_10_1_sell', 'PctlP_90_180_sell', 'PctlP_90_1_buy', 'MinP_15_buy', 'PctlP_45_180_sell', 'MaxP_180_sell', 'PctlP_45_180_buy', 'PctlP_45_60_buy', 'PctlP_10_180_buy', 'PctlP_25_60_buy', 'MinP_60_sell', 'PctlP_10_180_sell', 'VWAP_full_sell', 'PctlP_10_60_buy', 'MeanP_full_buy', 'PctlP_25_full_buy', 'MinP_180_buy', 'PctlP_90_full_sell', 'PctlP_45_full_buy']
	90	24	['LastP_full_sell', 'MaxP_1_sell', 'PctlP_90_1_sell', 'PctlP_90_5_sell', 'LastP_full_buy', 'PctlP_90_180_sell', 'MinP_15_sell', 'MaxP_180_sell', 'MaxP_5_buy', 'PctlP_45_180_buy', 'PctlP_25_180_sell', 'PctlP_75_60_buy', 'MinP_60_sell', 'PctlP_55_60_buy', 'PctlP_10_180_sell', 'VWAP_full_sell', 'PctlP_10_60_buy', 'MeanP_full_buy', 'PctlP_55_full_sell', 'PctlP_25_full_buy', 'VWAP_full_buy', 'MinP_180_buy', 'PctlP_90_full_sell', 'PctlP_45_full_buy']
ID1 DE qh	10	4	['MinP_15_buy', 'PctlP_10_1_buy', 'MinP_60_buy', 'MinP_180_buy']
	25	12	['PctlP_25_5_buy', 'PctlP_10_5_buy', 'MinP_5_buy', 'PctlP_25_5_sell', 'VWAP_60_sell', 'MaxP_5_sell', 'MaxP_1_sell', 'MeanP_60_buy', 'PctlP_90_1_sell', 'PctlP_75_60_buy', 'PctlP_45_5_buy', 'PctlP_90_15_sell']
	45	10	['PctlP_25_5_buy', 'PctlP_10_5_buy', 'MinP_5_buy', 'PctlP_25_5_sell', 'VWAP_60_buy', 'MaxP_1_sell', 'MeanP_60_buy', 'PctlP_90_1_sell', 'PctlP_75_60_buy', 'PctlP_90_15_sell']
	50	7	['PctlP_25_5_buy', 'PctlP_10_5_buy', 'MinP_5_buy', 'VWAP_60_buy', 'MaxP_1_sell', 'MeanP_60_buy', 'PctlP_90_1_sell']
	55	7	['PctlP_25_5_buy', 'PctlP_10_5_buy', 'PctlP_45_5_sell', 'VWAP_60_buy', 'MinP_1_buy', 'VWAP_5_sell', 'MedianP_5_buy']
	75	11	['PctlP_25_5_buy', 'PctlP_10_5_buy', 'VWAP_60_buy', 'MinP_15_buy', 'PctlP_10_1_buy', 'VWAP_180_sell', 'PctlP_90_180_buy', 'PctlP_10_60_buy', 'PctlP_90_5_sell', 'MaxP_1_sell', 'VWAP_full_buy']
	90	13	['VWAP_60_buy', 'MinP_15_buy', 'MeanP_5_buy', 'VWAP_180_sell', 'PctlP_25_1_buy', 'PctlP_90_60_buy', 'PctlP_90_180_buy', 'MeanP_1_sell', 'PctlP_10_60_buy', 'PctlP_90_5_sell', 'MaxP_1_sell', 'VWAP_full_buy', 'PctlP_10_5_sell']
ID1 AT qh	10	31	['MeanP_60_buy', 'VWAP_60_sell', 'VWAP_60_buy', 'VWAP_180_sell', 'PctlP_45_15_buy', 'MeanP_180_sell', 'PctlP_55_15_buy', 'PctlP_55_15_sell', 'PctlP_45_180_sell', 'PctlP_75_15_sell', 'MedianP_180_sell', 'MedianP_15_sell', 'MeanP_15_sell', 'PctlP_25_180_sell', 'VWAP_15_sell', 'PctlP_90_15_sell', 'PctlP_45_180_buy', 'MeanP_full_buy', 'PctlP_90_60_sell', 'PctlP_10_60_buy', 'MeanP_15_buy', 'VWAP_full_buy', 'VWAP_full_sell', 'PctlP_10_180_buy', 'PctlP_75_180_sell', 'PctlP_75_180_buy', 'FirstP_60_sell', 'PctlP_55_full_buy', 'MinP_15_buy', 'PctlP_25_full_sell', 'PctlP_75_5_sell']
	25	13	['PctlP_25_60_sell', 'PctlP_55_15_sell', 'PctlP_10_15_buy', 'PctlP_75_15_sell', 'MeanP_15_buy', 'PctlP_25_180_sell', 'VWAP_15_sell', 'MinP_15_buy', 'PctlP_10_180_sell', 'VWAP_full_sell', 'PctlP_75_5_sell', 'PctlP_90_5_sell', 'PctlP_10_full_buy']
	45	15	['PctlP_45_60_sell', 'PctlP_25_15_buy', 'PctlP_10_15_buy', 'PctlP_75_15_sell', 'MeanP_15_buy', 'PctlP_55_180_sell', 'PctlP_90_15_sell', 'MinP_15_buy', 'VWAP_full_sell', 'MaxP_15_sell', 'PctlP_75_15_buy', 'PctlP_90_5_sell', 'PctlP_25_full_buy', 'PctlP_55_full_buy', 'MedianP_full_buy']
	50	17	['MeanP_60_buy', 'PctlP_45_60_sell', 'PctlP_75_15_sell', 'PctlP_25_15_buy', 'PctlP_90_15_sell', 'VWAP_full_sell', 'VWAP_full_buy', 'VWAP_15_sell', 'PctlP_10_60_buy', 'PctlP_55_full_sell', 'PctlP_25_full_buy', 'PctlP_10_15_buy', 'PctlP_25_full_sell', 'VWAP_15_buy', 'PctlP_75_full_sell', 'PctlP_10_180_buy', 'MaxP_15_sell']
	55	21	['MeanP_60_buy', 'VWAP_180_sell', 'PctlP_75_60_sell', 'PctlP_55_15_sell', 'PctlP_75_15_sell', 'PctlP_75_60_buy', 'MeanP_full_buy', 'PctlP_25_15_buy', 'PctlP_25_180_sell', 'PctlP_90_15_sell', 'VWAP_full_buy', 'VWAP_15_sell', 'PctlP_55_15_buy', 'PctlP_10_60_buy', 'PctlP_55_full_sell', 'PctlP_25_full_buy', 'PctlP_10_15_buy', 'PctlP_25_full_sell', 'PctlP_75_full_sell', 'PctlP_10_180_buy', 'MaxP_15_sell']

Case Desc.	Quantile	Num Features	Features
	75	16	['PctlP_55_15_sell', 'MedianP_180_sell', 'MeanP_full_buy', 'PctlP_25_15_buy', 'MeanP_15_sell', 'PctlP_90_60_sell', 'VWAP_full_buy', 'PctlP_10_60_buy', 'PctlP_10_15_buy', 'PctlP_55_full_buy', 'PctlP_75_full_sell', 'PctlP_10_180_buy', 'MaxP_15_sell', 'PctlP_90_180_sell', 'PctlP_75_full_buy', 'PctlP_10_full_buy']
	90	19	['MedianP_60_sell', 'PctlP_45_180_sell', 'MedianP_180_sell', 'MedianP_15_sell', 'MeanP_full_buy', 'PctlP_25_15_buy', 'MeanP_15_sell', 'PctlP_90_60_sell', 'VWAP_full_buy', 'PctlP_75_180_sell', 'PctlP_45_full_sell', 'PctlP_10_60_buy', 'PctlP_10_15_buy', 'PctlP_10_180_buy', 'MaxP_15_sell', 'PctlP_90_180_sell', 'PctlP_75_full_buy', 'FirstP_60_buy', 'PctlP_10_full_buy']
ID2 DE qh	10	13	['MaxP_1_sell', 'MinP_15_buy', 'PctlP_75_1_sell', 'MeanP_15_buy', 'PctlP_25_1_sell', 'LastP_full_sell', 'FirstP_1_sell', 'MaxP_180_sell', 'PctlP_90_full_sell', 'MinP_60_buy', 'PctlP_25_15_sell', 'MeanP_15_sell', 'MinP_180_buy']
	25	20	['PctlP_10_15_buy', 'MinP_15_buy', 'MinP_5_buy', 'MaxP_15_sell', 'PctlP_90_1_sell', 'MaxP_1_sell', 'MeanP_60_sell', 'PctlP_10_60_buy', 'PctlP_75_15_sell', 'PctlP_75_1_sell', 'VWAP_60_buy', 'MeanP_180_sell', 'PctlP_45_180_sell', 'PctlP_45_15_sell', 'PctlP_90_180_sell', 'PctlP_75_180_buy', 'MaxP_60_sell', 'MinP_60_buy', 'PctlP_25_180_buy', 'PctlP_25_180_sell']
	45	21	['PctlP_10_15_buy', 'MinP_15_buy', 'MinP_5_buy', 'PctlP_90_5_sell', 'MaxP_5_sell', 'PctlP_90_1_sell', 'PctlP_75_60_buy', 'MaxP_1_sell', 'MeanP_60_sell', 'PctlP_10_60_buy', 'PctlP_75_15_sell', 'PctlP_55_1_sell', 'PctlP_45_5_sell', 'VWAP_60_buy', 'PctlP_55_180_buy', 'MeanP_180_sell', 'PctlP_90_180_sell', 'PctlP_75_180_buy', 'MaxP_60_sell', 'PctlP_25_180_buy', 'PctlP_25_180_sell']
	50	17	['PctlP_10_15_buy', 'MinP_15_buy', 'MinP_5_buy', 'MaxP_15_sell', 'PctlP_90_5_sell', 'MaxP_5_sell', 'MaxP_1_sell', 'MeanP_60_sell', 'PctlP_10_60_buy', 'PctlP_75_15_sell', 'MinP_1_buy', 'PctlP_45_5_sell', 'VWAP_60_buy', 'MeanP_180_sell', 'PctlP_75_180_buy', 'MaxP_60_sell', 'PctlP_25_180_buy']
	55	15	['PctlP_10_15_buy', 'MinP_15_buy', 'MinP_5_buy', 'MaxP_15_sell', 'PctlP_90_5_sell', 'MaxP_5_sell', 'PctlP_75_60_buy', 'MaxP_1_sell', 'PctlP_10_60_buy', 'PctlP_75_15_sell', 'MinP_1_buy', 'MeanP_180_sell', 'PctlP_75_180_buy', 'MaxP_60_sell', 'VWAP_5_sell']
	75	18	['PctlP_10_15_buy', 'PctlP_45_15_buy', 'MinP_15_buy', 'MinP_5_buy', 'MaxP_15_sell', 'PctlP_55_60_sell', 'MaxP_5_sell', 'PctlP_90_60_sell', 'PctlP_75_60_buy', 'MaxP_1_sell', 'PctlP_75_1_sell', 'PctlP_10_1_buy', 'MeanP_180_sell', 'PctlP_90_180_sell', 'MinP_60_buy', 'VWAP_5_sell', 'PctlP_25_1_buy', 'PctlP_25_180_sell']
	90	16	['MedianP_15_buy', 'MaxP_15_sell', 'PctlP_90_5_sell', 'PctlP_45_60_sell', 'PctlP_90_60_sell', 'MeanP_60_sell', 'PctlP_75_1_sell', 'PctlP_10_1_buy', 'PctlP_25_5_buy', 'PctlP_90_180_sell', 'MaxP_60_sell', 'MinP_60_buy', 'VWAP_5_sell', 'PctlP_25_1_buy', 'PctlP_25_180_sell', 'MeanP_180_buy']
ID2 AT qh	10	13	['LastP_full_sell', 'LastP_full_buy', 'MinP_1_sell', 'MinP_1_buy', 'MinP_15_sell', 'PctlP_75_180_buy', 'VWAP_full_sell', 'PctlP_10_180_buy', 'MinP_60_buy', 'PctlP_75_full_buy', 'MaxP_180_sell', 'PctlP_10_180_sell', 'PctlP_25_full_sell']
	25	16	['LastP_full_sell', 'PctlP_10_1_sell', 'PctlP_10_5_sell', 'PctlP_10_1_buy', 'MinP_1_sell', 'PctlP_10_15_sell', 'LastP_full_buy', 'MinP_1_buy', 'MinP_5_buy', 'MinP_15_buy', 'PctlP_10_180_buy', 'PctlP_25_full_sell', 'PctlP_10_180_sell', 'MinP_60_buy', 'PctlP_10_full_buy', 'MinP_60_sell']
	45	5	['MeanP_1_sell', 'MeanP_5_sell', 'MeanP_60_sell', 'VWAP_15_sell', 'MeanP_60_buy']
	50	21	['VWAP_15_sell', 'LastP_full_sell', 'PctlP_55_5_sell', 'MaxP_5_sell', 'PctlP_10_1_sell', 'PctlP_55_1_buy', 'LastP_full_buy', 'PctlP_10_15_sell', 'PctlP_10_5_buy', 'VWAP_180_sell', 'MinP_1_buy', 'MaxP_1_buy', 'MeanP_full_sell', 'FirstP_1_buy', 'PctlP_75_full_sell', 'MinP_60_buy', 'VWAP_full_buy', 'MedianP_full_buy', 'PctlP_45_full_buy', 'PctlP_90_full_sell', 'PctlP_25_full_buy']

Case Desc.	Quantile	Num Features	Features
	55	20	['VWAP_15_sell', 'PctlP_55_5_sell', 'LastP_full_sell', 'PctlP_55_1_buy', 'PctlP_10_5_buy', 'VWAP_180_sell', 'LastP_full_buy', 'MinP_1_buy', 'MaxP_1_sell', 'MaxP_5_sell', 'PctlP_90_60_sell', 'MeanP_full_buy', 'MeanP_full_sell', 'FirstP_1_buy', 'MaxP_1_buy', 'VWAP_full_buy', 'PctlP_45_full_buy', 'PctlP_90_180_sell', 'PctlP_75_full_sell', 'PctlP_75_full_buy']
	75	25	['VWAP_15_sell', 'LastP_full_sell', 'PctlP_45_60_buy', 'MaxP_1_sell', 'MaxP_15_sell', 'LastP_full_buy', 'PctlP_90_60_sell', 'MinP_1_buy', 'FirstP_15_sell', 'PctlP_25_60_sell', 'PctlP_45_180_sell', 'MaxP_1_buy', 'MeanP_full_buy', 'PctlP_90_180_sell', 'MaxP_15_buy', 'PctlP_25_180_sell', 'PctlP_75_full_sell', 'PctlP_10_180_buy', 'MedianP_full_buy', 'PctlP_75_full_buy', 'PctlP_90_180_buy', 'MaxP_180_sell', 'PctlP_10_180_sell', 'MaxP_60_buy', 'PctlP_25_full_sell']
	90	22	['VWAP_15_sell', 'LastP_full_sell', 'PctlP_90_15_sell', 'MaxP_1_sell', 'LastP_full_buy', 'FirstP_1_sell', 'PctlP_90_60_sell', 'FirstP_15_sell', 'PctlP_90_15_buy', 'MedianP_180_sell', 'MaxP_1_buy', 'MaxP_60_sell', 'MeanP_full_buy', 'MaxP_15_buy', 'PctlP_75_full_sell', 'PctlP_10_180_buy', 'PctlP_75_full_buy', 'PctlP_90_180_buy', 'MaxP_180_sell', 'PctlP_10_180_sell', 'MaxP_60_buy', 'PctlP_25_full_sell']
ID3 DE qh	10	7	['PctlP_10_60_buy', 'PctlP_75_15_sell', 'MeanP_60_sell', 'MinP_15_buy', 'PctlP_10_180_buy', 'MinP_60_buy', 'PctlP_90_180_sell']
	25	6	['PctlP_10_60_buy', 'PctlP_75_15_sell', 'MinP_15_buy', 'PctlP_10_180_buy', 'MinP_60_buy', 'PctlP_90_180_sell']
	45	10	['PctlP_25_60_buy', 'PctlP_45_60_sell', 'PctlP_10_60_buy', 'PctlP_90_15_sell', 'PctlP_75_15_sell', 'MaxP_15_sell', 'MinP_15_buy', 'PctlP_10_180_buy', 'MinP_60_buy', 'PctlP_90_180_sell']
	50	12	['PctlP_25_60_buy', 'PctlP_75_60_sell', 'PctlP_45_60_sell', 'PctlP_10_60_buy', 'PctlP_90_15_sell', 'MaxP_15_sell', 'VWAP_60_sell', 'PctlP_10_15_buy', 'MeanP_60_sell', 'MinP_15_buy', 'MinP_60_buy', 'PctlP_90_180_sell']
	55	8	['PctlP_25_60_buy', 'PctlP_45_60_buy', 'PctlP_75_60_sell', 'PctlP_10_60_buy', 'PctlP_90_15_sell', 'MaxP_15_sell', 'PctlP_10_15_buy', 'MinP_15_buy']
	75	16	['PctlP_25_60_buy', 'PctlP_75_60_sell', 'PctlP_45_60_sell', 'PctlP_90_60_sell', 'PctlP_90_15_sell', 'PctlP_55_180_sell', 'MaxP_15_sell', 'VWAP_60_sell', 'PctlP_10_15_buy', 'MeanP_60_sell', 'MinP_15_buy', 'PctlP_25_180_sell', 'PctlP_10_180_buy', 'VWAP_180_sell', 'MinP_60_buy', 'PctlP_90_180_sell']
	90	22	['PctlP_90_60_sell', 'PctlP_75_60_sell', 'PctlP_90_15_sell', 'MaxP_15_sell', 'PctlP_55_60_buy', 'PctlP_45_60_sell', 'PctlP_25_60_buy', 'MaxP_60_sell', 'PctlP_90_180_sell', 'PctlP_75_180_buy', 'PctlP_55_180_sell', 'MaxP_1_sell', 'PctlP_10_15_buy', 'PctlP_45_180_sell', 'PctlP_25_15_buy', 'MeanP_180_sell', 'MinP_60_buy', 'PctlP_25_180_sell', 'PctlP_45_15_sell', 'MaxP_180_sell', 'MinP_1_buy', 'PctlP_10_180_buy']
ID3 AT qh	10	24	['PctlP_75_180_buy', 'PctlP_90_180_sell', 'PctlP_75_180_sell', 'VWAP_180_sell', 'PctlP_90_5_buy', 'MedianP_180_buy', 'MaxP_180_sell', 'MaxP_5_buy', 'MaxP_60_buy', 'VWAP_full_buy', 'FirstP_5_buy', 'LastP_full_sell', 'VWAP_60_sell', 'FirstP_5_sell', 'FirstP_15_sell', 'VWAP_full_sell', 'PctlP_75_full_sell', 'PctlP_10_180_buy', 'MinP_5_buy', 'MinP_15_buy', 'PctlP_25_full_buy', 'PctlP_10_60_buy', 'MinP_1_sell', 'PctlP_90_full_sell']
	25	11	['PctlP_10_5_buy', 'LastP_full_buy', 'LastP_full_sell', 'PctlP_25_180_sell', 'VWAP_full_sell', 'PctlP_10_180_buy', 'MinP_15_buy', 'PctlP_25_full_buy', 'PctlP_10_60_buy', 'MinP_1_sell', 'PctlP_25_full_sell']
	45	5	['MeanP_180_buy', 'MeanP_180_sell', 'VWAP_1_buy', 'MeanP_1_buy', 'MeanP_15_buy']
	50	8	['MeanP_180_buy', 'MeanP_180_sell', 'VWAP_1_buy', 'VWAP_5_buy', 'PctlP_90_180_sell', 'MeanP_1_buy', 'MeanP_15_buy', 'PctlP_75_15_buy']
	55	7	['MeanP_180_buy', 'MeanP_180_sell', 'VWAP_1_buy', 'PctlP_90_180_sell', 'MeanP_1_buy', 'PctlP_90_180_buy', 'MeanP_15_buy']
	75	8	['MeanP_180_sell', 'VWAP_1_buy', 'PctlP_90_180_sell', 'MeanP_1_buy', 'PctlP_90_180_buy', 'PctlP_75_1_buy', 'MeanP_15_buy', 'PctlP_75_15_buy']

Case Desc.	Quantile	Num Features	Features
	90	7	['MaxP_180_sell', 'MaxP_1_buy', 'MaxP_180_buy', 'MaxP_1_sell', 'LastP_full_sell', 'PctlP_90_full_buy', 'PctlP_90_full_sell']

A.1.3. IPC Selection Results Analysis

Table A.3: Top five most important features selected by IPC

Case Desc.	Quantile	Top Five Features
ID1 DE h	10	['MinP_5_buy', 'PctlP_90_full_sell', 'MaxP_1_sell', 'MinP_1_buy', 'MaxP_60_sell']
	25	['MinP_5_buy', 'PctlP_75_60_buy', 'PctlP_25_60_buy', 'PctlP_10_5_buy', 'PctlP_45_5_sell']
	45	['PctlP_75_60_sell', 'MinP_5_buy', 'MeanP_60_sell', 'PctlP_10_5_buy']
	50	['MinP_5_buy', 'MeanP_60_sell', 'PctlP_10_5_buy']
	55	['MinP_5_buy', 'MeanP_60_sell', 'PctlP_10_5_buy']
	75	['PctlP_10_1_buy', 'MedianP_5_sell', 'PctlP_90_1_sell', 'PctlP_25_5_buy', 'MinP_60_buy']
	90	['PctlP_10_60_buy', 'PctlP_45_5_buy', 'MinP_15_buy', 'PctlP_10_1_buy', 'MedianP_60_buy']
ID1 AT h	10	['VWAP_5_sell', 'MaxP_180_sell', 'PctlP_10_180_sell', 'LastP_full_sell', 'PctlP_10_full_sell']
	25	['PctlP_10_15_buy', 'VWAP_5_sell', 'PctlP_90_1_sell', 'PctlP_25_15_sell', 'PctlP_45_60_sell']
	45	['PctlP_45_15_buy', 'PctlP_90_1_sell', 'MeanP_5_sell', 'VWAP_15_sell', 'PctlP_75_60_sell']
	50	['PctlP_45_15_buy', 'MeanP_1_sell', 'VWAP_5_sell', 'PctlP_75_60_sell', 'PctlP_75_5_sell']
	55	['MeanP_1_sell', 'PctlP_45_15_buy', 'PctlP_75_5_sell', 'PctlP_75_60_sell', 'VWAP_15_sell']
	75	['PctlP_10_1_buy', 'MaxP_60_sell', 'MedianP_15_buy', 'VWAP_full_buy', 'MinP_60_buy']
	90	['MaxP_full_sell', 'MaxP_15_sell', 'MaxP_60_sell', 'PctlP_55_180_buy', 'MinP_60_buy']
ID2 DE h	10	['PctlP_75_5_sell', 'MinP_60_buy', 'MinP_15_buy', 'PctlP_90_full_sell', 'PctlP_75_60_sell']
	25	['PctlP_75_5_sell', 'MinP_15_buy', 'PctlP_90_5_sell', 'PctlP_10_15_buy', 'PctlP_90_full_sell']
	45	['PctlP_90_5_sell', 'PctlP_10_15_buy', 'MaxP_5_sell', 'PctlP_75_5_sell', 'MinP_5_buy']
	50	['PctlP_90_5_sell', 'PctlP_10_15_buy', 'MaxP_5_sell', 'MinP_5_buy', 'MaxP_180_sell']
	55	['MaxP_5_sell', 'PctlP_90_5_sell', 'MinP_5_buy', 'PctlP_10_15_buy', 'PctlP_75_5_sell']
	75	['PctlP_10_5_buy', 'MaxP_15_sell', 'MaxP_5_sell', 'PctlP_90_180_sell', 'PctlP_45_full_sell']
	90	['MaxP_15_sell', 'PctlP_10_5_buy', 'PctlP_10_full_buy', 'MaxP_180_sell', 'MaxP_60_sell']
ID2 AT h	10	['MaxP_5_sell', 'MinP_180_buy', 'LastP_full_sell', 'FirstP_15_buy', 'MinP_1_buy']
	25	['MeanP_1_sell', 'VWAP_60_sell', 'PctlP_25_60_buy', 'PctlP_90_60_sell', 'VWAP_5_sell']
	45	['VWAP_1_sell', 'PctlP_45_60_buy', 'PctlP_25_60_buy', 'MaxP_1_sell', 'MaxP_5_sell']
	50	['VWAP_1_sell', 'PctlP_45_60_buy', 'MaxP_5_sell', 'PctlP_55_15_sell', 'VWAP_60_sell']
	55	['VWAP_60_buy', 'LastP_full_sell', 'PctlP_55_5_buy', 'PctlP_45_1_buy', 'LastP_full_buy']
	75	['MaxP_5_sell', 'LastP_full_sell', 'LastP_full_buy', 'MeanP_full_buy', 'PctlP_90_180_sell']
	90	['MinP_15_buy', 'MaxP_60_sell', 'FirstP_15_sell', 'MinP_180_buy', 'LastP_full_buy']
ID3 DE h	10	['PctlP_10_15_buy', 'MinP_15_buy', 'MaxP_5_sell', 'MaxP_180_sell', 'MinP_60_buy']
	25	['PctlP_10_15_buy', 'PctlP_90_5_sell', 'MinP_15_buy', 'PctlP_10_60_buy', 'PctlP_90_full_sell']
	45	['PctlP_10_15_buy', 'PctlP_90_5_sell', 'MaxP_5_sell', 'MinP_15_buy', 'PctlP_25_60_buy']

Case Desc.	Quantile	Top Five Features
	50	['PctlP_10_15_buy', 'PctlP_90_5_sell', 'MaxP_5_sell', 'PctlP_75_15_sell', 'MinP_15_buy']
	55	['PctlP_10_15_buy', 'PctlP_90_5_sell', 'PctlP_90_15_sell', 'PctlP_75_15_sell', 'PctlP_10_full_buy']
	75	['PctlP_90_15_sell', 'PctlP_10_full_buy', 'PctlP_10_15_buy', 'MaxP_5_sell', 'MaxP_15_sell']
	90	['PctlP_90_15_sell', 'PctlP_10_full_buy', 'PctlP_10_5_buy', 'MaxP_15_sell', 'MaxP_60_sell']
ID3 AT h	10	['PctlP_45_5_sell', 'MinP_5_buy', 'PctlP_10_full_buy', 'MinP_180_buy', 'FirstP_5_buy']
	25	['MinP_1_buy', 'MinP_60_buy', 'PctlP_25_5_sell', 'LastP_full_sell', 'PctlP_25_15_sell']
	45	['MinP_1_buy', 'LastP_full_sell', 'LastP_full_buy', 'MedianP_5_sell', 'FirstP_5_sell']
	50	['LastP_full_sell', 'LastP_full_buy', 'PctlP_45_5_sell', 'MinP_5_buy', 'FirstP_5_sell']
	55	['LastP_full_buy', 'LastP_full_sell', 'PctlP_45_5_sell', 'FirstP_5_sell', 'PctlP_45_full_buy']
	75	['LastP_full_buy', 'MaxP_1_sell', 'MeanP_full_buy', 'PctlP_25_60_buy', 'PctlP_10_60_buy']
	90	['LastP_full_buy', 'PctlP_90_full_sell', 'PctlP_90_1_sell', 'VWAP_full_sell', 'MaxP_5_buy']
ID1 DE qh	10	['MinP_15_buy', 'PctlP_10_1_buy', 'MinP_60_buy', 'MinP_180_buy']
	25	['MinP_5_buy', 'MeanP_60_buy', 'PctlP_75_60_buy', 'PctlP_10_5_buy', 'PctlP_90_15_sell']
	45	['MinP_5_buy', 'PctlP_25_5_buy', 'PctlP_10_5_buy', 'PctlP_90_1_sell', 'MaxP_1_sell']
	50	['MinP_5_buy', 'PctlP_25_5_buy', 'PctlP_10_5_buy', 'MaxP_1_sell', 'PctlP_90_1_sell']
	55	['PctlP_25_5_buy', 'MinP_1_buy', 'VWAP_60_buy', 'PctlP_10_5_buy', 'VWAP_5_sell']
	75	['PctlP_90_5_sell', 'PctlP_25_5_buy', 'MaxP_1_sell', 'PctlP_10_1_buy', 'VWAP_60_buy']
	90	['PctlP_90_5_sell', 'PctlP_10_60_buy', 'MaxP_1_sell', 'VWAP_full_buy', 'PctlP_90_180_buy']
ID1 AT qh	10	['PctlP_45_180_buy', 'MeanP_60_buy', 'PctlP_25_180_sell', 'PctlP_90_60_sell', 'VWAP_full_buy']
	25	['PctlP_25_180_sell', 'MinP_15_buy', 'VWAP_15_sell', 'PctlP_25_60_sell', 'PctlP_10_full_buy']
	45	['VWAP_full_sell', 'PctlP_25_full_buy', 'PctlP_10_15_buy', 'PctlP_75_15_sell', 'PctlP_55_180_sell']
	50	['PctlP_90_15_sell', 'PctlP_55_full_sell', 'PctlP_10_15_buy', 'PctlP_25_full_buy', 'PctlP_75_full_sell']
	55	['PctlP_90_15_sell', 'MeanP_60_buy', 'PctlP_25_full_buy', 'PctlP_75_full_sell', 'PctlP_10_15_buy']
	75	['MaxP_15_sell', 'MeanP_full_buy', 'PctlP_90_60_sell', 'PctlP_90_180_sell', 'PctlP_75_full_buy']
	90	['MaxP_15_sell', 'PctlP_90_60_sell', 'MeanP_full_buy', 'PctlP_90_180_sell', 'PctlP_75_full_buy']
ID2 DE qh	10	['MinP_180_buy', 'MinP_60_buy', 'MaxP_1_sell', 'MinP_15_buy', 'MaxP_180_sell']
	25	['MinP_15_buy', 'MaxP_1_sell', 'MinP_60_buy', 'PctlP_25_180_sell', 'PctlP_75_180_buy']
	45	['MinP_15_buy', 'MaxP_1_sell', 'PctlP_10_60_buy', 'MinP_5_buy', 'PctlP_10_15_buy']
	50	['MaxP_1_sell', 'PctlP_10_15_buy', 'PctlP_10_60_buy', 'MinP_15_buy', 'MinP_5_buy']
	55	['PctlP_10_15_buy', 'MaxP_1_sell', 'MinP_5_buy', 'PctlP_10_60_buy', 'PctlP_90_5_sell']
	75	['MaxP_15_sell', 'MinP_5_buy', 'PctlP_90_60_sell', 'MaxP_5_sell', 'MinP_15_buy']
	90	['MaxP_15_sell', 'PctlP_10_1_buy', 'PctlP_25_180_sell', 'MaxP_60_sell', 'MinP_60_buy']
ID2 AT qh	10	['PctlP_10_180_sell', 'MinP_1_buy', 'PctlP_10_180_buy', 'MinP_60_buy', 'MaxP_180_sell']
	25	['LastP_full_sell', 'PctlP_10_180_sell', 'MinP_1_buy', 'PctlP_25_full_sell', 'PctlP_10_180_buy']
	45	['MeanP_1_sell', 'MeanP_60_buy', 'MeanP_60_sell', 'VWAP_15_sell', 'MeanP_5_sell']
	50	['LastP_full_sell', 'LastP_full_buy', 'VWAP_180_sell', 'MinP_1_buy', 'MeanP_full_sell']
	55	['LastP_full_sell', 'MinP_1_buy', 'VWAP_15_sell', 'PctlP_75_full_sell', 'LastP_full_buy']

Case Desc.	Quantile	Top Five Features
	75	['LastP_full_sell', 'PctlP_75_full_sell', 'MaxP_1_buy', 'MeanP_full_buy', 'MaxP_1_sell']
	90	['MaxP_180_sell', 'MaxP_1_buy', 'MeanP_full_buy', 'PctlP_75_full_sell', 'LastP_full_sell']
ID3 DE qh	10	['MinP_60_buy', 'PctlP_90_180_sell', 'PctlP_10_180_buy', 'PctlP_75_15_sell', 'PctlP_10_60_buy']
	25	['MinP_60_buy', 'PctlP_75_15_sell', 'PctlP_10_60_buy', 'PctlP_90_180_sell', 'PctlP_10_180_buy']
	45	['PctlP_10_60_buy', 'PctlP_90_15_sell', 'MinP_60_buy', 'MinP_15_buy', 'PctlP_90_180_sell']
	50	['PctlP_90_15_sell', 'PctlP_10_60_buy', 'PctlP_25_60_buy', 'MinP_15_buy', 'PctlP_90_180_sell']
	55	['PctlP_90_15_sell', 'PctlP_10_60_buy', 'MinP_15_buy', 'PctlP_25_60_buy', 'MaxP_15_sell']
	75	['PctlP_25_60_buy', 'PctlP_90_60_sell', 'MaxP_15_sell', 'PctlP_90_180_sell', 'PctlP_10_15_buy']
	90	['MaxP_60_sell', 'PctlP_75_60_sell', 'PctlP_10_180_buy', 'PctlP_90_60_sell', 'PctlP_55_180_sell']
ID3 AT qh	10	['MinP_1_sell', 'PctlP_10_180_buy', 'MinP_5_buy', 'VWAP_full_sell', 'VWAP_180_sell']
	25	['MinP_1_sell', 'MinP_15_buy', 'PctlP_10_180_buy', 'LastP_full_sell', 'PctlP_25_full_sell']
	45	['MeanP_180_sell', 'VWAP_1_buy', 'MeanP_15_buy', 'MeanP_1_buy', 'MeanP_180_buy']
	50	['MeanP_180_sell', 'MeanP_15_buy', 'VWAP_1_buy', 'MeanP_1_buy', 'PctlP_75_15_buy']
	55	['MeanP_180_sell', 'MeanP_1_buy', 'VWAP_1_buy', 'MeanP_15_buy', 'PctlP_90_180_sell']
	75	['PctlP_90_180_sell', 'PctlP_75_1_buy', 'PctlP_90_180_buy', 'MeanP_15_buy', 'MeanP_180_sell']
	90	['MaxP_1_buy', 'PctlP_90_full_buy', 'MaxP_180_buy', 'MaxP_1_sell', 'MaxP_180_sell']

Table A.4: Shared features across quantiles

Case Desc.	Shared Features
ID1 DE h	[None]
ID1 AT h	[None]
ID2 DE h	[None]
ID2 AT h	[None]
ID3 DE h	['MaxP_5_sell']
ID3 AT h	['LastP_full_sell']
ID1 DE qh	[None]
ID1 AT qh	[None]
ID2 DE qh	[None]
ID2 AT qh	[None]
ID3 DE qh	[None]
ID3 AT qh	[None]

Table A.5: Shared features across indices

Case Desc.	Quantile	Shared Features
DE h	10	['MaxP_180_sell', 'MinP_15_buy', 'MinP_60_buy', 'PctlP_90_full_sell']
	25	[None]
	45	['MinP_5_buy']
	50	[None]
	55	[None]
	75	[None]
	90	[None]
AT h	10	['LastP_full_sell', 'MaxP_180_sell', 'VWAP_full_buy']
	25	[None]
	45	[None]
	50	[None]
	55	[None]
	75	['LastP_full_sell', 'PctlP_10_180_buy']
	90	['LastP_full_sell', 'MaxP_1_sell', 'MinP_180_buy', 'VWAP_full_buy']
DE qh	10	['MinP_15_buy', 'MinP_60_buy']
	25	[None]
	45	[None]
	50	[None]
	55	[None]
	75	['MinP_15_buy']
	90	[None]
AT qh	10	['PctlP_10_180_buy', 'PctlP_75_180_buy', 'VWAP_full_sell']
	25	['MinP_15_buy']
	45	[None]
	50	[None]
	55	[None]
	75	['PctlP_90_180_sell']
	90	[None]

Table A.6: Shared features across countries

Case Desc.	Quantile	Shared Features
ID1 h	10	['FirstP_15_buy', 'MaxP_180_sell', 'MinP_15_buy', 'PctlP_90_full_sell', 'VWAP_180_sell']
	25	[None]
	45	['PctlP_75_60_sell']
	50	[None]
	55	[None]

Case Desc.	Quantile	Shared Features
	75	['MedianP_5_sell', 'MinP_60_buy', 'PctlP_10_1_buy']
	90	['MaxP_1_sell', 'PctlP_10_1_buy', 'PctlP_25_5_sell']
ID2 h	10	['MaxP_180_sell', 'MinP_180_buy', 'MinP_60_buy', 'PctlP_25_60_sell', 'PctlP_25_full_sell', 'PctlP_90_full_sell', 'VWAP_60_buy', 'VWAP_60_sell', 'VWAP_full_sell']
	25	['MaxP_60_sell']
	45	['MaxP_5_sell', 'MeanP_5_sell', 'VWAP_60_buy']
	50	['MaxP_5_sell', 'PctlP_90_5_sell']
	55	['MaxP_5_sell', 'MaxP_60_sell', 'PctlP_90_5_sell']
	75	['MaxP_5_sell', 'PctlP_10_180_buy', 'PctlP_90_180_sell', 'VWAP_15_buy']
	90	['FirstP_60_buy', 'MaxP_15_sell', 'MaxP_180_sell', 'MaxP_60_sell', 'MinP_180_buy', 'MinP_60_buy', 'PctlP_10_full_buy']
ID3 h	10	['MaxP_180_sell', 'MinP_15_buy', 'MinP_180_buy', 'PctlP_10_15_buy']
	25	['PctlP_10_180_buy']
	45	['MinP_5_buy']
	50	[None]
	55	['MinP_15_buy']
	75	['MaxP_180_sell', 'PctlP_90_180_sell', 'PctlP_90_full_sell']
	90	['MaxP_180_sell', 'PctlP_25_full_buy', 'PctlP_90_180_sell', 'PctlP_90_full_sell']
ID1 qh	10	['MinP_15_buy']
	25	[None]
	45	['PctlP_90_15_sell']
	50	['MeanP_60_buy']
	55	[None]
	75	['PctlP_10_60_buy', 'VWAP_full_buy']
	90	['PctlP_10_60_buy', 'VWAP_full_buy']
ID2 qh	10	['LastP_full_sell', 'MaxP_180_sell', 'MinP_60_buy']
	25	['MinP_15_buy', 'MinP_5_buy', 'MinP_60_buy']
	45	['MeanP_60_sell']
	50	['MaxP_5_sell', 'MinP_1_buy']
	55	['MaxP_1_sell', 'MaxP_5_sell', 'MinP_1_buy']
	75	['MaxP_15_sell', 'MaxP_1_sell', 'PctlP_25_180_sell', 'PctlP_90_180_sell', 'PctlP_90_60_sell']
	90	['MaxP_60_sell', 'PctlP_90_60_sell']
ID3 qh	10	['MinP_15_buy', 'PctlP_10_180_buy', 'PctlP_10_60_buy', 'PctlP_90_180_sell']
	25	['MinP_15_buy', 'PctlP_10_180_buy', 'PctlP_10_60_buy']
	45	[None]
	50	['PctlP_90_180_sell']
	55	[None]
	75	['PctlP_90_180_sell']
	90	['MaxP_180_sell', 'MaxP_1_sell']

Table A.7: Shared features across resolutions

Case Desc.	Quantile	Shared Features
ID1 DE	10	['MinP_15_buy', 'MinP_60_buy', 'PctlP_10_1_buy']
	25	['MinP_5_buy', 'PctlP_10_5_buy', 'PctlP_75_60_buy', 'VWAP_60_sell']
	45	['MinP_5_buy', 'PctlP_10_5_buy']
	50	['MinP_5_buy', 'PctlP_10_5_buy']
	55	['PctlP_10_5_buy']
	75	['PctlP_10_1_buy', 'PctlP_25_5_buy']
	90	['MaxP_1_sell', 'MinP_15_buy', 'PctlP_10_60_buy', 'PctlP_25_1_buy', 'VWAP_60_buy']
ID1 AT	10	['MinP_15_buy', 'VWAP_180_sell', 'VWAP_full_buy']
	25	['PctlP_10_15_buy']
	45	[None]
	50	['VWAP_15_sell']
	55	['PctlP_75_60_sell', 'VWAP_15_sell']
	75	['MaxP_15_sell', 'PctlP_10_180_buy', 'PctlP_75_full_buy', 'VWAP_full_buy']
	90	['MaxP_15_sell', 'PctlP_45_full_sell', 'PctlP_75_full_buy', 'VWAP_full_buy']
ID2 DE	10	['MaxP_180_sell', 'MinP_15_buy', 'MinP_180_buy', 'MinP_60_buy', 'PctlP_90_full_sell']
	25	['MaxP_15_sell', 'MaxP_60_sell', 'MeanP_180_sell', 'MinP_15_buy', 'PctlP_10_15_buy', 'PctlP_10_60_buy', 'PctlP_75_1_sell']
	45	['MaxP_5_sell', 'MaxP_60_sell', 'MinP_15_buy', 'MinP_5_buy', 'PctlP_10_15_buy', 'PctlP_10_60_buy', 'PctlP_75_180_buy', 'PctlP_90_5_sell', 'VWAP_60_buy']
	50	['MaxP_5_sell', 'MinP_15_buy', 'MinP_5_buy', 'PctlP_10_15_buy', 'PctlP_90_5_sell']
	55	['MaxP_15_sell', 'MaxP_5_sell', 'MaxP_60_sell', 'MinP_5_buy', 'PctlP_10_15_buy', 'PctlP_90_5_sell']
	75	['MaxP_15_sell', 'MaxP_5_sell', 'MinP_60_buy', 'PctlP_90_180_sell']
	90	['MaxP_15_sell', 'MaxP_60_sell', 'MinP_60_buy']
ID2 AT	10	['LastP_full_buy', 'LastP_full_sell', 'MaxP_180_sell', 'MinP_15_sell', 'MinP_1_buy', 'MinP_1_sell', 'MinP_60_buy', 'PctlP_25_full_sell', 'VWAP_full_sell']
	25	[None]
	45	['MeanP_5_sell']
	50	['MaxP_5_sell']
	55	['FirstP_1_buy', 'LastP_full_buy', 'LastP_full_sell', 'MaxP_1_buy', 'MaxP_5_sell', 'MinP_1_buy', 'PctlP_55_1_buy', 'PctlP_75_full_sell', 'VWAP_15_sell', 'VWAP_180_sell']
	75	['FirstP_15_sell', 'LastP_full_buy', 'LastP_full_sell', 'MaxP_180_sell', 'MaxP_1_buy', 'MeanP_full_buy', 'PctlP_10_180_buy', 'PctlP_25_60_sell', 'PctlP_25_full_sell', 'PctlP_45_180_sell', 'PctlP_45_60_buy', 'PctlP_90_180_sell', 'VWAP_15_sell']
	90	['FirstP_15_sell', 'LastP_full_buy', 'LastP_full_sell', 'MaxP_180_sell', 'MaxP_1_buy', 'MaxP_1_sell', 'MaxP_60_sell', 'MeanP_full_buy', 'PctlP_25_full_sell', 'PctlP_90_15_sell', 'PctlP_90_180_buy']
ID3 DE	10	['MinP_15_buy', 'MinP_60_buy', 'PctlP_10_180_buy', 'PctlP_10_60_buy']
	25	['MinP_15_buy', 'PctlP_10_180_buy', 'PctlP_10_60_buy']
	45	['MinP_15_buy', 'PctlP_10_60_buy', 'PctlP_25_60_buy', 'PctlP_75_15_sell', 'PctlP_90_15_sell', 'PctlP_90_180_sell']
	50	['MinP_15_buy', 'PctlP_10_15_buy', 'PctlP_25_60_buy', 'PctlP_90_15_sell']
	55	['MinP_15_buy', 'PctlP_10_15_buy', 'PctlP_90_15_sell']

Case Desc.	Quantile	Shared Features
	75	['MaxP_15_sell', 'PctlP_10_15_buy', 'PctlP_25_180_sell', 'PctlP_90_15_sell', 'PctlP_90_180_sell', 'VWAP_60_sell']
	90	['MaxP_15_sell', 'MaxP_180_sell', 'MaxP_60_sell', 'PctlP_90_15_sell', 'PctlP_90_180_sell']
ID3 AT	10	['FirstP_15_sell', 'FirstP_5_buy', 'LastP_full_sell', 'MaxP_180_sell', 'MaxP_5_buy', 'MinP_15_buy', 'MinP_5_buy', 'PctlP_75_full_sell', 'PctlP_90_180_sell', 'VWAP_full_buy']
	25	['LastP_full_sell', 'PctlP_10_180_buy']
	45	[None]
	50	[None]
	55	[None]
	75	['PctlP_90_180_sell']
	90	['LastP_full_sell', 'MaxP_180_sell', 'MaxP_1_sell', 'PctlP_90_full_sell']

B

Experimental Results for Multi-Heads Models

B.1. Feature Selection

B.1.1. IPC Selecton Results

During the training and validation process, the selection results with the optimal quantile constraint q and number of top features n are presented in Table B.1.

The testing performance results are shown as Table B.2.

B.1.2. Experiment Conslusion

Selection Approaches Comparison

The testing performances are shown in Table B.2. The results indicate that IPC uses significantly fewer N_{input} across all cases, achieving the best performance in the majority of cases. Specifically, in terms of number of selected features, the average $\bar{N}_{\text{input}} = 4.67$ for IPC, whereas for PCA it is 37.08, and for L1-based it is 83.67. In terms of performance, the IPC selectors achieve the best AQL loss in 11 out of 12 cases. Moreover, IPC selectors have the lowest AQCR in all cases, suggesting that this selection method generally reduces the forecast AQCR. Furthermore, in pointwise forecast performance, IPC achieves optimal performance in 12, 11, and 10 cases for MAE, RMSE, and R2, respectively.

In conclusion, through comparative experiments, IPC selection demonstrates advantages in quantile forecast performance and pointwise forecast performance in most cases. Therefore, IPC selectors and selected features are used in the experiments in Sections B.2 and B.3.

Table B.1: Number of selected features (N_f) with optimal validation losses in all cases

Case Desc.	Filtered Features	q	n
ID1 DE h	['MinP_5_buy', 'PctlP_10_5_buy']	80	2
ID1 AT h	['PctlP_75_60_sell', 'PctlP_55_15_sell']	98	2
ID2 DE h	subset_1*	95	16
ID2 AT h	['PctlP_90_1_sell', 'PctlP_90_5_sell', 'PctlP_75_1_sell', 'VWAP_1_sell']	80	4
ID3 DE h	subset_2**	98	16
ID3 AT h	['LastP_sell', 'MedianP_1_sell']	99.5	2
ID1 DE qh	['PctlP_25_5_buy', 'PctlP_10_5_buy']	80	2
ID1 AT qh	['PctlP_45_15_buy', 'PctlP_25_15_buy']	99.5	2
ID2 DE qh	['PctlP_90_15_sell', 'PctlP_25_15_buy']	98	2
ID2 AT qh	['MeanP_60_buy', 'MeanP_15_sell', 'MeanP_1_sell', 'VWAP_15_sell']	99.5	4
ID3 DE qh	['PctlP_25_60_buy', 'PctlP_45_60_buy']	90	2
ID3 AT qh	['LastP_buy', 'VWAP_1_buy']	99.5	2

Note:

* `subset_1: ['PctlP_55_15_sell', 'PctlP_75_15_sell', 'PctlP_90_15_sell', 'PctlP_25_15_buy', 'MedianP_15_sell', 'PctlP_45_15_sell', 'PctlP_10_15_buy', 'PctlP_45_15_buy', 'MaxP_15_sell', 'MedianP_15_buy', 'PctlP_55_15_buy', 'MinP_15_buy', 'PctlP_90_5_sell', 'PctlP_25_5_buy', 'MaxP_5_sell', 'PctlP_10_5_buy']`.

** `subset_2: ['PctlP_75_15_sell', 'PctlP_90_15_sell', 'MaxP_15_sell', 'PctlP_25_15_buy', 'PctlP_10_15_buy', 'PctlP_55_15_sell', 'PctlP_90_5_sell', 'MaxP_5_sell', 'MinP_15_buy', 'PctlP_55_60_sell', 'PctlP_75_60_sell', 'MedianP_60_sell', 'PctlP_10_5_buy', 'PctlP_90_60_sell', 'PctlP_45_60_sell', 'MaxP_60_sell']`.

Table B.2: Testing performance of comparison among three selection modes in all cases. The best results are shown in **bold**. The units of AQL, RMSE, and MAE are expressed in /MWh, while AQCR is reported in %. All metrics are denormalized.

Case Desc.	**Selection Method**	N_{input}	**AQL**	**AQCR**	**MAE**	**RMSE**	**R2**
ID1 DE h	PCA	43	5.93	34.77	14.51	80.51	0.21
	L1	122	6.30	13.20	15.36	94.20	-0.09
	IPC	**2**	**4.85**	**0.23**	**11.69**	**30.48**	**0.89**
ID1 AT h	PCA	22	8.13	14.86	20.13	**42.03**	**0.74**
	L1	149	8.98	33.20	22.15	45.96	0.69
	IPC	**2**	**7.98**	**0.14**	**19.72**	47.79	0.66
ID2 DE h	PCA	33	4.35	**6.27**	10.54	26.99	**0.89**
	L1	96	4.80	23.62	11.48	28.87	0.88
	IPC	**16**	**3.84**	43.15	**9.45**	**26.69**	0.89
ID2 AT h	PCA	25	5.23	38.66	12.70	54.54	0.33
	L1	75	4.94	57.83	12.10	32.15	0.77

Case Desc.	Selection Method	N_{input}	AQL	AQCR	MAE	RMSE	R2
	IPC	**4**	**4.86**	**0.11**	**11.64**	**29.95**	**0.80**
ID3 DE h	PCA	34	4.47	23.04	10.90	28.99	0.86
	L1	115	7.96	26.16	19.50	42.13	0.71
	IPC	**16**	**4.10**	**3.42**	**10.13**	**27.91**	**0.87**
ID3 AT h	PCA	17	5.07	24.30	12.21	29.43	0.79
	L1	93	5.45	27.43	13.19	31.71	0.75
	IPC	**2**	**4.98**	**0.11**	**11.91**	**28.41**	**0.80**
ID1 DE qh	PCA	69	17.46	57.85	41.13	85.29	0.48
	L1	31	10.88	13.08	21.74	65.58	0.69
	IPC	**2**	**8.55**	**0.03**	**18.73**	**59.67**	**0.75**
ID1 AT qh	PCA	26	12.56	12.55	31.15	106.43	0.36
	L1	70	**12.33**	5.25	**30.48**	102.53	0.41
	IPC	**2**	12.56	**0.04**	30.97	**99.80**	**0.44**
ID2 DE qh	PCA	69	12.22	66.65	27.35	63.08	0.61
	L1	51	12.28	66.55	22.81	54.20	0.71
	IPC	**2**	**7.68**	**0.17**	**17.93**	**51.51**	**0.74**
ID2 AT qh	PCA	25	7.45	4.36	18.34	66.96	0.50
	L1	86	**7.39**	2.32	**18.12**	**66.04**	**0.52**
	IPC	**4**	7.48	**0.02**	18.22	66.74	0.51
ID3 DE qh	PCA	67	16.03	69.78	37.46	69.24	0.47
	L1	59	16.04	78.85	39.67	70.90	0.44
	IPC	**2**	**7.70**	**0.18**	**17.96**	**51.48**	**0.71**
ID3 AT qh	PCA	15	7.35	6.89	17.86	52.35	0.57
	L1	57	**7.32**	1.16	17.62	52.20	0.57
	IPC	**2**	7.35	**0.02**	**17.61**	**51.58**	**0.58**

Insights on Features Candidates' Correlation

The N_p results shown in Table 4.1 from PCA compression show notable differences between Germany and Austria. Firstly, for the same index, i.e., when Δ, which means the time interval between prediction time and delivery time, is equal, Austria achieves the same EVR thresholds with significantly fewer N_p compared to Germany. Furthermore, as Δ increases from 60 minutes to 180 minutes, the N_p in Austria decreases monotonically across all EVR thresholds, whereas in Germany, the N_p remains almost unchanged.

These results highlight the differences in feature candidates between Germany and Austria. One potential insight from the PCA N_p results is that the correlation between feature candidates in Austria may be stronger than in Germany, and this correlation seems to increase with the extension of Δ within a certain range in Austria, while remaining stable in Germany.

Insights on IPC Selected Features

Firstly, the volume-related feature candidates were seldom deemed to have a significant impact on any labels.

Secondly, in addition to the handcrafted features such as VWAP, mean value, and last transaction prices, the introduction of percentile prices has proven to have a significant impact on the labels. For clarity, percentile prices that exclude the median are defined as biased percentile prices. According to the IPC results, shown in Table B.1, any percentile prices features are only considered less important in 3 and 2 cases, respectively. Of the 56 instances of selected features mentioned across all cases, BPP and FPP were referred to 36 and 40 times, respectively.

Moreover, biased percentile prices do not exhibit axis symmetry between the buy and sell sides; instead, they display a form of central symmetry, to some extend, as shown in Figure B.1. This result indicates that, on the buying side, low percentiles below the 50th percentile are prioritized, whereas on the selling side, high percentiles above the 50th percentile are given more attention. This insight aligns with the clearing model in IDM.

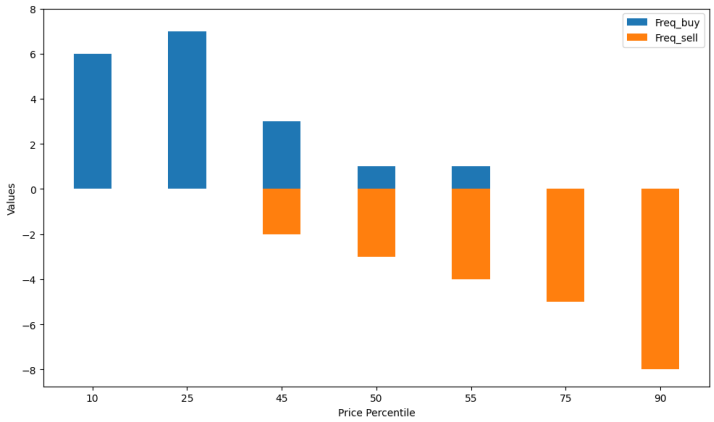

Figure B.1: Frequency of each percentile price appearing in the IPC results of both buying (+) and selling (-) sides

B.2. Probabilistic Price Prediction

B.2.1. Experiments Results & Conclusion

After training and validation using the same selected features, the testing performance is presented in Table B.3.

The results show that the deep learning models, QMLP and QKAN, outperform the tree-based models, LightGBM and XGBoost, in all cases, as demonstrated in terms of quantile forecast performance, model AQCR, and pointwise forecast performance. Specifically, in terms of quantile forecast performance, the traditional neural network-based QMLP achieves the lowest AQL in 9 out of 12 cases, while QKAN shares the remaining 3 cases. In terms of model AQCR, QMLP achieves the lowest crossing rate in 7 cases, whereas QKAN performs better in the remaining 5 cases. QMLP consistently maintains an AQCR below 5% across all cases, whereas QKAN exceeds this threshold in two cases of ID1_h. From the perspective of pointwise forecast performance, QMLP outperforms in MAE, RMSE, and R^2 in 8, 12, and 12 cases, respectively, while QKAN excels in MAE in 4 cases. This suggests QMLPs advantage in handling extreme values.

In conclusion, the above experiments confirm the superiority of deep learning methods in terms of quantile forecast performance, model AQCR and pointwise forecast performance. Additionally, as an innovative deep learning architecture, QKAN can be considered as an alternative, demonstrating better performance than QMLP in some cases.

Table B.3: Testing performance of models comparison. The best results are shown in **bold**. The units of AQL, RMSE,and MAE are expressed in /MWh, while AQCR is reported in %. All metrics are denormalized.

Case Desc.	Model	AQL	AQCR	MAE	RMSE	R2
ID1 DE h	QKAN	5.00	6.43	12.07	34.13	0.86
	QLGBM	6.56	56.99	12.69	43.86	0.76
	QMLP	**4.85**	**0.23**	**11.69**	**30.48**	**0.89**
	QXGB	5.34	22.70	12.57	43.03	0.77
ID1 AT h	QKAN	8.17	85.16	20.36	50.13	0.63
	QLGBM	8.89	76.29	20.17	53.77	0.57
	QMLP	**7.98**	**0.14**	**19.72**	**47.79**	**0.66**
	QXGB	8.74	45.84	20.18	53.91	0.57
ID2 DE h	QKAN	3.89	**1.13**	9.52	27.37	0.89
	QLGBM	4.98	90.17	10.04	33.45	0.83
	QMLP	**3.84**	43.15	**9.45**	**26.69**	**0.89**
	QXGB	4.29	58.98	9.99	33.51	0.83
ID2 AT h	QKAN	**4.86**	0.27	**11.64**	30.17	0.79
	QLGBM	6.59	63.17	11.82	30.97	0.78
	QMLP	4.86	**0.11**	11.64	**29.95**	**0.80**
	QXGB	5.17	27.00	11.75	30.89	0.78
ID3 DE h	QKAN	4.15	**0.05**	10.23	28.28	0.87
	QLGBM	5.62	98.23	12.97	38.57	0.76
	QMLP	**4.10**	3.42	**10.13**	**27.91**	**0.87**
	QXGB	4.50	69.11	10.37	30.39	0.85
ID3 AT h	QKAN	5.07	0.27	12.05	28.79	0.80
	QLGBM	7.49	76.38	12.93	29.69	0.78
	QMLP	**4.98**	**0.11**	**11.91**	**28.41**	**0.80**
	QXGB	5.36	34.63	12.02	28.85	0.80
ID1 DE qh	QKAN	8.69	**0.01**	18.83	60.53	0.74
	QLGBM	10.11	31.56	19.97	74.55	0.60
	QMLP	**8.55**	0.03	**18.73**	**59.67**	**0.75**
	QXGB	9.31	15.23	20.05	74.74	0.60
ID1 AT qh	QKAN	12.64	0.26	**30.90**	110.31	0.32
	QLGBM	13.67	29.35	31.37	113.97	0.27
	QMLP	**12.56**	**0.04**	30.97	**99.80**	**0.44**
	QXGB	13.19	11.92	31.44	114.21	0.27

Case Desc.	Model	AQL	AQCR	MAE	RMSE	R2
ID2 DE qh	QKAN	7.75	**0.12**	18.01	53.42	0.72
	QLGBM	8.10	62.66	18.49	58.41	0.67
	QMLP	**7.68**	0.17	**17.93**	**51.51**	**0.74**
	QXGB	8.26	39.45	18.50	58.40	0.67
ID2 AT qh	QKAN	**7.47**	**0.01**	**18.03**	67.80	0.49
	QLGBM	8.78	62.94	18.30	69.63	0.46
	QMLP	7.48	0.02	18.22	**66.74**	**0.51**
	QXGB	7.77	17.59	18.23	69.41	0.47
ID3 DE qh	QKAN	**7.62**	0.21	**17.93**	52.56	0.69
	QLGBM	9.77	98.06	18.13	53.14	0.69
	QMLP	7.70	**0.18**	17.96	**51.48**	**0.71**
	QXGB	7.92	27.53	18.15	53.24	0.69
ID3 AT qh	QKAN	7.37	0.12	17.97	51.85	0.58
	QLGBM	8.92	47.76	17.93	51.87	0.58
	QMLP	**7.35**	**0.02**	**17.61**	**51.58**	**0.58**
	QXGB	7.63	13.70	17.90	51.78	0.58

B.3. Generalization Assessment

B.3.1. Cross-Market Generalization

Based on the conclusions from Section B.1 and Section B.2, generalization across markets (between Germany and Austria) experiments were conducted using four transfer learning strategies. To assess the statistical significance of the differences between the results of separate training and other strategies, the DM test on AQL, as proposed in Section 3.5.3, was employed. The results include the DM_stat and p_value. These results are presented in Table B.4. The Case Desc. in the table refers to the target case (case B).

Table B.4: Generation results with different transfer learning strategies across countries. All results are based on testing datasets of hourly products. The best results are highlighted in **bold**. The units of AQL, RMSE, and MAE are expressed in /MWh, while AQCR is reported in %. All metrics are denormalized. The **Case Desc.** refers to case B. In the **DM test results**, model 1 corresponds to the separate training approach for the current case, while model 2 represents the strategy applied in this row.

Case Desc.	Trans. Strategy	AQL	AQCR	MAE	RMSE	R2	DM_stat	p_value
ID1 DE h	zero	5.25	0.34	12.62	27.45	0.91	-7.16	0.00
	1 shot	4.94	53.79	11.52	25.27	0.92	-0.58	0.56
	5 shot	5.34	2.79	**11.41**	**25.23**	**0.92**	-6.66	0.00
	10 shot	5.29	12.48	12.83	29.82	0.89	-13.85	0.00
	50 shot	5.14	18.73	11.84	30.00	0.89	-7.87	0.00
	100 shot	5.61	0.48	13.86	30.26	0.89	-20.36	0.00
	500 shot	5.15	1.79	11.76	28.92	0.90	-9.98	0.00
	1000 shot	5.01	10.03	11.66	29.59	0.89	-5.73	0.00

Case Desc.	Trans. Strategy	AQL	AQCR	MAE	RMSE	R2	DM_stat	p_value
	Sepa	**4.90**	0.05	11.80	31.75	0.88	0.00	nan
	joint	5.16	**0.20**	12.10	29.33	0.89	-4.97	0.00
ID1 AT h	zero	7.92	0.09	19.32	33.34	0.84	0.07	0.95
	1 shot	8.05	29.69	19.29	33.79	0.83	-1.36	0.17
	5 shot	7.89	8.74	**19.24**	**33.06**	**0.84**	0.38	0.70
	10 shot	7.97	13.64	19.37	33.87	0.83	-0.44	0.66
	50 shot	7.90	0.72	19.51	35.13	0.82	0.37	0.71
	100 shot	7.88	0.07	19.30	33.35	0.84	0.50	0.62
	500 shot	7.88	49.01	19.53	34.79	0.82	0.62	0.54
	1000 shot	7.81	0.07	19.63	35.91	0.81	1.47	0.14
	Sepa	7.93	0.59	19.65	44.56	0.71	0.00	nan
	joint	**7.80**	**0.00**	19.57	42.75	0.73	2.97	0.00
ID2 DE h	zero	4.10	32.14	9.58	26.57	0.90	-5.77	0.00
	1 shot	4.04	0.36	9.65	26.41	0.90	-3.97	0.00
	5 shot	4.02	**0.20**	9.57	26.32	0.90	-2.19	0.03
	10 shot	4.02	0.20	9.58	26.32	0.90	-2.46	0.01
	50 shot	4.02	0.48	**9.51**	26.46	0.90	-2.41	0.02
	100 shot	3.99	5.84	9.54	26.56	0.90	-1.16	0.25
	500 shot	4.07	0.20	9.53	26.45	0.90	-5.36	0.00
	1000 shot	3.98	0.41	9.55	26.54	0.90	-0.57	0.57
	Sepa	**3.97**	22.92	9.55	**26.29**	**0.90**	0.00	nan
	joint	3.97	0.34	9.52	27.41	0.89	-0.08	0.94
ID2 AT h	zero	4.84	0.05	**11.55**	29.36	0.80	0.56	0.58
	1 shot	4.90	3.90	11.57	29.34	0.81	-1.68	0.09
	5 shot	4.81	0.36	11.63	29.44	0.80	1.33	0.18
	10 shot	4.98	**0.02**	11.80	29.44	0.80	-4.12	0.00
	50 shot	4.84	0.02	11.59	29.45	0.80	0.36	0.72
	100 shot	4.82	0.63	11.67	29.52	0.80	1.35	0.18
	500 shot	4.81	5.25	11.63	29.53	0.80	1.47	0.14
	1000 shot	4.83	0.14	11.76	29.66	0.80	0.85	0.40
	Sepa	4.85	0.07	11.64	29.80	0.80	0.00	nan
	joint	**4.77**	6.30	11.70	**29.15**	**0.81**	2.20	0.03
ID3 DE h	zero	4.30	0.45	**10.24**	27.72	0.87	-7.62	0.00
	1 shot	4.22	21.79	10.35	27.76	0.87	-2.66	0.01
	5 shot	4.50	0.52	11.71	28.68	0.87	-11.21	0.00
	10 shot	4.45	20.57	11.23	28.05	0.87	-17.60	0.00
	50 shot	4.34	0.18	10.86	27.95	0.87	-8.37	0.00
	100 shot	4.28	41.86	10.35	27.72	0.87	-7.46	0.00
	500 shot	4.20	0.09	10.26	**27.71**	**0.87**	-2.27	0.02
	1000 shot	4.19	0.05	10.27	27.75	0.87	-1.85	0.06
	Sepa	**4.16**	**0.14**	10.47	27.77	0.87	0.00	nan

Case Desc.	Trans. Strategy	AQL	AQCR	MAE	RMSE	R2	DM_stat	p_value
	joint	4.18	0.18	10.24	27.82	0.87	-1.05	0.29
ID3 AT h	zero	5.00	0.50	11.92	28.45	0.80	1.39	0.16
	1 shot	5.15	32.71	12.23	28.58	0.80	-9.45	0.00
	5 shot	5.19	26.12	12.93	29.37	0.79	-4.61	0.00
	10 shot	5.25	1.93	12.19	28.50	0.80	-15.84	0.00
	50 shot	5.01	0.70	12.09	28.71	0.80	-0.02	0.99
	100 shot	5.07	0.34	12.48	28.93	0.79	-1.93	0.05
	500 shot	4.99	0.07	12.07	28.64	0.80	1.50	0.13
	1000 shot	5.00	14.18	12.14	28.73	0.80	0.79	0.43
	Sepa	5.01	**0.00**	11.89	**28.44**	**0.80**	0.00	nan
	joint	**4.95**	0.09	**11.86**	28.84	0.80	2.05	0.04

To investigate the impact of scaler (whether the scalers for case B are the same as those for case A) and the use of layer freezing on prediction results during fine-tuning, we conducted experiments focusing on fine-tuning. For clarity, we use b_{scaler} to represent the scaler choice, where a value of True indicates that the scalers for case A and case B are the same, and False indicates that the scalers differ. We use $b_{freezing}$ to represent the choice of layer freezing, where True indicates that layer freezing is applied, and False indicates that it is not. The results are presented in Table B.5 and Table B.6, respectively.

Table B.5: The experiment results of fine-tuning of hourly products between the same and different scalers between case A and case B. The units for AQL, RMSE, and MAE are expressed in /MWh, while AQCR is reported as a %. All metrics are denormalized. The **Case Desc.** refers to case B. In the **DM test results**, model 1 corresponds to the groups with $b_{scaler} = True$ for the current case, while model 2 represents the groups with $b_{scaler} = False$.

Case Desc.	x	b_{scaler}	AQL	AQCR	MAE	RMSE	R2	DM_stat	p_value
ID1 DE h	1	True	4.94	53.79	11.52	25.27	0.92	0.00	nan
	1	False	4.94	34.52	11.51	25.30	0.92	0.57	0.57
	5	True	5.34	2.79	11.41	25.23	0.92	0.00	nan
	5	False	5.34	2.17	11.46	25.09	0.92	-0.23	0.82
	10	True	5.29	12.48	12.83	29.82	0.89	0.00	nan
	10	False	5.24	0.57	12.79	29.87	0.89	13.08	0.00
	50	True	5.14	18.73	11.84	30.00	0.89	0.00	nan
	50	False	5.11	17.24	11.78	28.60	0.90	3.62	0.00
ID1 AT h	1	True	8.05	29.69	19.29	33.79	0.83	0.00	nan
	1	False	8.05	29.69	19.29	33.79	0.83	9.62	0.00
	5	True	7.89	8.74	19.24	33.06	0.84	0.00	nan
	5	False	7.88	0.82	19.30	33.65	0.83	2.02	0.04
	10	True	7.97	13.64	19.37	33.87	0.83	0.00	nan
	10	False	7.94	10.01	19.37	34.14	0.83	3.54	0.00
	50	True	7.90	0.72	19.51	35.13	0.82	0.00	nan
	50	False	7.89	7.93	19.39	34.35	0.83	0.73	0.46
ID2 DE h	1	True	4.04	0.36	9.65	26.41	0.90	0.00	nan

Case Desc.	x	b_{scaler}	AQL	AQCR	MAE	RMSE	R2	DM_stat	p_value
	1	False	4.04	0.34	9.65	26.41	0.90	11.16	0.00
	5	True	4.02	0.20	9.57	26.32	0.90	0.00	nan
	5	False	4.03	5.59	9.57	26.31	0.90	-8.06	0.00
	10	True	4.02	0.20	9.58	26.32	0.90	0.00	nan
	10	False	4.03	0.18	9.58	26.32	0.90	-11.63	0.00
	50	True	4.02	0.48	9.51	26.46	0.90	0.00	nan
	50	False	4.02	0.48	9.53	26.51	0.90	-2.84	0.00
ID2 AT h	1	True	4.90	3.90	11.57	29.34	0.81	0.00	nan
	1	False	4.92	0.05	11.65	29.32	0.81	-8.11	0.00
	5	True	4.81	0.36	11.63	29.44	0.80	0.00	nan
	5	False	4.81	0.14	11.67	29.47	0.80	-0.25	0.80
	10	True	4.98	0.02	11.80	29.44	0.80	0.00	nan
	10	False	5.01	0.05	11.93	29.45	0.80	-14.35	0.00
	50	True	4.84	0.02	11.59	29.45	0.80	0.00	nan
	50	False	4.86	0.07	11.64	29.42	0.80	-7.50	0.00
ID3 DE h	1	True	4.22	21.79	10.35	27.76	0.87	0.00	nan
	1	False	4.21	1.09	10.35	27.76	0.87	9.50	0.00
	5	True	4.50	0.52	11.71	28.68	0.87	0.00	nan
	5	False	4.50	0.43	11.68	28.64	0.87	2.11	0.04
	10	True	4.45	20.57	11.23	28.05	0.87	0.00	nan
	10	False	4.47	5.19	11.23	28.12	0.87	-2.01	0.04
	50	True	4.34	0.18	10.86	27.95	0.87	0.00	nan
	50	False	4.36	0.14	11.07	28.14	0.87	-2.27	0.02
ID3 AT h	1	True	5.15	32.71	12.23	28.58	0.80	0.00	nan
	1	False	5.16	11.37	12.17	28.56	0.80	-18.18	0.00
	5	True	5.19	26.12	12.93	29.37	0.79	0.00	nan
	5	False	5.17	24.89	12.64	29.15	0.79	6.18	0.00
	10	True	5.25	1.93	12.19	28.50	0.80	0.00	nan
	10	False	5.33	6.36	12.45	28.61	0.80	-11.96	0.00
	50	True	5.01	0.70	12.09	28.71	0.80	0.00	nan
	50	False	5.02	0.14	12.05	28.69	0.80	-0.74	0.46

Table B.6: The comparison experiment results of fine-tuning of hourly products between the with and without layers freezing. The units for AQL, RMSE, and MAE are expressed in /MWh, while AQCR is reported as a percentage. All metrics are denormalized. The **Case Desc.** refers to case B. In the **DM test results**, model 1 corresponds to the groups with $b_{freezing} = True$ for the current case, while model 2 represents the groups with $b_{freezing} = False$.

Case Desc.	x	$b_{freezing}$	AQL	AQCR	MAE	RMSE	R2	DM_stat	p_value
ID1 DE h	1	True	4.94	53.79	11.52	25.27	0.92	0.00	nan
	1	False	4.86	21.54	11.43	25.23	0.92	5.10	0.00
	5	True	5.34	2.79	11.41	25.23	0.92	0.00	nan
	5	False	5.38	3.04	12.50	26.29	0.92	-2.37	0.02

Case Desc.	x	$b_{freezing}$	AQL	AQCR	MAE	RMSE	R2	DM_stat	p_value
	10	True	5.29	12.48	12.83	29.82	0.89	0.00	nan
	10	False	5.25	21.79	12.54	33.12	0.87	1.38	0.17
	50	True	5.14	18.73	11.84	30.00	0.89	0.00	nan
	50	False	5.09	28.06	11.78	30.85	0.88	2.04	0.04
ID1 AT h	1	True	8.05	29.69	19.29	33.79	0.83	0.00	nan
	1	False	8.10	13.07	19.31	33.85	0.83	-11.95	0.00
	5	True	7.89	8.74	19.24	33.06	0.84	0.00	nan
	5	False	8.15	2.29	19.52	32.84	0.84	-12.54	0.00
	10	True	7.97	13.64	19.37	33.87	0.83	0.00	nan
	10	False	8.04	22.97	19.88	35.56	0.81	-1.91	0.06
	50	True	7.90	0.72	19.51	35.13	0.82	0.00	nan
	50	False	8.03	19.75	19.90	34.87	0.82	-5.48	0.00
ID2 DE h	1	True	4.04	0.36	9.65	26.41	0.90	0.00	nan
	1	False	4.04	26.46	9.94	26.51	0.90	-0.28	0.78
	5	True	4.02	0.20	9.57	26.32	0.90	0.00	nan
	5	False	4.03	15.11	9.79	26.27	0.90	-1.23	0.22
	10	True	4.02	0.20	9.58	26.32	0.90	0.00	nan
	10	False	4.03	21.77	9.83	26.29	0.90	-0.93	0.35
	50	True	4.02	0.48	9.51	26.46	0.90	0.00	nan
	50	False	3.97	8.90	9.52	26.46	0.90	14.07	0.00
ID2 AT h	1	True	4.90	3.90	11.57	29.34	0.81	0.00	nan
	1	False	4.97	8.74	11.63	29.32	0.81	-20.74	0.00
	5	True	4.81	0.36	11.63	29.44	0.80	0.00	nan
	5	False	4.92	0.45	12.18	29.42	0.80	-5.84	0.00
	10	True	4.98	0.02	11.80	29.44	0.80	0.00	nan
	10	False	5.09	10.85	12.16	30.06	0.80	-5.87	0.00
	50	True	4.84	0.02	11.59	29.45	0.80	0.00	nan
	50	False	5.06	0.39	12.57	30.47	0.79	-7.36	0.00
ID3 DE h	1	True	4.22	21.79	10.35	27.76	0.87	0.00	nan
	1	False	4.28	19.52	10.33	27.77	0.87	-8.61	0.00
	5	True	4.50	0.52	11.71	28.68	0.87	0.00	nan
	5	False	6.42	0.09	17.85	33.56	0.82	-34.66	0.00
	10	True	4.45	20.57	11.23	28.05	0.87	0.00	nan
	10	False	5.51	9.83	15.37	30.27	0.85	-33.58	0.00
	50	True	4.34	0.18	10.86	27.95	0.87	0.00	nan
	50	False	4.26	52.59	10.32	27.66	0.87	6.00	0.00
ID3 AT h	1	True	5.15	32.71	12.23	28.58	0.80	0.00	nan
	1	False	5.15	8.36	12.06	28.51	0.80	-0.03	0.98
	5	True	5.19	26.12	12.93	29.37	0.79	0.00	nan
	5	False	5.59	20.50	14.02	30.62	0.77	-13.76	0.00
	10	True	5.25	1.93	12.19	28.50	0.80	0.00	nan

Case Desc.	x	$b_{freezing}$	AQL	AQCR	MAE	RMSE	R2	DM_stat	p_value
	10	False	6.12	0.52	14.85	29.74	0.78	-38.53	0.00
	50	True	5.01	0.70	12.09	28.71	0.80	0.00	nan
	50	False	5.13	0.36	12.11	28.70	0.80	-10.18	0.00

B.3.2. Cross-Product Generalization

Based on the conclusions from Section B.1 and Section B.2, generalization across different types of products experiments were conducted using four transfer learning strategies. To assess the statistical significance of the differences between the results of separate training and other strategies, the DM test based on quantile loss, as proposed in Section 3.5.3, was employed. The results include the DM_stat and p_value. These results are presented in Table B.7. The Case Desc. in the table refers to the target case (case B).

Table B.7: Generation results with different transfer learning strategies across products in German market. All results are based on testing datasets. The best results are highlighted in **bold**. The units of AQL, RMSE, and MAE are expressed in /MWh, while AQCR is reported in %. All metrics are denormalized. The **Case Desc.** refers to case B. In the **DM test results**, model 1 corresponds to the separate training approach for the current case, while model 2 represents the strategy applied in this row.

Case Desc.	Trans. Strategy	AQL	AQCR	MAE	RMSE	R2	DM_stat	p_value
ID1 DE h	zero	5.58	**0.00**	12.41	31.76	0.88	-18.60	0.00
	1 shot	5.44	14.36	12.30	31.33	0.88	-13.79	0.00
	5 shot	5.46	0.00	**11.70**	**29.32**	**0.89**	-13.48	0.00
	10 shot	5.82	26.05	13.72	34.21	0.86	-23.07	0.00
	50 shot	5.67	12.55	12.77	34.24	0.86	-20.43	0.00
	100 shot	5.89	11.94	13.71	34.52	0.85	-23.33	0.00
	500 shot	5.73	0.02	13.42	34.49	0.85	-20.90	0.00
	1000 shot	5.57	**0.00**	12.62	33.71	0.86	-17.51	0.00
	Sepa	**4.92**	0.18	11.78	31.42	0.88	0.00	nan
	joint	5.46	0.00	11.89	30.32	0.89	-15.19	0.00
ID2 DE h	zero	4.36	**0.00**	10.29	27.38	0.89	-13.26	0.00
	1 shot	4.14	33.64	9.54	26.18	0.90	-8.63	0.00
	5 shot	4.33	14.50	9.75	**25.85**	**0.90**	-19.53	0.00
	10 shot	4.30	17.60	9.61	25.89	0.90	-18.26	0.00
	50 shot	4.34	52.87	9.88	27.05	0.89	-11.28	0.00
	100 shot	4.23	27.18	9.67	27.19	0.89	-9.88	0.00
	500 shot	4.29	28.79	9.63	27.07	0.89	-11.14	0.00
	1000 shot	4.15	14.43	9.63	27.20	0.89	-7.18	0.00
	Sepa	**3.92**	0.63	**9.49**	26.99	0.89	0.00	nan
	joint	4.16	0.18	9.68	27.00	0.89	-7.45	0.00
ID3 DE h	zero	4.59	0.18	10.63	29.86	0.85	-8.55	0.00
	1 shot	4.42	11.30	10.24	29.27	0.86	-6.22	0.00
	5 shot	4.92	0.20	12.83	31.93	0.83	-10.58	0.00

Case Desc.	Trans. Strategy	AQL	AQCR	MAE	RMSE	R2	DM_stat	p_value
	10 shot	4.90	0.48	12.47	30.76	0.84	-13.66	0.00
	50 shot	4.68	0.27	11.60	30.24	0.85	-8.89	0.00
	100 shot	4.56	14.72	10.83	29.82	0.85	-7.89	0.00
	500 shot	4.50	15.45	10.42	29.78	0.85	-6.61	0.00
	1000 shot	4.43	0.14	10.60	30.15	0.85	-5.04	0.00
	Sepa	**4.11**	3.44	**10.12**	**27.77**	**0.87**	0.00	nan
	joint	4.40	**0.11**	10.21	28.38	0.87	-10.71	0.00
ID1 DE qh	zero	8.43	**0.00**	19.38	61.43	0.73	5.72	0.00
	1 shot	8.40	1.55	19.94	63.14	0.71	5.56	0.00
	5 shot	**8.28**	14.91	19.09	61.39	0.73	10.11	0.00
	10 shot	8.62	0.91	19.58	63.11	0.72	0.30	0.76
	50 shot	8.33	**0.00**	**19.08**	63.57	0.71	6.10	0.00
	100 shot	8.53	**0.00**	19.49	63.51	0.71	2.13	0.03
	500 shot	8.45	**0.00**	19.30	61.45	0.73	5.32	0.00
	1000 shot	8.64	**0.00**	19.67	61.14	0.73	-0.28	0.78
	Sepa	8.63	0.60	19.25	60.67	0.74	0.00	nan
	joint	8.54	0.01	18.30	**57.15**	**0.77**	2.89	0.00
ID2 DE qh	zero	7.64	0.16	18.07	54.12	0.71	1.54	0.12
	1 shot	7.67	3.06	18.37	54.82	0.71	0.79	0.43
	5 shot	7.68	0.44	18.24	55.09	0.70	0.50	0.62
	10 shot	7.65	0.50	18.05	55.04	0.70	1.15	0.25
	50 shot	7.64	9.30	18.06	55.25	0.70	1.41	0.16
	100 shot	7.65	0.37	18.04	55.17	0.70	1.25	0.21
	500 shot	7.66	0.22	18.06	55.20	0.70	0.86	0.39
	1000 shot	7.71	0.30	18.10	54.96	0.70	-0.33	0.74
	Sepa	7.70	**0.07**	17.73	51.31	0.74	0.00	nan
	joint	**7.45**	0.16	**17.55**	**50.61**	**0.75**	15.56	0.00
ID3 DE qh	zero	7.63	0.03	18.18	51.56	0.71	-2.21	0.03
	1 shot	7.77	30.33	18.12	51.49	0.71	-13.08	0.00
	5 shot	7.78	17.32	18.33	51.51	0.71	-7.57	0.00
	10 shot	7.80	0.19	18.98	51.60	0.71	-10.39	0.00
	50 shot	7.69	35.46	18.08	51.43	0.71	-4.60	0.00
	100 shot	7.72	0.38	18.05	51.67	0.70	-7.51	0.00
	500 shot	7.61	0.12	17.96	51.70	0.70	-0.41	0.68
	1000 shot	7.67	**0.01**	18.06	51.69	0.70	-6.35	0.00
	Sepa	7.60	6.90	18.13	51.36	0.71	0.00	nan
	joint	**7.38**	1.11	**17.53**	**49.73**	**0.73**	5.46	0.00

To investigate the impact of scaler selection (whether the scalers for case B are the same as those for case A) and the use of layer freezing on prediction results during fine-tuning, we conducted comparison experiments focusing on fine-tuning. For clarity, we use b_{scaler} and $b_{freezing}$ proposed in Section B.3.1. The results are presented in Table B.5 and Table B.6, respectively.

Table B.8: The comparison experiment results of fine-tuning in German market between the same and different scalers between case A and case B. The units for AQL, RMSE, and MAE are expressed in /MWh, while AQCR is reported as a percentage. All metrics are denormalized. The **Case Desc.** refers to case B. In the **DM test results**, model 1 corresponds to the groups with $b_{scaler} = True$ for the current case, while model 2 represents the groups with $b_{scaler} = False$.

Case Desc.	x	b_{scaler}	**AQL**	**AQCR**	**MAE**	**RMSE**	**R2**	**DM_stat**	**p_value**
ID1 DE h	1	True	5.44	14.36	12.30	31.33	0.88	0.00	nan
	1	False	5.35	17.15	11.68	29.71	0.89	4.64	0.00
	5	True	5.46	0.00	11.70	29.32	0.89	0.00	nan
	5	False	5.39	0.00	11.75	29.40	0.89	9.00	0.00
	10	True	5.82	26.05	13.72	34.21	0.86	0.00	nan
	10	False	5.44	0.66	12.11	32.45	0.87	13.87	0.00
	50	True	5.67	12.55	12.77	34.24	0.86	0.00	nan
	50	False	5.39	0.02	11.72	30.17	0.89	7.14	0.00
ID2 DE h	1	True	4.14	33.64	9.54	26.18	0.90	0.00	nan
	1	False	4.31	30.85	9.99	26.11	0.90	-13.61	0.00
	5	True	4.33	14.50	9.75	25.85	0.90	0.00	nan
	5	False	4.32	11.80	9.62	25.87	0.90	0.96	0.34
	10	True	4.30	17.60	9.61	25.89	0.90	0.00	nan
	10	False	4.35	9.69	9.70	25.99	0.90	-3.90	0.00
	50	True	4.34	52.87	9.88	27.05	0.89	0.00	nan
	50	False	4.25	14.04	9.48	26.15	0.90	4.82	0.00
ID3 DE h	1	True	4.42	11.30	10.24	29.27	0.86	0.00	nan
	1	False	4.60	9.45	10.72	29.29	0.86	-18.33	0.00
	5	True	4.92	0.20	12.83	31.93	0.83	0.00	nan
	5	False	4.97	1.22	13.04	32.22	0.83	-12.61	0.00
	10	True	4.90	0.48	12.47	30.76	0.84	0.00	nan
	10	False	4.77	0.50	11.85	29.74	0.85	9.32	0.00
	50	True	4.68	0.27	11.60	30.24	0.85	0.00	nan
	50	False	4.61	6.46	11.02	29.34	0.86	5.49	0.00
ID1 DE qh	1	True	8.40	1.55	19.94	63.14	0.71	0.00	nan
	1	False	8.50	19.90	20.48	63.93	0.71	-18.19	0.00
	5	True	8.28	14.91	19.09	61.39	0.73	0.00	nan
	5	False	8.30	14.90	19.19	63.60	0.71	-1.30	0.19
	10	True	8.62	0.91	19.58	63.11	0.72	0.00	nan
	10	False	8.29	16.34	19.13	63.42	0.71	16.45	0.00
	50	True	8.33	0.00	19.08	63.57	0.71	0.00	nan
	50	False	8.28	32.54	19.10	63.10	0.72	9.91	0.00
ID2 DE qh	1	True	7.67	3.06	18.37	54.82	0.71	0.00	nan
	1	False	7.70	0.82	18.74	55.32	0.70	-11.81	0.00
	5	True	7.68	0.44	18.24	55.09	0.70	0.00	nan
	5	False	7.68	0.62	18.24	54.98	0.70	0.82	0.41
	10	True	7.65	0.50	18.05	55.04	0.70	0.00	nan

Case Desc.	x	b_{scaler}	AQL	AQCR	MAE	RMSE	R2	DM_stat	p_value
	10	False	7.64	0.44	18.05	54.98	0.70	12.23	0.00
	50	True	7.64	9.30	18.06	55.25	0.70	0.00	nan
	50	False	7.65	0.52	18.16	55.05	0.70	-5.66	0.00
ID3 DE qh	1	True	7.77	30.33	18.12	51.49	0.71	0.00	nan
	1	False	7.88	43.73	18.59	51.77	0.70	-18.53	0.00
	5	True	7.78	17.32	18.33	51.51	0.71	0.00	nan
	5	False	7.74	0.78	18.08	51.45	0.71	4.95	0.00
	10	True	7.80	0.19	18.98	51.60	0.71	0.00	nan
	10	False	7.95	14.29	19.24	51.74	0.70	-18.11	0.00
	50	True	7.69	35.46	18.08	51.43	0.71	0.00	nan
	50	False	7.66	16.21	18.28	51.60	0.70	2.24	0.03

Table B.9: The comparison experiment results of fine-tuning between the with and without layers freezing in German market. The units for AQL, RMSE, and MAE are expressed in /MWh, while AQCR is reported as a percentage. All metrics are denormalized. The **Case Desc.** refers to case B. In the **DM test results**, model 1 corresponds to the groups with $b_{freezing} = True$ for the current case, while model 2 represents the groups with $b_{freezing} = False$.

Case Desc.	x	$b_{freezing}$	AQL	AQCR	MAE	RMSE	R2	DM_stat	p_value
ID1 DE h	1	True	5.44	14.36	12.30	31.33	0.88	0.00	nan
	1	False	5.27	12.80	12.57	32.38	0.87	20.35	0.00
	5	True	5.46	0.00	11.70	29.32	0.89	0.00	nan
	5	False	5.69	0.43	11.92	29.25	0.90	-18.97	0.00
	10	True	5.82	26.05	13.72	34.21	0.86	0.00	nan
	10	False	5.82	0.59	14.45	36.51	0.84	-0.40	0.69
	50	True	5.67	12.55	12.77	34.24	0.86	0.00	nan
	50	False	5.48	0.25	12.46	33.68	0.86	24.41	0.00
ID2 DE h	1	True	4.14	33.64	9.54	26.18	0.90	0.00	nan
	1	False	4.08	10.44	9.46	26.46	0.90	16.68	0.00
	5	True	4.33	14.50	9.75	25.85	0.90	0.00	nan
	5	False	4.45	1.47	9.97	25.78	0.90	-6.32	0.00
	10	True	4.30	17.60	9.61	25.89	0.90	0.00	nan
	10	False	4.32	50.83	9.59	25.78	0.90	-1.72	0.09
	50	True	4.34	52.87	9.88	27.05	0.89	0.00	nan
	50	False	4.32	27.86	9.98	27.09	0.89	6.58	0.00
ID3 DE h	1	True	4.42	11.30	10.24	29.27	0.86	0.00	nan
	1	False	4.33	20.54	10.18	29.56	0.86	11.16	0.00
	5	True	4.92	0.20	12.83	31.93	0.83	0.00	nan
	5	False	5.91	0.32	16.99	35.85	0.79	-28.19	0.00
	10	True	4.90	0.48	12.47	30.76	0.84	0.00	nan
	10	False	5.46	0.32	15.28	32.18	0.83	-30.13	0.00
	50	True	4.68	0.27	11.60	30.24	0.85	0.00	nan

Case Desc.	x	$b_{freezing}$	AQL	AQCR	MAE	RMSE	R2	DM_stat	p_value
	50	False	4.80	51.87	11.36	29.97	0.85	-13.10	0.00
ID1 DE qh	1	True	8.40	1.55	19.94	63.14	0.71	0.00	nan
	1	False	8.50	22.30	19.99	62.98	0.72	-18.75	0.00
	5	True	8.28	14.91	19.09	61.39	0.73	0.00	nan
	5	False	8.12	63.01	18.45	59.80	0.74	12.91	0.00
	10	True	8.62	0.91	19.58	63.11	0.72	0.00	nan
	10	False	8.55	25.59	20.01	63.03	0.72	10.08	0.00
	50	True	8.33	0.00	19.08	63.57	0.71	0.00	nan
	50	False	8.60	0.00	19.30	68.07	0.67	-9.29	0.00
ID2 DE qh	1	True	7.67	3.06	18.37	54.82	0.71	0.00	nan
	1	False	7.73	27.08	18.32	55.97	0.69	-7.76	0.00
	5	True	7.68	0.44	18.24	55.09	0.70	0.00	nan
	5	False	8.22	7.55	19.67	60.87	0.64	-15.21	0.00
	10	True	7.65	0.50	18.05	55.04	0.70	0.00	nan
	10	False	7.85	0.29	18.48	60.02	0.65	-6.34	0.00
	50	True	7.64	9.30	18.06	55.25	0.70	0.00	nan
	50	False	7.76	9.48	18.25	59.88	0.65	-4.15	0.00
ID3 DE qh	1	True	7.77	30.33	18.12	51.49	0.71	0.00	nan
	1	False	8.43	31.21	18.16	51.68	0.70	-76.37	0.00
	5	True	7.78	17.32	18.33	51.51	0.71	0.00	nan
	5	False	8.48	0.83	19.31	51.88	0.70	-52.31	0.00
	10	True	7.80	0.19	18.98	51.60	0.71	0.00	nan
	10	False	9.26	21.28	21.70	52.79	0.69	-58.40	0.00
	50	True	7.69	35.46	18.08	51.43	0.71	0.00	nan
	50	False	7.66	8.64	18.26	51.55	0.71	5.62	0.00

B.3.3. Experiments Conclusion

The results in B.4 illustrate the similarities in the underlying structure between the German and Austrian markets, as reflected in the hourly product prices. However, there are notable differences in generalization between the two countries. In predicting all three cases for the German market, various transfer learning strategies that involved Austrian datasets were found to be no significantly better than the separate training approach, in terms of quantile forecast performance. Additionally, the zero-shot quantile forecast performance was significantly worse than that of separate training. However, for the Austrian market, in all three cases, joint learning was found to significantly outperform separate training, while zero-shot performance showed no significant difference from separate training.

The results in B.7 illustrate the similarities in the structure between the hourly and quarter-hourly products in the German market, while also highlighting the significant differences in generalization between the two types of products. In predicting all three cases for the prices of hourly products, any transfer learning strategies, including zero-shot, fine-tuning and joint learning, which involved quarter-hourly product prices were found to perform significantly worse than separate training in terms of quantile forecast performance. However, for quarter-hourly products, joint learning was found to provide

significant improvement in quantile forecast performance compared to separate training. Additionally, the improvement from joint learning was observed in pointwise forecast.

Next, we focus on the impact of the choice of scalers and layer freezing on the fine-tuning results. The results in B.5 and B.8 illustrate the effect of whether the scalers selected for case A and case B are the same or different on the testing quantile forecast results. In most experiments, this difference was found to be statistically significant, as confirmed by the DM test. However, the groups with the same and different scalers did not show a clear advantage in terms of quantile forecast performance, and the similarities across cases were difficult to capture. One possible explanation for this is that the features and labels distributions between the cases are similar, as partially demonstrated in Figure 4.2 with respect to label distributions.

Additionally, B.6 and B.9 show the impact of layer freezing on the results. In the German market, the use or non-use of layer freezing was found to significantly affect quantile forecast performance in most experiments, as confirmed by the DM test. However, there is no clear conclusion on whether the use of freezing improves or worsens the prediction performance.

In conclusion, the fine-tuning results show uncertainties how the choice of scalers or layer freezing affects quantile forecast performance.

C

Results of Extended Explorations

C.1. Effect of Sides Lock Correction on Results

In the feature selection process, to validate whether features should exhibit axis symmetry between the selling and buying sides, we introduce the concept of **sides lock**. This approach forces the selected features on one side to be mirrored by the same features on the opposite side, while maintaining their uniqueness. Comparative experiments were conducted on the MLP and KAN models to test this approach. The results of these tests are presented in the tables below, where $b_{sides\_lock} = \text{True}$ indicates that the feature lock is enabled, while $b_{sides\_lock} = \text{False}$ indicates that the feature lock is disabled.

Table C.1: Testing performance of comparison between sides lock usage utilizing MLP in all cases. The units of AQL, RMSE, and MAE are expressed in /MWh, while AQCR is reported in %. All metrics are denormalized.

Case Desc.	b_{sides_lock}	AQL	AQCR	MAE	RMSE	R2
ID1 DE h	False	5.00	6.43	12.07	34.13	0.86
	True	7.33	15.40	17.00	42.87	0.77
ID1 AT h	False	8.17	85.16	20.36	50.13	0.63
	True	8.19	0.02	20.23	49.53	0.64
ID2 DE h	False	3.89	1.13	9.52	27.37	0.89
	True	9.32	41.16	15.31	35.62	0.81
ID2 AT h	False	4.86	0.27	11.64	30.17	0.79
	True	4.82	0.02	11.62	30.93	0.78
ID3 DE h	False	4.15	0.05	10.23	28.28	0.87
	True	15.82	24.17	31.92	67.83	0.24
ID3 AT h	False	5.07	0.27	12.05	28.79	0.80
	True	4.96	1.31	11.96	28.82	0.80

Case Desc.	b_{sides_lock}	AQL	AQCR	MAE	RMSE	R2
ID1 DE qh	False	8.69	0.01	18.83	60.53	0.74
	True	8.58	7.77	18.84	58.39	0.76
ID1 AT qh	False	12.64	0.26	30.90	110.31	0.32
	True	12.60	0.03	30.89	111.22	0.31
ID2 DE qh	False	7.75	0.12	18.01	53.42	0.72
	True	9.73	7.79	19.52	58.44	0.67
ID2 AT qh	False	7.47	0.01	18.03	67.80	0.49
	True	7.62	0.89	18.35	69.38	0.47
ID3 DE qh	False	7.62	0.21	17.93	52.56	0.69
	True	7.67	0.35	18.09	51.74	0.70
ID3 AT qh	False	7.37	0.12	17.97	51.85	0.58
	True	7.38	0.05	17.92	53.01	0.56

Table C.2: Testing performance of comparison between sides lock usage utilizing KAN in all cases. The units of AQL, RMSE, and MAE are expressed in /MWh, while AQCR is reported in %. All metrics are denormalized.

Case Desc.	b_{sides_lock}	AQL	AQCR	MAE	RMSE	R2
ID1 DE h	False	5.05	0.18	12.38	33.11	0.87
	True	5.43	1.00	13.14	46.03	0.74
ID1 AT h	False	7.98	0.02	19.69	45.65	0.69
	True	8.07	0.54	20.01	48.53	0.65
ID2 DE h	False	3.88	11.48	9.51	27.16	0.89
	True	14.00	65.32	32.18	77.65	0.10
ID2 AT h	False	4.88	0.11	11.89	30.10	0.80
	True	4.85	50.06	11.57	29.48	0.80
ID3 DE h	False	4.14	0.14	10.42	27.89	0.87
	True	16.22	36.87	29.69	56.35	0.48
ID3 AT h	False	5.24	1.90	13.22	29.20	0.79
	True	4.98	0.02	11.87	28.64	0.80
ID1 DE qh	False	8.55	0.03	18.73	59.67	0.75
	True	15.33	2.66	34.07	248.71	-3.42
ID1 AT qh	False	12.56	0.04	30.97	99.80	0.44
	True	12.57	0.00	30.80	103.35	0.40
ID2 DE qh	False	7.68	0.17	17.93	51.51	0.74
	True	7.81	1.57	18.08	51.69	0.74
ID2 AT qh	False	7.48	0.02	18.22	66.74	0.51

Case Desc.	b_{sides_lock}	AQL	AQCR	MAE	RMSE	R2
	True	7.47	0.01	18.19	67.05	0.50
ID3 DE qh	False	7.70	0.18	17.96	51.48	0.71
	True	8.13	1.02	18.00	51.46	0.71
ID3 AT qh	False	7.35	0.02	17.61	51.58	0.58
	True	7.32	0.05	17.77	52.23	0.57

The results in Table C.1 and Table C.2 suggest that the use of sides lock may introduce instability in quantile forecast performance, greatly worsening the forecast in certain cases. This finding confirms that, after introducing feature candidates in percentiles, axis symmetry in feature selection between the selling and buying sides does not hold.

C.2. Time-Window Selection based on Deep Learning Methods

This section presents the conclusions from time-window selection using MLP, GRU, LSTM, and 2DCNN models. Since the quantile sets selected for quantile regression (as shown in Formula C.1) differ from those used in other results in this report, the findings here are provided for reference only. The features input contains all price candidates shown in Table 3.2.

$$A_{tw} = \{10\%, 25\%, 50\%, 75\%, 90\%\} \tag{C.1}$$

Table C.3: Time-window selection experiment results utilizing deep learning benchmarks in prediction of ID1 and ID3 in Germany and Austria. The units of AQL, RMSE, and MAE are expressed in /MWh, while AQCR is reported in %. All metrics are denormalized.

Case Desc.	Model	Optimal Time-window	AQL	AQCR	MAE	RMSE	R2
ID1 DE h	2DCNN	['60']	4.83	83.67	15.29	33.50	0.87
	GRU	['60']	5.02	82.81	15.85	38.66	0.82
	LSTM	['60']	4.98	82.72	16.06	39.47	0.82
	MLP	['60']	4.80	80.91	15.49	29.45	0.90
ID1 AT h	2DCNN	['1', '5', '15', '60', '180', 'full']	7.22	85.66	22.36	41.02	0.74
	GRU	['60']	7.29	83.33	22.98	45.51	0.69
	LSTM	['1', '5', '15', '60']	7.26	83.90	22.71	45.62	0.68
	MLP	['1', '5', '15', '60', '180']	7.27	85.35	23.71	44.73	0.70
ID3 DE h	2DCNN	['180']	3.83	82.40	12.77	30.38	0.85
	GRU	['full']	3.94	74.63	12.09	29.52	0.86
	LSTM	['1', '5']	3.92	85.62	12.63	27.97	0.87
	MLP	['180']	3.85	84.35	12.80	29.62	0.86
ID3 AT h	2DCNN	['15']	4.59	84.58	14.39	31.45	0.76
	GRU	['1', '5', '15', '60', '180']	4.58	81.83	14.44	31.85	0.76

Case Desc.	Model	Optimal Time-window	**AQL**	**AQCR**	**MAE**	**RMSE**	**R2**
	LSTM	['1', '5', '15', '60', '180']	4.56	77.51	13.83	31.67	0.76
	MLP	['1', '5', '15', '60', '180', 'full']	4.59	82.74	14.95	32.52	0.75
ID1 DE qh	2DCNN	['1', '5', '15']	14.08	83.31	39.24	77.55	0.60
	GRU	['1']	9.33	91.73	26.54	65.75	0.71
	LSTM	['1']	9.98	92.49	27.78	70.01	0.67
	MLP	['15']	10.55	92.64	28.74	65.48	0.71
ID1 AT qh	2DCNN	['15']	11.08	82.02	37.08	96.73	0.39
	GRU	['1', '5', '15', '60', '180', 'full']	11.06	84.60	36.13	102.39	0.32
	LSTM	['15']	11.30	84.55	35.95	95.24	0.41
	MLP	['1', '5', '15']	11.12	85.82	36.96	92.77	0.44
ID3 DE qh	2DCNN	['15']	7.27	81.82	20.21	51.18	0.71
	GRU	['1', '5']	7.36	86.22	21.70	54.16	0.68
	LSTM	['5']	7.41	86.19	20.99	53.22	0.69
	MLP	['15']	7.42	85.92	21.39	53.55	0.69
ID3 AT qh	2DCNN	['60']	6.63	81.00	21.31	48.99	0.59
	GRU	['60']	6.60	82.96	21.31	49.17	0.59
	LSTM	['60']	6.67	85.57	21.40	49.38	0.59
	MLP	['1', '5', '15', '60', '180']	6.64	79.36	21.10	49.56	0.58

The results exhibit the following general trends. First, when all price candidates are included, the models' reliability is generally poor. Second, for the same Δ, the optimal time window in Austria is generally longer than in Germany. Third, for the same country, as Δ increases from 60 minutes to 180 minutes, the required time window also increases.

D

Interpretable Deep Learning Pointwise Forecast via KAN

D.1. Motivation and Objective

Due to the Rashomon effect [84], different models or even different iterations of the same modelcan yield significantly divergent results for the same price prediction. This variability introduces substantial risks for traders, as inconsistent or unreliable forecasts may lead to suboptimal bidding strategies and, ultimately, financial losses [85]. Therefore, to mitigate these risks, interpretability can be considered as an objective in IDM price prediction.

However, in the previous studies discussed in Section 2.1, deep learning approaches are typically considered black-box models. While they perform well in capturing the nonlinear relationships between features and labels, the learned relationships are often difficult for human researchers to interpret or understand.

Building on this research gap, the objective of this work package is to achieve accurate IDM price prediction while maintaining strong interpretability through the use of deep learning models.

D.2. Kolmogorov–Arnold Network (KAN) Model Theory

Liu et al. [86] introduced the Kolmogorov-Arnold Networks (KANs) as an innovative neural network architecture. A key feature of KANs is the replacement of the traditional learnable parametersweights (w) and biases (b)and fixed activation functions in MLP models with learnable activation functions. Uniquely, in KANs, activation functions are relocated from the neurons to the edges, offering a new approach to network design. When combined with visualization and symbolization tools, KANs become particularly useful for scientists seeking to (re)discover underlying mathematical and physical laws [87].

This section will provide an overview of KAN, focusing on its integration with fully connected neural networks (FNNs). In Section D.2.1, we will present the overall structure of KAN and delve into its elegant mathematical foundations. Section D.2.2 will focus on the concept of learnable activation

functions. In Sections D.2.3 and D.2.4, we will explore the current sparsity and symbolification tools available for KAN. Finally, Section D.2.5 will cover the current applications of KAN across various fields.

D.2.1. Overall Structure and Mathematical Foundations

The current structure of KAN closely resembles that of a MLP, consisting of a fully connected input layer, output layer, and hidden layers. In the KAN model, the nodes in each layer are similar to neurons in an MLP. However, unlike MLP neurons, each node in a KAN performs only basic operations and does not require any parameters to be trained. The concept of edges in the KAN model is akin to that in MLP, where edges represent the connections between nodes in adjacent layers. What distinguishes KAN is the introduction of learnable activation functions, which provide a richer and more dynamic meaning to these edges. As illustrated in the Figure D.1, both MLP and KAN models are depicted with 2 input features, 1 output label, and 1 hidden layer containing 5 nodes (neurons).

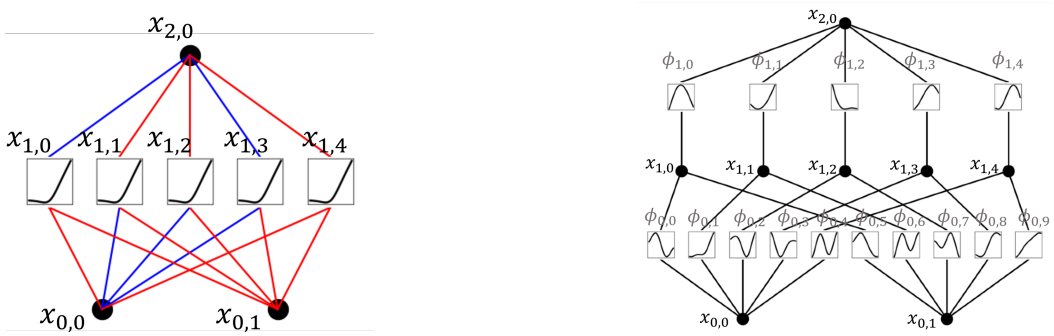

(a) MLP model. **(b)** KAN model.

Figure D.1: Comparison of the structure of a model with 2 input features, 1 output label, and 1 hidden layer containing 5 nodes (neurons).[86]

Taking the output label $x_{2,0}$ from the figure as an example, the MLP model can be represented by the following formula:

$$x_{2,0} = \sum_{i=0}^{4} \boldsymbol{w_{2,1,i}} \phi \left(\sum_{j=0}^{1} \boldsymbol{w_{1,1,j}} x_{0,j} + \boldsymbol{b_{1,i}} \right) + \boldsymbol{b_2} \tag{D.1}$$

where ϕ represents the fixed activation functions, w and b represent the weight and bias, respectively, which are the key parameters during training. In contrast, the same output in KAN is expressed by the following formula:

$$x_{2,0} = \sum_{i=0}^{4} \phi_{1,i}(x_{1,i}) = \sum_{i=0}^{4} \phi_{1,i} \left(\sum_{j=0}^{1} \phi_{0,4j+i}(x_{0,j}) \right) \tag{D.2}$$

where the core parameters during training are the activation functions themselves. This allows KAN to model complex non-linear relationships with greater flexibility and expressiveness. The approach enables KAN to capture intricate patterns in data, particularly in scientific tasks where traditional neural networks may struggle to provide interpretability or accurate modeling.

KANs are built upon an elegant mathematical foundation, the Kolmogorov-Arnold representation theorem [88]. This theorem asserts that any real-valued function f of d variables can be represented as a sum of one-dimensional functions, specifically:

$$f(x_1, x_2, \ldots, x_d) = \sum_{i=1}^{d} g_i(h_i(x_1, x_2, \ldots, x_d)) \tag{D.3}$$

where g_i are one-dimensional functions, and h_i are functions mapping from $\mathbb{R}^d$ to $\mathbb{R}$. This representation suggests that a high-dimensional function can be approximated by simpler one-dimensional functions, providing a foundation for modeling complex relationships with fewer parameters.

D.2.2. Relocation of Learnable Activation Functions

The relocation of activation functions is the key structural feature of KAN models. This learnable activation function can be viewed as the mapping relationship between the nodes at both ends of each edge, and it forms the core component that KAN learns.

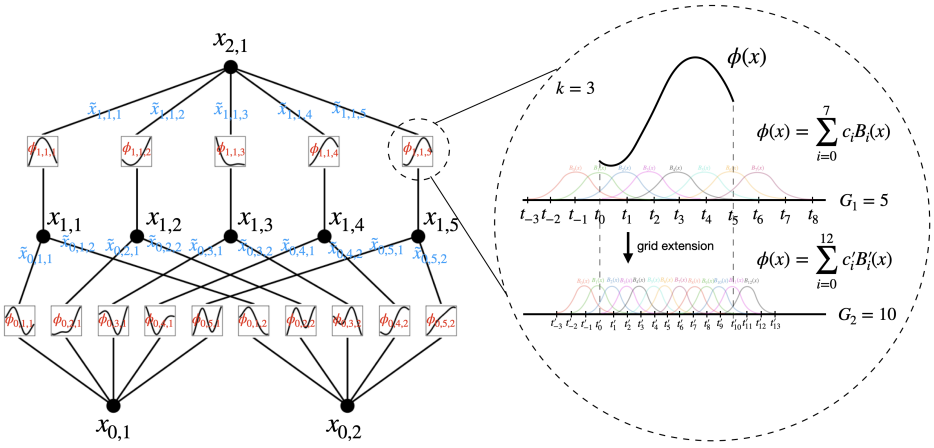

Figure D.2: Notations of activations that flow through the network and an activation function is parameterized as a B-spline. [86]

Currently, KAN uses B-splines to fit these mapping relationships. B-splines are chosen due to their numerous advantages, such as flexibility, ease of local control, high-order continuity, and the ability to perform interpolation or approximation effectively [89]. Of course, in certain scenarios, B-splines can be replaced by other curve-fitting methods, such as Fourier series [90]. As shown in Figure D.2, the mapping relationship is learned through a linear combination of multiple fixed B-splines, and the formula is as follows:

$$\phi(x) = \sum_{i=0}^{G} c_i B_i(x) \tag{D.4}$$

where c_i represents the learnable coefficient of each B-spline, B_i denotes the fixed basis function, and G indicates the number of grid intervals. During training, the c_i values serve as the key parameters for learning the activation functions. Additionally, G is an important hyperparameter, which can be considered analogous to the resolution of the fitting process.

D.2.3. Sparsity Tools

Adding L1 regularization and implementing a pruning process [91] are common strategies to induce sparsity in DL models, helping to mitigate overfitting and reduce model complexity. In a typical DL model, L1 regularization is incorporated into the cost function to achieve better training outcomes. While L1 regularization can be applied to KAN models in a similar manner as in MLP models, the pruning process in KAN offers a more intuitive approach to sparsification, facilitated by visualization tools.

For KAN models, due to the relocation of activation functions discussed earlier, pruning is preferred to performed on the edges rather than the nodes. This edge-based pruning offers a significant advantage: it enables more precise and targeted sparsification. Consider a scenario where a node x is connected to several other nodes through edges with varying degrees of importance. In a traditional node pruning approach, deciding whether to discard or retain the node can be problematic. Discarding the node may result in the loss of high-importance edges, which could significantly degrade the model's performance. Conversely, retaining the node might not fully eliminate low-importance factors. Edge pruning, however, avoids these issues, as it targets specific connections, allowing for more effective sparsification.

In the implementation of this process, KAN first calculates the attribute of each edge, defined as follows:

$$|\phi|_{L1} = \frac{1}{N_p} \sum_{s=0}^{N_p} |\phi(x^{(s)})| \tag{D.5}$$

where N_p represents the number of training inputs, $x^{(s)}$ means the s-th training input. The attribute of each edge is defined by the L1 norm of the corresponding edge. Any edges with attributes below a predefined pruning threshold are discarded.

However, node-based pruning can still be applied in KANs in a manner similar to that in MLPs, providing a rapid means of achieving model sparsity. The definition of importance score is provided as Formula D.6.

$$\begin{aligned} I_{l,i} &= \max_k \left(|\phi_{l-1,i,k}|_1 \right), \\ O_{l,i} &= \max_j \left(|\phi_{l,j,i}|_1 \right), \\ |x|_{L1,i,j} &= \min(I_{l,i}, O_{l,i}) \end{aligned} \tag{D.6}$$

Where $|x|_{L1,i,j}$ represents the importance score of a node, and $I_{l,i}$ and $O_{l,i}$ denote the highest importance scores of the edges between the current node and any nodes in the lower and higher layers, respectively. When pruning nodes, all nodes with importance scores lower than the threshold are deactivated. Similarly, when pruning edges, all edges with importance scores lower than the threshold are deactivated.

Sparsity is not an essential step in all studies. However, as illustrated in the Figure D.3, a simple toy example involving the function fitting of two variables demonstrates that, in KAN models, an excessive number of nodes does not necessarily lead to a reduction in loss.

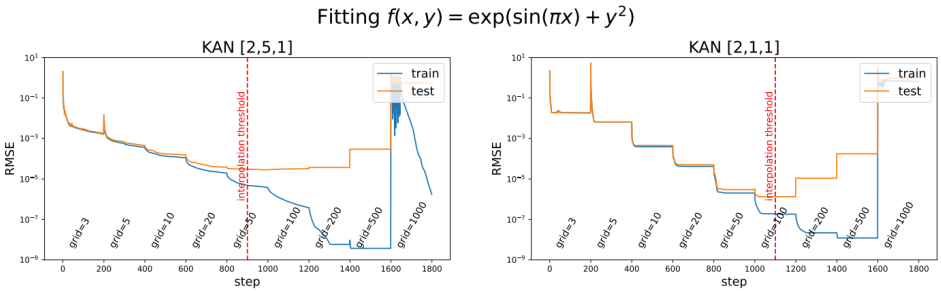

Figure D.3: The results of a training progress of a toy example of function fitting. [86]

D.2.4. Symbolification

The symbolification process refers to the replacement of the predictions from the "black box" model with a formulaic representation, thereby enhancing the interpretability and transparency of the model. In the KAN model, this process involves utilizing a predefined library of functions to fit the mapping learned by each edge. The functions within this library can be expressed in the form illustrated as Formula D.7, where the four coefficients a, b, c and d are optimized to maximize R^2 . These symbolized functions with optimized coefficients are then used to replace the activation function of the edge, providing a more transparent representation of the learned relationships.

$$f(x) = cf(ax + b) + d \tag{D.7}$$

This process bears similarities to symbolic regression, wherein the goal is to derive a symbolic expression that accurately captures the underlying relationship between variables.

D.2.5. Applications of KAN in Previous Researches

KAN has demonstrated significant success across various forecasting applications, highlighting its potential as a powerful modeling tool. For example, Vaca-Rubio et al. [92] applied KAN to forecast satellite traffic performance, finding that it provides a viable alternative to traditional MLPs in traffic management. Similarly, Bresson et al. [93] showcased KAN's superior performance over MLPs in graph regression tasks, emphasizing its applicability to more complex regression problems. While these studies primarily focused on the predictive accuracy of KAN, they effectively illustrated its practical utility and established it as a robust tool for forecasting tasks, even without fully exploiting KAN's interpretability capabilities.

D.3. Methodology

D.3.1. Auto Prune-Fine-tuning-Symbolification Cycle (APPSC)

To obtain the optimal white-box KAN pointwise forecast, the Auto Prune-Fine-tuning-Symbolification Cycle (APPSC) is employed. This cycle includes circular pruning and fine-tuning steps on the pretrained model (Model A), followed by symbolizing steps on both pruned models (Model B_k) and fine-tuned models (Model D_k) to generate symbolized pruned (Model B_k^s) and symbolized fine-tuned models (Model D_k^s), respectively. Here, k denotes the current round number.

Specifically, the pruning strength rank (PSR) is defined as the pruning threshold on edges, as shown in

the formula. As k increases, the PSR for that round also increases, indicating stronger pruning.

$$\delta = \frac{Mean(|\phi(x^{(s)})|) - Min(|\phi(x^{(s)})|)}{N_\delta}$$
$$PSR_k = Min(|\phi(x^{(s)})|) + k \times \delta, k \in \{0, 1, 2, ...\} \tag{D.8}$$

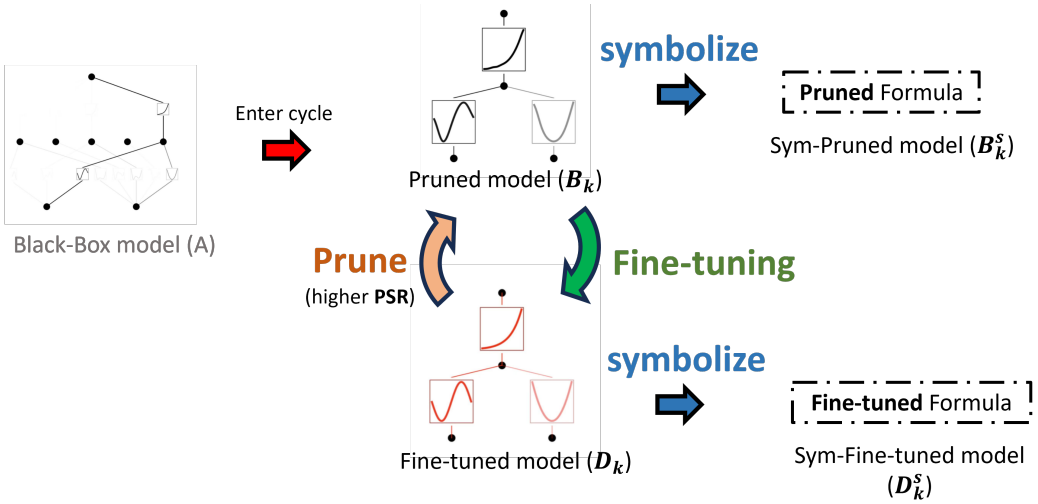

Figure D.4: Progress of APPSC

D.3.2. Dynamic Edge Rebear (DER)

Dynamic Edge Rebear (DER)

Dynamic Edge Rebear (DER) is introduced to address the issue of over-pruning in the current pruning process by providing a fixed probability of re-activation for edges that have been deactivated. Specifically, this involves randomly re-activating edges before each round of fine-tuning in the APPSC.

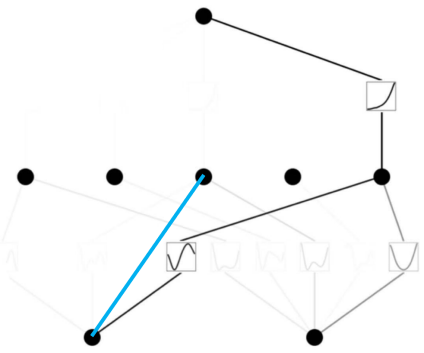

Figure D.5: Progress of APPSC

D.3.3. Benchmarks

In this package, white-box KAN (after symbolizing), black-box KAN (without symbolizing), linear regression (SR) and symbolic regression (SR) are mentioned.

Symbolic regression is a type of regression analysis that seeks to find a mathematical expression or symbolic equation that best fits a given set of data. Unlike traditional regression methods, which assume a predefined functional form, symbolic regression automatically discovers both the form of the equation and the parameters that optimize the fit to the data.Symbolic regression is implemented using evolutionary algorithms, such as genetic programming, to explore a large space of potential equations.

D.4. Experiments and Results

D.4.1. Experimental Setup

The features input in this package contain VWAP, minimum prices, maximum prices and sum of volume with a timewindow of 15 minutes prior to the prediction time. The label is the ID3 index of hourly products in German market. The order book data are split into training (Jan 2022–Dec 2023), validation (Jan–Jun 2024), and testing (Jul–Dec 2024) datasets. All experiments were conducted using the NVIDIA GeForce RTX 4060 GPU.

D.4.2. Experimental Results

The pointwise forecast performance experiments for all four benchmarks are presented in Table D.1. For clarity, KAN in this table refers to the white-box KAN. The white-box KAN results are derived from the white-box KAN models with the highest testing R2.

Table D.1: KAN testing results with other benchmarks

Model	mae	rmse	r2	dm stat	p value
KAN with DER	12.00	31.28	0.84	0.00	nan
KAN without DER	13.00	31.34	0.84	-0.25	0.80
SR	10.80	29.92	0.85	0.86	0.39
black-box KAN	10.89	28.61	0.87	2.33	0.02
LR	11.71	32.45	0.83	-1.24	0.22

D.5. Package Conclusion

This package represents an exploration and attempt to apply white-box deep learning in IDM price prediction. However, the experimental results do not demonstrate a significant advantage of white-box KAN in pointwise forecast performance. On the contrary, white-box KAN does not outperform SR or LR significantly. A possible explanation for this is that, during the symbolification phase, white-box KAN is subjected to a significantly higher loss compared to black-box KAN. Furthermore, the proposed DER does not show a substantial improvement in the performance of white-box KAN.

E

Anomaly Detection

E.1. Motivation and Objective

Models trained with different loss functions are considered to have the potential to exhibit varying performance in predicting anomalies versus normal values [94]. To further improve the performance of pointwise forecasts, anomaly detectors need to be developed that can predict whether the labels are anomalous based on the features, and apply the appropriate model for current predictions.

Therefore, the objective of this work package is to develop a pointwise forecasting system that integrates anomaly detectors with multiple deep learning models. The main tasks include: (1) validating that models trained with different loss functions exhibit varying performance on anomalies and normal values; and (2) training a classifier capable of accurately detecting anomalies.

E.2. Methodology

E.2.1. Loss Functions with Different Powers

As defined in 3.35, we introduce a new pointwise forecast loss, the mean absolute error with an m-power (MAE-m), as defined in Formula E.1.

$$MAE_m = \frac{1}{N}\sum_{i=0}^{N}|\hat{y}_i - y_i|^m \tag{E.1}$$

where N means the length of dataset, $\hat{y}_i$ means i-th predicted value, y_i means i-th true target value, m is definded the power of loss.

In this work package, the considered values of m are shown as Formula E.2.

$$m \in [1, 2, 4, 8, 16] \tag{E.2}$$

E.2.2. Definition of Anomaly and Focal Loss

In the field of IDM prices, there is currently no widely accepted definition of "abnormal price." In this work package, prices below the Q95 value of the training set labels are defined as normal prices, while prices greater than or equal to the Q95 value are defined as abnormal prices.

Typically, classifiers use cross-entropy (CE) as their loss function, as shown in Formula E.3.

$$CE = -y \cdot \log(p) - (1 - y) \cdot \log(1 - p) \tag{E.3}$$

However, the number of samples in the normal group of the anomaly detectors developed here is much larger than that in the abnormal group, which causes the classifiers to primarily focus on detecting abnormal prices. Therefore, we use focal loss [95] as the loss function for the anomaly detection classifiers, as defined in Formula E.4. The set of considered α is shown in Formula E.5.

$$FL = -\alpha \cdot y \cdot \log(p) - (1 - \alpha) \cdot (1 - y) \cdot \log(1 - p) \tag{E.4}$$

$$\alpha \in [0.1, 0.25, 0.5, 0.6, 0.7, 0.75, 0.85, 0.9, 0.95, 0.99, 0.999, 0.9999] \tag{E.5}$$

E.3. Experiments and Results

E.3.1. Experimental Setup

In all experiments within this work package, the prediction target is the ID3 price index of QH contracts in the German market. The input features include VWAP, P_{min}, and P_{max} with $\delta = 15\,\text{min}$. The split of the training, validation, and testing datasets is the same as described in Section 4.1.1.

E.3.2. Results of Models with MAE-m Losses

The experimental results for both the normal and abnormal datasets are shown in Table E.1. When $m > 2$ is used, the losses in metrics such as $MAE-4$, $MAE-8$, and $MAE-16$ are significantly lower compared to models with $m = 1$ or 2 when predicting the normal dataset. However, when predicting the abnormal dataset, larger values of m do not lead to improved pointwise forecast performance.

Table E.1: Testing performance comparison under different loss functions. The best results are shown in **bold**.

Data State	m	MAE	RMSE	MAE-4	MAE-8	MAE-16
normal	1	13.87	23.15	63.47	147.73	240.80
	2	13.95	24.55	75.97	190.17	326.85
	4	**13.80**	**22.45**	61.93	167.35	292.86
	8	14.27	23.11	**55.75**	**123.80**	**201.86**
	16	14.03	22.98	57.89	132.03	215.61

Data Set	m	MAE	RMSE	MAE-4	MAE-8	MAE-16
abnormal	1	103.92	**206.42**	494.72	983.86	1485.17
	2	**103.77**	206.43	**494.22**	**981.97**	**1482.43**
	4	107.49	222.90	527.38	1034.18	1560.69
	8	113.83	243.18	559.14	1047.89	1568.48
	16	105.76	213.55	508.18	1004.72	1517.16

E.3.3. Anomaly Detectors

We trained different classifiers based on focal loss with 12 different values of α, and the testing results are shown in Table E.2. Different values of α are reflected in the tradeoff between false positive and false negative errors. The anomaly detector with the best performance achieves an F1 score of approximately 0.46. Further experiments also confirm that using multiple classifiers with a voting mechanism does not effectively improve performance.

Table E.2: Testing performance of anomaly detectors. The best results are shown in **bold**.

α	Accuracy	Recall	F1 Score
0.1	0.9535	0.0702	0.1311
0.25	0.9538	0.0781	0.1447
0.5	0.9534	0.0691	0.1291
0.6	0.9553	0.1076	0.1941
0.7	0.9554	0.111	0.1994
0.75	0.9561	0.1246	0.2209
0.85	0.9587	0.1846	0.3087
0.9	0.9595	0.2061	0.337
0.95	**0.9638**	0.3092	**0.4608**
0.99	0.783	0.7418	0.2547
0.999	0.6241	0.8958	0.1924
0.9999	0.2999	**0.9943**	0.1244

E.4. Package Conclusion

In conclusion, the experimental results from this work package do not support the hypothesis that models with loss functions involving higher powers of m (such as those greater than the MAE and MSE) offer improved pointwise forecasting performance on the abnormal dataset. Furthermore, the anomaly detectors, which were based on focal loss, did not exhibit strong performance, suggesting that the chosen loss function may not be optimal for anomaly detection in this context.

F

Academic Publication

Learning from Orderbook Features: Generalizing Across Countries and Product Types in Intraday Electricity Markets

Runyao Yu*†, Ruochen Wu*, Yongsheng Han*, Jochen L. Cremer*†
* Department of Electrical Sustainable Energy, Delft University of Technology
† Department of Integrated Energy Systems, Austrian Institute of Technology
Email: runyao.yu@tudelft.nl

Index terms– Intraday electricity market, orderbook, feature selection, probabilistic prediction, generalization assessment.

Intraday electricity markets are characterized by high volatility and rapid price fluctuations, which pose challenges for forecasting and decision-making. Accurate probabilistic forecasting is essential for market participants to assess risks and make informed bidding and trading decisions. Existing studies typically rely on a limited set of handcrafted features such as Volume-Weighted Average Price (VWAP) or last transaction price [1], [2], [3]. However, the rich data available from the orderbook remains largely underutilized. Moreover, current methods often apply conventional statistical learning models such as Linear Quantile Regression (LQR) or Least Absolute Shrinkage and Selection Operator (LASSO) [4], [5], while advanced machine learning approaches—capable of capturing nonlinear dependencies and complex uncertainty structures—remain underexplored in the field. Furthermore, existing approaches are often developed and validated within a single country and product type, making it unclear whether learned patterns are context-specific or generalizable. Studying generalization across countries and product types can reveal structural similarities, offering insights that benefit both model development and market regulation.

In this paper, a total of 384 features—including the momentum, percentiles, and volatility of prices and volumes over multiple look-back windows for both buy and sell sides—are extracted from the continuous intraday trading sessions, covering the temporal range from January 2022 to January 2025. We introduce a novel dynamic feature selection algorithm for the extracted 384 features based on correlation with both normal and extreme price labels. This method is shown to outperform conventional techniques such as pure L1-penalized regression and Principal Component Analysis (PCA) for probabilistic forecasting. Using the selected features, we provide a comprehensive benchmark of probabilistic forecasting performance across various advanced statistical and deep learning models, such as Quantile Extreme Gradient Boosting (QXGB), Quantile Multilayer Perceptron (QMLP), and Quantile Kolmogorov–Arnold Network (QKAN). These models, which leverage non-linear representation learning, remain underexplored in the context of intraday electricity markets. We further perform a systematic generalization study using the best-performing model across two countries (Germany and Austria) and two product types (hourly and quarter-hourly), evaluating model transferability under full retraining, zero-shot and few-shot transfer learning, and joint training scenarios. The evaluation metrics on unseen data are Average Quantile Loss (AQL), Root Mean Squared Error (RMSE), Mean Absolute Error (MAE), and the Coefficient of Determination (R^2), ensuring a comprehensive assessment of the predictive performance.

The full paper will present the identified optimal feature set derived from orderbook data, selected through the proposed feature selection method. It will further demonstrate the well-performing model architectures for probabilistic prediction with these identified features. In addition, the paper will analyze structural similarities and differences across markets and product types through model transferability, providing insights relevant for both operational deployment and regulatory decision-making.

References

[1] G. Marcjasz, B. Uniejewski, and R. Weron, "Beating the naïve—combining lasso with naïve intraday electricity price forecasts," *Energies*, vol. 13, no. 7, 2020.
[2] M. Narajewski and F. Ziel, "Econometric modelling and forecasting of intraday electricity prices," *Journal of Commodity Markets*, vol. 19, p. 100107, 2020.
[3] T. Serafin, G. Marcjasz, and R. Weron, "Trading on short-term path forecasts of intraday electricity prices," *Energy Economics*, vol. 112, p. 106125, 2022.
[4] J. R. Andrade, J. Filipe, M. Reis, and R. J. Bessa, "Probabilistic price forecasting for day-ahead and intraday markets: Beyond the statistical model," *Sustainability*, vol. 9, no. 11, p. 1990, 2017.
[5] B. Uniejewski, G. Marcjasz, and R. Weron, "Understanding intraday electricity markets: Variable selection and very short-term price forecasting using lasso," *International Journal of Forecasting*, vol. 35, no. 4, pp. 1533–1547, 2019.

Submitted to the 24th Power Systems Computation Conference (PSCC 2026).

G

Large Language Model Usage Statement

During the course of this report, artificial intelligence (AI) tools, specifically ChatGPT, were employed to assist with grammar detection and correction. The AI provided suggestions for textual improvements, which were then carefully reviewed and manually proofread to ensure accuracy and coherence. These tools were used solely for support, and the author takes full responsibility for the content, analysis, and conclusions presented in this report.